



UNIVERSIDAD NACIONAL AUTÓNOMA DE MÉXICO

**POSGRADO EN CIENCIAS DE LA TIERRA
INSTITUTO DE GEOFISICA UNAM
CIENCIAS ATMOSFERICAS ESPACIALES Y PLANETARIAS**

**ESTUDIO DE LA ACELERACIÓN ESTOCÁSTICA Y DETERMINÍSTICA DE LAS
PARTÍCULAS SOLARES RELATIVISTAS**

TESIS

QUE PARA OPTAR POR EL GRADO DE DOCTOR EN CIENCIAS DE LA TIERRA

**PRESENTA:
JUAN CARLOS MÁRQUEZ ADAME**

**TUTOR
Dr. Jorge Alberto Pérez y Peraza
Instituto de Geofísica UNAM**

**MIEMBROS DEL COMITÉ TUTOR
Dr. Víctor Manuel Velasco Herrera
Instituto de Geofísica UNAM
Dr. Luis Xavier González Méndez
Instituto de Geofísica UNAM**

Ciudad Universitaria, CDMX

Octubre 2019



Universidad Nacional
Autónoma de México



UNAM – Dirección General de Bibliotecas
Tesis Digitales
Restricciones de uso

DERECHOS RESERVADOS ©
PROHIBIDA SU REPRODUCCIÓN TOTAL O PARCIAL

Todo el material contenido en esta tesis esta protegido por la Ley Federal del Derecho de Autor (LFDA) de los Estados Unidos Mexicanos (México).

El uso de imágenes, fragmentos de videos, y demás material que sea objeto de protección de los derechos de autor, será exclusivamente para fines educativos e informativos y deberá citar la fuente donde la obtuvo mencionando el autor o autores. Cualquier uso distinto como el lucro, reproducción, edición o modificación, será perseguido y sancionado por el respectivo titular de los Derechos de Autor.

AGRADECIMIENTOS:

- A la Universidad Nacional Autónoma de México,*
- A Conacyt por su apoyo económico.*
- Al Programa de Posgrado en Ciencias de la Tierra.*
- Al Instituto de Geofísica de la UNAM.*

TUTOR DE TESIS:

Dr. Jorge Alberto Pérez y Peraza

Así como al comité Tutorial:

Dr. Víctor Manuel Velasco Herrera

Dr. Luis Xavier González Méndez

JURADO

<i>Dr. José Francisco Valdés Galicia</i>	<i>Presidente</i>
<i>Dr. Luis Xavier González Méndez</i>	<i>Vocal</i>
<i>Dr. Jorge Alberto Pérez y Peraza</i>	<i>Secretario</i>
<i>Dr. Ernesto Ortiz Fragoso</i>	<i>Suplente</i>
<i>Dr. Oscar Morales Olivares</i>	<i>Suplente</i>

DEDICATORIA...

A mi mujer y a mis hijos...

INDICE GENERAL:

ESTRUCTURA DE LA TESIS	5
INTRODUCCION	6
OBJETIVOS GENERALES DEL TRABAJO	10
MARCO TEORICO	11
RESULTADOS	20
PRESENTACION DEL CAPITULO EN LIBRO: <i>“Exploration of Solar Cosmic Ray Sources by Means of Particle Energy Spectra”</i>	25
<i>“Exploration of Solar Cosmic Ray Sources by Means of Particle Energy Spectra”</i>	26
PRESENTACION DEL ARTICULO: <i>“Source Energy Spectrum of the 17 May 2012 GLE”</i>	70
<i>“Source Energy Spectrum of the 17 May 2012 GLE”</i>	71
PRESENTACION DEL ARTICULO: <i>““Spectra of the Two Official GLEs of Solar Cycle 24”</i>	82
<i>““Spectra of the Two Official GLEs of Solar Cycle 24””</i>	83
PRESENTACION DEL ARTICULO: <i>“The Quasi-Biennial Oscillation of 1.7 years in Ground Level Enhancement Events”</i>	116
<i>“The Quasi-Biennial Oscillation of 1.7 years in Ground Level Enhancement Events”</i>	117
PRESENTACION DEL ARTICULO: <i>“Determination of GLE of Solar Energetic Particles by Means of Spectral Analysis”</i>	124
<i>“Determination of GLE of Solar Energetic Particles by Means of Spectral Analysis”</i>	125
PRESENTACION DEL ARTICULO: <i>“An Alternative Classification of Solar Particle Events that Reach the Earth Ground Level”</i>	131
<i>“An Alternative Classification of Solar Particle Events that Reach the Earth Ground Level”</i>	132
DISCUSION Y CONCLUSIONES GENERALES	140
REFERENCIAS	142

ESTRUCTURA DE LA TESIS

La presente tesis se encuentra dentro de la modalidad de ***artículos publicados***. Consta de:

-Introducción.

-Objetivos generales del trabajo.

-Marco Teórico.

-Resultados.

-Un capítulo en libro con su respectiva presentación.

-Cinco artículos con sus respectivas presentaciones. Todos ellos en revistas internacionales arbitradas. Tres publicados (incluido uno como primer autor) y dos aceptados para publicación, todos con su respectiva presentación.

-Una discusión y conclusión general.

-Referencias.

Introducción.

La interdependencia entre la Física Espacial y otras disciplinas científicas, particularmente con los plasmas de laboratorio, ha sido ampliamente discutida en la literatura

Esta complementación se debe al hecho de que ambas disciplinas exploran diferentes regiones de los parámetros físicos del plasma, lo que ha permitido aprender acerca de ciertos rangos de parámetros que son inaccesibles en experimentos de laboratorio. Las configuraciones de plasma en el laboratorio se construyen intencionalmente, mientras que en el espacio los plasmas asumen formas espontáneas. Los plasmas de laboratorio son más densos que los plasmas espaciales. Estos últimos están prácticamente libres de efectos de frontera, en contraste con los de laboratorio, los cuales están sujetos al efecto de los dispositivos contenedores que producen a menudo fuerte contaminación superficial. Debido a la diferencia de escalas, el sondeo de los plasmas de laboratorio introduce perturbaciones del sistema, en tanto que el sondeo de los plasmas espaciales no los perturba notablemente. Los plasmas calientes de laboratorio están regidos normalmente por el equilibrio estático, en tanto que los plasmas espaciales son flujos de gran escala fuertemente dependientes del tiempo. En base a las diferencias y similitudes de ambos contextos, las pérdidas turbulentas de partículas confinadas en los reactores de fusión y en los anillos de radiación de Van Allen han sido estudiadas en paralelo (Pérez-Peraza, 1990).

En los Tokamaks, los procesos de reconexión magnética similares a los de los plasmas espaciales determinan la estabilidad global del plasma y afectan también el transporte microscópico. Los experimentos de interacción haz-plasma han sido muy útiles para interpretar fenómenos de la Física de las Auroras. Las ondas de choque estudiadas actualmente en los laboratorios fueron estudiadas y parametrizadas originalmente en los plasmas espaciales. Problemas relacionados con la aceleración y transporte de partículas energéticas son estudiados más intensivamente en el espacio, mientras que estudios paramétricos de geometría y comportamiento de los plasmas en reconexión son investigados en laboratorio (Pérez-Peraza, 1990).

El diagnóstico de los plasmas de laboratorio utiliza técnicas de sondeo directo. En contraste, el sondeo de los plasmas espaciales se realiza por percepción-remota, salvo algunas excepciones de sondeos in situ de nuestra vecindad espacial, con las naves espaciales. El sondeo de los plasmas en otras instancias cósmicas más lejanas, concierne al ámbito de la Astrofísica Geofísica, cuyo principal agente de sondeo son las emisiones electromagnéticas que se emiten en todo el espectro, desde rayos gamma hasta las radio-ondas. Los aceleradores terrestres más potentes hoy en día alcanzan apenas energías de 10^{15} eV en el centro de masa, como es el caso con el acelerador LHC en el CERN. En contraste, los aceleradores cósmicos producen rayos cósmicos que alcanzan energías de hasta de 10^{21} eV. La aceleración de partículas cargadas ocurre en cualquier lugar del universo en el que se produce turbulencia magnética, o bien, intensos campos eléctricos seculares, en virtud de variaciones espaciales y temporales de los campos magnéticos.

El laboratorio cósmico más cercano para estudiar los procesos de aceleración de partículas a energías mayores de 10 MeV es el Sol, en particular durante los fenómenos asociados a la actividad solar, entre los cuales las llamadas *Fulguraciones Solares* (*solar flares* como se les designa internacionalmente) son la principal fuente generadora de partículas de alta energía. Los campos eléctricos generados en este fenómeno son capaces de acelerar, en un lapso promedio de 100 s, a las partículas termales, cuyas energías locales son del orden de 1–100 eV, y llevarlas a energías superiores a los 10^{10} eV. Los mecanismos aceleradores fueron originalmente estudiados en el contexto de los rayos cósmicos galácticos, en la década de los treinta, cuando la física de aceleradores daba sus primeros pasos, lo que condujo a otro ejemplo más de la interdependencia entre la física de laboratorio y la física del espacio (Pérez-Peraza, 1990).

En virtud de que la generación de ***Partículas Solares Energéticas (ESP por sus siglas en inglés)*** es un fenómeno que se puede seguir prácticamente en tiempo real, en contraste con los rayos cósmicos galácticos cuya vida media es de millones de años, el estudio de los procesos de aceleración se polarizó hacia la atmósfera solar. **Dentro de esta categoría (ESP) se producen esporádicamente partículas solares que alcanzan energías relativistas (> 450 MeV) capaces de atravesar la magnetosfera terrestre, las cuales se detectan a nivel terrestre. Los eventos relativos a estas partículas relativistas se les denomina incrementos al nivel del suelo (Ground Level Enhancements, GLEs)** (Pérez-Peraza, et al., 1994).

Los agentes aceleradores de las partículas cargadas son en última instancia los campos eléctricos, cuya naturaleza en la atmósfera solar son del tipo **estocástico**, cuando la turbulencia es relativamente débil, y **seculares (determinísticos)** en situaciones en las que la turbulencia es muy intensa. Las propiedades fundamentales de las partículas aceleradas son su **perfil-temporal**, su **espectro de carga** y su **espectro de energía**. El primero nos proporciona información sobre el proceso de transporte y las estructuras magnéticas a través de las cuales se propagan, en tanto que el espectro de carga nos indica las abundancias relativas de los iones solares y la evolución de su estado de carga. El espectro de energía nos da información sobre el proceso mismo de su generación en las fuentes aceleradoras y modulación fuera de ellas. ***Es decir, el espectro de energía es una firma del proceso acelerador, precisamente este aspecto crucial es el tema principal que se aborda en este trabajo de tesis Doctoral, tanto para aceleración estocástica como para aceleración determinística.*** (Pérez-Peraza et al., 1994).

A partir del conteo del incremento de partículas detectado por la red global de monitores de neutrones (www.nmdb.eu) se obtienen los espectros de energía observacionales para cada GLE, en este trabajo desarrollamos el marco matemático para generar los espectros de energía teóricos, los cuales ajustándolos a los observacionales nos dan por resultado los parámetros necesarios para reconstruir los diferentes escenarios posibles en la fuente, dígame en la fulguración solar. En el primer trabajo: ***“Exploration of Solar Cosmic Ray Sources by Means of Particle Energy Spectra”***, se abordan los estudios iniciales en el tema donde no se considera la dependencia del tiempo, y en el segundo trabajo: ***“Source Energy Spectrum of the 17 May 2012 GLE”***, así como en el tercer trabajo: ***“Spectra of the Two Official***

GLEs of Solar Cycle 24", ya se consideran los espectros de energía dependientes del tiempo y estacionarios, resolviéndose la ecuación de transporte de energía para todo el rango de energías (Pérez-Peraza & Gallegos-Cruz, 1994; Gallegos-Cruz & Pérez-Peraza, 1995) por medio del método de aproximación WKB de forma analítica. Esta solución analítica es de suma relevancia debido al escenario que prevalecía hasta inicios de los años noventa, ya que los primeros enfoques para resolver analíticamente este tipo de ecuación se relacionaron con soluciones en rangos de energía limitados: en el rango ultrarrelativista Kaplan (1956), Ginzburg (1958), Kardashev (1962), Ginzburg y Syrovatskii (1964), Tverskoi (1967), Ramaty (1979), y Melrose (1980); en el rango no relativista de Tverskoi (1967), Ramaty (1979), y Barbosa (1979). Schlickeiser (1984), Droge & Schlickeiser (1986), y Steinacker & Schlickeiser (1989) obtuvieron soluciones analíticas solo para el estado estacionario sobre todo el rango de energías. Mullan (1980) y Miller et al., (1987), obtuvieron soluciones numéricas dependientes del tiempo solo en intervalos no relativistas y por último Miller, Guessoum, & Ramaty (1990) obtuvieron soluciones en todo el rango de energías, pero también de forma numérica. Es relevante subrayar que en los trabajos previamente citados se resolvió por primera vez el problema dependiente del tiempo para todo el rango de energías de manera analítica considerando la deceleración por pérdidas adiabáticas, cabe mencionar que en el presente trabajo ya se incluye el tratamiento matemático de la deceleración por pérdidas colisionales. En las subsiguientes secciones: Marco Teórico y Resultados, se presenta el tratamiento de la **deceleración debida a pérdidas colisionales y a la degradación energética por colisiones Protón-Protón**, siendo lo anterior el objetivo original del presente trabajo.

Es importante mencionar que el equipo australiano de Bombardieri et al., 2006 y 2008, demostró que para los eventos del 14 de julio del 2000 y del 20 de enero del 2005, donde se usó la formulación dada en Pérez-Peraza & Gallegos-Cruz, 1994 y Gallegos-Cruz & Pérez-Peraza, 1995, el espectro observacional es mejor reproducido por la aceleración estocástica, en lugar de una aceleración de choque.

Inicialmente en la presente tesis solo se había planteado el **estudio de la aceleración estocástica y determinística de las partículas solares relativistas** que llegan a la tierra y provocan los incrementos a nivel del suelo que son detectados por la red global de estaciones de Monitores de Neutrones (MN), sin embargo, el trabajo se extendió al análisis de otros aspectos importantes de los GLEs, como lo es su **ocurrencia, periodicidad y prognosis**. Se suele suponer que estos eventos esporádicos ocurren al azar. Sin embargo, en el cuarto trabajo: **"The Quasi-Biennial Oscillation of 1.7 years in Ground Level Enhancement Events"**, encontramos que al estudiar los últimos 56 eventos de incrementos a nivel del suelo registrados de 1966 hasta 2014, aplicando el Análisis de Coherencia Wavelet a los datos de GLEs, de Rayos Cósmicos Galácticos proporcionados por la red global de estaciones de MN así como de la serie de tiempo no estacionaria propia de la actividad solar: Solar Flare Index (FSI por sus siglas en inglés), se obtuvo que estos eventos ocurren preferentemente en la fase positiva de la oscilación cuasi-bienal de la periodicidad de 1.7 años. Siendo las periodicidades correspondientes los armónicos en tiempo encontrados en la serie de tiempo bajo estudio. También se observa en este trabajo en gran medida, que su tasa de ocurrencia sigue el ciclo de actividad solar de Schwabe de 11 años, íntimamente relacionado con el fenómeno de las manchas solares. En Pérez-Peraza et al., 2011, 2015 ya se había evidenciado el comportamiento armónico de los GLEs. Siguiendo en la misma línea de análisis, en el

quinto trabajo: ***“Determination of GLE of Solar Energetic Particles by Means of Spectral Analysis”***, utilizando las tres series de tiempo propias de la actividad solar no estacionarias: Solar Flare Index (FSI), Sunspots Index (SS) y Solar Flux Index (F10.7), volvemos a aplicar el Análisis de Coherencia Wavelet de Morlet para determinar los armónicos dominantes de la actividad solar, de los cuales la combinación de las periodicidades de 1.73, 3.27, 4.9, 10.4 y 11 años.

Posteriormente usamos algunos conceptos de Lógica Difusa descritos por Mendel (1995). La teoría de conjuntos difusos y de lógica difusa establecen los aspectos específicos del mapeo no lineal. En general, un sistema de lógica difusa (FLS por sus siglas en inglés) es un mapeo no lineal de un conjunto de datos de entrada (característicos) en una salida escalar (Función de Pertenencia, FP), y puede expresarse matemáticamente como una combinación lineal de funciones de base difusa, en nuestro caso se mapea el comportamiento armónico de las series de tiempo involucradas en momentos de interés dados por las fechas de ocurrencia de los GLE, desde 1942 a 2006, tomadas como fechas de entrenamiento, a partir de lo cual se genera una FP que puede reproducir el comportamiento periódico de la información ingresada (zona de entrenamiento), de tal forma que proyectando dicha FP a tiempos posteriores podemos generar zonas de prognosis, en nuestro caso para cubrir el final del Ciclo Solar 24 y el inicio del Ciclo Solar 25. Todo lo anterior le da un aspecto previsorio al trabajo; esto es de sumo interés en vista de la gran controversia despertada en relación con la aparición de GLEs muy débiles durante el presente Ciclo Solar 24.

La gran controversia mencionada en el párrafo anterior es tratada en el sexto y último trabajo: ***“An Alternative Classification of Solar Particle Events that Reach the Earth Ground Level”***. Se realizó una revisión exhaustiva en la literatura existente sobre el tema, en donde se encontró una gran discrepancia en la asignación de los GLEs como tales y en su denominación, al grado de definirse un nuevo tipo de evento denominado Sub-GLE. Se revisaron minuciosamente los incrementos a nivel terrestres dados en la red global de estaciones de MN para cada evento mencionado en la literatura, considerando la variabilidad diurna, es importante considerar la posibilidad de que algunos incrementos débiles hayan llegado a nivel terrestre, pero fuesen enmascarados por dicho fenómeno. Se aplicaron los últimos criterios aceptados por la comunidad internacional para definir un GLE y/o lo que es un Sub-GLE (Poluianov et al., 2017). De los 15 eventos encontrados originalmente, llegamos a la conclusión de que solo 4 cumplen los criterios de un GLE y ninguno con el criterio de Sub-GLE. De igual manera propusimos una nomenclatura basada en la fecha del evento y no en la numeración consecutiva de tales eventos. Esta también es una aportación importante al estudio del tema la cual esperamos sea tomada en cuenta por la comunidad internacional encargada del estudio de los GLEs.

Objetivos generales del trabajo.

Dentro de las Ciencias Espaciales existen diferentes áreas: Física Solar, Física de Plasmas, Física de Relaciones Sol-Tierra, Física de la Magnetosfera, Física del medio interplanetario etc.; en nuestro caso, en particular, corresponde al área de la Percepción Remota Espacial aplicada al estudio de partículas solares de altas energías como única herramienta para realizar nuestro trabajo.

El método de sondeo para diagnósticos de plasmas, particularmente de fuentes aceleradoras de rayos cósmicos en base a las propiedades de los flujos de partículas, es absolutamente original, pues hasta ahora todo método de sondeo indirecto está basado en la radiación electromagnética que se emite en todo el rango de frecuencias por la interacción de partículas supraterrales con la materia y los campos electromagnéticos, mas ningún método está basado en el estudio de las propias partículas como mecanismo de sondeo y diagnóstico (Pérez-Peraza, et al., 1994).

En este trabajo proponemos como objetivo principal una nueva alternativa de diagnóstico, mediante el sondeo de los plasmas, no por su radiación fotónica intrínseca, sino en base a la materia misma del universo, es decir partículas del plasma local en las diferentes estancias del universo, que son aceleradas a muy altas energías, conocidas como Rayos Cósmicos Galácticos, y por otro lado las Partículas Solares Energéticas (ESP por sus siglas en inglés).

En el sondeo de las características en la fuente de los eventos GLEs, en Pérez-Peraza et al., 2008, 2009; Vashenyuk, et al., 1994, se puso en evidencia que en general se muestran dos componentes, una componente retardada y otra componente pronta. Cada componente con un espectro de energía diferente, uno estocástico y el otro determinístico.

Se ha publicado una gran cantidad de trabajos en relación con las características observacionales obtenidas con diferentes instrumentos. En este sentido otro de los objetivos del trabajo es analizar los fenómenos de origen, en relación con los procesos de generación y los parámetros físicos de origen, mediante la confrontación de los diferentes enfoques de los espectros observacionales con nuestros espectros teóricos analíticos basados en la aceleración estocástica y la aceleración determinística del campo eléctrico desde los procesos de reconexión. De esta manera, en los primeros tres trabajos: *“Exploration of Solar Cosmic Ray Sources by Means of Particle Energy Spectra”*, *“Source Energy Spectrum of the 17 May 2012 GLE”* y *“Spectra of the Two Official GLEs of Solar Cycle 24”*, derivamos un conjunto de parámetros que caracterizan las fuentes de las dos componentes mencionadas para cada GLE estudiado, lo que nos lleva a proponer posibles escenarios de generación de partículas en la fuente para el evento en cuestión.

Como mencionamos anteriormente, el objetivo principal de los trabajos 4 y 5 es dejar en claro la naturaleza armónica en la ocurrencia de los eventos GLEs, así como definir técnicas robustas de pronóstico de dichos eventos.

El presente Ciclo Solar 24 ha sido peculiar, arrojando un gran número de eventos débiles, provocando controversia en la comunidad internacional para catalogarlos como GLEs, definiéndose nuevos criterios para tal efecto, así como un nuevo tipo de evento denominado Sub-GLE, en este sentido el objetivo principal del último trabajo es definir con toda claridad cuáles de los eventos mencionados en la literatura cumplen dichos criterios y proponer una nueva nomenclatura basada en la fecha de ocurrencia del evento y en un número consecutivo para tal.

Marco Teórico

Por medio de la teoría cuasi-lineal, e introduciendo los efectos del transporte espacial a un determinado tiempo (Schlickeiser 1989), se obtiene una ecuación de difusión en el espacio de momentos a partir de la ecuación de Vlasov (ecuación de Boltzmann sin colisiones). Esto también se puede derivar de la ecuación de Chapman-Kolmogorov (e.g., Schatzman 1966).

$$\frac{\partial f(p,t)}{\partial t} = \frac{1}{p^2} \frac{\partial}{\partial p} \left[p^2 D(p) \frac{\partial f(p,t)}{\partial p} \right] \quad (1)$$

Aquí $f(p, t)$ es el ángulo de paso de la densidad promedio de las partículas de momento p que interactúan con la turbulencia en el tiempo t , y $D(p)$ es el coeficiente de difusión que caracteriza la dinámica de interacción entre las partículas y el tipo específico de turbulencia, que se supone homogéneo e independiente del tiempo (Tsytovich, 1977). Además, se puede encontrar una solución alternativa para esta ecuación de difusión por su transformación en una ecuación de tipo Fokker-Planck en el espacio de energía de las partículas (Ginzburg & Syrovatskii 1964):

$$\frac{\partial N(E,t)}{\partial t} = \frac{1}{2} \frac{\partial^2}{\partial E^2} [D(E)N(E, t)] - \frac{\partial}{\partial E} [B(E)N(E, t)] \quad (2)$$

donde E es la energía cinética de las partículas, y $N(E, t)$ es el número de partículas por intervalo de energía en el tiempo t ; $D(E)$ es la tasa de cambio de energía difusiva producida por la dispersión en la ganancia de energía en torno al valor de la tasa sistemática de ganancia de energía, dada por $B(E)$. El efecto de las pérdidas de energía sistemáticas o cualquier otro efecto de aceleración sistemática se puede introducir en el segundo término de la derecha de la ecuación anterior al establecer $A(E) = B(E) \pm$ *Procesos de cambio de energía sistemáticos adicionales* (Ginzburg, 1958). Además, se agrega un término fuente $Q(E, t)$, (que indica la inyección de partículas externas en la región de aceleración) y un término de sumidero, que se supone describe cualquier tipo de proceso de desaparición de partículas del volumen de aceleración en el tiempo característico de desaparición (o de escape) $\tau(E, t)$. Empleando estos argumentos, la ecuación anterior generalmente se reescribe como:

$$\frac{\partial N(E,t)}{\partial t} = \frac{1}{2} \frac{\partial^2}{\partial E^2} [D(E)N(E, t)] - \frac{\partial}{\partial E} [A(E)N(E, t)] - \frac{N(E,t)}{\tau(E,t)} + Q(E, t) \quad (3)$$

Aquí $A(E)$ es el efecto sistemático de los procesos de aceleración y desaceleración estocásticos como cualquier efecto secular eventual de cambio de energía. Y $D(E)$ son los efectos difusivos debido a la dispersión alrededor de la tasa de cambio de energía sistemática $A(E)$; $D(E)$ se discutió en Pérez-Peraza

& Gallegos-Cruz, 1994. En este sentido ya mencionamos que los primeros enfoques para resolver analíticamente este tipo de ecuación se relacionaron con soluciones en rangos de energía limitados: en el rango ultrarrelativista Kaplan (1956), Ginzburg (1958), Kardashev (1962), Ginzburg y Syrovatskii (1964), Tverskoi (1967), Ramaty (1979), y Melrose (1980); en el rango no relativista de Tverskoi (1967), Ramaty (1979), y Barbosa (1979). Schlickeiser (1984), Droge y Schlickeiser (1986), y Steinacker & Schlickeiser (1989) obtuvieron soluciones analíticas solo para el estado estacionario sobre todo el rango de energías. Mullan (1980) y Miller et al., (1987), obtuvieron soluciones numéricas dependientes del tiempo solo en intervalos no relativistas y por último Miller et al., (1990), obtuvieron soluciones en todo el rango de energías, pero también de forma numérica.

Entre las simplificaciones habituales para resolver la ecuación se encuentran considerar la independencia con respecto al tiempo y la energía de los procesos de inyección, el tiempo de escape así como para la eficiencia de aceleración, debido a que cada evento tiene diferente comportamiento, difieren por ejemplo debido a las condiciones locales de evento a evento, igual que los campos magnéticos y eléctricos debido a las diversas topologías que puede tomar la lámina magnética de corriente neutra (MNCS por sus siglas en ingles), Pérez-Peraza et al., 1977 y 1978, en la estructura propia de cada fulguración, por lo que estos parámetros (eficiencia de aceleración, tiempo de escape, intensidad del campo magnético, densidad del plasma y longitud de la MNCS) se toman como parámetros libres, y en base a ellos se realizan los ajustes teóricos contra los espectros observacionales de energía.

Consideramos, de igual manera, para simplificar, el supuesto general de que el flujo $N(E, t)$ se está inyectando a una velocidad $Q(E) = q(E)\Theta(t) \approx q(E)$ [donde $\Theta(t)$ es la función escalón] a una velocidad de escape τ^{-1} (Gallegos-Cruz & Pérez-Peraza, 1995).

Los espectros teóricos desarrollados en la presente tesis son:

1. Espectro de energía dependiente del tiempo con turbulencia MHD, inyección monoenergética y deceleración adiabática.

El espectro dependiente del tiempo para la turbulencia de MHD, con inyección monoenergética, $\tau = cte.$ y $D(p) \approx p^2/\beta$ se ha dado en la Ecuación 41 en Gallegos-Cruz & Pérez-Peraza (1995), Ec. 3 en Pérez-Peraza et al., (2009): esta formulación con la incorporación de pérdidas de energía adiabática se empleó en Pérez-Peraza et al., 2018:

$$N(E, t) \cong \frac{(\beta_0/\beta)^{1/4}(\varepsilon/\varepsilon_0)^{1/2}(\beta_0^{3/2}\varepsilon_0)^{-1}}{(4\pi\alpha/3)^{1/2}} \left[\left(\frac{N_0}{t^{1/2}} \right) \exp \left(-a_f t - \frac{3J_f^2}{4\alpha t} \right) + \left(\frac{q_0}{2} \right) \left(\frac{\pi}{a_f} \right)^{\frac{1}{2}} R_5(\varepsilon_0, \varepsilon) \right] [F_{ad}(\rho_0, \varepsilon)/4\pi R_{SE}^2] \text{ protones}/(MeV s cm^2 str) \quad (4)$$

donde $\left(\frac{dE}{dt} \right)_{acc} = 4\alpha\beta\varepsilon/3 (MeV/s)$ = la razón de aceleración estocástica;

$$y \quad \left(\frac{dE}{dt}\right)_{ad} = -\rho_0 \beta^2 \varepsilon \text{ (MeV/s)} = \text{la razón de deceleración adiabática,}$$

con α (s^{-1}) la eficiencia de aceleración y $\rho_0 = (2/3)(V_r/R)$ (s^{-1}) es la eficiencia de desaceleración debida al enfriamiento adiabático. Además, V_r y R son la velocidad de expansión y la extensión lineal de la estructura magnética en expansión, respectivamente; $N_0 = \text{protones}$; $q_0 = \text{protones}$ y $R_{SE} = 1.5 \times 10^{13} \text{ cm} = \text{distancia sol-tierra}$

$$R_5(\varepsilon_0, \varepsilon) = [\text{erf}(Z_1) - 1] \exp[(3a_f/2\alpha)J_f^2] + [\text{erf}(Z_2) + 1] \exp[-(3a_f/2\alpha)J_f^2];$$

$$Z_{1,2} = (a_f t)^{1/2} \pm (3a_f/4\alpha t)^{1/2} J_f; \quad a_f = \left(\frac{\alpha}{3}\right) \left(\bar{F} + \frac{3}{\alpha\tau} - 3\rho(4 - \beta^2 - \beta_0^2)/2\alpha\right);$$

$$\bar{F} = 0.5[\beta^{-1} + 3\beta - 2\beta^3 + \beta_0^{-1} + 3\beta_0 - 2\beta_0^3];$$

$$\beta = (\varepsilon^2 - m^2 c^4)^{1/2} / \varepsilon; \quad \beta_0 = (\varepsilon_0^2 - m^2 c^4)^{1/2} / \varepsilon_0$$

$$J_f = \tan^{-1} \beta^{1/2} - \tan^{-1} \beta_0^{1/2} + 0.5 \ln \left[\frac{(1 + \beta^{1/2})(1 - \beta_0^{1/2})}{(1 - \beta^{1/2})(1 + \beta_0^{1/2})} \right];$$

$$F_{ad}(\rho_0, \varepsilon) = \left[\frac{\varepsilon_0(1 + \beta_0)}{\varepsilon(1 + \beta)} \right]^{3\rho_0/2\alpha} \text{ con } \varepsilon_0 \text{ (MeV) la inyección de energía.}$$

(Nótese que la Ec. 4 es la que aparece graficada en las figuras 2, 3, 4, 5 y 7 del artículo "Source Energy Spectrum of the 17 May 2012 GLE")

2. Espectro de energía en estado estacionario con turbulencia MHD, inyección monoenergética y deceleración adiabática para $\tau = cte.$

El Espectro de estado-estacionario para turbulencia MHD, inyección monoenergética, $\tau = cte.$, y $D(p) \approx p^2/\beta$, se ha dado en la Ec. 42 en Gallegos-Cruz & Pérez-Peraza (1995): esta formulación también se desarrolló con la inclusión de pérdidas de energía adiabáticas:

$$N(E) \approx (q_0/2)(a_f \alpha/3)^{-1/2} (\beta_0^{3/2} \varepsilon_0)^{-1} (\beta_0/\beta)^{1/4} (\varepsilon/\varepsilon_0)^{1/2} \exp \left[-(3a_f/\alpha)^{1/2} J_f \right] [F_{ad}(\rho_0, \varepsilon)/4\pi R_{SE}^2] \\ \text{protones/(MeV cm}^2 \text{ str)} \quad (5)$$

donde: $\alpha, \rho_0, a_f, \bar{F}, J_f, \beta, \beta_0, \varepsilon_0, F(\rho_0)$ y R_{SE} son las mismas que en la Ecuación (4).

(Nótese que la Ec. 5 es la que aparece graficada en la figura 7 del artículo "Source Energy Spectrum of the 17 May 2012 GLE")

3. Espectro de energía en estado estacionario con turbulencia MHD, inyección monoenergética y deceleración adiabática para $\tau \approx 1/\beta.$

El espectro de estado estacionario para turbulencia MHD, inyección monoenergética, $\tau \approx 1/\beta$, y $D(p)$

$\approx p^2/\beta$, se ha dado en la Ecuación 43 en Gallegos-Cruz & Pérez-Peraza (1995): esta formulación con la incorporación de pérdidas de energía adiabática se empleó en Pérez-Peraza et al., (2018):

$$N(E) = \frac{(q_0/2)(\beta_0/\beta)^{\frac{1}{4}}(\varepsilon/\varepsilon_0)^{\frac{1}{2}}}{(4\pi R_{SE}^2)(\alpha/3)^{\frac{1}{2}}a^{\frac{1}{4}}(E)a^{\frac{1}{4}}(E_0)\beta_0^{\frac{3}{2}}\varepsilon_0} \left[\frac{\varepsilon + \beta\varepsilon}{\varepsilon_0 + \beta_0\varepsilon_0} \right]^{-\left(b+\frac{1}{2b}\right)} \exp \left[\left(\frac{-1}{2b} \right) (\beta^{-1} - \beta_0^{-1}) \right] [F_{ad}(\rho_0, \varepsilon)/4\pi R_{SE}^2] \quad (6)$$

protones/ (MeV cm² str)

donde $\alpha, \rho_0, a_f, \bar{F}, J_f, \beta, \beta_0, \varepsilon_0, F(\rho_0)$ y R_{SE} son las mismas que en la Ec. (4).

(Nótese que la Ec. 6 es la que aparece graficada en las figuras 4 y 7 del artículo “Source Energy Spectrum of the 17 May 2012 GLE”)

4. Espectro de energía en estado estacionario por un campo eléctrico directo en una hoja de corriente magnética neutra (MNCS).

El espectro de estado estacionario por un campo eléctrico directo en una hoja de corriente magnética neutra (MNCS), se ha dado en Pérez-Peraza et al., (1978) y la Ecuación 1 en Pérez-Peraza et al. (2009):

$$N(E) = N_0 (E/E_c)^{-1/4} \exp[-1.12(E/E_c)^{3/4}] \quad \text{protones/ (MeV cm}^2 \text{ str)} \quad (7)$$

con $N_0 = 8.25 \times 10^5 \left(\frac{nL^2}{B} \right) \left(\frac{1}{E_c} \right) / 4\pi R_{SE}^2$ protones/(MeV cm² str), asumiendo una conductividad anómala; $E_c = 1.792 \times 10^3 \left(\frac{B^2 L}{n} \right) \text{ MeV}$, B = intensidad del campo magnético (gauss), L = longitud de la MNCS (cm); y n = densidad del plasma (cm⁻³).

(Nótese que la Ec. 7 es la que aparece graficada en las figuras 1 y 6 del artículo “Source Energy Spectrum of the 17 May 2012 GLE”)

5. Espectro de energía dependiente del tiempo para turbulencia MHD con inyección monoenergética, deceleración adiabática y deceleración por pérdidas colisionales.

El espectro dependiente del tiempo para la turbulencia de MHD, con inyección monoenergética, $\tau = cte.$ y $D(p) \approx p^2/\beta$ se ha dado en la Ecuación 41 en Gallegos-Cruz & Pérez-Peraza (1995), Ec. 3 en Pérez-Peraza et al., (2009), esta formulación con la incorporación de pérdidas de energía adiabática se empleó en Pérez-Peraza et al., 2018. En este paso agregamos la **deceleración por pérdidas colisionales**:

$$N(E, t) \cong \frac{(\beta_0/\beta)^{1/4}(\varepsilon/\varepsilon_0)^{1/2}(\beta_0^{3/2}\varepsilon_0)^{-1}}{(4\pi\alpha/3)^{1/2}} \left[\left(\frac{N_0}{t^{1/2}} \right) \exp \left(-a'_f t - \frac{3J_f^2}{4at} \right) + \right.$$

$$\left(\frac{q_0}{2}\right) \left(\frac{\pi}{a'_f}\right)^{\frac{1}{2}} R'_5(\varepsilon_0, \varepsilon) \left[F_{ad}(\rho_0, \varepsilon) F_{col} / 4\pi R_{SE}^2 \right] \quad \text{Protones}/(\text{MeV s cm}^2 \text{ str}) \quad (8)$$

dónde:

$$R'_5(\varepsilon_0, \varepsilon) = [\text{erf}(Z_{f1}) - 1] \exp[(3a'_f/2\alpha)J_f^2] + [\text{erf}(Z_{f2}) + 1] \exp[-(3a'_f/2\alpha)J_f^2];$$

$$Z_{f1,f2} = (a'_f t)^{1/2} \pm (3a'_f/4\alpha t)^{1/2} J_f;$$

y $\alpha, \rho_0, \bar{F}, J_f, \beta, \beta_0, \varepsilon_0$ y R_{SE} son las mismas que en la Ec. (4)

Para los términos a'_f y F_{col} considerando pérdidas de energía por colisión se tienen dos casos:

5.1.- El primero es cuando solo se consideran las perdidas colisionales a altas energías arriba de la velocidad de Bohr (las llamadas antiguamente perdidas por ionización del plasma) y que convencionalmente se expresa de la forma siguiente (Ginsburg & Sirovatski, 1964), en donde la tasa de pérdidas por colisión, en un medio de densidad n , es:

$$\left(\frac{dE}{dt}\right)_{ion} = - \frac{7.62 \times 10^{-9} n L}{\beta} \quad (\text{eV/s}) \quad (9)$$

con $\beta = v/c$ la velocidad de la partícula en términos de la velocidad de la luz, L es un factor unidimensional y depende logarítmicamente de la energía de la partícula. Asumiremos un valor de $L \sim 27$ para las condiciones de una fulguración solar, cuando la concentración del medio es $n \sim 10^{12} - 10^{13} \text{ cm}^3$.

En estas condiciones los términos a'_f y F_{col} obtenidos son los siguientes:

$$a'_f = a_f - \frac{h}{2} \left[\frac{\beta^2 - 1}{\varepsilon \beta^3} - \frac{\beta_0^2 - 1}{\varepsilon_0 \beta_0^3} \right] \quad \text{y}$$

$$F_{col} = F_{col}(n, \varepsilon) = \left[\frac{\beta^2 \varepsilon^2 (\varepsilon_0 - mc^2)}{\beta_0^2 \varepsilon_0^2 (\varepsilon - mc^2)} \right]^{\frac{3h}{4\alpha mc^2}} \exp \left\{ \frac{3h}{4\alpha} \left(\frac{1}{\varepsilon \beta^2} - \frac{1}{\varepsilon_0 \beta_0^2} \right) \right\}$$

donde $h = 7.62 \times 10^{-9} n L$ y a_f es la mismas que en la Ec. (4), la cual incluye aceleración y pérdidas adiabáticas.

5.2.- El segundo caso es considerar la descripción completa de las pérdidas por colisión a lo largo de todo el rango de energía desde energías termaltes hasta ultrarrelativistas, incluidas las pérdidas en la parte de baja energía (el llamado frenado nuclear y frenado electrónico), Buttler & Buckingham (1962) y posteriormente optimizada (Perez-Peraza & R. Lara-A. 1979; Perez-Peraza, 1981) como:

$$\left(\frac{dE}{dt}\right)_{col} = A_{col} = -\frac{1.57 \times 10^{-35} n Q^2}{\beta} H(x) \ln \Lambda \quad (\text{eV/ns}) \quad (10)$$

dónde

$$x_e = 5.44 \times 10^4 \beta T^{-0.5}, x_p = 2.33 \times 10^6 \beta T^{-0.5}, H(x) = \xi_1 H_e(x_e) + \xi_2 H_p(x_p) \quad \text{con}$$

$$H_e(x_e) = 0.88 \text{erf}(x_e) - (1 - 5.48 \times 10^{-4}/A) x_e e^{-x_e^2} \quad \text{para electrones,}$$

$$H_p(x_p) = 0.88 \text{erf}(x_p) - (1 + \frac{1}{A}) x_p e^{-x_p^2} \quad \text{para protones,}$$

$$\xi_1 = 1.097803296 \times 10^{27}, \quad \xi_2 = 5.979073244 \times 10^{23},$$

$$n = \text{densidad del plasma (cm}^{-3}\text{)} \ \& \ \Lambda = [4.47 \times 10^{16} A (T/n)^{0.5} \beta^2] / Q$$

Para este caso los términos \mathbf{a}'_f y \mathbf{F}_{col} obtenidos son los siguientes:

$$a'_f = a_f - \frac{1}{2} \left(a_{fcol}(E) + a_{fcol}(E_0) \right) \quad \text{donde}$$

donde a_f es la misma que en la Ecuación 4 y

$$\begin{aligned} a_{fcol}(E) &= \frac{dA_{col}}{dE} = \\ &= \frac{k_1(\beta^2 - 1)}{\varepsilon \beta^3} \ln(k_2 \beta^2) [k_3 \text{erf}(k_4 \beta) - k_5 k_4 \beta e^{-k_4^2 \beta^2} + k_6 \text{erf}(k_7 \beta) - k_8 k_7 \beta e^{-k_7^2 \beta^2}] \\ &+ \frac{k_1 \ln(k_2 \beta^2)}{\beta} \left[\varepsilon^{-1} (\beta^{-1} - \beta) \left\{ e^{-k_4^2 \beta^2} \left[\frac{2k_3}{\sqrt{\pi}} - k_4 k_5 (1 - 2k_4^2 \beta) \right] \right. \right. \\ &+ \left. \left. e^{-k_7^2 \beta^2} \left[\frac{2k_6}{\sqrt{\pi}} - k_8 k_7 (1 - 2k_7^2 \beta) \right] \right\} \right] \\ &+ \frac{2k_1(\beta^2 - 1)}{\varepsilon \beta} [k_3 \text{erf}(k_4 \beta) - k_5 k_4 \beta e^{-k_4^2 \beta^2} + k_6 \text{erf}(k_7 \beta) - k_8 k_7 \beta e^{-k_7^2 \beta^2}] \end{aligned}$$

Y por último:

$$F_{col} = F_{col}(T, n, \varepsilon) = \exp \left\{ -\frac{1}{2} \int_{E_0}^E P_{1col}(\beta(E)) dE \right\}$$

donde

$$\begin{aligned} P_{1col}(\beta(E)) &= \frac{3k_1}{\alpha} \left\{ k_3 \int_{\beta_0}^{\beta} \frac{\ln(k_2 \beta) \text{erf}(k_4 \beta)}{\varepsilon \beta^3 (1 - \beta^2)} d\beta + k_4 k_5 \int_{\beta_0}^{\beta} \frac{\ln(k_2 \beta) \exp(-k_4^2 \beta)}{\varepsilon \beta^2 (1 - \beta^2)} d\beta \right. \\ &\left. - k_6 \int_{\beta_0}^{\beta} \frac{\ln(k_2 \beta) \text{erf}(k_7 \beta)}{\varepsilon \beta^3 (1 - \beta^2)} d\beta + k_7 k_8 \int_{\beta_0}^{\beta} \frac{\ln(k_2 \beta) \exp(-k_7^2 \beta)}{\varepsilon \beta^2 (1 - \beta^2)} d\beta - \right\} \end{aligned}$$

con:

$$k_1 = -1.57 \times 10^{-35} n Q^2 / A$$

$$k_2 = [4.47 \times 10^{16} A (T/n)^{0.5}] / Q$$

$$k_3 = 0.88 \xi_1$$

$$k_4 = 5.44 \times 10^4 T^{-0.5}$$

$$k_5 = \xi_1 (1 - 5.48 \times 10^{-4} / A)$$

$$k_6 = 0.88 \xi_2$$

$$k_7 = 2.33 \times 10^6 T^{-0.5}$$

$$k_8 = \xi_2 (1 + \frac{1}{A})$$

$Q = \text{carga atómica}$ y $A = \text{masa atómica}$

6. Espectro de energía dependiente del tiempo para turbulencia MHD con inyección monoenergética, deceleración adiabática, deceleración por pérdidas colisionales y deceleración por degradación energética por colisiones protón-protón.

En la actualidad, hay evidencias de la aparición de reacciones nucleares entre los núcleos solares y el material solar, que producen rayos gamma de alta energía, aunque no está absolutamente claro si las reacciones nucleares de las partículas energéticas solares y el material solar tienen lugar, cuando se inyectan protones en la fotosfera, o pasan a través de condensaciones coronales, o durante su aceleración dentro del material denso de las regiones de la fulguración. Asumiremos que las interacciones nucleares ocurren al menos en el volumen de aceleración, donde es muy probable que el movimiento de las partículas energéticas sea completamente aleatorio con respecto al material solar local. El movimiento isotrópico de las partículas aceleradas se sugiere mediante un análisis de los flujos de neutrones, Ifedili (1974). A los efectos de los cálculos de pérdida de energía, no tenemos en cuenta los protones de colisiones con otras especies nucleares, porque el cambio máximo de energía en la dispersión elástica se produce cuando las partículas en colisión tienen una masa similar. Aunque se cree que la disipación de energía de las colisiones p:p se debe principalmente a la dispersión elástica, sin embargo, a altas energías (> 750 MeV), la sección transversal inelástica se vuelve muy importante, Hess (1958), y aumenta hasta un máximo en algunos GeV, donde permanece prácticamente constante. De hecho, como la producción de piones se inicia a ~ 285 MeV y una fracción $\geq 35\%$ de la energía cinética del protón incidente se convierte en energía pión, entonces, la disipación de energía de la dispersión inelástica de p:p no es despreciable en un medio de alta densidad ($n \geq 10^{12} \text{ cm}^{-3}$). Con respecto a las interacciones inelásticas de p:p, la línea de rayos gamma a 2.2 MeV debido a la rápida producción de neutrones, parece ser una fuerte evidencia de la aparición de colisiones de p:p en las erupciones solares. Todo esto depende en gran medida del modelo de producción: la geometría supuesta y la forma espectral considerada, Bai & Ramaty (1976). De hecho, la sección transversal para las interacciones posteriores es 10-100 veces mayor, es decir, su umbral es ≤ 36 MeV/nucleón, mientras que para la dispersión inelástica de p:p es ~ 285 MeV. Sin embargo, se sabe desde hace mucho tiempo, Cameron

(1967), que las abundancias solares de *CNO* y *He* son del orden de $\sim 1.5-7\%$ con respecto al *H* local, de tal manera que este tipo de equilibrio entre las abundancias locales y las secciones transversales de interacción indican una alta probabilidad de que ocurran colisiones *p:p* en el propio cuerpo del material de la fulguración solar. El principal problema relacionado con estas características es que algunas reacciones rinden a altas energías, y otras por decaimiento producen rayos gamma solares de alta energía (50 MeV) que, según nuestro conocimiento, no han sido explicados satisfactoriamente, ni su posible absorción en el material solar. De hecho, el amplio pico predicho para estos rayos gamma que van desde $\sim 38.5-118$ MeV, Bland, (1966), probablemente podría dificultar su identificación debido a la presencia de fotones de alta energía esperados por la Bremsstrahlung de electrones solares de muy alta energía. Además, existe el hecho de que las reacciones *p:p* de alta energía deben ocurrir con mayor frecuencia, ya que la sección transversal inelástica aumenta progresivamente desde 290 MeV hasta un máximo de aproximadamente 1 GeV, donde permanece prácticamente constante. Chupp (1971) & Chupp et al., (1974), han revisado los problemas relacionados con los productos secundarios de las interacciones nucleares en las fulguraciones solares. Sin embargo, más adelante en este trabajo, mostramos que solo se esperan colisiones *p:p* en algunos GLE. Por lo tanto, aunque el flujo medido de partículas no distingue si los protones solares han sufrido colisiones nucleares o no, la modulación del espectro de energía por sus efectos proporciona información disponible sobre su ocurrencia. La importancia de la degradación de la energía de las colisiones *p:p* en la física de los rayos cósmicos se señaló por primera vez en Vernov et al., (1955). La tasa de pérdida de energía por interacciones nucleares está de acuerdo con Ginzburg (1969)

$$\frac{dE}{dt} = -\sigma cn\beta\varepsilon \text{ (eV/s)}$$

donde σ en colisiones *p:p* se compone de $\sigma_{p-p}^{ine} + \sigma_{p-p}^{el}$, como la sección transversal inelástica es débilmente dependiente de la energía, puede ser aproximada a su valor medio a altas energías ($\sigma_{p-p}^{ine} \sim 26$ mb). Con respecto a las colisiones elásticas, un ajuste razonable de los datos de la sección transversal diferencial viene dado por una expresión analítica, Ramudarai & Biswas (1974). Como la sección transversal diferencial es altamente isotrópica, podemos suponer simetría alrededor de 90° , de modo que su expresión se puede reescribir como $\sigma_{p-p}^{el} = hE^{-2} + jE^{-1}$ (si $E \leq 110$ MeV) y $\sigma_{p-p}^{el} = hE^{-2} + f$ (si $E > 110$ MeV), donde $h = 96.09$ mb-MeV², $j = 5.497 \times 10^3$ mb MeV y $f = 46.49$ mb. Tenemos entonces de la ecuación anterior:

$$\begin{aligned} \left(\frac{dE}{dt}\right)_{p-p} &= -cn(hE^2 + jE)\beta\varepsilon \text{ (Si } E \leq 110 \text{ MeV)} \\ \left(\frac{dE}{dt}\right)_{p-p} &= -cn(hE^2 + f)\beta\varepsilon \text{ (Si } 110 < E \leq 290 \text{ MeV)} \\ \left(\frac{dE}{dt}\right)_{p-p} &= -[\eta + cn(hE^2 + f)]\beta\varepsilon \text{ (Si } E \geq 290 \text{ MeV), donde } \eta = cn\sigma_{in} \end{aligned}$$

Para que el cambio energético neto pueda ser compactado como:

$$\left(\frac{dE}{dt}\right)_{p-p} = -(hE^2 + jE + f + \eta)\beta\varepsilon \text{ (eV/s)} \quad (11)$$

donde $h(n) = 2.88 \times 10^{-15} n \text{ MeV}^2 \text{ s}^{-1}$, $j(n) = 1.65 \times 10^{-13} n \text{ MeV s}^{-1}$ (si $E \leq 110 \text{ MeV}$), $j = 0$ y $f(n) = 1.39 \times 10^{-15} n \text{ s}^{-1}$ (si $E > 110 \text{ MeV}$), $f = 0$ (si $E \leq 110 \text{ MeV}$), $\eta(n) = 8.1 \times 10^{-16} n \text{ s}^{-1}$, (si $E > 290 \text{ MeV}$) y $\eta = 0$ (si $E < 290 \text{ MeV}$).

Dentro de las **Pérdidas Colisionales** también vamos a considerar este caso (colisiones coulombianas + colisiones proton-proton). En consecuencia, considerando la última ecuación del espectro de energía dependiente del tiempo para la turbulencia MHD, con inyección monoenergética, $\tau = cte$ y $D(p) \approx p^2/\beta$, considerando la deceleración por pérdidas adiabáticas, colisionales y las debidas a la **Degradación Energética por Colisiones Protón-Protón** toma la siguiente forma:

$$N(E, t) \cong \frac{(\beta_0/\beta)^{1/4}(\varepsilon/\varepsilon_0)^{1/2}(\beta_0^{3/2}\varepsilon_0)^{-1}}{(4\pi\alpha/3)^{1/2}} \left[\left(\frac{N_0}{t^{1/2}}\right) \exp\left(-a_f''t - \frac{3J_f^2}{4\alpha t}\right) + \left(\frac{q_0}{2}\right) \left(\frac{\pi}{a_f''}\right)^{\frac{1}{2}} R_5''(\varepsilon_0, \varepsilon) \right] [F_{ad}(\rho_0, \varepsilon)F_{col}(T, n, \varepsilon)F_{p-p}(n, \varepsilon)/4\pi R_{SE}^2] \text{ Protones}/(\text{MeV s cm}^2 \text{ str}) \quad (12)$$

dónde:

$$R_5''(\varepsilon_0, \varepsilon) = [\text{erf}(Z_{f1}) - 1] \exp[(3a_f''/2\alpha)J_f^2] + [\text{erf}(Z_{f2}) + 1] \exp[-(3a_f''/2\alpha)J_f^2];$$

$$Z_{f1, f2} = (a_f''t)^{1/2} \pm (3a_f''/4\alpha t)^{1/2}J_f;$$

y $\alpha, \rho_0, \bar{F}, J_f, \beta, \beta_0, \varepsilon_0$ y R_{SE} son las mismas que en la Ec. 4

Para los términos a_f'' y F_{p-p} considerando **Degradación Energética por Colisiones Protón-Protón** tenemos:

$$a_f'' = a_f' - \frac{1}{2} \left(a_{fp-p}(E) + a_{fp-p}(E_0) \right)$$

donde a_f' es la misma que la Ec. 8 y ya incluye pérdidas adiabáticas y colisionales, y

$$a_{fp-p}(E) = \frac{dA_{p-p}}{dE} = \frac{3hE^3 + (5hmc^2 + 2j)E^2 + (3jmc^2 + f + \eta)E + (f + \eta)mc^2}{\sqrt{E^2 + 2Emc^2}}$$

por último:

$F_{p-p}(\varepsilon(E), n)$

$$= \exp \left\{ \frac{-3}{2\alpha} \left[(j - 2hmc^2) \ln \left(\left| \sqrt{E(E + 2mc^2)} + E + mc^2 \right| \right) + \frac{f + \eta - (j - hmc^2)mc^2}{mc^2} \tan^{-1} \left(\frac{\sqrt{E(E + 2mc^2)}}{mc^2} \right) + h\sqrt{E(E + 2mc^2)} \right] \right\}_{E_0}^E$$

donde $h(n) = 2.88 \times 10^{-15} n \text{ MeV}^2 \text{ s}^{-1}$, $j(n) = 1.65 \times 10^{-13} n \text{ MeV s}^{-1}$ (si $E \leq 110 \text{ MeV}$), $j = 0$ y $f(n) = 1.39 \times 10^{-15} n \text{ s}^{-1}$ (si $E > 110 \text{ MeV}$), $f = 0$ (si $E \leq 110 \text{ MeV}$), $\eta(n) = 8.1 \times 10^{-16} n \text{ s}^{-1}$, (si $E > 290 \text{ MeV}$) y $\eta = 0$ (si $E < 290 \text{ MeV}$).

RESULTADOS.

En seguida ajustamos los espectros teóricos a los observacionales aplicando la Ec. 12 a los 12 eventos estudiados en Pérez-Peraza & Márquez-Adame, 2018.

La Figura 1 corresponde a los eventos calientes (28-Enero-1967 y 01-Septiembre-1971), podemos observar los parámetros de ajuste en la Tabla 1.

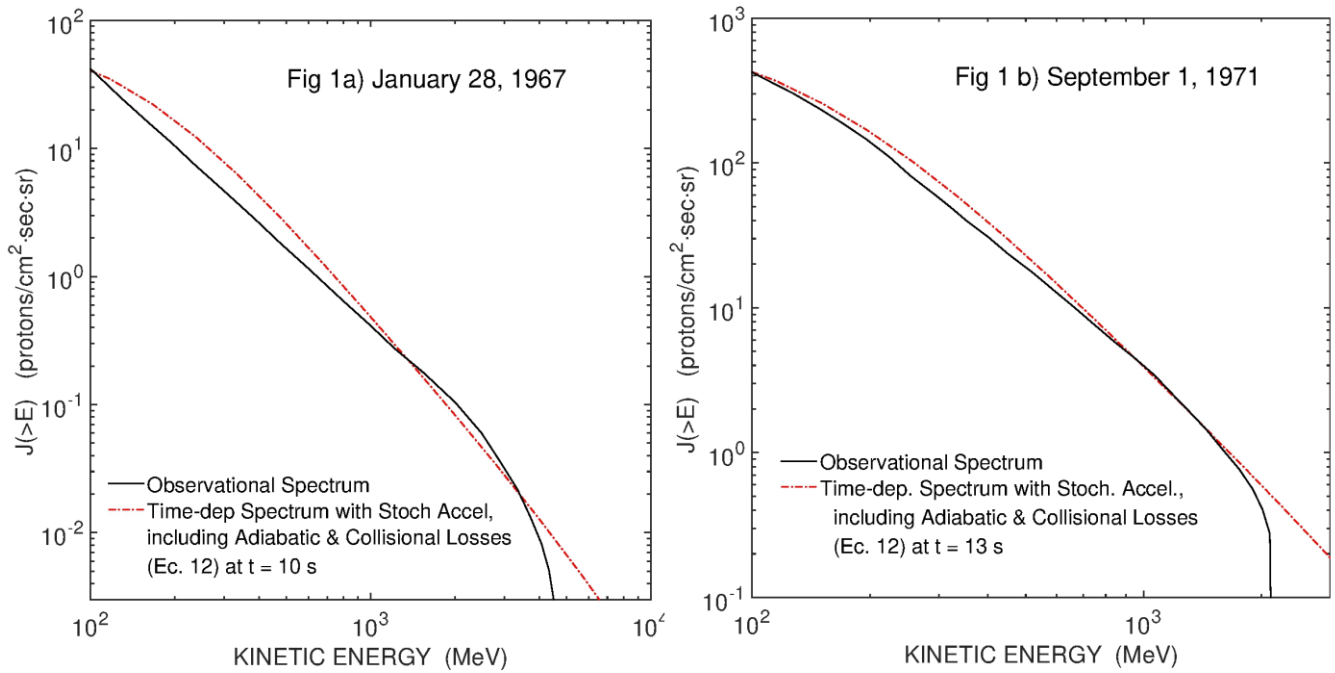


Figura 1. Espectros de energía observacionales y ajustes teóricos de eventos calientes.

GLE	alfa	rho	n	T	t	Tau	B	L
January 28, 1967	0.215	0.95	1.00E+12	1.00E+07	10	1	500	5.00E+07
September 1, 1971	0.23	0.83	5.00E+12	3.00E+07	13	1	570	3.00E+07

Tabla 1. Parámetros en la fuente de producción de partículas solares relativistas obtenidas a partir del ajuste entre los espectros de energía observacionales y los teóricos para eventos calientes.

En la Figura 2 se muestran los eventos fríos (12-Noviembre-1960, 04-Agosto-1972, 03-Septiembre-1960, 30-Marzo-1969 y 02-Noviembre-1969), y sus parámetros de ajuste se despliegan en la Tabla 2.

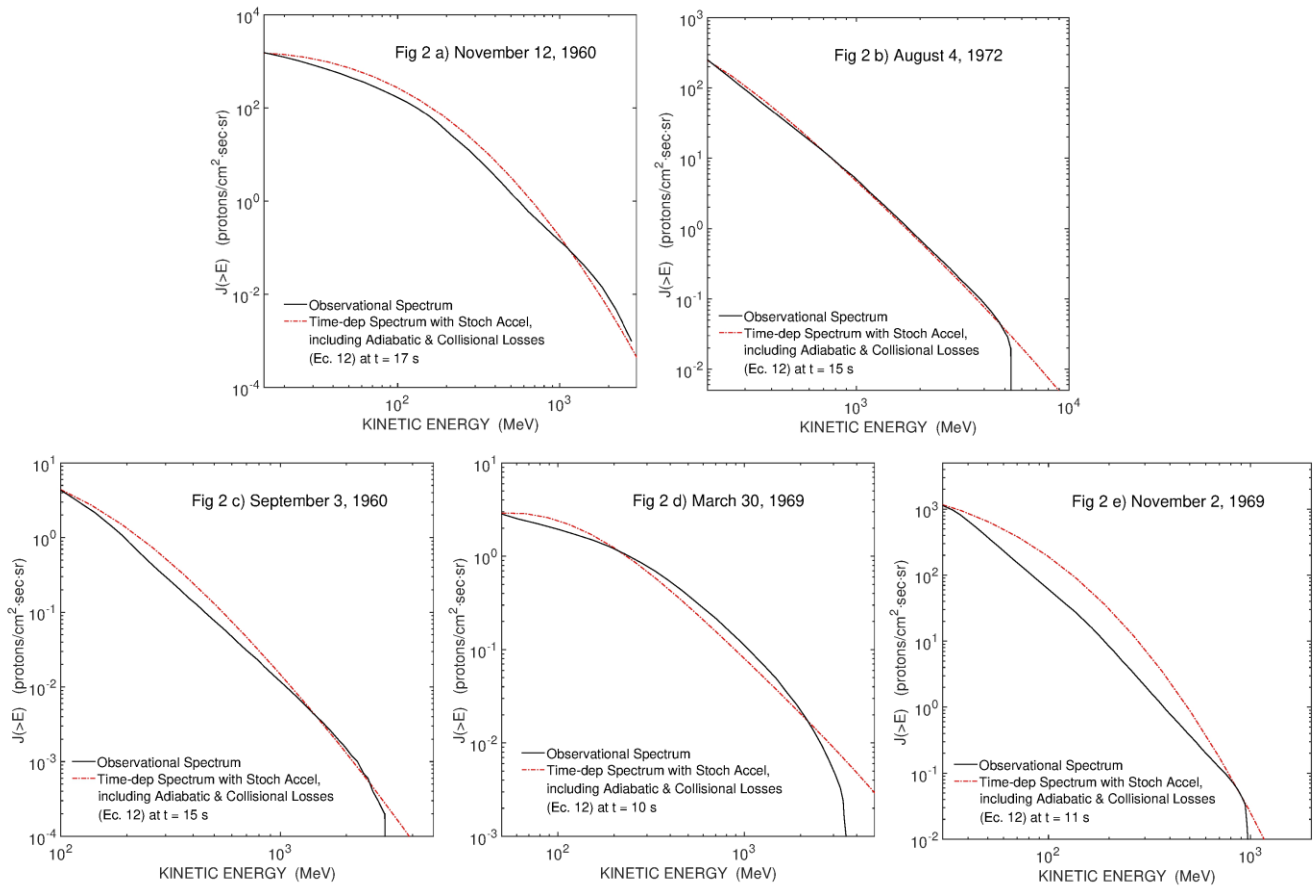


Figura 2. Espectros de energía observacionales y ajustes teóricos de eventos fríos.

GLE	alfa	rho	n	T	t	Tau	B	L	
November 12, 1960	0.14	0.48	7.00E+12	6.00E+04	10	10	1	550	3.00E+07
August 4, 1972	0.63	0.88	5.00E+12	9.00E+04	15	15	1	550	4.00E+07
September 3, 1960	0.8	0.75	1.00E+12	1.00E+05	15	15	1	510	6.00E+07
March 30, 1969	0.9	0.7	2.00E+12	1.00E+05	10	10	1	500	5.00E+07
November 2, 1969	1.17	0.5	7.00E+12	5.00E+04	11	11	1	545	4.00E+07

Tabla 2. Parámetros en la fuente de producción de partículas solares relativistas obtenidas a partir del ajuste entre los espectros de energía observacionales y los teóricos para eventos fríos.

Por último en la Figura 3 se muestran los eventos cálidos(15-Noviembre-1960, 18-Noviembre-1968, 07-Julio-1966, 24-Enero-1971 y 25-Febrero-1969), y sus parámetros de ajuste se despliegan en la Tabla 3.

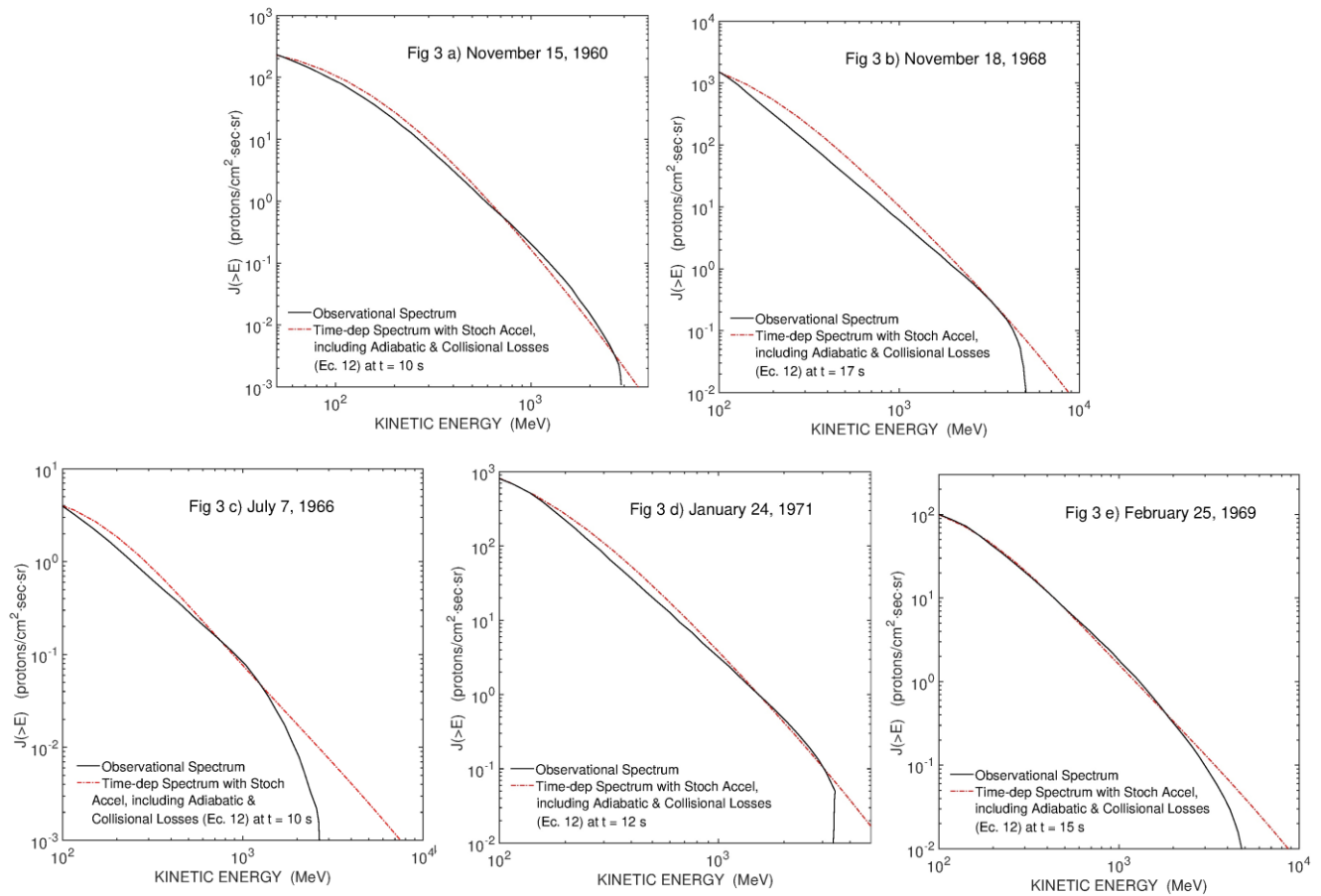


Figura 3. Espectros de energía observacionales y ajustes teóricos de eventos cálidos.

GLE	alfa	rho	n	T	t	Tau	B	L
November 15, 1960	0.2	0.9	1.00E+12	1.00E+06	10	1	530	5.00E+07
November 18, 1968	0.23	0.83	3.00E+12	8.00E+05	17	1	545	1.00E+07
July 7, 1966	0.3	0.99	1.00E+12	1.00E+06	10	1	530	5.00E+07
January 24, 1971	0.405	0.83	3.00E+12	7.00E+05	12	1	570	4.00E+07
February 25, 1969	0.45	0.95	2.00E+12	1.00E+05	15	1	515	6.00E+07

Tabla 3. Parámetros en la fuente de producción de partículas solares relativistas obtenidas a partir del ajuste entre los espectros de energía observacionales y los teóricos para eventos cálidos.

En este trabajo también se ajustaron teóricamente los espectros observacionales obtenidos por nuestro grupo de trabajo de los GLE71 y GLE72, dichos ajustes se muestran en la Figura 4, y los parámetros de ajuste se despliegan en la Tabla 4.

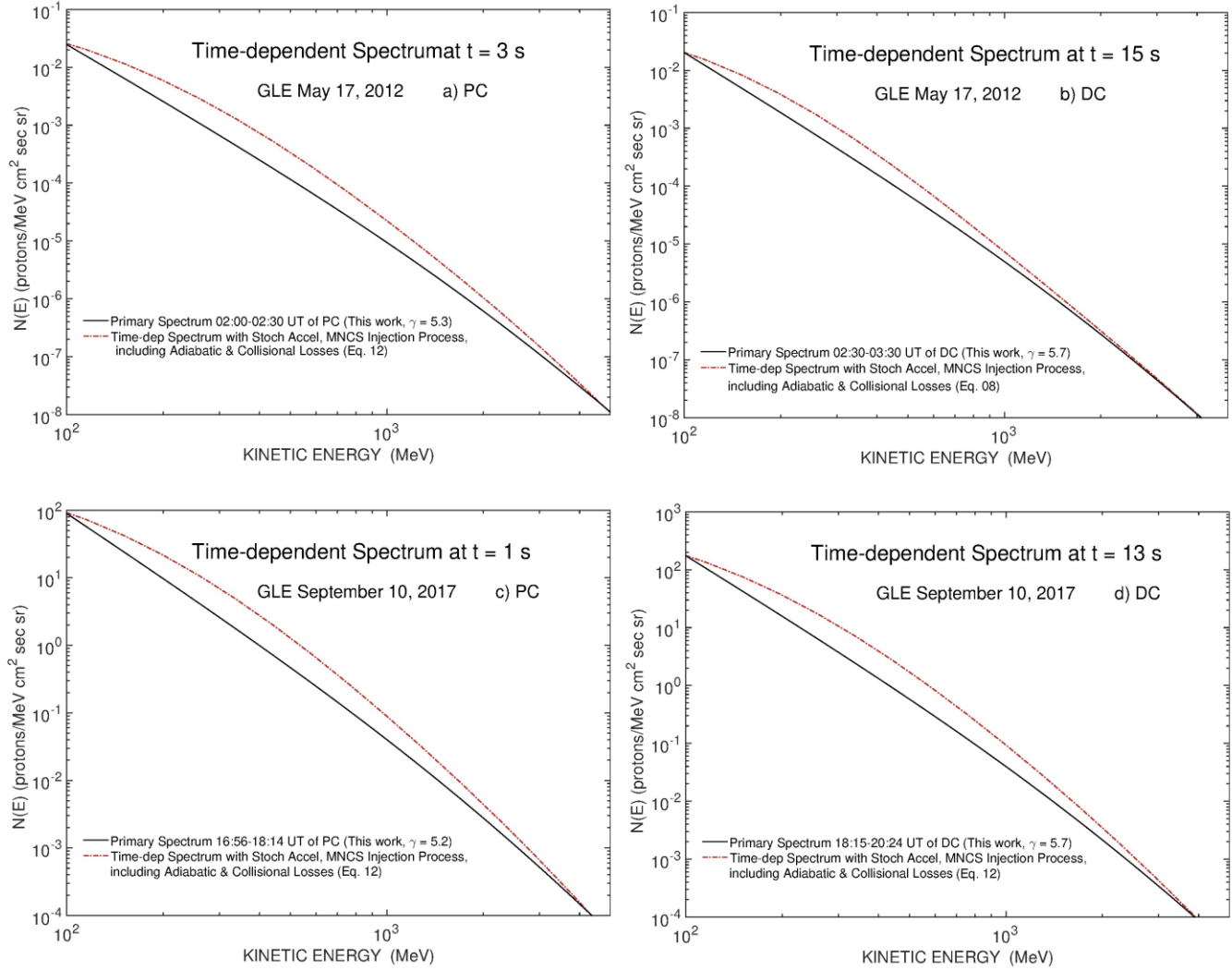


Figura 4. Espectros de energía observacionales y ajustes teóricos de los GLE 71 y 72

EVENTO	alfa (s^{-1})	rho (s^{-1})	n (cm^{-3})	T ($^{\circ}K$)	t (s)	Tau (s)	B (gauss)	L (cm)
GLE71-PC	0.3	0.83	3.00E+12	1.00E+07	3	1	530	3.00E+08
GLE71-DC	0.27	0.82	1.00E+12	1.00E+07	15	1	500	7.00E+08
GLE72-PC	0.3	0.83	5.00E+12	1.00E+07	1	1	550	1.00E+08
GLE72-DC	0.28	0.85	3.00E+12	1.00E+07	13	1	490	5.00E+08

Tabla 4. Parámetros en la fuente de producción de partículas solares relativistas obtenidas a partir del ajuste entre los espectros de energía observacionales y los teóricos para los eventos GLEs 71 y 72.

Enseguida continuamos con el material publicado y/o aceptado para publicación.

PRESENTACION DEL CAPITULO EN LIBRO:

Exploration of Solar Cosmic Ray Sources by Means of Particle Energy Spectra

A través del análisis del espectro de energía de 12 incrementos a nivel del suelo (GLE) de los protones solares, se intenta realizar una contribución en la comprensión del proceso de generación de partículas en las fulguraciones solares. Los espectros teóricos de protones se derivan considerando que no hay pérdida de energía dentro del volumen de aceleración o que se desaceleran durante el proceso de aceleración. Al comparar los espectros teóricos de la fuente con los espectros experimentales, se afirma que el proceso de generación de partículas solares se desarrolla bajo tres regímenes principales de temperatura: la eficiencia de aceleración de las partículas es relativamente alta en los regímenes fríos y disminuye a la vez que aumenta la temperatura del medio. Se muestra que en algunos eventos las pérdidas de energía son capaces de modular el espectro de aceleración dentro de la fuente durante la breve escala de tiempo del fenómeno, mientras que en otros eventos las pérdidas de energía son completamente insignificantes durante la aceleración. Se argumenta que la aceleración tiene lugar en líneas de campo magnético cerrado y se predice la expansión y compresión del material de origen en asociación con el proceso de generación de las partículas. Este estudio nos permite estimar el rango de variación de varios parámetros de la fuente de un evento a otro, así como el proceso de aceleración en sí.

Estatus: Publicado.



IntechOpen

Cosmic Rays

Edited by Zbigniew Szadkowski



Cosmic Rays

<http://dx.doi.org/10.5772/intechopen.72533>

Edited by Zbigniew Szadkowski

Contributors

Jorge Perez Peraza, Juan Carlos Marquez Adame, Julia Tjus, Mehmet Guenduez, Björn Eichmann, Francis Halzen, Francesco Higgi, Domenico Lo Presti, Paola La Rocca, William R Webber, Svetlana Veretenenko, Maxim Ogurtsov, Markus Lindholm, Risto Talkanen, Agnieszka Janiuk, Konstantinos Sapountzis, Zbigniew Piotr Szadkowski

© The Editor(s) and the Author(s) 2018

The rights of the editor(s) and the author(s) have been asserted in accordance with the Copyright, Designs and Patents Act 1988. All rights to the book as a whole are reserved by INTECHOPEN LIMITED. The book as a whole (compilation) cannot be reproduced, distributed or used for commercial or non-commercial purposes without INTECHOPEN LIMITED's written permission. Enquiries concerning the use of the book should be directed to INTECHOPEN LIMITED rights and permissions department (permissions@intechopen.com).

Violations are liable to prosecution under the governing Copyright Law.



Individual chapters of this publication are distributed under the terms of the Creative Commons Attribution 3.0 Unported License which permits commercial use, distribution and reproduction of the individual chapters, provided the original author(s) and source publication are appropriately acknowledged. If so indicated, certain images may not be included under the Creative Commons license. In such cases users will need to obtain permission from the license holder to reproduce the material. More details and guidelines concerning content reuse and adaptation can be found at <http://www.intechopen.com/copyright-policy.html>.

Notice

Statements and opinions expressed in the chapters are those of the individual contributors and not necessarily those of the editors or publisher. No responsibility is accepted for the accuracy of information contained in the published chapters. The publisher assumes no responsibility for any damage or injury to persons or property arising out of the use of any materials, instructions, methods or ideas contained in the book.

First published in London, United Kingdom, 2018 by IntechOpen

IntechOpen is the global imprint of INTECHOPEN LIMITED, registered in England and Wales, registration number: 11086078, The Shard, 25th floor, 32 London Bridge Street

London, SE19SG – United Kingdom

Printed in Croatia

British Library Cataloguing-in-Publication Data

A catalogue record for this book is available from the British Library

Additional hard copies can be obtained from orders@intechopen.com

Cosmic Rays, Edited by Zbigniew Szadkowski

© 2018

Print ISBN 978-1-78923-592-0

Online ISBN 978-1-78923-593-7

Contents

Preface VII

- Section 1 Extragalactic Cosmic Rays 1**
- Chapter 1 **Introductory Chapter: Ultrahigh-Energy Cosmic Rays 3**
Zbigniew Szadkowski
- Chapter 2 **Gamma Ray Bursts: Progenitors, Accretion in the Central Engine, Jet Acceleration Mechanisms 13**
Agnieszka Janiuk and Konstantinos Sapountzis
- Section 2 Galactic Cosmic Rays 39**
- Chapter 3 **Cosmic Ray Muons as Penetrating Probes to Explore the World around Us 41**
Paola La Rocca, Domenico Lo Presti and Francesco Riggi
- Chapter 4 **Galactic Cosmic Rays from 1 MeV to 1 GeV as Measured by Voyager beyond the Heliopause 61**
William R. Webber
- Chapter 5 **Galactic Cosmic Rays and Low Clouds: Possible Reasons for Correlation Reversal 79**
Svetlana Veretenenko, Maxim Ogurtsov, Markus Lindholm and Risto Jalkanen
- Chapter 6 **Cosmic Ray Cradles in the Galaxy 99**
Mehmet Guenduez, Julia Becker Tjus, Bjorn Eichmann and Francis Halzen
- Chapter 7 **Exploration of Solar Cosmic Ray Sources by Means of Particle Energy Spectra 121**
Jorge Perez Peraza and Juan C. Márquez Adamec

Exploration of Solar Cosmic Ray Sources by Means of Particle Energy Spectra

Jorge Perez-Peraza and Juan C. Márquez-Adame

Additional information is available at the end of the chapter

Abstract

Through the analysis of the energy spectrum of 12 ground level enhancements (GLE) of solar protons, a contribution in the understanding of the generation process of flare particles is attempted. Theoretical spectra of protons are derived by considering either they do not lose energy within the acceleration volume or that they are decelerated during the acceleration process. By comparing the theoretical source spectra with the experimental spectra, it is claimed that the generation process of solar particles develops under three main temperature regimes: the efficiency of particles acceleration is relatively high in cold-regimens decreasing while increasing the temperature of the medium. It is shown that in some events energy losses are able to modulate the acceleration spectrum within the source during the short time scale of the phenomenon, whereas in other events energy losses are completely negligible during the acceleration. It is argued that acceleration takes place in closed magnetic field lines and predicted the expansion and compression of the source material in association with the generation process of particles. This study allows us to estimate the range of variation from event to event of several parameters of the source and the acceleration process itself.

Keywords: solar protons, energy spectrum, solar sources, GLE

1. Introduction

Most of the information on solar flares has been generally supplied by the analysis of their electromagnetic spectrum; however, the confrontation of timing synchronization between

electromagnetic flare emissions with those of energetic particles and coronal mass ejections (CME) is the method utilized to explore the physical conditions and processes taking place in the sources of particle generation. For example, results obtained from the SEPS server project and future HESPERIA HORIZON 2020 project. However, the study of the corpuscular radiation emitted in some flares can also provide us with very valuable information about the physical conditions and processes occurring in association with this solar phenomenon. It is known, for instance, that the processes involved in the generation of solar particles are probably of a non-thermal nature, because the intensity of particles usually decays more softly than an exponential of a the thermal type does, and so other properties may be deduced in order to investigate how and where multi-GeV solar protons originate, that means the source parameters and the parameters involved in the generation process of particle [69, 70]. In this chapter, we attempt to draw some inferences concerning solar sources by the analysis of 12 ground level enhancements (GLE) of solar cycles 19 and 20.

It has been shown [40] that the best representation of the energy spectrum of solar protons through the whole energy domain explored experimentally at present is given by an inverse power law with an upper cutoff in its high energy portion. In fact, a good fit of the experimental data can be obtained with an exponential law in a limited energy band; however, a strong deflection is obtained with them as soon as a wider energy domain is involved. Besides, it has been established [11] that the measured differential intensity in solar proton events, as well as the source spectrum (inferred as an inverse power law in energy) are both velocity-dependent. Therefore, we infer that the acceleration rate of particles in the sun must provide the spectral shape and velocity dependence such as suggested by those results. This is the case with an energy gain rate of the form

$$\left(\frac{dW}{dt}\right)_{acc} = \alpha\beta W = \alpha(W^2 - (Mc^2)^2)^{1/2} \quad (1)$$

where β is the velocity of the particles in units of light velocity and W the total energy of particles. The parameter α denotes the efficiency of the acceleration mechanism, which in the case of solar sources may be considered as roughly constant when the acceleration process reaches the steady-state in a given event [79, 80]. It has been generally thought that the energy loss processes of solar particles acceleration stage are not important in practice, and have only been taken into account after the acceleration stage in order to explain some features of electromagnetic emissions in solar flares and heating of the chromosphere [87].

In this chapter we shall consider, together with acceleration, energy loss processes occurring in the high density plasma of the solar source. It will be shown that energy losses in some proton flares can modulate the acceleration spectrum, thus implying that if such a small effect compared to the acceleration rate is able to modify the spectrum during the short lapse of the acceleration process, then the source spectrum is actually the result of a strong modulation due to local energy losses during acceleration and not only through interplanetary propagation; thus in Section 2, we discuss the basic equations of the more plausible energy loss processes in

particle sources. In Section 3, we present the observational energy spectrum of the concerned GLE as reported by several authors. In Section 4, we deduce theoretical source spectra, without and with energy losses during acceleration, disregarding energy changes of after acceleration while traversing the dense medium of the solar atmosphere to attain the interplanetary medium. In Section 5, we describe the criterion employed to construct integral energy spectra of solar proton (GLE) as well as the methods used in calculations; the results are presented graphically. In Section 6, the interpretation and significance of our results are discussed. In Section 7, the concluding remarks are summarized.

2. Energy losses of protons during acceleration in solar flares

Some researchers who study radiation and secondary particle fluxes consider an acceleration stage followed by a slowing down phase in the solar material once the action of the acceleration mechanism on particles has ceased (e.g. [86, 87, 88, 89]); and they generally neglect the simultaneous occurrence of energy loss and acceleration.

However, particle acceleration is not performed in the vacuum but in the high density medium of flare regions; therefore, we shall study the local modulation of the acceleration spectrum as the protons are broken during the short-time scale of solar particle generation. The most important processes occurring in astrophysical plasmas capable of affecting the net energy change rate of particles in the range of kinetic energies of energetic solar protons ($E \sim 10^6 - 10^{10}$ eV) are:

2.1. Collisional energy losses

These depend strongly on the density and temperature of the plasma; thus we assume that the main energy dissipation of particles must occur in the generation region, in the body of the flare itself. The rate of collisional losses in a medium of density n has been given in a simplified expression [37]

$$\left(\frac{dW}{dt}\right)_{ion} = -\frac{7.62 \times 10^{-9} n L}{\beta} \text{ (eV/sec)} \quad (2)$$

where $\beta = v/c$ is the particle velocity in terms of the light velocity, L is a unidimensional factor and logarithmically depending marginally on the particle energy. We shall assume a value of $L \sim 27$ for solar flare conditions, when the medium concentration is $n \sim 10^{12} - 10^{13} \text{ cm}^3$. In **Figure 1**, the behavior of Eq. (2) with energy is shown. The complete description of collisional losses through the entire energy range including losses in the low energy portion (the so called nuclear stopping and electronic stopping) has been given by [10] for fully ionized hydrogen as:

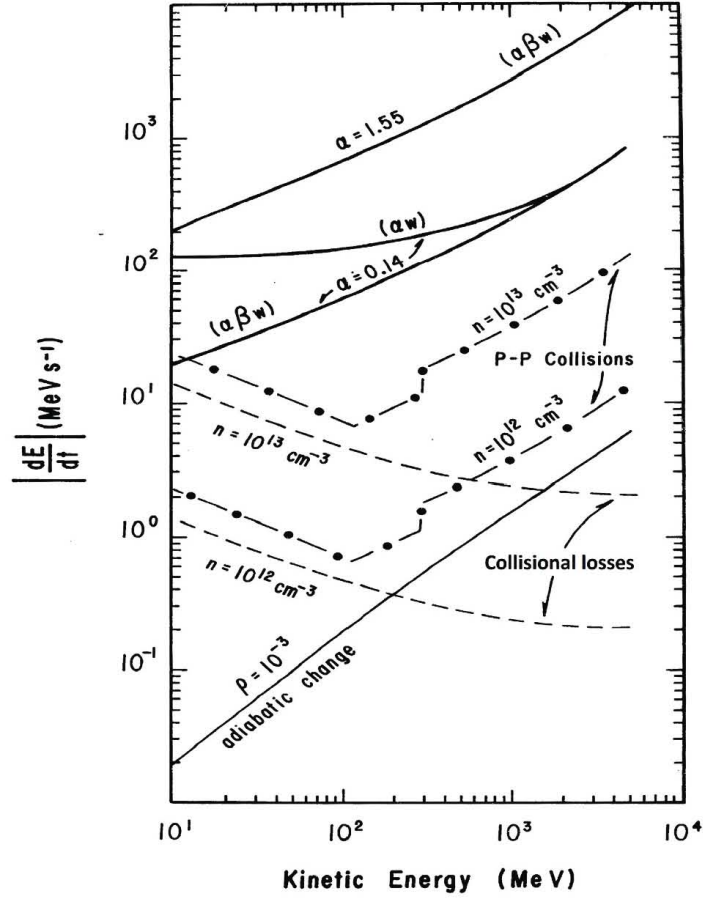


Figure 1. Energy change rates of protons (acceleration for two different rates) and deceleration for collisional losses p-p nuclear collisions and adiabatic cooling in a medium of density $n = 10^{12}-10^{13} \text{ cm}^{-3}$.

$$\frac{dE}{dt} = -\frac{1.57 \times 10^{-35} N Q^2}{\beta A} H(x) \ln \Lambda \quad (\text{eV/ns}) \quad (2.1)$$

where $x = 5.44 \times 10^4 \beta T^{-0.5}$, $H(x) = \xi_1 H_e(x_e) + \xi_2 H_p(x_p)$ with

$H_e(x_e) = 0.88 \text{erf}(x_e) - (1 - 5.48 \times 10^{-4}/A) x_e e^{-x_e^2}$ for electrons,

$H_p(x_p) = 0.88 \text{erf}(x_p) - (1 + \frac{1}{A}) x_p e^{-x_p^2}$ for protons,

$$\xi_1 = 1.097803296 \times 10^{27}, \xi_2 = 5.979073244 \times 10^{23} \text{ and } \Lambda = \left[4.47 \times 10^{16} A (T/N)^{0.5} \beta^2 \right] / Q$$

For the task of simplicity and because we are dealing in this work with GLE (high energy protons), we will use preferentially Eq. (2).

2.2. Energy degradation from proton-proton collisions

At present, there are evidences of the occurrence of nuclear reactions between solar nuclei and solar material, producing high energy gamma rays although is not absolutely clear whether nuclear reactions of solar energetic particles and solar material take place, when protons are injected into the photosphere, or they pass through coronal condensations, or during their acceleration within the dense material of flare regions. We shall assume that nuclear interactions occur at least in the acceleration volume where very likely the motion of energetic particles is completely random with respect to the local solar material. The isotropic motion of the accelerated particles is suggested by an analysis of neutron fluxes [45]. For purposes of energy loss calculations, we do not take into account collisions protons with other nuclear species, because the maximum energy change in elastic scattering occurs when the colliding particles have similar mass. Although the energy dissipation from $p:p$ collisions is believed to appear mainly from elastic scattering, however at high energies (>750 MeV), the inelastic cross-section becomes highly important [44] increasing up to a maximum at some GeV, where it remains practically constant. In fact, as pion production initiates at ~ 285 MeV and a fraction $\geq 35\%$ of the kinetic energy of the incident proton goes into pion energy, then, energy dissipation from inelastic $p:p$ scattering is not negligible in a high density medium ($n \geq 10^{12}$ cm $^{-3}$). Concerning inelastic $p:p$ interactions, the gamma ray line at 2.2 MeV due to fast neutron production, seems to be strong evidence of the occurrence of $p:p$ collisions in solar flares. All this depends strongly on the production model: The assumed geometry and the spectral shape considered [2]. In fact, the cross-section for the later interactions is 10: 100 times higher, that is, their threshold is ≤ 36 MeV/nucleon, while that for inelastic $p:p$ scattering are ~ 285 MeV. Nevertheless, it has been known for a long time from [12] that solar abundances of CNO and he are of the order of $\sim 1.5: 7\%$ with respect to the local H , in such a way that this kind of equilibrium between local abundances and interaction cross-sections states a high probability for the occurrence of $p:p$ collisions in the body itself of the solar flare material. The main problem related with these features is that some reactions, as for instance $p(p; a\pi^0)p$ and multiple pion yielding at high energies, $p(p; a\pi^+)p$ or $p(p; a\pi^-, b\pi^0)p$ or $p(p;n, \pi^+, a\pi^+, a\pi^{--}, b\pi^0)$ by π^0 decay produce high energy solar gamma rays (50 MeV) that have neither been detected to our knowledge nor their plausible absorption into the solar material satisfactorily explained. In fact, the predicted wide peak for these gamma rays ranging from $\sim 38.5: 118$ MeV [6] could probably render their identification difficult due to the presence of high energy photons expected from bremsstrahlung of very high energy solar electrons. In addition, there is the fact that high energy $p:p$ reactions must occur more frequently, since the inelastic cross-section rises progressively from 290 MeV up to a maximum of about 1 GeV where it remains practically constant. Refs. [14, 15] have reviewed the problems connected with secondary products of nuclear interactions in solar flares. Nevertheless we show later in this work that $p:p$ collisions are only expected in some few GLE. Hence, although the measured flux of particles does not distinguish whether solar protons have suffered nuclear collisions or not, the modulation of the energy spectrum by their effects furnish available information about their occurrence. The importance of energy degradation from $p:p$ collisions in cosmic rays physics has been pointed out for the first time by [129]. The energy loss rate by nuclear interactions is agreement with [38]

$$\frac{dW}{dt} = -\sigma cn\beta W \quad (\text{eV/sec}) \quad (3)$$

where σ in p - p collisions is composed of $\sigma_{p-p}^{ine} + \sigma_{p-p}^{el}$. As the inelastic cross-section is weakly energy dependent, it may be approximated to its mean value at high energies ($\sigma_{p-p}^{ine} \sim 26$ mb). Concerning elastic collisions, a reasonable fit of the differential cross-section data by an analytical expression has been given by [91]. As the differential cross-section is highly isotropic, we can assume symmetry around 90° , such that their expression may be rewritten as $\sigma_{p-p}^{el} = hE^{-2} + jE^{-1}$ (if $E \leq 110$ MeV) and $\sigma_{p-p}^{el} = hE^{-2} + f$ (if $E > 110$ MeV), where $h = 96.09$ mb-MeV², $j = 5.497 \times 10^3$ mb MeV and $f = 46.49$ mb. We have then from Eq. (3):

$$\begin{aligned} \left(\frac{dW}{dt}\right)_{p-p} &= -cn(h\bar{E}^2 + j\bar{E})\beta W \quad (\text{if } E \leq 110 \text{ MeV}) \\ \left(\frac{dW}{dt}\right)_{p-p} &= -cn(h\bar{E}^2 + f)\beta W \quad (\text{If } 110 < E < 290 \text{ MeV}) \\ \left(\frac{dW}{dt}\right)_{p-p} &= -[\eta + cn(h\bar{E} + f)]\beta W \quad (\text{If } E \geq 290 \text{ MeV}), \text{ where } \eta = cn\sigma_{in} \end{aligned}$$

So that the net energy change can be compacted as:

$$\left(\frac{dW}{dt}\right)_{p-p} = -(hE^{-2} + jE^{-1} + f + \eta)\beta W \quad (\text{eV/sec}) \quad (4)$$

where $h = 2.88 \times 10^{-15}$ n Me² s⁻¹, $j = 1.65 \times 10^{-13}$ n MeV s⁻¹ (if $E \leq 110$ MeV), $j = 0$ and $f = 1.39 \times 10^{-15}$ n s⁻¹ (if $E > 110$ MeV), $f = 0$ (if $E \leq 110$ MeV), $\eta = cn\sigma_{p-p}^{ine} = 8.1 \times 10^{-16}$ n s⁻¹, (if $E > 290$ MeV) and $\eta = 0$ if ($E < 290$ MeV). We have plotted Eq. (4) in **Figure 1** for two different values of the density n .

2.3. Adiabatic deceleration at the source level

Adiabatic cooling of cosmic particles in the solar wind has been proved long ago (e.g. [34]). However, here we are dealing with adiabatic cooling at the sources of solar energetic protons in GLE and not in the interplanetary or interstellar media medium. It is well-known that great flares are associated with magnetic arches, such as loop prominences and flare nimbuses (e.g. [7, 97, 98]) which occur between regions of opposite-polarity in the photosphere. Observations show that magnetic flux tubes expand from flare regions [23, 66, 107, 109, 117]. These configurations identified as “magnetic bottles” are usually related to the development of flare phenomena (e.g. [14, 83, 84, 96, 104, 110, 123]), therefore, we shall investigate the relationship between these magnetic structures and the phenomenon of particle generation through the study of the energy spectra of solar protons in GLE: We assume the hypothesis that particles are enclosed within those “magnetic bottles”, where they are accelerated up to high energies.

Therefore, while the acceleration mechanism is in effect, and a fraction of particles are escaping from the flare region, the bulk of particles lose energy by adiabatic cooling due to the work that protons exert on the expanding material. Mechanisms for the expansion (or compression) of magnetic structures have been widely discussed (e.g. [96, 99]). It has been shown through energetic estimations that when particle kinetic density exceeds magnetic field pressure, the sunspot field lines are transported upward by the accelerated plasma; and thus, owing to the decrease of magnetic field density according to the altitude over the photosphere [1, 101], the magnetic bottles blow open at an altitude lower than $0.6: 1 R_s$ allowing particles to escape into the interplanetary medium. Particles that have left the acceleration region before the magnetic bottle blows up may escape due to drift by following the field lines, or they remain stored therein losing energy until the magnetic structure is opened. We shall not consider this eventual deceleration during particle storage but only energy losses inside the acceleration volume. According to [46, 77], the energy change rate of particles by expansion (or compression) of magnetic fields producing adiabatic cooling or heating of the solar cosmic ray gas, when the non-radial components of the plasma velocity are negligible is given as

$$\left(\frac{dE}{dt}\right)_{ad} = \pm \frac{2V_r}{3R} \mu E \text{ (eV/sec)} \quad (5)$$

where V_r and R are the velocity and distance of the plasma displacement, respectively, $\mu = 1 + \gamma^{-1}$ and $\gamma = W/Mc^2$. Hence, in terms of total energy W the adiabatic deceleration rate in the expanding magnetic fields may be expressed as

$$\left(\frac{dW}{dt}\right) = -\rho\beta^2 W \text{ (eV/sec)} \quad (6)$$

In order to estimate an approximate value for $\rho = (2/3) (V_r/R)$ in flare conditions, we extend the following considerations: it is known that the hydromagnetic velocity of the coronal expansion is in average of the order 400 km s^{-1} and that in association with proton flares type IV sources systematically appear expanding with velocities in the range of 10^2 – 10^3 km s^{-1} depending on the direction of the expansion (e.g. [100, 101, 136]). Observations also show displacements with velocities of 650 – 2600 km s^{-1} in association with type II burst [95] and expansion of flare knots in limb flares with velocities in the range 5.3 – 110 km s^{-1} [54, 55, 83, 84]. Besides, it is also known that closed magnetic arches have a mean altitude of $0.6 R_s$ above the photosphere [122]. Therefore, assuming that the average velocity of 400 km s^{-1} is a typical value of magnetic motions in the chromosphere and low corona and an average expanded distance of the source of $0.3 R_s$ while acceleration is operating, we obtain thus $\rho \approx 10^{-3} \text{ s}^{-1}$. On the other hand, if we take into account the results usually associated with multi-GeV proton flares (GLE), then, magnetic loops expand $\sim 30,000 \text{ km}$ with a velocity of $\sim 45 \text{ km s}^{-1}$ at the time of the flare start, thus giving a value for ρ of the same order. We have illustrated Eq. (6) with $\rho = 10^{-3} \text{ s}^{-1}$ in **Figure 1**.

It is expected that if the physical conditions in the source of multi-GeV solar proton flares and processes acting on solar particles must be similar, the behavior of the theoretical source spectra of solar protons from event to event will be similar, and thus by comparing the rates (1)–(6) the influence of each process on the acceleration spectrum can be established. For

instance, it can be seen from **Figure 1** that in the energy range $1\text{--}10^3$ MeV and medium concentration $n = 10^{13} \text{ cm}^{-3}$, the ratio $r_1 = (dW/dt)_{p-p}/(dW/dt)_{coll}$ changes from $r_1 = 1.7\text{--}16$ and the ratio $r_2 = (dW/dt)_{ad}/(dW/dt)_{coll}$ varies from $r_2 = 4.6 \cdot 10^{-5}\text{--}0.64$; therefore if all processes would act simultaneously in solar flares, the acceleration spectrum is mainly affected by energy degradation from $p\text{--}p$ collisions, whose effects are stronger in the high energy portion of the spectrum. Collisional losses are more important in the non-relativistic region, whereas adiabatic losses become important in the relativistic region of the spectrum. Using experimental data of several GLE of solar protons, we shall investigate if the same processes occur in all events, and thus similar physical conditions are prevalent at the sources, or if they vary from event to event, in which, case it is interesting to investigate why and how they vary.

3. Experimental integral spectra of multi-GeV solar proton events

The description of the spectral distribution of solar particle fluxes of a given event is concerned, the result is a strong spread of spectral shape representations, according to the different detection methods employed, the energy bands and time intervals studied. The most plausible spectral shapes are described either by inverse power laws in kinetic energy or magnetic rigidity and exponential laws in magnetic rigidity (e.g. [53]). One of the most popular methods was developed by Forman et al, published in Ref. [59].

For example, in the case of the GLE of January 28, 1967, for which experimental measurements of fluxes through a wide energy range are available, several different spectral shapes have been analyzed: from the study of the relativistic portion of the spectrum, [60, 61, 62] proposes an exponential rigidity law $\{\sim \exp. (-P/0.6 \text{ (GV)})\}$ and alternatively a differential power law spectrum in rigidity ($\sim P^{-5}$); [8] proposed a differential spectrum of the form ($\sim P^{-4.8}$) for relativistic protons of the event. Taking into consideration data from balloon, polar satellite and neutron monitors (N.M.), [3] gives an integral spectrum of the form ($\sim P^{-4}$); similarly, [40] deduced an integral spectrum as a power law in kinetic energy ($\sim E^{-2}$) with an upper cutoff at $E_m = 4.3$ GeV or in magnetic rigidity P as ($\sim P^{-3.1}$) with an upper cutoff at $P_m = 5.3$ GV. These authors have shown that as far as the whole energy spectrum through the different energy bands is concerned, any spectral shape that does not take into an upper cutoff is strongly deflected from the experimental data.

It would seem, therefore, that the description of energy spectra of solar particles is one of the most particular topics connected with solar cosmic ray physics: that is, owing to the lack of global measurements of the whole spectrum at a given time and to the lack of simultaneity in the measurements of differential fluxes, the integral spectra must be constructed with the inhomogeneous data available for each event. Therefore, in order to do so for 12 GLE during solar cycles 19 and 20, we have used low rigidity data (high latitude observations) for the following events: for September 3, 1960 event we have employed the 14:10 U.T. data from Rocket Observations [18] in the (0.1–0.7) GV band. For November 12 and 15, 1960 GLE's, we have used the 18:40 U.T. and 05:00 U.T. data, respectively, from rocket observations in the (6.16–1.02) GV band [73]. For July 7, 1966 GLE, we have used the 19:06 U.T. data given by [57, 58] in the (0.13–0.19) GV band, and the spectrum given by [118] in the (0.19–0.44) GV band;

for higher rigidities (> 0.44 GV) we have employed the 03:00 U.T. measurements on Balloon and N.M. data given by [39]. In the events of November 18, 1968, February 25, 1969, March 30, 1969, November 2, 1969 and September 1, 1971, we have used the peak flux data in the (0.1–0.7) GV band, given by [47] from the IMP4 and IMP5 satellite measurements. For January 24, 1971 GLE, we have employed the 06:05 flux data and at 07:20 U.T. in the (0.28–0.7) GV band from [134]. For August 4, 1972 event, we have considered the HEOS2 graphical fluxes in the (0.15–0.45) GV band at 16:00 U.T. by [61] which lie between the 09:57–22:17 U.T. data of [4] and is in good agreement with N.M. measurements; for the (0.6–1.02) GV band we have employed the balloon extrapolated data by [61]. For the high rigidity portion of the spectrum (> 1.02 Gy), we have made use of the measurements given by [41–43] from NM data, in the following form:

$$J(> P) = K \int_P^{P_m} P^{-\Phi} dP \quad (7)$$

where K is a constant, P_m the high rigidity cutoff and Φ the spectral slope of the differential fluxes.

The values of P_m and Φ were taken through several hours around the peak flux of the event, as explained by the latter authors. The values of Φ were found to be systematically lower than other values furnished by GLE measurements due to the presence of the high rigidity cutoff parameter. For November 2, 1969 event we have taken the high rigidity power law spectrum as given by [61]; according to this data, we have considered a characteristic upper cutoff at 1.6 GV. In the case of August 4, 1972 event, we have taken the upper bound of Φ given for August 7 event by [43] considering that the particle spectrum became flatter with time during August 1972 events [4]. For the high rigidity cutoff, we have tested that within the error band, the value was essentially the same of that of August 7 event.

The extrapolation of the high rigidity power laws to the integral fluxes of the lower rigidity branches, has allowed us to determine K from Eq. (7) and thus to construct the high rigidity branches of the proton fluxes. By smoothing fluxes of both branches we have obtained the experimental integral spectra, which we have represented in the kinetic energy scale with solid lines through **Figures 2–4**. We have verified the good agreement of the high energy power law shape deduced in this manner, with the corresponding integral slope of the differential power law in kinetic energy $\int_E^{E_m} E^{-\Phi} dE$ reported in several works by (e.g. [41–43]). However, although it is systematically true that the best fit for the experimental points is given by such a power law, it is also true that there are some points that do not fit perfectly with that kind of curve; we have attempted to include these points in the experimental curves in the case of some GLE events. For January 28, 1967 event, we employed the integral spectrum deduced by [40] with the previously mentioned characteristics. It must be emphasized that the choice of these 12 multi-GeV proton events (GLE) follows from the fact that they furnish particle fluxes through a large range of energy bands and because of the information of the experimental value of E_m in these cases, which unlike the other parameters of the spectrum is the only one that does not vary through the propagation of particles into the interplanetary space as shown by [40]) and therefore, can be directly related to the acceleration process

An excellent review of solar cosmic ray events has been given in [130].

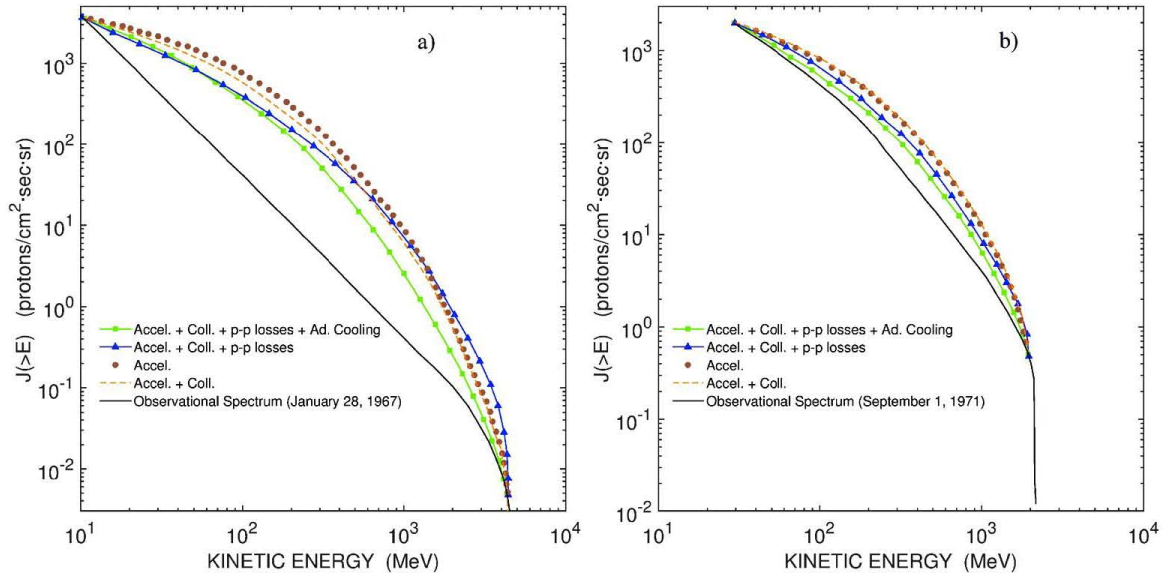


Figure 2. Theoretical and observational integral energy spectrum of *hot* events.

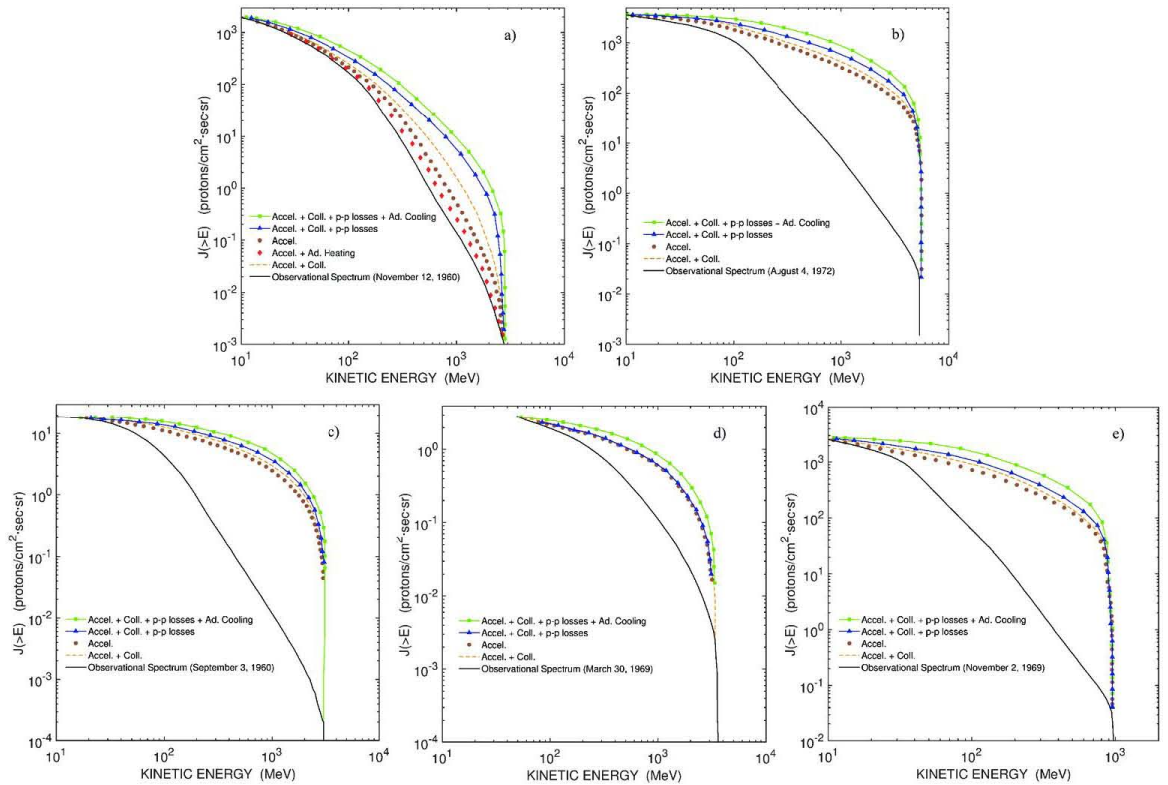


Figure 3. Theoretical and observational integral energy spectrum of *cold* events.

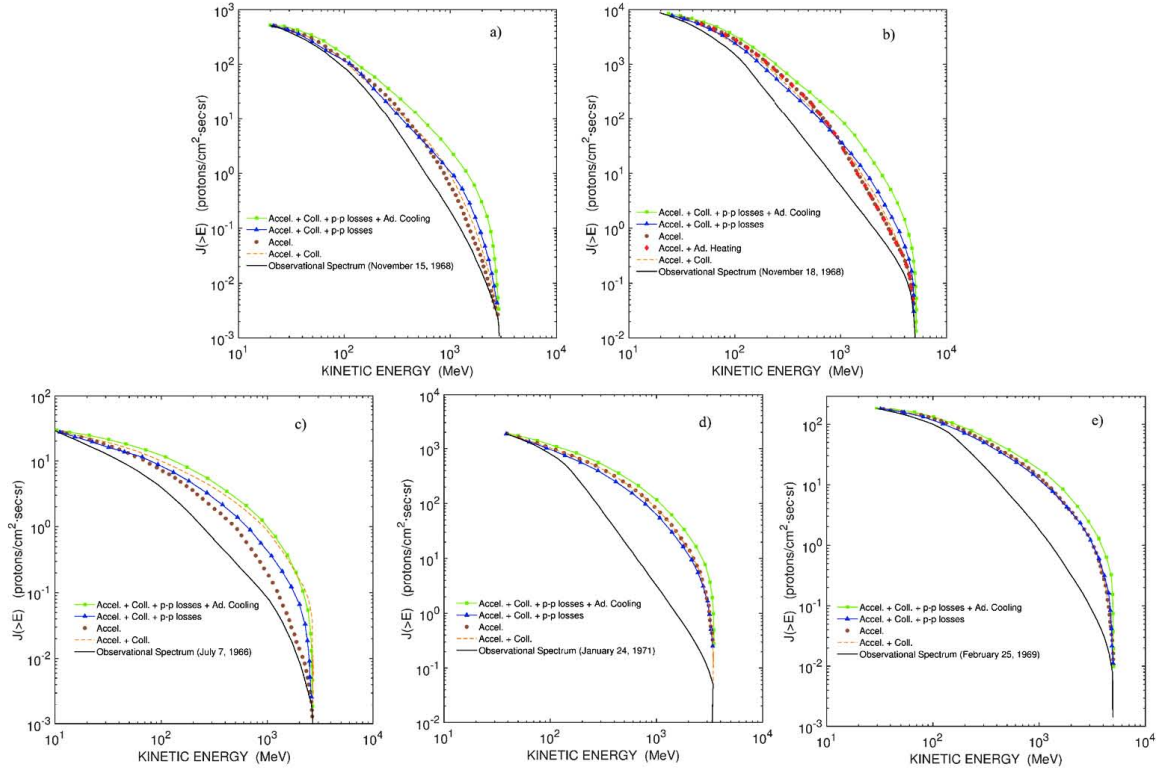


Figure 4. Theoretical and observational integral energy spectrum of *warm* events.

4. Theoretical spectra of solar protons in the source

In order to deduce the velocity and time dependent theoretical spectrum of the accelerated protons, one must take into account the various processes which affect particles during the remaining time within the acceleration volume. The main processes acting on particles during acceleration in a high density plasma are related either to catastrophic changes of particle density from the accelerated flux or to energy losses. Whereas the first kind of processes affect mainly the number density of the spectrum, energy losses entail a shift of the particle distribution toward lower energies, and a certain degradation of the number density due to thermalization of the less energetic particles. The number density changes on the accelerated proton flux may occur from catastrophic particle diffusion out of the flare source or by nuclear disintegration or creation of solar protons by nuclear reactions. Given the lack of knowledge about the exact magnetic field configuration and thus of the confinement efficiency of these fields, we do not consider here the effects of plausible escape mechanisms [26, 27, 104] on the theoretical spectrum. Therefore, to make a clear distinction between the energy loss effects (Section 2) on the spectrum of acceleration, we shall also neglect nuclear transformation during acceleration, local modulation post-acceleration and interplanetary modulation [67, 68] in this approach.

In addition, we shall not take into account spatial spread in the energy change rates within the acceleration process such that energy fluctuations [81, 82] which are considered minor for the purpose of this work.

It must be emphasized that since we are dealing with solar energetic particles, the well-known phenomena of Forbush decreases are rather related with galactic cosmic rays but not necessarily with solar energetic protons (e.g. [20]).

To establish the particle spectrum, we shall follow the assumptions that under the present simplified conditions lead to similar results that are obtained by solving a Fokker-Planck type transport equation on similar conditions [36, 81], that is, when the steady-state is reached in the source: we assume that a suprathermal flux with similar energy or a Maxwellian particle distribution is present in the region where the acceleration process is operating and a fraction N_0 of them can be accelerated during the time interval in which the stochastic acceleration mechanism is acting [93]. The selection of particles follows to the fact that their energy must be \geq than a critical energy, E_c , determined by the competition of acceleration and by local energy losses. By analogy with radioactive decay the energy distribution of cosmic ray particles is assumed as an exponential distribution in age of the form

$$N(E)dE = N(t)dt = \frac{N_0}{\tau} \exp(-t/\tau)dt \quad (8)$$

which in terms of the Lorentz factor is expressed as

$$N(\gamma)d\gamma = (1/Mc^2)N(t)dt \quad (8.1)$$

where t is the necessary time to accelerate particles up to the energy E and τ is considered as a mean confinement time of particles in the acceleration process. Eq. (8) represents hence the differential spectrum of the accelerated particles; to obtain the integral spectrum we take the integration of (8) up to the maximum energy of the accelerated protons, E_m (corresponding to the upper cutoff in the particle spectrum) the existence of which has been shown by [43] as discussed before.

$$J(> E) = \int_E^{E_m} N(E)dE = \int_t^{t_m} N(t)dt = N_0 \int_t^{t_m} \frac{e^{-t/\tau}}{\tau} dt = N_0 [e^{-t/\tau} - e^{-t_m/\tau}] \quad (9)$$

where t_m is the acceleration time up to the high energy cutoff. Because the acceleration process is competing with energy loss processes, the net energy gain rate is effectively fixed on particles, only beginning at a certain threshold value, E_c defined by $(dE/dt) = 0$, such that only particles with $E > E_c$ are able to participate in the acceleration process (the flux N_0). Thus the acceleration time t is defined as

$$t = \int_{E_c}^E \left(\frac{dE}{dt} \right) dt = t(E) - t(E_c) \quad (10)$$

Similarly the constant value t_m , representing the acceleration time up to the high energy cutoff, E_m defined as $t_m = t(E_m) - t(E_c)$, where $t(E_c)$ denotes the time of the acceleration onset. Therefore, Eq. (9) can be rewritten as

$$J(> E) = N_0 e^{t(E_c)/\tau} \left[e^{-t(E)/\tau} - e^{-t(E_m)/\tau} \right] \quad (11)$$

4.1. The spectrum of acceleration

For the case in which energy losses are completely unimportant within the acceleration time scale, the net energy change rate is determined by the acceleration rate, Eq.(1), which for simplicity's sake, we shall represent hereafter in terms of the Lorentz factor γ as

$$\left(\frac{d\gamma}{dt} \right) = \alpha (\gamma^2 - 1)^{1/2} \quad (12)$$

the condition $(d\gamma/dt) = (d\gamma/dt)_{acc} - (d\gamma/dt)_{loss} = 0$ gives $\gamma_c = 1$ (and hence $E_c = 0$), such that by integration of (12) we obtain the acceleration time up to the energy $E = Mc(\gamma - 1)$ as

$$t = \frac{1}{\alpha} \ln \left[\gamma + (\gamma^2 - 1)^{1/2} \right] \quad (13)$$

Now, by substitution of (13) in Eq. (8.1), we obtain the following differential spectrum

$$N(\gamma) = \frac{N_0}{\alpha \tau M c^2} (\gamma^2 - 1)^{-1/2} \left[\gamma + (\gamma^2 - 1)^{1/2} \right]^{-1/\alpha \tau} \quad (14)$$

which in terms of total energy W is expressed as

$$N(W) = \frac{N_0}{\alpha \tau} (M c^2)^{1/\alpha \tau} \frac{(1 + \beta)^{-1/\alpha \tau}}{\beta} W^{-(1+1/\alpha \tau)} = \frac{N_0}{\alpha \tau} (M c^2)^{1/\alpha \tau} \frac{\left\{ W + (W^2 - (M c^2)^{1/2}) \right\}^{1/\alpha \tau}}{(W^2 - (M c^2)^2)^{1/2}} \quad (14.1)$$

When the parameter β is considered outside of the integrating equations a somewhat different expression is obtained:

$$N(W) = \frac{N_0}{\alpha \beta \tau} (M c^2)^{1/\alpha \beta \tau} W^{-(1+1/\alpha \beta \tau)}$$

The corresponding integral spectrum of the accelerated particles appears from Eqs. (11)–(13) as

$$J(> E) = N_0 \left[\left[\gamma + (\gamma^2 - 1)^{1/2} \right]^{-1/\alpha \tau} - \left[\gamma_m + (\gamma_m^2 - 1)^{1/2} \right]^{-1/\alpha \tau} \right] \quad (15)$$

(where) $\gamma_m = (E_m + M c^2) / M c^2$

the integral spectrum expressed in terms of kinetic energy becomes,

$$J(> E) = N_0 (M c^2)^{1/\alpha \tau} \left\{ \left[E + M c^2 + \sqrt{E^2 + 2 M c^2 E} \right]^{-1/\alpha \tau} - \left[E_m + M c^2 + \sqrt{E_m^2 + 2 M c^2 E_m} \right]^{-1/\alpha \tau} \right\} \quad (15.1)$$

4.2. The modulated spectrum in the acceleration region

In order to study local modulation of spectrum (14) or (15) during acceleration, we shall proceed to consider energy loss processes together with the energy gain rate (12), according to the processes discussed in Section 2.

4.2.1. Modulation by collisional losses

When collisional losses are not negligible during acceleration, the net energy change rate is determined by (2) and (12) as

$$\frac{d\gamma}{dt} = \alpha(\gamma^2 - 1)^{1/2} - (b/Mc^2)\gamma(\gamma^2 - 1)^{-1/2} \quad (16)$$

where $b = 7.62 \times 10^{-9}$ nL, then, the solution of (16) is easily performed by employing a change of variable of the form $x = [(\gamma - 1)/(\gamma + 1)]$ [90], such that the acceleration time from the critical energy E_c up to the energy E , in terms of the Lorentz factor is

$$t = \ln \left| \frac{1+x}{1-x} \right|^{1/\alpha} \left| \frac{\phi^{1/2}x - (-Y_2)^{1/2}}{\phi^{1/2}x - (-Y_2)^{1/2}} \right|^p + \xi \tan^{-1} \left[x(\phi/Y_1)^{1/2} \right] \Big|_{x_c}^x = t(x) - t(x_c) \quad (17)$$

with $\phi = b/Mc^2$, $Y_1 = 2\alpha + (4\alpha^2 + \phi^2)^{1/2}$, $Y_2 = 2\alpha - (4\alpha^2 + \phi^2)^{1/2}$, $p = Y_3/[2(-Y_2)^{1/2}\phi^{1/2}]$, $Y_3 = (2\phi/\alpha)[(\phi - Y_2)/(Y_1 - Y_2)]$, $Y_4 = (2\phi/\alpha)[(Y_1 - \phi)/(Y_1 - Y_2)]$, $\zeta = Y_4/(\phi Y_1)^{1/2}$ and $x_c = [(Y_c - 1)/(Y_c + 1)]^{1/2}$, where $Y_c = (b/2\alpha Mc^2) + 1$ is the critical value for acceleration determined by $(d\gamma/dt) = 0$, and the constant value $t(x_c)$ corresponds to the value of $t(E_c)$ appearing in Eq. (10). The differential spectrum of particles is obtained by substituting of (Eq. 17) in Eq. (8') as follows

$$N(\gamma) = \frac{N_0}{\tau Mc^2} e^{t(x_c)/\tau} \frac{(\gamma^2 - 1)^{1/2}}{[\alpha(\gamma^2 - 1) - \phi\gamma]} \left(\frac{1+x}{1-x} \right)^{-1/\alpha\tau} \left[\frac{\phi^{1/2}x - (-Y_2)^{1/2}}{\phi^{1/2}x + (-Y_2)^{1/2}} \right]^{-\phi/2} \exp \left[(-q/\tau) \tan^{-1} \left[x(\phi/Y_1)^{1/2} \right] \right] \quad (18)$$

The integral spectrum is then from Eq. (11) and Eq. (17)

$$J(> E) = N_0 \exp(t(x_c)/\tau) \left\{ \left(\frac{1+x}{1-x} \right)^{-1/\alpha\tau} \left(\frac{\phi^{1/2}x - (-Y_2)^{1/2}}{\phi^{1/2}x + (-Y_2)^{1/2}} \right)^{-p/2} \exp \left[\left(-\frac{q}{\tau} \right) \tan^{-1} \left[x(\phi/Y_1)^{1/2} \right] \right] \right. \\ \left. - \exp(-t(x_m)/\tau) \right\} \quad (19)$$

where $t(x_m)$ corresponding to $t(E_m)$ in Eq. (11), appearing from the evaluation of Eq. (17) in the constant value $x_m = [(\gamma_m - 1)/(\gamma_m + 1)]^{1/2}$. It can be seen that spectra (18) or (19) reduces to (14) or (15) when $b = 0$. The integral spectrum in terms of kinetic energy is expressed as

$$\begin{aligned}
 J(> E) = N_0 \exp\left(\frac{t(E_i)}{\tau}\right) & \left\{ \left[\left| \frac{\varepsilon + E + Mc^2}{Mc^2} \right|^{-1/\alpha\tau} \left| \frac{(E-E_1) - \varepsilon + [E_1(E_1+2Mc^2)]^{1/2}}{(E-E_1) - \varepsilon - [E_1(E_1+2Mc^2)]^{1/2}} \right| \right]^{-p} \right. \\
 & \times \exp\left(\frac{-[E_2(-E_2 - 2Mc^2)]^{1/2}}{\alpha\tau(E_1 - E_2)} \tan^{-1}\left(\frac{E(E_2 + Mc^2) + Mc^2 E_2}{\varepsilon E_2(-E_2 - 2Mc^2)}\right)\right) \left. - \exp\left(\frac{-t(E_m)}{\tau}\right) \right\} \quad (19.1)
 \end{aligned}$$

with $p = \frac{[E_1(E_1+2Mc^2)]^{1/2}}{\alpha\tau(E_1-E_2)}$, $= (E^2 + 2Mc^2 E)^{1/2}$, $E_i = b/2$ α is the threshold value for effective acceleration and E_1, E_2 correspond respectively to $\left\{ \left[b \pm (b^2 + 4\alpha^2 (Mc^2)^2)^{1/2} \right] / 2\alpha \right\}$. It can be seen that spectrum (19.1) reduces a spectrum (15.1) when $b = 0$.

The corresponding particle energy spectrum to Eq. (2') is developed in the Appendix.

4.3. Modulation by proton-proton nuclear collisions

In the event that proton-proton collisions are important during the acceleration process. By adding Eq. (4), the net energy rate (16) turns into the following expression

$$\frac{d\gamma}{dt} = \alpha(\gamma^2 - 1)^{1/2} - (b/Mc^2)\gamma(\gamma^2 - 1)^{-1/2} - \left[h \left[Mc^2(\gamma - 1)^{-2} + j \left[Mc^2(\gamma - 1) \right]^{-1} + f + \eta \right] \right] (\gamma - 1)^{1/2} \quad (20)$$

The critical value γ_c for acceleration resulting when $(d\gamma/dt) = 0$ is obtained by solving a cubic equation of the form $A\gamma^3 + B\gamma^2 + C\gamma + D = 0$ with $A = \alpha(Mc^2)^2$, $B = -A - (b + j)Mc^2$, $C = -A + bMc^2 - h$, $D = A + jMc^2 - h$ if $E \leq 110$ MeV, or, $A = (\alpha - f)(Mc^2)^2$, $B = -A - bMc^2$, $C = -A + bMc^2 - h$, $D = A - h$ if $110 < E \leq 290$ MeV and for the range $E > 290$ MeV similar to the last one but with $A = (\alpha - f - \eta)(Mc^2)^2$. Therefore, the roots a_1, a_2 and a_3 depend on α, b, h, j, f and η , such that when a medium concentration n is fixed, the basic dependence remains on α . Given that for the bulk of the involved parameters the conditions $a_1 > 1, a_2 \leq -1$ and $0 < a_3 \leq 1$ are systematically satisfied through all the energy ranges the relation $E_c = Mc^2 (\gamma_c - 1)$ states a_1 as the critical value for effective acceleration. The acceleration time of particles beginning with this critical value up to the energy E is obtained from Eq. (20) as

$$\begin{aligned}
 t = \frac{1}{\lambda} & \left\{ \ln \left[\left| 2(\gamma^2 - 1)^{1/2} + 2\gamma \right|^{A_1 a_1 + A_2 a_2 + A_3 a_3} \left| \frac{\gamma - a_1}{2(a_1^2 - 1)^{1/2}(\gamma^2 - 1)^{1/2} + 2a_1\gamma - 2} \right|^{A_1(a_1^2 - 1)^{1/2}} \right] \right. \\
 & \left. - \left[A_2(1 - a_2^2)^{1/2} \sin^{-1}\left(\frac{a_2\gamma - 1}{|\gamma - a_2|}\right) + A_3(1 - a_3^2)^{1/2} \sin^{-1}\left(\frac{a_3\gamma - 1}{|\gamma - a_3|}\right) \right] - t(\gamma_c) \right\} \quad (21)
 \end{aligned}$$

where the constants. $A_1 = (a_1 - 1)(a_2 - a_3)/\xi$, $A_2 = (a_2 - 1)(a_3 - a_1)/\xi$ and $A_3 = (a_3 - 1)(a_1 - a_2)/\xi$ emerge from the integration by partial fractions of Eq. (20), with $\xi = a_1^2(a_2 - a_3) + a_2^2(a_3 - a_1) + a_3^2(a_1 - a_2)$, and take on different values according to the energy range concerned;

$\lambda = \alpha$ (if $E \leq 110$ MeV), $\lambda = \alpha - f$ (if $110 < E \leq 290$ MeV) and $\lambda = \alpha - f - \eta$ (if $E > 290$ MeV). The differential spectrum in this case follows from Eqs. (8.1) and (20) as

$$N(\gamma) = \frac{N_0 M c^2}{\tau} e^{t(\gamma_c)/\tau} \left| 2(\gamma^2 - 1)^{1/2} + 2\gamma \right|^{-\delta} \left| \frac{\gamma - a_1}{2(a_1\gamma - 1) + 2(a_1^2 - 1)^{1/2}(\gamma^2 - 1)^{1/2}} \right|^{-\delta_1} \quad (22)$$

$$\exp \left[-\delta_2 \sin^{-1} \left(\frac{a_2\gamma - 1}{|\gamma - a_2|} \right) - \delta_3 \sin^{-1} \left(\frac{a_3\gamma - 1}{|\gamma - a_3|} \right) \right] \frac{(\gamma - 1)(\gamma^2 - 1)^{1/2}}{A\gamma^3 + B\gamma^2 + C\gamma + D}$$

where $\delta = (A_1 a_1 + A_2 a_2 + A_3 a_3)/\lambda\tau$, $\delta_1 = A_1(a_1^2 - 1)^{1/2}\lambda\tau$, $\delta_2 = A_2(1 - a_2^2)^{1/2}/\lambda\tau$ and $\delta_3 = A_3(1 - a_3^2)^{1/2}/\lambda\tau$; therefore, the integral spectrum is given from (Eq. 11) and Eq. (21) as

$$J(> E) = N_0 (M c^2)^2 \left\{ e^{t(\gamma_c)/\tau} \left| 2(\gamma^2 - 1)^{1/2} + 2\gamma \right|^{-\delta} \left| \frac{\gamma - a_1}{2(a_1\gamma - 1) + 2(a_1^2 - 1)^{1/2}(\gamma^2 - 1)^{1/2}} \right|^{-\delta_1} \right. \quad (23)$$

$$\left. \times \exp \left[-\delta_2 \sin^{-1} \left(\frac{a_2\gamma - 1}{|\gamma - a_2|} \right) - \delta_3 \sin^{-1} \left(\frac{a_3\gamma - 1}{|\gamma - a_3|} \right) \right] \exp \left[-t(\gamma_m)/\tau \right] \right\}$$

which in terms of kinetic energy becomes,

$$J(> E) = N_0 \exp \left(\frac{t(E_i)}{\tau} \right) \left\{ \left[\left| \frac{2}{M c^2} \left[(E^2 + 2M c^2 E)^{1/2} + E + M c^2 \right] \right|^{-\delta_1} \left| \frac{2(a_1^2 - 1)(E^2 + 2M c^2 E)^{1/2} + 2a_1 E + 2M c^2(a_1 - 1)}{E + M c^2(1 - a_1)} \right|^{-\delta_2} \right. \right. \quad (23.1)$$

$$\left. \cdot \left(\exp \left[A_2(1 - a_2^2)^{1/2} \sin^{-1} \left(\frac{a_2 E + (a_2 - 1)M c^2}{|E + (1 - a_2)M c^2|} \right) + A_3(1 - a_3^2)^{1/2} \sin^{-1} \left(\frac{a_3 E + (a_3 - 1)M c^2}{|E + (1 - a_3)M c^2|} \right) \right] \right)^{\delta_3} - \exp \left(\frac{-t(E_m)}{\tau} \right) \right\}$$

where

$\delta_1 = \left[(M c^2)^2 / Q \tau \right] (a_1 A_1 + a_2 A_2 + a_3 A_3)$, $\delta_2 = \left[(M c^2)^2 / Q \tau \right] A_1 (a_2 - 1)^{1/2}$, $\delta_3 = (M c^2)^2 / Q \tau$ and $Q, A_1, A_2, A_3, a_1, a_2, a_3$, are constants that depend on α, b, η, h, j and f which emerge from the integration by partial fractions and take different values throughout the three different range considered.

4.4. Modulation by adiabatic processes

Under the consideration of adiabatic deceleration of protons while the acceleration mechanism is acting, the net energy change rate Eq. (20), is transformed by addition of Eq. (6) in

$$\frac{d\gamma}{dt} = \alpha(\gamma^2 - 1)^{1/2} - (M c^2)\gamma(\gamma^2 - 1)^{-1/2} - \left\{ h[M c^2(\gamma - 1)]^{-2} + j[M c^2(\gamma - 1)^{-1} + f + \eta] \right\} \quad (24)$$

$$\times (\gamma^2 - 1)^{1/2} - \rho(\gamma^2 - 1)\gamma^{-1}$$

The condition $(d\gamma/dt) = 0$ for determining γ_c in this case, leads to a transcendental equation of the form $E\gamma^4 + F\gamma^3 + G\gamma^2 + H\gamma + I(\gamma - 1)(\gamma^2 - 1)^{3/2} = 0$, whose solution depends only on α, n and

very weakly on ρ , and where $E = \alpha(Mc^2)^2$, $F = -E - (b + j)Mc^2$, $G = -E - h + bMc^2$, $H = E - h + jMc^2$ and $I = -\rho(Mc^2)^2$ in the range $E \leq 110$ MeV. Therefore, since critical energy for acceleration is defined in the low energy range, the wide interval $1.0 \leq \gamma \leq 1.1$ states a unique value of γ_c for any acceleration parameter α when the values of n and ρ are fixed. In order to deduce the particle spectrum, we have simplified Eq. (24) by changing variable $Z = \gamma - (\gamma^2 - 1)^{1/2}$, thus, obtaining in this way a rational function which integration by partial fractions gives the following acceleration time

$$t = \frac{1}{k} \left\{ \left[\ln \left(|z^2 + R_1z + R_2|^{c_1/2} |z^2 + R_3z + R_4|^{c_3/2} |z^2 + R_5z + R_6|^{c_5/2} |z^2 + R_7z + R_8|^{c_7/2} z^{c_9} \frac{|2z + R_1 - (\Delta_1)^{1/2}|^{k_1}}{|2z + R_1 + (\Delta_1)^{1/2}|} \right) + k_2 \tan^{-1} \left(\frac{2z + R_3}{(-\Delta_2)^{1/2}} \right) + k_3 \tan^{-1} \left(\frac{2z + R_5}{(-\Delta_3)^{1/2}} \right) + k_4 \tan^{-1} \left(\frac{2z + R_7}{(-\Delta_4)^{1/2}} \right) \right] - t(z_c) \right\} \quad (25)$$

where $K_1 = (2C_2 - R_1C_1)/2\Delta_1^{1/2}$, $K_2 = (2C_4 - R_3C_3)/(-\Delta_2)^{1/2}$, $K_3 = (2C_6 - R_5C_5)/(-\Delta_3)^{1/2}$, $K_4 = (2C_8 - R_7C_7)/(-\Delta_4)^{1/2}$; R_1, R_2, \dots, R_8 are the coefficients of the quadratic factors $\Delta_1, \Delta_2, \Delta_3$ and Δ_4 their discriminants, corresponding to two real and six complex roots of the nine roots of the rational function denominator, and C_1, C_2, \dots, C_9 are the coefficients of the linear factors. For a given value of the acceleration efficiency α all the quantities involved in (25) become constants and take on different values according to the three energy intervals studied. The factor κ is given as $\kappa = \alpha + \rho$ (if $E \leq 110$ MeV), $\kappa = \alpha - f - \eta$ (if $110 < E \leq 290$ MeV) and $\kappa = \alpha - f - \eta + \rho$ (if $E > 290$ MeV). As in the preceding cases, the substitution of Eq. (25) in (8') furnishes us with a differential spectrum of the form

$$N(\gamma) = \frac{N_0}{Mc^2\kappa\tau} e^{t(z_c)/\tau} \left(\frac{-z^8 + 2z^7 - 2z^5 + 2z^4 - 2z^3 + 2z - 1}{z^8 + Jz^7 + Mz^6 + Nz^5 + Pz^4 + Qz^3 + Rz^2 + Sz + V} \right) \times \left\{ \left(|z^2 + R_1z + R_2|^{-\theta_1} |z^2 + R_3z + R_4|^{-\theta_2} |z^2 + R_5z + R_6|^{-\theta_3} |z^2 + R_7z + R_8|^{-\theta_4} \times \frac{|2z + R_1 - (\Delta_1)^{1/2}|^{-\theta_5}}{|2z + R_1 + (\Delta_1)^{1/2}|} z^{-\theta_6} \right) \exp \left[\theta_7 \tan^{-1} \left(\frac{2z + R_3}{(-\Delta_2)^{1/2}} \right) + \theta_8 \tan^{-1} \left(\frac{2z + R_5}{(-\Delta_3)^{1/2}} \right) + \theta_9 \tan^{-1} \left(\frac{2z + R_7}{(-\Delta_4)^{1/2}} \right) \right] \right\} \quad (26)$$

$\Theta_1 = c_1/2\kappa\tau$, $\Theta_2 = c_3/2\kappa\tau$, $\Theta_3 = c_5/2\kappa\tau$, $\Theta_4 = c_7/2\kappa\tau$, $\Theta_5 = K_1/2\kappa\tau$, $\Theta_6 = c_9/2\kappa\tau$, $\Theta_7 = (-K_2)/\kappa\tau$, $\Theta_8 = (-K_3)/\kappa\tau$ and $\Theta_9 = (-K_4)/\kappa\tau$, $J = 2(F + I)/V$, $M = (4E + 4G + 2I)/V$, $N = (6F + 8H - GI)/V$, $P = (GE + 8G)/V$, $Q = (GP + 8H + GI)/V$, $R = (4E + 4c - 2I)/I$, $S = 2(F - I)/V$, $V = (E + I)/V$ and $V = E - I$. The values of E, F, G, H, I in the range $E < 110$ MeV are the values given above; in the range $110 < E \leq 290$ MeV, $E = (\alpha - f)(Mc^2)^2$, $F = E - bMc^2$, $G = -E + bMc^2$, $H = E - h$ and $I = \rho(Mc^2)^2$. In the range $E > 290$ MeV the only difference with the precedent range is $E = (\alpha - f - \eta)(Mc^2)^2$. The constant $t(Z_c)$ is the evaluation of (25) in the threshold value $Z_c = \gamma_c - (\gamma_c^2 - 1)^{1/2}$. The integral spectrum according Eq. (11) is,

$$\begin{aligned}
J(> E) = N_0 e^{t(z_c)/\tau} \left\{ \left(|z^2 + R_1 z + R_2|^{-\theta_1} |z^2 + R_3 z + R_4|^{-\theta_2} |z^2 + R_5 z + R_6|^{-\theta_3} |z^2 + R_7 z \right. \right. \\
+ R_8|^{-\theta_4} \left. \left. \frac{|2z + R_1 - (\Delta_1)^{1/2}|^{-\theta_5}}{|2z + R_1 + (\Delta_1)^{1/2}|} |z^{-\theta_6}| \right) \exp \left[\theta_7 \tan^{-1} \left(\frac{2z + R_3}{(-\Delta_2)^{1/2}} \right) + \theta_8 \tan^{-1} \left(\frac{2z + R_5}{(-\Delta_3)^{1/2}} \right) \right. \right. \\
\left. \left. + \theta_9 \tan^{-1} \left(\frac{2z + R_7}{(-\Delta_4)^{1/2}} \right) \right] - \exp(-t(z_m)/\tau) \right\} \quad (27)
\end{aligned}$$

where $t(Z_m)$ is the evaluation of Eq. (25) in $Z = \gamma_m - (\gamma_m^2 - 1)^{1/2}$ corresponding to the high energy cutoff value in the acceleration process.

In order to express the previous equation as a function of the kinetic energy E , the variable Z should be written as $Z(E) = (E + Mc^2) - (E^2 + 2EMc^2)^{1/2}$ and $Z(E)_m = (E_m + Mc^2) - (E_m^2 + 2E_m Mc^2)^{1/2}$.

It is also interesting to analyze the opposite case, when instead of an expansion of the source materials, there is a compression of the source medium (e.g. [101–103]) with a consequent adiabatic acceleration of the flare particles, which entail a change of sign in the last term of the net energy change rate (24). Let us develop the situation for which energy losses are completely negligible in relation to the acceleration rate during the stochastic particle acceleration and compression of the local material

$$(d\gamma/dt) = \alpha(\gamma^2 - 1)^{-1/2} + \rho(\gamma^2 - 1)\gamma^{-1} \quad (28)$$

As in the case of Eq. (12) the threshold for acceleration is meaningless, and thus the acceleration time up to the energy E is given as

$$t = \ln \left(\left| \frac{\gamma}{\alpha\gamma + \rho(\gamma^2 - 1)^{1/2}} \right|^{\chi} \left| \frac{\gamma + (\gamma^2 - 1)^{1/2}}{\gamma - (\gamma^2 - 1)^{1/2}} \right|^{\psi} \gamma^{\omega} |\alpha|^{\chi} \right) \quad (29)$$

where $\chi = \frac{\rho}{(\alpha^2 - \rho^2)}$, $\psi = \frac{\alpha}{2(\alpha^2 - \rho^2)}$ and $\omega = \frac{\rho}{\rho^2 - \alpha^2}$, consequently, the differential spectrum of particles is

$$N(\gamma)d\gamma = \frac{N_0}{mc^2\tau|\alpha|^{\chi/2}} \left| \frac{\gamma}{\alpha\gamma + \rho(\gamma^2 - 1)^{1/2}} \right|^{-\chi/\tau} \left| \frac{\gamma + (\gamma^2 - 1)^{1/2}}{\gamma - (\gamma^2 - 1)^{1/2}} \right|^{-\psi/\tau} \frac{\gamma^{(1-\omega/\tau)} d\gamma}{(\gamma^2 - 1)^{1/2} [\alpha\gamma + \rho(\gamma^2 - 1)^{1/2}]} \quad (30)$$

and then the integral spectrum is simply given as

$$J(> E) = \frac{N_0}{|\alpha|^{\chi/2}} \left(\left| \frac{\gamma}{\alpha\gamma + \rho(\gamma^2 - 1)^{1/2}} \right|^{-\chi/\tau} \left| \frac{\gamma + (\gamma^2 - 1)^{1/2}}{\gamma - (\gamma^2 - 1)^{1/2}} \right|^{-\psi/\tau} \gamma^{-\omega/\tau} - e^{-t(\gamma_m)/\tau} \right) \quad (31)$$

which in terms of kinetic energy becomes,

$$J(> E) = \frac{N_0}{|\alpha|^{\chi/2}} \left(\left| \frac{E + Mc^2}{\alpha(E + Mc^2) + \rho(E^2 + 2EMc^2)^{1/2}} \right|^{-\chi/\tau} \left| \frac{(E + Mc^2) + (E^2 + 2EMc^2)^{1/2}}{(E + Mc^2) - (E^2 + 2EMc^2)^{1/2}} \right|^{-\psi/\tau} \right) \left[(E + Mc^2)/Mc^2 \right]^{-\omega/\tau} - e^{-t[(E_m + Mc^2)/Mc^2]/\tau} \quad (31.1)$$

It is worth mentioning that although it is expected that the critical energy for acceleration E_c increases while adding energy loss process to the net energy charge rate, nevertheless, the value of E_c resulting from Eq. (24) is essentially the same as that obtained from Eq. (20). This can be understood from **Figure 1**, because adiabatic cooling is practically negligible at low energies.

5. Procedure and results

As seen in the preceding section, the calculation of our theoretical spectra, Eqs. (15),(19), (23), (27) and (31) requires three fundamental parameters, one of them directly related to the physical state of flare regions, that is, the medium concentration n , and the others concerning the acceleration mechanism itself, that is, the acceleration efficiency α and the mean confinement time τ . These last two depend of course on some of the physical parameters of the source, which we attempt to estimate from the appropriate values of α and τ . In the case of the solar source, we have considered the mean value of the electron density and a conservative value for the proton population as $n_e \approx n_H = 10^{13} \text{ cm}^{-3}$ (e.g. [19, 35, 56, 113, 114, 116, 118]).

This assumption locates the acceleration region in chromospheric densities in agreement with some analysis of the charge spectrum of solar cosmic rays [64, 92].

Besides, since our expressions contain the acceleration parameter as the product $\alpha\tau$ and since we are dealing with particles of the same species, for the sake of simplicity we have adopted the assumption $\tau = 1 \cdot s$ which allows us to separate the behavior of the acceleration efficient α in order to analyze it through several events and several source conditions. In any event, this value falls within the generally accepted range (e.g. [130, 131]); we shall discuss the implications of this assumption in the next section.

The determination of α has been carried out through the following procedure: in order to represent the theoretical spectrum within the same scale as that of the experimental curve, we have normalized both fluxes at the minimum energy for which available experimental data are effectively trustworthy, in such a way as to state the maximum flux of particles at the normalization energy, E_{nor}

$$[J(> E)_{acc}]_{E_{nor}} = q [J(> E)_{earth}]_{E_{nor}} \quad (32)$$

where q is the normalization factor. Since our expressions do not directly furnish the source

integral spectrum but rather $J(>E)/N_0$, we have deduced in this way a normalization flux K_0 , keeping the same proportion with the differential flux N_0 appearing in our expressions

$$N_0 = qk_0 = \text{protons}/4\pi R_{SE}^2 s \quad (\text{protons}/\text{cm}^2 \text{ str } s) \quad (33)$$

where $R_{SE} = 1.5 \times 10^{13} \text{ cm} = \text{sun-earth distance}$. We have listed E_{nor} for every event on columns 8 of **Tables 1–3**.

The value of N_0 for every event is tabulated on columns 10 of **Tables 1–3**.

Assuming that the theoretical curve among Eqs. (15), (19), (23), (27) and (31) is near the experimental curve in a given event, describes the kind of phenomena occurring at the source better, we have proceeded to perform this intercomparison according to the following criterion: first, the condition stated by Eq. (32) at the normalization energy and, second, that $J(>E) \approx 0$ at the high energy cutoff E_m . In order to compare each one of the theoretical spectra with an experimental curve under the same conditions, we could proceed to fix the value of the acceleration

Hot Events		Spectrum (31)	Spectrum (15)	Spectrum (19)	Spectrum (23)	Spectrum (27)	E_m (GeV)	E_n (MeV)	N_0 (protons/ $\text{m}^2 \text{ s str}$)
28/01/1967	$\alpha(s^{-1})$	0.18	0.18	0.19	0.23	0.21	4.30	10.00	2.1×10^{-12}
	E_c (MeV)	*****	*****	5.26	11.57	12.67			
01/09/1971	$\alpha(s^{-1})$	0.21	0.21	0.22	0.24	0.23	2.30	30.00	9.9×10^{-13}
	E_c (MeV)	*****	*****	4.54	11.09	11.57			

Table 1. Characteristic parameters of the acceleration process in solar protons *hot* events: acceleration efficiency α , high energy cutoff E_m , normalization energy E_n , flux of accelerated particles in the source N_0 and heliographic coordinates of the flare according to different reports.

Hot Events		Spectrum (31)	Spectrum (15)	Spectrum (19)	Spectrum (23)	Spectrum (27)	E_m (GeV)	E_n (MeV)	N_0 (protons/ $\text{cm}^2 \text{ s str}$ MeV)
12/11/1960	$\alpha(s^{-1})$	0.13	0.14	0.17	0.26	0.26	2.600	15.000	3.891×10^{-11}
	E_c (MeV)	15.32	14.30	13.45	9.67	10.58			
04/08/1972	$\alpha(s^{-1})$	0.59	0.50	0.70	0.90	0.93	4.280	15.000	1.979×10^{-11}
	E_c (MeV)	4.28	4.21	3.87	3.06	2.97			
03/09/1960	$\alpha(s^{-1})$	0.72	0.73	0.83	0.98	0.99	2.960	10.000	4.704×10^{-16}
	E_c (MeV)	2.96	2.92	2.77	2.40	2.39			
30/03/1969	$\alpha(s^{-1})$	0.91	0.92	0.95	0.99	1.08	2.340	50.000	1.449×10^{-15}
	E_c (MeV)	2.34	1.18	2.42	2.38	2.48			
02/11/1969	$\alpha(s^{-1})$	1.54	1.55	1.76	2.10	2.59	0.915	10.000	2.342×10^{-11}
	E_c (MeV)	0.84	0.84	0.81	0.66	1.05			

Table 2. Characteristic parameters of the acceleration process in solar protons *cold* events: acceleration efficiency α , high energy cutoff E_m , normalization energy E_n , flux of accelerated particles in the source N_0 and heliographic coordinates of the flare according to different reports.

Hot Events		Spectrum (31)	Spectrum (15)	Spectrum (19)	Spectrum (23)	Spectrum (27)	E_m (GeV)	E_n (MeV)	N_0 (protons/ $\text{cm}^2 \text{ s str}$ MeV)
15/11/1968	$\alpha(\text{s}^{-1})$	0.16	0.16	0.18	0.23	0.25	2.60	20.00	4.550x10-13
	$E_c(\text{MeV})$	*****	*****	12.68	11.22	11.03			
18/11/1968	$\alpha(\text{s}^{-1})$	0.20	0.20	0.21	0.26	0.28	4.80	20.00	6.400x10-11
	$E_c(\text{MeV})$	*****	*****	13.17	11.62	10.84			
07/07/1966	$\alpha(\text{s}^{-1})$	0.23	0.23	0.35	0.36	0.39	2.70	10.00	1.376x10-16
	$E_c(\text{MeV})$	*****	*****	2.85	7.40	6.83			
24/01/1971	$\alpha(\text{s}^{-1})$	0.34	0.34	0.35	0.39	0.41	6.90	40.00	1.365x10-12
	$E_c(\text{MeV})$	*****	*****	6.90	6.62	6.56			
25/02/1969	$\alpha(\text{s}^{-1})$	0.40	0.40	0.41	0.46	0.48	6.57	30.00	6.300x10-15
	$E_c(\text{MeV})$	*****	*****	6.57	6.18	6.14			

Table 3. Characteristic parameters of the acceleration process in solar protons *warm* events: acceleration efficiency α , high energy cutoff E_m , normalization energy E_n , flux of accelerated particles in the source N_0 and heliographic coordinates of the flare according to different reports.

parameters in advance, which would entails making a priori inferences about the physical parameters of the source involved in the acceleration process of a given solar event; furthermore, this would result in a bias for the interpretation of the phenomenology involved in each event depending on the selected value of the efficiency α ; that is, high values would give systematically the best fit with spectrum (27), whereas low values would show a systematically better fit with spectrum (15). Therefore, we proceeded conversely by determining the appropriate parameters of the source from the value of α in the theoretical spectra that best represents the experimental curve. The optimum values of α , obtained for each of the theoretical curves allows us to determine the critical energy E_c and the normalization flux K_0 appropriate to each case. We have tabulated the values of α , E_c and K_0 obtained for every event through calculations of the spectra (15) (19), (23), (27) and (31) in **Tables 1–3**. We have illustrated the optimum theoretical curves on **Figures 2–4**. From an examination of these results, it can be observed that no general conclusion can be drawn about the behavior of our theoretical spectra by the simple comparison of energy change rates (1), (2), (4) or (6) at different energy values 7 as if the medium density n were the only important parameter in determining the processes occurring at the source. Other factors must intervene, as can be seen from the fact that spectra behavior changes from event to event. Nevertheless, according to the behavior of particle spectra, we can group the solar events in three groups of similar characteristics: those illustrated in **Figure 2**, which we shall denominate *hot events*, where it can be seen that theoretical spectra progressively approach the experimental curves while adding energy loss processes to the acceleration rate. Therefore, the physical processes taking place at the source in those events are described by spectrum (27) indicating that adiabatic cooling of protons together with energy degradation from p - p collisions and collisional losses may have taken place. In this case spectrum (31) (illustrated only in the January 28, 1967 event) is systematically the more deflected curve, showing the absence of adiabatic compression, at least during the acceleration period. **Figure 3** shows the second group which we will call *cold events*, and

where it can be seen that energy losses are not important within the time scale of the acceleration process because theoretical curves get progressively separate from the experimental one while adding energy loss processes. Actually the best systematic approach in these cases is obtained with spectrum (31) (illustrated only for November 12, 1960 event) indicating that acceleration of protons by adiabatic compression could have taken place. The third group that we shall distinguish as *warm* events is represented in **Figure 4**, where we can observe that there is no systematic tendency as compared to the previous groups. Nevertheless, it can be seen that at least at low energies the best approach to the experimental curve is described by spectrum (23), whereas at high energies the best fit is obtained with spectrum (15), thus indicating that to greater or lesser degree energy losses by collisional losses and proton-proton collisions may be important on low energy protons but they become negligible in relation to the acceleration rate in high energy particles. The point where this change may occur varies from very low energies in some events (July 7, 1966) to very high energies in others (January 24, 1971). The larger deflection from the experimental curve in these cases is obtained with spectrum (27), indicating that adiabatic expansion do not take place; furthermore, the fact that spectrum (31) (illustrated only for the November 18, 1968 event) is systematically deflected in relation to the acceleration spectrum (15) indicates that there is no adiabatic compression either. The values of the parameters describing the most adequate theoretical spectrum of events of **Figures 2–4** are tabulated on columns 7, 3 and 6 of **Tables 1–3**, respectively.

In order to estimate the amount of local plasma particles that must be picked up by the acceleration process to produce the observed spectrum, we must know the value of N_0 in (8) when $t = 0$. Therefore, roughly assuming that at least for events of (**Figure 3, Table 2**), the picked up protons originate in a thermal plasma where the velocities distribution is of a Maxwellian-type, or that they appear from a preliminary heating related to turbulent thermal motions, then, it can be inferred that the primary differential flux is given as, related with the flux defined in Eq. (33).

$$N_0 = \left[9/(2\pi)^{3/2} \right] (k/M)^{1/2} e^{3/2} n T^{1/2} \quad (34)$$

where M is the mass of protons and k the of Boltzman's constant. Then, by assuming that K_0 is related to the flux of protons involved in the acceleration process and the flux N_0 related to the original concentration of the medium, we have estimated from Eq. (33) the fraction of the local plasma particles that were accelerated in each event and tabulated them on columns 10 of **Tables 1–3**. In evaluating (34), we have assumed a different value of temperature T for each one of the 3 groups of events, before discussing them in the next section.

Now let us summarize the results which emerge from **Figures 2–4** and **Tables 1–3**, before extending their interpretation in next section:

1. The events illustrated in **Figure 2**, show the following features:

- i. In September 1, 1971 event, the best fit of the experimental spectrum is obtained with

(27) whereas the worst fit is given by (15) and (31).

- ii. The January 28, 1967 event follows the same tendency as the preceding event up to ~ 800 MeV, with an exception at very low energies (≤ 30 MeV) where it can be seen that spectrum (23) is slightly better than (27). Beyond ~ 800 MeV spectrum (23) becomes the more deflected curve. The low particle energy flux tail is noticeably similar to the minimum theoretical energy for effective acceleration ($E_c \sim 12$ MeV).

2. The events of **Figure 3** show that:

The best fit of the experimental curve is systematically given by spectrum (31) and (15) (e.g. the November 12, 1960 event), whereas spectrum (27) is systematically the most deflected one.

3. The events of **Figure 4** show the following characteristics

- a. The theoretical curve which best approximates the experimental one at low energies is spectrum (23) followed by spectrum (19).
- b. At given energy (from ~ 500 to ~ 3000 MeV) the previous tendency is abandoned, such that spectrum (15) interchanges sequential order with spectrum (23).
- c. Spectrum (27) is systematically the most deflected curve at all energies.
- d. Spectrum (31) is systematically deflected in relation to spectrum (15) (e.g. November 18, 1968 event).
- e. The July 7, 1966 event, however, by following the feature (a) at $E \leq 25$ MeV, beyond this energy spectrum (15) comes nearer to the experimental curve than spectrum (23), whereas spectrum (19) through a progressive, separation becomes the most deflected curve beyond ~ 2000 MeV.

4. Examination of **Tables 1–3** shows the following features:

- a. For a given event the obtained value of acceleration efficiency α is the same with spectrum (31) and (15) (columns 3 and 4 of **Tables 1** and **3**) contrary to the events of **Table 2**, in which case α is lower with spectrum (31) than with (15).
- b. Examination of a given spectrum (same column 5, or, 6 or 7) shows that α and E_c behave in an inversely proportional manner.
- c. For a given event, the values of α in the events of **Tables 2** and **3** (columns 4, 5, 6, and 7) increase monotonically while adding energy loss processes to the acceleration rate, with the exception of the events of **Table 1**, in which case the obtained values of α with spectrum (27) decrease in relation to the value of α from spectrum (23).
- d. For a given event of **Table 1**, the value of E_c increases monotonically with the addition of an energy loss process to the net energy change rate, whereas in the events of **Tables 2** and **3** the value of E_c obtained from (27) (column 7) decreases in relation to the values obtained from spectrum (23).
- e. The obtained value of K_0 , (column 10) is related only to the magnitude of the event (i.e. the value of $J(>E)$ at E_n).
- f. There is no correlation between E_m and the other parameters of the tables α , E_c , K_0 , or heliographic coordinate; neither is there any correlation between the maximum flux at E_n and α or E_c .

- g. If we ignore the fact that the assumed heliographic position of the flare associated to the January 28, 1967 event is relatively uncertain, it can be noted that there is a south asymmetry in the what we designate as *hot events* (**Table 1**), a north asymmetry in *cold* and *warm events* (**Table 2**) and a certain west and north asymmetry among the events of **Table 3**.
- h. The critical energy E_c from *cold* and *warm* events is correlated with the temperature of the source in the sense that their values increase from *cold* to *warm* and from *warm* to *hot* events. The significance of the association of the parameter temperature to solar proton events will be discussed in Section 6.

6. Discussion

It has been said that we cannot give a general interpretation of our theoretical source spectra behavior on the sole basis of the relationships between the energy change rates (1)–(6) since their behavior in the events of **Figure 2** is different from that in **Figure 3** and both differ from that in **Figure 4**, implying that the kind of processes, their sequence of occurrence and their importance is not the same from event to event. To interpret this behavior we cannot remit ourselves to the amount of traversed material, positing that particles originated in the invisible side of the sun or in the eastern hemisphere have lost more energy, because in that case events as such as the March 30, 1969 or February 2, 1969 ones would behave like the events of **Table 1**. Moreover, our hypothesis does not consider deceleration of particles after acceleration, while they traverse the solar atmosphere. Therefore, we believe that the explanation is on the basis of the parameter temperature: that is, we argue that solar proton flares develop under three main different temperature regimes, a low one that we shall denominate *cold* events ($T \approx 10^3 - 10^5$ K) (**Table 3**), an intermediate regime that we shall call *warm* events ($\approx 10^5 - 10^7$ K) (**Table 4**), and a high temperature regime that we shall call hereafter *hot* events ($T > 10^7$ K) (**Table 3**). On the basis of this conjecture, let us discuss the main results of the preceding section:

Concerning points 1(a), 1(b) and 1(c), we can comment that as the medium was very hot, collisional losses were very high, making spectrum (18) better than spectrum (15); due to the high temperature and high density in the source nuclear reactions took place and thus spectrum (23) is even closer than (18) to the experimental curve.

Furthermore, the fact that the best fit is given by (27) seems to indicate that beyond a certain temperature, the source material is able to expand and consequently particles which have not escaped the source are adiabatically cooled. In addition, since spectrum (15) is better than (31) it is assumed that compression of the medium did not take place in high temperature regions, and so neither did adiabatic heating of protons. The irregular behavior of spectrum (23) at $E \leq 30$ MeV and $E \geq 800$ MeV in the January 28, 1967 event in relation to the tendency outlined in the last section, may be interpreted as indicating that the low energy protons observed in this event did not originate in the same process, which explains why the observations show a high flux of protons at energy lower than the threshold acceleration value for in a medium of density $n \approx 10^{13} \text{ cm}^{-3}$. Therefore, these particles may form part of the high energy tail of a preliminary heating process which were not transported by the expanding material. This

would mean that only deceleration by collisional losses and p - p collisions took place during the acceleratory process. At high energies, although energy losses from p - p collisions are stronger than collisional losses (**Figure 1**), it can be speculated that the low flux of high energy protons escape very fast from the acceleration region, so that the contribution of this process at high energies was not very important during the time scale of the acceleration.

Concerning point 2 of the last section, we assume that the acceleration process in the events of **Figure 3** was carried out in a low temperature regime so that collisional losses were completely unimportant in relation to the acceleration rate, and nuclear reactions did not take place, at least within the acceleration phase. Furthermore, a compression of the local material is associated with low temperature regimes as indicated by the fact that spectrum (31) systematically gives the best fit to the experimental curves (e.g. November 12, 1960 event).

Points 3(a)–3(d) are interpreted as follows: the temperature and density associated with the acceleration region was high enough to favor nuclear reactions, but not the expansion of source material; consequently, collisional losses of low energy protons were important in the events of **Figure 4**, providing spectrum (23) with a better description of the experimental curve. Also, because the higher temperature does not allow for a compression of the material, spectrum (31) is systematically deflected in relation to spectrum (15). Furthermore, the sudden change in the order of the sequence of curves (15) (19) and (23) is the combined effect of the temperature associated to each event and the importance of the accelerated flux of high energy protons as discussed above with respect to the January 28, 1967 event; the lower the temperature the faster spectrum (19) deflects in relation to (15) (e.g. the November 15, 1960 and November 18, 1968 events); and the higher the flux of the accelerated high energy protons, the later spectrum (23) deflects in relation to (19) (e.g. the February.25, 1969 and January 24, 1971 events).

Related to point 3(e) of last section, it would appeal that the temperature associated with this event was not very high, so that collisional losses were significant only on the low energy protons. Because of the low flux of the accelerated protons in this event, the effect of p - p collisions diminishes as energy increases. This event behaves almost like the cold events of **Figure 3**, since energy losses are negligible in relation to the acceleration rate of high energy protons. The reason why beyond 2 GeV spectrum (19) is more deflected than (27) is that the latter includes the p - p contribution to this event and collisional losses are unimportant on high energy particles (**Figure 1**). Interpretation of 3(b) and 3(e) must also consider the fact that high energy particles escape faster from the acceleration volume, and so, they are subject to energy degradation by p - p collisions during the acceleration time.

The interpretation of 4(a) follows from the fact that in cold events the contribution of the adiabatic heating is translated into a lower effort of the acceleration mechanism; however, in the hot and warm events (**Tables 1** and **3**) adiabatic heating did not occur, and so no effect was produced.

In relation to the interpretation of 4(b) to 4(d) it must be pointed out that the inverse proportionality between α and E_c follows from the fact that for a given situation the requirement for effective acceleration is lowered while the acceleration efficiency becomes progressively higher. On the other hand, the addition of energy losses to a given situation (same row in the

Tables) generally entails an increase in the requirement of energy E_c , and thus an increase of α in order to exceed the new barrier. However, the irregularities synthesized in points 4(c) and 4(d) of last section, which can be seen on **Tables 1–3**, that may be explained in the following manner: the critical energy, E_c is defined at low energies where the effect of adiabatic deceleration is negligible in relation to the other processes involved (**Figure 1**), and thus for a same value of α the values of E_c from (19) and (23) are remarkably similar. Nevertheless, the decrease of the values of α in column 7 of **Table 1** may be explained by the fact that although the requirement for acceleration is the same, as in column (6), a supplementary process is acting on the particles, and efficiency of the process is being lowered. Since E_c and α behave inversely, the value of E_c appears to increase; but in fact the real value of E_c in this event was ~ 11.6 MeV. Besides, we see from columns 6 and 7 of **Tables 2** and **3** that under the hypothetical situation of the presence of adiabatic cooling in these events, the efficiency α appears higher in relation to that of column 6, given that there is an additional barrier to overtake. The value of E_c should behave similarly, but since the value of E_c in (13) is the same as that in (19), then, this hypothetical increase of α shown in column 7 in relation to that of column (6) implies a decrease of the value of E_c in column 7; this in fact does not occur because adiabatic cooling did not take place and thus the real values of α and E_c in events of **Tables 1** and **3** were those of columns 3 and 6 respectively. The interpretation of 4(e) follows from the definitions of Eqs. (31) and (32), whereas points 4(f) and 4(g) cannot have a coherent interpretation, what can be attributed to the complexity and variability of conditions from flare to flare (e.g. the medium density, temperature, conductivity, magnetic field strength, magnetic topologies, etc.). In relation to point 4(h) it must be mentioned that deduce the same result by discussing three main different temperature regimes in the acceleration region of solar particles [105]; they estimate threshold values for proton acceleration of 1, 2.7 and 5.5 MeV for a cold region, an intermediate one and a hot region. These values are slightly lower than ours, since they do not take into account all the energy loss processes we did. In any event, as we discussed previously, the threshold value E_c increases with the temperature because energy loss processes are increased with this parameter.

In addition to the suggestion of three temperature regions in acceleration regions extended by [105], several other suggestions have been presented in this direction: the author in [78] has discussed temperatures of 10^4 K suggested by the central peak of hydrogen emission lines, up to more than 10^8 K suggested by thermal emissions of X-rays. Furthermore, the flare phenomenon has usually been interpreted on basis of a dual character): the optical flare of $T \sim 10^4$ K and high electron density, and on the other hand, the high energy flare plasma of $T \sim 10^7 - 10^9$ K and relatively low electron density. The existence of several temperature regimes during a given flare has also been evoked by suggesting that the emitting regions have a filamentary and intermingling structure with hot filaments about 1 km. of diameter imbedded in cooler material [113, 115], or by suggesting a cooling of a hot region during the flare development [17, 135]. Some other models for explaining the flare energy output suggest several phases of the phenomenon, each associated with a different temperature; for example, a of relatively low temperature thermal phase followed by an explosive high temperature phase [13, 50, 51, 52, 111] posit similar models. We have not attempted to place our results into the framework of what of any of these interpretations of the flare phenomenon, but rather only to demonstrate that the generation of solar particles is accompanied by, several processes whose occurrence is narrowly related to, the

temperature of the medium, and to suggest that the acceleration regions must be associated alternately with the hot and cold aspects present during a flare or even in a pre-flare state, but certainly under very different temperature regimes from flare to flare.

Related with the expansion and compression of the source medium, there are some observational indications [84] which propose a minimum value of $\sim 3 \times 10^7$ K for expansion. The author in [102, 103] has studied hydromagnetic criteria for expansion and compression of the sunspot magnetic lines, which he distinguishes as two different phases of the flare development; although he shows that sometimes the expansion phase may not present itself according to our findings such as we found in warm and cold events. However, in Sakurai's model acceleration occurs during the compression phase, whereas our results indicate that expansion of the source material may also occur during the acceleration process; moreover, our analysis does not show indications of expansion and compression during the same event during the phase of particle acceleration. Nevertheless, we see that, with exception of the November 12, 1960 event, the acceleration efficiency is very high where there is a compression (cold event), presumably due to the strong spatial variations of the of the longitudinal and transversal field lines, as suggested by [101, 102].

It must be emphasized that we have taken into account that expansion of closed structures occurs only within a height lower than ~ 0.6 to 1 solar radius, and thus expansions beyond this distance may be associated with propagation of shock waves generated in relation to type II burst or CME; therefore, our assumptions concern only adiabatic cooling through the local expansion of the source and not in higher the solar envelope.

In the specific case of the November 18, 1968 event, for which our results do not indicate any expansion of the source, observations reported a loop expansion; however s it is usually supported the fact that there is no mass motion but only a traveling excitation front. It must also be mentioned that it is generally accepted that low energy protons are much more likely to be subject to adiabatic cooling since high energy protons are rather dominated by drifts and scattering in field inhomogeneities [27, 33]; Moreover, according to [131, 132, 133] adiabatic deceleration disappears as the density of the accelerated particles decreases, so that when particle velocity is much higher than both the velocity of the medium and the Alfvén velocity, the adiabatic cooling is null. This would imply that in the case of our hot events (**Figure 2**) protons of energy much higher than ~ 670 MeV should not be adiabatically cooled in a medium of $T > 10^8$ K, however, our results show that even higher energy protons were adiabatically decelerated. Therefore, we claim that at least in these two events, our results support the hypothesis that particles were accelerated in closed magnetic field lines with high confinement efficiency.

Now turning to the problem of p - p nuclear collisions in some solar flares: we had mentioned that the value of $N_H \sim 10^{13} \text{ cm}^{-3}$ was an average value in flare regions, since in fact concentrations as high as 10^{16} cm^{-3} have been reported (e.g. [118]) which implies that Eq. (23) and Eq. (27) will remain near the observational curves. This feature leads us to speculate that some flares have a high proton concentration medium (e.g. January 24, 1971), whereas in others the concentration is much lower (e.g. July 7, 1966), and that a great spread in high energy gamma rays and neutron fluxes is expected from flare to flare. The difference between observational and theoretical fluxes of gamma ray and neutrons is not a matter of discussion here, we only

want to note that these fluxes are mainly generated from the most energetic protons which are in fact the first to escape and do not frequently interact with the medium, as discussed previously in relation with some events of **Figures 2** and **4**. This implies that depending on the magnetic confinement efficiency in each flare, the expected flux of the secondary radiation will be of greater or lesser importance. According to **Figures 2** and **4** a high gamma ray flux must be generated in the February 25, 1969, January 24, 1971 and September 1, 1971 events, whereas a lower flux should be expected from the July 7, 1966 event and no gamma-ray fluxes from nuclear collision in the acceleration volume must be expected in the events of **Figure 3**. The variability of the expected high energy gamma-ray fluxes has been previously discussed in [25]. Concerning neutron fluxes we argue that they are strongly absorbed by a neutron capture reaction ($n + H_e^3 \rightarrow H^3 + p$).

It must be pointed out that the need of protons for a minimum energy in order to overtake energy losses and to be accelerated upwards, measured energies may not be a strong requirement since the temporal and spatial sequence of phenomena in a flare seem to indicate the occurrence of a two-step acceleration of solar particles (e.g. [19, 16, 123]). A great variety of preliminary acceleration processes capable of accelerating particles up to some MeV has been suggested (e.g. [104, 112], etc.). It can be assumed that a certain portion of the low energy tail of the particle spectrum may belong to the first acceleration step. By smoothing the experimental data we have obtained a peculiar shape for this low energy tail of some spectra, although a similar shape is predicted from the theoretical point of view [5]. Moreover, authors in [94] discuss a noticeable deviation of the power spectrum below ≈ 4 MeV in low energy proton events, which they attribute to collisional losses during storage in the ionized medium of the low corona. We are aware of the difficulty of estimating the exact shape of the low energy spectrum, due to the strong modulation of these particles either within or outside of the source. Therefore, we argue that in addition to energy losses, this particular slope change in the low energy tail of some spectra may be due to an upper cutoff in the preliminary acceleration process.

Now let us discuss the assumption made in Section 5 in taking τ as a constant value: although it is expected that the mean confinement time varies according to particle rigidity, it is not clear if the escape mechanism from the source occurs through leakage, by thin or thick scattering, by curvature drifts, by gradient drifts or even by a sudden catastrophic disruption of a closed magnetic structure at the source; therefore, we opted for a mean value $\tau = 1$ sec. Whose implications can be seen as follows: we note from Eq. (11) that if the value of τ increases, then $J(>E)$ increases, whereas if τ decreases, then $J(>E)$ decreases and so the theoretical spectra will approximate the experimental curves. At any rate, what can be deduced is that if τ is either lower or higher than the assumed value, the sequence of theoretical spectra does not change or consequently our conclusions are not altered. In order to evidence that the value of τ is in general of the order assumed, we shall develop the following considerations: if we make the extreme assumption that acceleration of solar protons is performed by a low efficiency process, such as a second-order Fermi-type mechanism then we know that in these cases the acceleration efficiency is given as $\alpha = V_a^2/v\iota$, where v is the velocity of protons, ι the acceleration step within the acceleration volume, and V_a the hydromagnetic velocity of the magnetic field irregularities. Taking into account that our values of α in a given event can be considered as

an average value for different energies of protons, we shall estimate the average value of ι for a 50 MeV proton and assume that the value of ι is typical of the acceleration region configuration; hence for a field strength of 500 G and density $n = 10^{13} \text{ cm}^{-3}$, the extreme values of α obtained are $\alpha = 0.1$ and 1.54 s^{-1} leading to the following values: $\iota = 10 \text{ Km}$ and 0.84 Km respectively, which are of the same order as the values found by Perez-Peraza (1975) for multi-GeV solar protons. To estimate τ in a magnetic field (H) where the field gradient is $\approx H/\iota$, we use the fact that $\tau = L^2 / v\iota$, where L is the linear size of the acceleration region; an approximate value of L may be deduced by the fact that the volume of flare regions varies from 10^{25} to 10^{29} cm^3 from flare to flare [19, 54, 55], and hence a linear dimension of $\sim 10^9 \text{ cm}$ may be considered as a typical value [30, 31] Assuming that the acceleration volume cannot be greater, than the flare volume, we shall consider $L = 10^8 \text{ cm}$ as a typical linear dimension for acceleration regions [116]. In such conditions we obtain $\tau = 1$ and 12.6 s . for solar events where $\alpha = 0.13$ and 1.54 s^{-1} respectively. We should say that if a shorter length scale L than the assumed one were taken values of $\tau < 1$ could be obtained, and hence our theoretical fluxes $J(>E)$ would come closer to experimental curve as discussed above. In fact, it can be observed in **Figure 3**, that the theoretical curve corresponding to $\alpha = 0.13$ and thus to a low value of τ (the November 12, 1960 event) is nearer the experimental curve than to the theoretical curve corresponding to higher values of α , where it is supposed that τ must be higher. It must be noted that a higher value of α in one event with respect to another event does not imply a shorter escape time for particles in the former with respect to the latter, because the source conditions are not the same from one event to the other, as can be seen from the fact that magnetic inhomogeneities are much closer between them in events of high acceleration efficiency. We have considered a second-order Fermi-type mechanism to illustrate that even in the extreme case of such low efficiency the acceleration process may be performed within the flare time scale and to show that the assumption of $\tau = 1 \text{ s}$ is well justified. If instead of a second-order Fermi mechanism we consider a first-order Fermi-type process in a shock wave, such as is usually attributed to the acceleration of solar particles (e.g. [32, 110]) the resulting value of τ is then lower than 1 s . From the study of heavy nuclei overabundances in solar cosmic rays it can be predicted that the value of τ is comprised between 0.1 and 0.4 s ; these values when included in our calculations result in a much better fit of the theoretical spectra to the observational curves that the one illustrated with $\tau = 1 \text{ s}$.

The acceleration time scale of protons in solar flares, can be estimated from the following expression: $t = \int_{E_c}^E \frac{dE}{f(E)}$. In the energy range $10^6 \lesssim E \lesssim 10^{10} \text{ eV}$ we have according our results discussed in last section that,

$$f(E) = \begin{cases} \alpha\beta W \\ (\alpha\beta + \rho\beta^2)W \end{cases} \text{ in low temperature regimens}$$

$$f(E) = (d - hE^{-2} - jE^{-1})\beta W - b/\beta \text{ in intermediate temperature regions}$$

$$f(E) = [(d - hE^{-2} - jE^{-1})\beta - \rho^2]W - b/\beta \text{ in high temperature regimens}$$

$$\text{(where) } d = \alpha - f - \eta$$

Therefore, a consideration of the parameters obtained α and E_c for a medium density $n = 10^{13} \text{ cm}^{-3}$ give acceleration times much lower than the time scale of the explosive phase of the flare phenomenon. For instance, for a low efficiency event ($\alpha = 0.14$) in a high temperature regime, the time necessary to accelerate a proton from 10 MeV to 5000 MeV, is only of the order of 8 sec.

It is interesting to comment on the estimated parameter ι on the basis of our results of the parameter α : as pointed out by [102] the time scale of the explosive phase in solar flares, is $\sim 10^3 \text{ s}$, and it is believed to be that of the stored magnetic energy dissipation, which is given as

$$\tau_d = 4\pi\sigma l^2 / c^2 \quad (35)$$

where l is the characteristic length of the system and σ the electrical conductivity in flare material is of the order of $2.1 \times 10^{12} - 2.4 \times 10^{14} \text{ s}^{-1}$. A single calculation with (35) shows us that $l = 1.7 \times 10^4 - 1.8 \times 10^5 \text{ cm}$ which agrees well with the values estimated in this work and previously deduced by [79].

It worth comment on the discrepancy between the predicted theoretical energy spectra at the source and the experimental spectra measured in the earth environment: first we note that the physical processes that can occur in a medium as dense as the sun's atmosphere are undoubtedly very diverse, and so, we do not claim to have included in our treatment all loss processes for charged particles, but only those of greatest interest that can affect protons within the energy range we are concerned with and during the short time scale of the acceleration durability. In fact, although Cerenkov losses are included in Eq. (2) we have ignored other losses from collective effects, however, some of them, such as energy loss by plasma perturbations see to be negligible for protons of $E > 23 \text{ MeV}$; also we have not considered energy losses caused by viscosity and Joule dissipation as suggested by [120]. On the other hand, we have not included nuclear transformation within the acceleration volume, as for instance proton production by neutron capture, nor loss of particles from the accelerated flux as leakage from the acceleration volume. Therefore, it is expected that the consideration of these neglected processes, together with a lower value of τ as discussed above and a higher proton concentration of the medium would depress our theoretical fluxes in greater congruency with the experimental curves. Again, local modulation of particles at the source level after acceleration are not examined here, either by an energy degradation step in a closed magnetic structure, or while traversing the dense medium of the solar atmosphere as studied by [121].

In fact, observations of low energy particles indicate the existence of a strong modulation within a small envelope of $\sim 0.2-0.3 \text{ A.U.}$ (e.g. [34]). Furthermore, studies of relativistic solar flare particles during the May 4, 1960 and November 18, 1968 events have shown that particles diffuse in the solar envelope ($< 30 R_s$) [9, 21, 22, 63] which entails a modulation of the solar fluxes. Evidences of particle storage in the sun, where particles can be strongly decelerated, have been widely mentioned in the literature (e.g. [1, 65, 106]). Modulation in interplanetary space is a complicated process (e.g. [28, 29]) which provokes both the depression in the number density of particles and their strong deceleration: estimations of [74] indicate that particles lose $\sim 10-64\%$ of their energy through propagation, while [75, 76] sustains a loss of

\sim a half of their energy before escaping into interstellar space. Moreover, the acceleration of particles in interplanetary space [21, 22, 85] may strongly disturb the spectrum. Given the strong modulation of solar particles at different levels, one cannot expect a good fit between the predicted source spectrum and the experimental one. Nevertheless, we believe that the kind of intercomparison performed here permits the clarification of ideas about the processes related to the generation of solar flare particles.

7. Concluding remarks

In order to provide some answers to the numerous questions associated with the generation of solar particles (e.g. [24, 26, 71, 102, 119]) we have attempted to study the physical processes and physical conditions prevailing in solar cosmic ray sources by separating source level effects from interplanetary and solar atmospheric effects. On this basis, we have drawn some inferences from the intercomparison of the predicted theoretical energy spectra of protons in the acceleration region with the experimental spectra of multi-GeV proton events. Concerning this kind of events a number of modern techniques have been recently developed e.g.: [72]) and the, the PGI group in Apatity, Murmansk, Russia [124–128]. In some of GLE it has been frequent to discern two particles populations: a prompt component and a delayed one. A new kind of classification has been proposed, *GLE's* and *SubGLE's* depending the number of station that register the earth level enhancement, location and latitude of NM stations.

We have chosen to study this particular kind of solar events (GLE) because they allow the study of the behavior of local modulation on protons, through the widest range of solar particle energies. Although one should expect that local modulation by particle energy losses at the source should follow the behavior illustrated in **Figure 1**, our results on source energy spectra indicate that is not the general case, but local modulation varies from event to event, depending on the particular phenomena that take place at the source according to the particular physical parameters prevailing in each event, such as density, temperature, magnetic field strength as well as the acceleration efficiency and particle remaining time before they escape from the source.

In drawing conclusions about the physical processes at the source, we have assumed a fixed value of the parameter n , taking into account that although spectroscopic measurements show a variation in the value of n from flare to flare, these fluctuations are nonetheless very near the value $n = 10^{13} \text{ cm}^{-3}$ [115]), and thus our conclusions about energy loss processes in the acceleration region are not significantly altered by small fluctuation on this parameter. Moreover, an analysis of the electromagnetic emission associated with flares indicate a spread of several decades on the medium temperature in flare regions ($\sim 10^4$ – 10^8 K), hence we have chosen to fix the parameter n in order to concentrate our analysis on the parameter temperature. On the other hand, in drawing conclusions about the physical parameter of the acceleration process we have selected a mechanism with an energy gain rate proportional to particle energy as is the case of stochastic acceleration by MHD turbulence [36]); nevertheless, we believe that our results can in general be considered as valid, in the sense that whatever the

acceleration mechanism may be, the physical conditions of the medium (density, temperature, field strength) state undoubtedly state the kind of phenomena occurring at the source. We have shown that even a low efficient mechanism (low values of α) is able to explain the generation process within the observation time scale of the explosive phase of flares, when severe conditions in the density of the medium are assumed.

Finally, let us discuss the global conception of the generation process of solar particles, according to the results obtained in this work: it is first assumed that in association with the development of solar flare conditions for the acceleration of particles may be such that it can take place either in a hot medium or in a cold one; in the first case, as a result of some powerful heating process, the local plasma must be strongly heated and acceleration of particles up to some few MeV must take place. This preliminary heating must follow to a some specific kind of hydromagnetic instability or a magnetic field annihilation process in a magnetic neutral current sheet, so that by means of electron-ion and electron-neutral collisions, Joule dissipation, viscosity, slow and fast Alfvén modes or even acoustic and gravity waves, the local plasma attain very high temperature $\geq 10^7$ K. The processes involved in this preliminary process of particle acceleration is not yet completely well understood; several plausible processes capable to accelerate particles up to some MeV have been suggested in the literature (e.g. [112]). Among many possibilities suggested, we believe that the one proposed by [108] presents a very plausible picture: a very select group of fast particles appearing from the preliminary heating can be reaccelerated up to very high energies, probably by a Fermi-type mechanism as proposed by [108]). Because the medium is very hot and dense we propose that collisional and $p-p$ nuclear collisions between the fast protons and particles of the medium take place. Besides, we predict that up to some definite temperature the kinetic pressure of the gas is such that it favors the hydromagnetic expansion of a closed field line configuration, and thus adiabatic deceleration of particles takes place during their acceleration in the expanding plasma. Those particles with very low energy with respect a threshold energy E_c (determined by the competition between the acceleration and the deceleration rates) cannot escape from the sunspot magnetic field configuration because of their low rigidity, and thus, by scattering with the atoms, ions and electrons of the turbulent plasma, their energy is rapidly converted into heat to rise the local plasma temperature while the selected particles go into the main acceleration process. As noted by [110] the increase of electron temperature tends to decrease the efficiency of acceleration, such as that obtained in the case of *hot* events (**Table 1**) with regard to the events of **Tables 2** and **3**. This low efficiency is also related to the relatively large characteristic length- scale of the magnetic field, so that the acceleration time of particles up to high energies is relatively long. A second kind of solar event may be distinguished from the previous one, when the temperature is not so high (*warm* events in **Table 3** and **Figure 4**) and thus expansion of the source material does not take place, at least during the time of the particle acceleration process. The temperature being lower and the characteristic magnetic field length shorter than in hot events, the acceleration efficiency is higher and consequently the acceleration time is relatively shorter. In these events or in *hot* events a low flux of high energy gamma rays generated by nuclear collisions of highly energetic protons is expected, because these fast particles spend very short time in the source before they escape. On the other hand, conditions in solar flares may be such that energy losses of protons are negligible during the

acceleration process, because particles are generated by a very efficient process in a shorter acceleration time. This kind of events are assumed to occur when the acceleration region is associated with a relatively cold plasma, such that below a certain critical temperature, a compression of the sunspot field lines takes place and thus particles are more efficiently accelerated because the characteristic magnetic field length scale is reduced. Moreover, adiabatic heating of protons into the compressed plasma may occur within the short acceleration time of these events raising the net energy exchange rate. Since the energy loss rate is negligible by rapport to the energy gain rate in these events, particles may practically be accelerated regardless of their energies, so that a preferential acceleration of heavy nuclei as suggested by [48, 49], must be expected when acceleration occurs in a region of low temperature regime. Either by assuming that in *cold* events particles are picked up from a thermal plasma or that in *warm* and *hot* events the preliminary heating is of quasi-thermal nature, a very small fraction ($N_0 \sim 10^{-11} - 10^{-18}$) of plasma particle of the source volume need to be picked up by the acceleration process in order to explain the experimental spectra.

The most important parameters concerning the source and acceleration process of solar particles deduced under the assumptions made in in this work may be summarized as follows: acceleration efficiency $\alpha = 0.1 - 1.5 \text{ s}^{-1}$, characteristic magnetic field length in the acceleration volume $l = 3 \times 10^4 - 10^6 \text{ cm}$, linear dimension of the acceleration volume $L = 10^9 \text{ cm}$, field strength of magnetic field inhomogeneities $\sim 500 \text{ G}$, hydromagnetic velocity $V_a = 3.5 \times 10^7 \text{ cm s}^{-1}$, medium density $n \sim 10^{13} \text{ cm}^{-3}$, mean confinement time of particles within the acceleration volume $\tau \sim 0.1 - 4 \text{ s}$, average acceleration time of individual protons $t = 12 \text{ s}$, medium temperature $T \sim 10^4 - 10^8 \text{ K}$. Finally, we add that whatever the approach may be in developing flare models, an expansion and compression of the source material (e.g. [96]) local modulation of particles after the acceleration processes and a plausible absorption of secondary radiation from nuclear collisions in the solar environment must be considered.

Epilogue

We would like to emphasize that this work is to some extent with the aim to pay homage to the forefathers-founders of solar cosmic ray physics and space physics.

Acknowledgements

We are very grateful to the B.S. **Alejandro Sánchez Hertz** for his valuable help in the preparation of the figures.

A. Appendix

Energy spectrum of energetic particles accelerated in a plasma by a stochastic type-Fermi acceleration process ($\sim \alpha\beta W$) while losing energy simultaneously by collisional losses

according to the general expression of [10], operative throughout all the range from suprathermal to ultrarelativistic energies, given in Eq. (2.1) in Section II. In this case, the equation to be solved when only collisional losses are competing with acceleration is

$$\frac{dW}{dt} = \alpha\beta W - \frac{k}{\beta} \ln(k_1\beta^2) \left[R_4 H(\chi_e) + R_5 H(\chi_p) \right] \quad \left(\frac{\text{MeV}}{\text{seg}} \right) \quad (\text{A.1})$$

where all the factors appearing in (A1) were defined below Eq. (2.1) in Section II

Now we proceed to a variable change, in terms of $\gamma = \frac{1}{(1-\beta^2)^{\frac{1}{2}}}$ since $W = Mc^2\gamma$, $dW = Mc^2 d\gamma$ and

$$\beta = \frac{\sqrt{\gamma^2 - 1}}{\gamma} \quad (\text{A.2})$$

Hence

$$\alpha\beta W = \alpha \frac{\sqrt{\gamma^2 - 1}}{\gamma} Mc^2\gamma = Mc^2\alpha\sqrt{\gamma^2 - 1} \quad (\text{A.3})$$

Therefore, Ec. (A.1) as a function of γ can be rewritten in the following form

$$\frac{d\gamma}{dt} = \alpha\sqrt{\gamma^2 - 1} - \frac{\kappa}{Mc^2} \frac{\gamma}{\sqrt{\gamma^2 - 1}} \ln\left(\frac{\kappa_1(\gamma^2 - 1)}{\gamma^2}\right) [R_4 H(x_e) + R_5 H(x_p)] \quad (\text{A.4})$$

From where

$$dt = \frac{d\gamma}{\alpha\sqrt{\gamma^2 - 1} - \frac{\kappa}{Mc^2} \frac{\gamma}{\sqrt{\gamma^2 - 1}} \ln\left(\frac{\kappa_1(\gamma^2 - 1)}{\gamma^2}\right) [R_4 H(x_e) + R_5 H(x_p)]} \quad (\text{A.5})$$

and thus

$$t = \frac{1}{\sqrt{b^2 - 4ac}} \left[\ln \left| \frac{2a(\sqrt{\gamma^2 - 1}/\gamma) + b - \sqrt{b^2 - 4ac}}{2a(\sqrt{\gamma^2 - 1}/\gamma) + b + \sqrt{b^2 - 4ac}} \right| \left| \frac{2a(\sqrt{\gamma_c^2 - 1}/\gamma_c) + b - \sqrt{b^2 - 4ac}}{2a(\sqrt{\gamma_c^2 - 1}/\gamma_c) + b + \sqrt{b^2 - 4ac}} \right| \right] \quad (\text{A.6})$$

For integration of (A.5) we have assumed the case when $b^2 > 4ac$

$$\text{(were) } a = -\alpha; b = -f'(\gamma_T); c = \alpha - f(\gamma_T) + \frac{\sqrt{\gamma_T^2}}{\gamma_T} f'(\gamma_T);$$

$$f(\gamma) = \frac{1}{\gamma^3 - \gamma} \frac{\kappa}{Mc^2} \ln\left(\frac{k_1(\gamma^2 - 1)}{\gamma^2}\right) [R_4 H(x_e) + R_5 H(x_p)] \quad (\text{and})$$

$$f'(\gamma) = \frac{\kappa}{Mc^2} \frac{[R_4 H(x_e) + R_5 H(x_p)]}{\sqrt{\gamma^2 - 1}} \left[\left(-3 - \frac{2}{\gamma^2 - 1} \right) \ln\left(\frac{k_1(\gamma^2 - 1)}{\gamma^2}\right) + \frac{2}{\gamma^2 - 1} \right] \\ + \frac{\kappa}{Mc^2} \frac{1}{\gamma(\gamma^2 - 1)} \ln\left(\frac{k_1(\gamma^2 - 1)}{\gamma^2}\right) \left\{ R_4 R_2 e^{-x_e^2} [1 - c_4(1 - 2x_e^2)] + R_5 R_3 e^{-x_p^2} [1 - c_5(1 - 2x_p^2)] \right\}$$

Now, according to Eq. (8.1) in Section IV the differential spectrum in terms of γ is,

$$N(\gamma)d\gamma = \frac{N_0}{\tau Mc^2} e^{-t/\tau} dt \quad (\text{A.7})$$

And from (A.6) we obtain

$$e^{-t/\tau} = \left[\frac{2a(\sqrt{\gamma^2-1}/\gamma) + b - \sqrt{b^2-4ac}}{2a(\sqrt{\gamma^2-1}/\gamma) + b + \sqrt{b^2-4ac}} \middle| \frac{2a(\sqrt{\gamma_c^2-1}/\gamma_c) + b - \sqrt{b^2-4ac}}{2a(\sqrt{\gamma_c^2-1}/\gamma_c) + b + \sqrt{b^2-4ac}} \right]^{\frac{1}{\tau\sqrt{b^2-4ac}}} \quad (\text{A.8})$$

in such a way that Eq. (A.7) can be rewritten

$$N(\gamma)d\gamma = \frac{N_0}{\tau Mc^2} \frac{\left[\frac{2a(\sqrt{\gamma^2-1}/\gamma) + b - \sqrt{b^2-4ac}}{2a(\sqrt{\gamma^2-1}/\gamma) + b + \sqrt{b^2-4ac}} \middle| \frac{2a(\sqrt{\gamma_c^2-1}/\gamma_c) + b - \sqrt{b^2-4ac}}{2a(\sqrt{\gamma_c^2-1}/\gamma_c) + b + \sqrt{b^2-4ac}} \right]^{\frac{1}{\tau\sqrt{b^2-4ac}}} d\gamma}{\alpha \sqrt{\gamma^2-1} - \frac{\kappa}{\mu c^2} \frac{\gamma}{\sqrt{\gamma^2-1}} \ln \left(\frac{\kappa_1(\gamma^2-1)}{\gamma^2} \right) [R_4 H(x_e) + R_5 H(x_p)]} \quad (\text{A.9})$$

which is the differential spectrum as a function of gamma.

To obtain the integral spectrum we resort to Eq. (9) of Section IV,

$$J(> \gamma) = \int_{\gamma}^{\gamma_m} N(\gamma)d\gamma = \frac{N_0}{Mc^2} e^{t(\gamma_c)/\tau} \left[e^{-t(\gamma)/\tau} - e^{-t(\gamma_m)/\tau} \right] \quad (\text{A.10})$$

Introducing A.8 in A.10 we obtain the integral spectrum

$$J(> \gamma) = \frac{N_0}{Mc^2} \left[\frac{2a(\sqrt{\gamma_c^2-1}/\gamma_c) + b - \sqrt{b^2-4ac}}{2a(\sqrt{\gamma_c^2-1}/\gamma_c) + b + \sqrt{b^2-4ac}} \right]^{\frac{1}{\tau\sqrt{b^2-4ac}}} - \left[\frac{2a(\sqrt{\gamma^2-1}/\gamma) + b - \sqrt{b^2-4ac}}{2a(\sqrt{\gamma^2-1}/\gamma) + b + \sqrt{b^2-4ac}} \right]^{\frac{1}{\tau\sqrt{b^2-4ac}}} \quad (\text{A.11})$$

Eqs. A.9 and A.12 may become very important for the study of all the entire range of particle energy of solar particles, particularly low energy protons measured by satellites in the interplanetary space, that presumably they have been affected in their sources. Eventually this approach could be used at laboratory scale for experiments of particle energization in plasmas.

Author details

Jorge Perez-Peraza* and Juan C. Márquez-Adame

*Address all correspondence to: perperaz@geofisica.unam.mx

Instituto de Geofisica, Universidad Nacional Autonoma de Mexico, D.F. for CDMX, Mexico

References

- [1] Alhualia. 12th ICRC, Tasmania, Hobart; 1971. p. 468
- [2] Bai T, Ramaty R. Solar Physics. 1976;**49**:343
- [3] Barcus JG. Solar Physics. 1969;**8**:186
- [4] Bazilevskaya GA, Charakhchyan AN, Charakhchyan TN, Lozutin IL. 12th I.C.R.C., Tasmania. 1971;**5**:1825
- [5] Biswas S, Radhakishnan·B. Solar Physics. 1973;**28**:211
- [6] Bland. Nuovo Cimento. 1966;**13**:427
- [7] Bruzek A. Solar Physics. 1972;**26**:94
- [8] Bukata RP, Gronstal PI, Palmeira RAR, McCracken KG, Rao UR. Solar Physics. 1969;**10**:198
- [9] Burlaga. Solar Physics. 1970;**13**:348
- [10] Buttler ST, Buckingham MJ. Physical Review. 1962;**126**:1
- [11] Bryant DA, Cline TL, Desai VD, McDonald FB. Astrophysical Journal. 1965;**141**:478
- [12] Cameron AGW. The Astrophysical Journal Letters. 1967;**1**:35
- [13] Cheng C-C. Solar Physics. 1972;**22**:178-188
- [14] Chupp EL. Space Science Reviews. 1971;**12**:486
- [15] Chupp EL, Forrest DJ, Highbie PR, Suri AN, Tsai C, Dunphy PP. Nature. 1974;**241**:333
- [16] Cline T. NASA-X-661-7133, GSFC, Greenbelt, Maryland;1970
- [17] Datlowe D. Solar Physics. 1971;**17**:436
- [18] Davis L. In: Mackin RJ, Neugebauer M, editors. The Solar Wind. NY: Pergamon Press;1966
- [19] De Jager C. Solar Physics. 1967;**2**:327
- [20] Dessai UD. Canadian Journal of Physics. 1971;**49**:265
- [21] Duggal SP, Guidi I, Pomerantz MA. Solar Physics. 1971;**18**:234
- [22] Duggal SP. Reviews of geophysics. Space Physics. 1979;**17**:1021
- [23] Dulk GA, Altschuler MD, Smerd SF. Astrophysical Journal Letters. 1971;**8**:235
- [24] Elliot H. In: Wilson JG. Progress in Cosmic Ray Physics, Vol. 1;1952
- [25] Elliot H. Planetary and Space Science. 1964;**12**:657
- [26] Elliot H. In: De Jager C, Svestka Z, editors. N Solar Flares and Space Research. Amsterdam: North Holland Pub; 1969. p.356

- [27] Elliot H. In: De Jager C, editor. Solar-Terrestrial Physics, Part I; 1972. p.134
- [28] Englade RC. 12th International Conference on Cosmic Rays. 1971;2:502
- [29] Englade RC. Journal of Geophysical Research. 1972;77:6266
- [30] Ellison MA, McKenna SMP, Reid. Dunsink Observatory Publications. 1961. 53
- [31] Ellison MA, Reid JA. Research in Geophys. 1964 M.I.T. Presstime 1,43
- [32] Fichtel CE, McDonald FB. Annual Review of Astronomy and Astrophysics. 1967;5:359
- [33] Fisk LA, Axford WI. Journal of Geophysical Research. 1968:73. DOI: 10.1029/JA073i013p04396 ISSN 0148-0227
- [34] Fisk LA. 14th ICRC; Munich. 1975;2:810
- [35] Fritzoza-Svestkova, Svetska. Solar Physics. 1967;2:87
- [36] Gallegos-Cruz A, Pérez-Peraza J. Astrophysical Journal. 1995;446:669
- [37] Ginzburg VL, Syrovatskii SI. The Origin of Cosmic Rays. Oxford: Pergamon Press;1964
- [38] Ginzburg VL. Elementary Processes for Cosmic Ray. Astrophys, Gordon & Breach;1969
- [39] Heristchi Dj, Kangas J, Kremser G, Legrand JP, Masse P, Palous M, Pfozter G, Riedler W, Whilhem K. Annals of the International Quiet Year. 1967;3:267
- [40] Heristchi Dj, Trottet G. Physical Review Letters. 1971;26:197
- [41] Heristchi DJ, Perez-Peraza J, Trottet G. In: Lincoln V, editor. Bulletin of the World Data Center A, Upper Atmosphere Geophysics, Boulder Colorado. Vol. 24; 1972. 182
- [42] Heristchi Dj, Perez-Peraza J, Trottet G. Paper SP-5.3-9 14th ICRC. 1975;5:1841
- [43] Heristchi Dj, Trottet G, Perez-Peraza J. Solar Physics. 1976;49:141
- [44] Hess WN. Reviews of Modern Physics. 1958;30:368
- [45] Ifedili SO. Solar Physics. 1974;39:233
- [46] Jokipii JR. Reviews of Geophysics and Space Physics. 1971;9:1
- [47] King JH. J. Spacecraft Rockets. 1974;11:401
- [48] Korchak AA, Sirovatskii SI. Soviet Doklady. 1958;3:983
- [49] Korchak AA, Sirovatskii SI. Proc of the 6th ICRC 3, 216. Moscow: Izd AN SSSR (in Russian); 1960
- [50] Korchak AA. Astronomicheskii Zhurnal. 1967a;11:258
- [51] Korchak AA. Doklady AN SSSR. 1967b;12:192
- [52] Korchak AA, Platov YV. Astronomicheskii Zhurnal. 1968;45(6):1185
- [53] Krimigis SM. Journal of Geophysical Research. 1965:70, 2943

- [54] Krivsky. *Acta Physica Academiae Scientiarum Hungaricae*. 1970;**29**:427
- [55] Krivsky L. *Nuovo Cimento Series*. 1965;**10-27**:1017
- [56] Kurochka LN. *Astronomicheskii Zhurnal*. 1970;**47**:111
- [57] Lin RP. *Journal of Geophysical Research*. 1968;**73**:3066
- [58] Lin RP, Kahler SW, Roelof EC. *Solar Physics*. 1960;**4**:338
- [59] Lingelfelter RE, Ramaty R. In: Shen BSP, editor. *High Energy Nuclear Reactions in Astrophysics*. New York: Benjamin WA, Inc; 1967. p. 99
- [60] Lockwood JA. *Journal of Geophysical Research*. 1967;**72**:3395
- [61] Lockwood JA. *Journal of Geophysical Research*. 1968;**73**:4247
- [62] Lockwood JA, Webber WR, Hsieh L. *Journal of Geophysical Research*. 1974;**79**:4149
- [63] Lust R, Simson JA. *Physical Review*. 1957;**108**:1563
- [64] McCracken KG. 1969 in *Solar Flares and Space Research*, Ed. by De Jager, C. and Svetska, Z. North Holland Pub, Amsterdam, p. 202.
- [65] McDonald FB, Dessai. *Journal of Geophysical Research*. 1971;**76**:808
- [66] Malville JM, Smith SF. *Journal of Geophysical Research*. 1963;**68**:3181
- [67] Miroshnichenko L, Sorokin MO. *Geomagn and Aeronomy*. 1985;**25**(4):534
- [68] Miroshnichenko LI, Sorokin MO. *Geomagnetism and Aeronomy*. 1986;**26**(4):535
- [69] Mirosnichenko LI, Pérez-Peraza J. *Astrophysical Aspects in the studies of solar cosmic rays*. *International Journal of Modern Physics*. 2008;**23**:1
- [70] Mirosnichenko LI, Vashenyuk EV, Pérez-Peraza J. *Bulletin of the Russian Academy of Sciences*. 2009;**73**(3):297
- [71] Miroshnichenko L. *Solar cosmic rays: Fundamental and applications*. *Astrophysics and Space Science Library*. 2015;**405**
- [72] Mishev AL, Kocharov LG, Usoskin G. *J.G.R.: Space Physics*. 2014;**119**:670
- [73] Ogilvie KW, Bryant DA, Davis LR. *Journal of Geophysical Research*. 1962;**67**(3):929
- [74] Palmer IA. *Reviews of Geophysics and Space Physics*. 1982;**20**:335
- [75] Parker EN. *Interplanetary Dynamical Processes*. New York: John Wiley & Sons, Interscience;1963a
- [76] Parker EN. *ApJ*. 1963b. Suppl 77;**8**:177
- [77] Parker. *Planetary and Space Science*. 1965;**13**(1):9
- [78] Parker EN. *Space Science Reviews*. 1969;**9**:325

- [79] Perez-Peraza J. Journal of Geophysical Research. 1975;**80**:3535
- [80] Perez-Peraza J, Galindo Trejo J. Revista Mexicana De Astronomia Y Astrofisica. 1975;**1**:273
- [81] Perez-Peraza J, Gallegos-Cruz A. The Astrophysical Journal Supplements. 1994a;**669**:90-92
- [82] Perez-Peraza J, Gallegos-Cruz A. Geofisica Internacional. 1994b;**33-2**:311
- [83] Pinter S. Solar Physics. 1969;**8**:149
- [84] Pinter S. Proc. IV Leningrad Cosmic Phys. Seminar, Phys. Techn. Inst., Leningrad; 1972p.63
- [85] Pomerantz, Duggal. Journal of Geophysical Research. 1974;**79**:913
- [86] Ramaty R, Lingelfetter RE. High Energy Phenomenon on the sun NASA SP-342; 1973. 301
- [87] Ramaty R, Lingelfetter RE. Journal of Geophysical Research. 1967;**72**:879
- [88] Ramaty R, Stone RG. High Energy Phenomenon on the Sun NASA SP-342;1973. 341
- [89] Ramaty R, Lingelfetter RE. In: Kane RS, editor. N Solar Gamma, X and EUV Radiation, IAU Symposium 68. Dordrecht, Holland: Reidel Pub Co; 1975. p. 363
- [90] Ramudarai S, Biswas S. 12th International Cosmic Rays Conference. Vol. 21971. p. 793
- [91] Ramudarai S, Biswas S. Astrophysics and Space Science. 1974;**30**:187
- [92] Reames DF, Fichtel CE. 10th ICRC, CAL. 1967;**2**:546
- [93] Reid JH. Dunsink Obs. Publ.1961;53
- [94] Rotwell PL. Journal of Geophysical Research. 1976;**81**:709
- [95] Sakurai K. Journal of Geomagnetism and Geoelectricity. 1963;**14**:144
- [96] Sakurai K. Publications of the Astronomical Society of Japan. 1965;**19**:408
- [97] Sakurai K. Publications of the Astronomical Society of Japan. 1966a;**18**:77
- [98] Sakurai K. Report of Ionosphere and Space Research in Japan 20 519. 1966b;**20**:233
- [99] Sakurai K. Report of Ionosphere and Space Research in Japan 21. 1967;**21**:113, 213
- [100] Sakurai K. NASA Report X- 693-71-268 GSFC, Greenbelt Md1971
- [101] Sakurai K. Solar Physics. 1973;**31**:483
- [102] Sakurai K. Physics of Solar Cosmic Rays. Tokio, Japan: University of Tokyo Press; 1974
- [103] Sakurai K. Publications of the Astronomical Society of Japan. 1976;**28**:177
- [104] Schatzman E. Solar Physics. 1967;**1**:411
- [105] Severnii, Shabanskii. Soviet Astronomy - Astrophysical Journal. 1961;**4**:583
- [106] Simnet. Solar Physics. 1971;**20**:448

- [107] Smerd SF, Dulk GA. Solar Magnetic Fields, IAU 431971. p. 616
- [108] Smith EVP. In: Oman Y, editor. N Mass Motions in Solar Flares and Related Phenomena, Nobel Symposium 9. Stockholm: Almqvistand Wiksell; 1968. p. 137
- [109] Smith SF, Ramsay HE. Solar Physics. 1967;2:158
- [110] Smith DF. Advances in Space Research. 1986;6(6):135
- [111] Somov BV, Syrovatskii SI. Solar Physics. 1974;39:415
- [112] Sonnerup. In: Ramaty R, Stone RG, editors. High Energy Phenomena on the Sun, NASA X-693-73-193. 1973. p. 357
- [113] Suemoto, Hiei. Publications of the Astronomical Society of Japan. 1959;11:185
- [114] Suemoto, Hiei. Publications of the Astronomical Society of Japan. 1962;14:33
- [115] Svestka Z. BAC. 1963;14:234
- [116] Svetska Z. Bulletin of the Astronomical Institute of Czechoslovakia. 1966;17:262
- [117] Svetska Z. Solar Physics. 1968;4(1):18
- [118] Svetska, Z. 1969 in Solar Flares and Space Research (ed. By de Jager, C. and Svestka, Z.) North-Holland Pub., Amsterdam, p. 16.
- [119] Svetska Z. Solar Flares Geophysical and Astrophysics Monographs. Dordrecht Holland: Reidel Publishing Company; 1976
- [120] Syrovatskii SI. Soviet Physics - Journal of Experimental and Theoretical Physics. 1961;13: 1257
- [121] Syrovatskii SI, Shmelevae OP. Soviet Astronomy - Astrophysical Journal. 1972;16:273
- [122] Takakura T. Space Science Reviews. 1966;5:80
- [123] Takakura T. Solar Physics. 1969;6:133
- [124] Vashenyuk EV, Balabin YV, Perez-Peraza J, Gallegos-Cruz A, Miroshnichenko LI. Advances in Space Research. 2006;38(3):411
- [125] Vashenyuk EV, Balabin YV, Miroshnichenko LI, Pérez-Peraza J, Gallegos-Cruz A. 30th Int. Cosmic Ray, Mérida. Vol. 12007a. p. 249
- [126] Vashenyuk EV, Miroshnichenko LI, Balabin Y-V, Pérez-Peraza J, Gallegos-Cruz A. 30th Int. Cosmic Ray Conf., Merida. 2007b;1:253
- [127] Vashenyuk EV, Balabin YV, Miroshnichenko LI. Advances in Space Research. 2008;41(6):926
- [128] Vashenyuk EV. Bulletin of the Russian Academy of Sciences. 2011;75(6):767
- [129] Vernov SN, Grigorov NL, Zatespin GT, Chudakov AE. Izvstia Akademii Nauk Sssr, Deriya Series Fizika (English Translation). 1955;19:45

- [130] Webber WR. In: Hess WW, editor. AAS-NASA SP-50 Symp. On the physics of Solar flares, GSFC. 1964. p. 515
- [131] Wentzel DG. Journal of Geophysical Research. 1965;**70**:2716
- [132] Wentzel DG. ApJ. 1969a;**156**:303
- [133] Wentzel DG. ApJ. 1969b;**157**:545
- [134] West HI Jr, Buck RM, Walton JR, D'Arcy RG Jr. Upper Atmosph. Geophys World Data Center A, NOAA, Rep. 241972. p. 113
- [135] Widding KG. IAU Symposium. 1975;**68**:153
- [136] Wild JP. Journal of the Physical Society of Japan. 1962;**17**(Suppl. A II):249

PRESENTACION DEL ARTÍCULO: “*Source Energy Spectrum of the 17 May 2012 GLE*”

Entre los diversos GLEs que presumiblemente ocurrieron en el período 2012-2015, el del 17 de mayo de 2012 es el más ampliamente aceptado como un GLE, en vista del alto número de estaciones de monitoreo de neutrones en latitudes altas que lo registraron. A pesar de su pequeña magnitud, fue el más prominente de los previstos para la presente década (Pérez-Peraza y Juárez-Zuñiga, 2015). Sin embargo, la falta del efecto de latitud dificulta el estudio de las características de su espectro en el extremo de las altas energías. Varios autores han podido derivar espectros observacionales en la parte superior de la atmósfera terrestre para este peculiar GLE. Algunos de estos trabajos encuentran que el flujo de protones se caracteriza por dos componentes. Se han publicado un gran número de trabajos en relación a las características observacionales obtenidas por diferentes instrumentos, pero la fenomenología de la fuente, con respecto a los procesos de generación y sus parámetros físicos, no se han examinado. El objetivo principal del artículo es analizar dichos aspectos mediante la confrontación de los diferentes enfoques de los espectros observacionales con nuestros espectros teóricos analíticos basados en la aceleración estocástica y en la aceleración del campo eléctrico a partir de los procesos de reconexión. De esta forma, derivamos un conjunto de parámetros que caracterizan la fuente de cada una de las dos componentes del GLE, lo que nos lleva a proponer posibles escenarios para la generación de las partículas solares reactivas.

Estatus: Publicado.

RESEARCH ARTICLE

10.1002/2017JA025030

Source Energy Spectrum of the 17 May 2012 GLE

Jorge Pérez-Peraza¹, Juan C. Márquez-Adame¹, Leonty Miroshnichenko^{2,3}, and Victor Velasco-Herrera¹ 

Key Points:

- We make a review of the observational spectra of the GLE of May 17, 2012, noting that there is some dispersion due to the different techniques used in its derivation
- We observe that certain authors discern two different components of the spectrum: a prompt one and a delayed one
- Confrontation of these results with the theoretical spectra published previously leads to a plausible scenario of the source phenomena; we propose a set of parameters characterizing the source and acceleration process

Supporting Information:

- Supporting Information S1

Correspondence to:

J. Pérez-Peraza,
perperaz@geofisica.unam.mx

Citation:

Pérez-Peraza, J., Márquez-Adame, J. C., Miroshnichenko, L., & Velasco-Herrera, V. (2018). Source energy spectrum of the 17 May 2012 GLE. *Journal of Geophysical Research: Space Physics*, 123. <https://doi.org/10.1002/2017JA025030>

Received 20 NOV 2017

Accepted 6 MAR 2018

Accepted article online 14 MAR 2018

©2018. American Geophysical Union.
All Rights Reserved.

¹Instituto de Geofísica, Universidad Nacional Autónoma de México, México City, Mexico, ²Pushkov Institute of Terrestrial Magnetism, Ionosphere and Radio Wave Propagation of the Russian Academy of Sciences, Moscow, Russia, ³Skobeltsyn Institute of Nuclear Physics, Lomonosov Moscow State University, Moscow, Russia

Abstract Among the several GLEs (ground level enhancements) that have presumptuously occurred in the period 2012–2015, the 17 May 2012 is that which is more widely accepted to be a GLE, in view of the high number of high-latitude neutron monitor stations that have registered it. In spite of the small amplitude, it was more prominent of the predicted GLE's of the present decade (Pérez-Peraza & Juárez-Zuñiga, 2015, <https://doi.org/10.1088/0004-637X/803/1/27>). However, the lack of latitude effect makes it difficult to study the characteristics of this event in the high-energy extreme of the spectrum. Nevertheless, several outstanding works have been able to derive observational spectra at the top of the Earth atmosphere for this peculiar GLE. Some of these works find that the flow of protons is characterized by two components. Quite a great number of works have been published in relation with observational features obtained with different instrumentation, but the source phenomena, regarding the generation processes and source physical parameters, have not been scrutinized. The main goal of this work is to look at such aspects by means of the confrontation of the different approaches of the observational spectra with our analytical theoretical spectra based on stochastic acceleration and electric field acceleration from reconnection processes. In this way, we derive a set of parameters which characterize the sources of these two GLE components, leading us to propose possible scenarios for the generation of particles in this particular GLE event.

1. Introduction

The importance of the study of relativistic solar particles that produce the so-called GLEs (ground level enhancements) has been highlighted long ago in the literature (e.g., Miroshnichenko & Pérez-Peraza, 2008; Miroshnichenko, 2014) emphasizing solar phenomena features and terrestrial effects. It is assumed that the time profile of particles gives information about the interplanetary transport processes and structure of the interplanetary magnetic field, whereas the energy spectrum gives information about the source phenomena: involved processes (acceleration and deceleration processes), plasma parameters magnetic field strength (B), density (n), temperature (T) and so on. Usually, the confrontation of timing synchronization between electromagnetic flare emissions with those of energetic particles and coronal mass ejections (CME) is the method utilized to explore the physical conditions and processes taking place in the sources of particle generation. This synchronization method has been exhaustively exemplified by Malandraki et al. (2012) in connection with the SEPServer project for the case of the 13 July 2005 event. Besides, by means of the HESPERIA HORIZON 2020 project the first inversion of the neutron monitor (NM) observations has been carried out that infers directly the release timescales of relativistic Solar Energetic Particles (SEPs) at or near the Sun (Malandraki et al., 2015). Recently, the Fermi-LAT collaboration (Ackermann et al., 2017) proposes that >10 -GeV protons (accelerated in the CME environment) produce >100 -MeV gamma rays which correlates by the interaction of >10 -GeV protons in a thick target photospheric source away from the original flare site and the hard X-ray emission. In the particular case of the GLE71 (17 May 2012) several outstanding synchronization between particles and electromagnetic radiation studies have been done (e.g., Battarbee et al., 2017; Li et al., 2013).

Another method to infer about the source physical parameters and the kind of acceleration mechanisms involved in the phenomenon is by means of the confrontation of the observational and theoretical particle energy spectra (Pérez Peraza et al., 2011; Pérez-Peraza et al., 2006, 2008, 2009; Miroshnichenko et al., 2009). Based on this last alternative, in this work, we attempt here to determine the physical parameters and acceleration processes at the source of the 17 May 2012 GLE. This leads us to build possible scenarios for the particle generation process.

Among the descriptions for describing particle spectra of GLE at the top of the Earth atmosphere, a number of proposals can be found in the literature: an exponential over rigidity (e.g., Freier & Weber, 1963; Lockwood et al., 1974), a power law with an exponential roll-off (e.g., Ellison & Ramaty, 1985), or alternatively the so-called Band function (Band et al., 1993) based on a suitable model to parameterize the event-integrated fluence (Tylka & Dietrich, 2009); this approach describes the integral rigidity spectrum by a double power law in rigidity with a smooth exponential junction in between (Usoskin et al., 2011). Some of these propositions describe nicely the observational data for some particular GLE, though according to some authors (e.g., Bombardieri et al., 2006, 2007, 2008; Shea & Smart, 2012) these simple approximations often do not work well, especially for high energies above several GeV. Nevertheless, whatever the approach, the observational spectra obtained at the Earth level give scarce information about the source phenomena at the Sun level. This is due to the fact that, in general, the spectrum at the top of the atmosphere is not necessarily the same than the one at the source.

The reconstruction of solar cosmic rays spectra at the source from observations at the top of the Earth atmosphere is a complicated problem, since the spectrum goes considerable modulation along the way from the source to the Earth; the observed time profile is a superposition of the effects of particle azimuthal propagation in the solar corona and modulation during their transport in the interplanetary space. Because of the stochastic nature of the solar and interplanetary magnetic fields, the inverse problem of Solar Cosmic Rays (SCR) propagation, that is, the reconstruction of their characteristic near the roots of the interplanetary field lines at the high corona cannot be solved exactly. It can only be done under certain model approximations (e.g., Miroshnichenko & Sorokin, 1985, 1986, 1987a, 1987b, 1989): one must assume that the demodulated spectrum for interplanetary transport corresponds approximately to the spectrum only when the emitted particles from the upper corona occur near the longitude of the Sun-Earth connection ($\theta \approx 60^\circ\text{W}$). For further demodulation of the spectrum, after the interplanetary demodulation obtained up to the top of the solar corona field lines, one must allow for the azimuthal transport of particles in the magnetic fields of the solar corona as proposed originally by Reinhard and Wibberenz (1973, 1974), Wibberenz and Reinhard (1975), Schatten and Mullan (1977), Martinell and Pérez-Peraza (1981), Pérez-Peraza and Martinell (1981) and Pérez-Peraza et al. (1985) and reviewed in Pérez-Peraza (1986). This method proposes two coronal regions of particle transport (in the ecliptic plane), a fast propagation region and a slow propagation region. According to Álvarez-Madriral et al. (1986), in their conclusion no. 4, if the fast propagation region contains the solar longitude of connection between the Earth and the Sun, then the observed spectrum and the full demodulated spectrum (spectrum of the source) practically coincide. On the other hand, it is well known that Forman et al. (1986) have developed a method to derive the observational energy spectrum on the basis of the fluences at the *time of maximum intensity* at each particle energy, usually known as the TOM method. These authors pointed out that this method is suitable for very high energy particles, when the source is in the well-connected region of the Sun (55°W – 88°W), to avoid effects of coronal and interplanetary transport. This assumption allows estimating suitable integral energy spectra of several GLE that have taken place since 23 February 1956 (Miroshnichenko, 1994, 1996, 2001). Therefore, taking into account that under those particular conditions the source spectrum can be approximated to the observational one, we have proceeded to study the source processes by solving the Vlasov equation (collisionless Boltzman equation) in the frame of the quasi-linear theory; such equation leads us to a Fokker Planck kind equation in energy space, which we have analytically solved by means of the WKB method (Gallegos-Cruz & Pérez-Peraza, 1995, hereafter G-P, Ap.J. 1995), through all the energy range, from suprathermal to ultrarelativistic energies. It is in this way that considering the observational spectra as a proxy of the source spectra, we have proceeded, in the past, to the confrontation of the theoretical spectra with the observational one for several GLE (Bombardieri et al., 2006, 2007; Pérez-Peraza et al., 2006, 2008, 2009; Vashenyuk et al., 2006).

In the particular case of the GLE in consideration, the GLE71, which has presented at least two different components (what may be interpreted as two different sources), we have assumed that most of the observational spectra given by different authors were measured around the TOM. Besides, since the responsible flare was located at 13°N , 83°W , it can be considered that it is within the fast propagation region of the corona, allowing us to consider the observational spectrum as a proxy of the source spectrum.

2. Energy Spectrum of the 17 May 2017

On 17 May 2012 took place a peculiar GLE that has been conventionally designated as GLE71. As mentioned above, determination of the observational energy spectra of GLE has been done historically by several

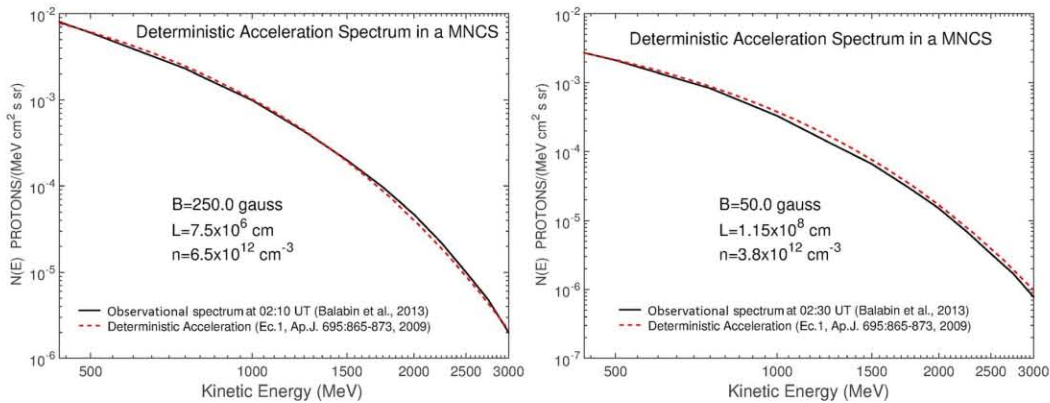


Figure 1. Confrontation of the observational spectra at 02:10 and 02:30 universal time (UT) (Balabin et al., 2013) versus theoretical spectra with deterministic acceleration in a magnetic neutral current sheet (MNCS).

different methods. The standard conventional method is based on a given spectral function, specific yield functions, pitch angle distribution, asymptotic cones, an inversion method, and so on (see, e.g., Miroshnichenko, 2014). This method usually requires data of NM stations well distributed in latitude, which is not precisely the case of GLE71.

The event was mainly observed in high-latitude polar NM and some few stations at lower latitudes with geomagnetic cutoff < 3 GV. It was an event of small intensity and highly anisotropic: the maximal enhancement ($\sim 25\%$ according to 5-min data) was registered at the South Pole station. Particles of $E < 433$ MeV were recorded by several spacecraft, for example, Geostationary Operational Environmental Satellite (GOES) and Anomalous Long Term Effects in Astronauts (ALTEA) (e.g., Berrilli et al., 2014). The observational characteristics of the associated flare and electromagnetic emissions have been widely described by many authors (e.g., Augusto et al., 2013; Firoz et al., 2014; Heber et al., 2013; Li et al., 2013; Papaioannou et al., 2014).

Studies of the observational spectrum have been done by Kuwabara et al. (2012), Balabin et al. (2013), Plainaki et al. (2014), Mishev et al. (2014), and Asvestari et al. (2017). For the confrontation of our theoretical spectra (G-P, Ap.J. 1995) and the observational spectra of the several authors, previously mentioned, we have limited the span in kinetic energy of protons up to the top of the observational fluences by the NM stations. Then, we begin with the spectra given by Balabin et al. (2013) derived for three different times; though their results are presented up to 7 GeV, we have only considered them up to the observed top by NM stations, that is, near 3 GeV. Our best fit of their spectrum is by assuming *deterministic acceleration* from a *magnetic neutral current sheet (MNCS)*. In Figure 1 we show such adjustment, at times 02:10 and 02:30, with equation (4) in the supporting information (corresponding to equation (1) in Pérez-Peraza et al., 2009). The obtained source parameters point toward an expanding chromospheric MNCS, which is lengthening as acceleration is taking place in the first phase of the event. It could be considered that such spectra correspond to the so-called prompt component (PC; e.g., Vashenyuk et al., 2006, 2008); however, the authors do not give such specification nor a spectrum later than 02:30 that could be considered as a *delayed component (DC)*.

Another observational spectrum, the first published one of the GLE71 (to our knowledge), was given by Kuwabara et al. (2012). This was done on the basis of the data of the large Antarctic installation (South Pole monitors), the IceTop Cherenkov detector, the NM64 NM, and the Polar Bare NM. They use a standard-kind model to derive the energy spectrum. Figure 2 shows their derived spectrum between 02:35 and 03:35 UT. We have adjusted their curve with a *time-dependent spectrum* from *stochastic acceleration* and *injection* from a preacceleration stage, fed by a *monoenergetic* fluence of protons of $E_0 = 1$ MeV (from the top of a plasma thermal distribution at about 10^7 K) while being decelerated by *adiabatic* losses. The employed spectrum is given in the supporting information as equation (1) (corresponding to equation (41) in G-P, Ap.J. 1995), where we have added adiabatic energy losses during acceleration in the expanding structures of the source up to the moment that particles escape to the interplanetary space. This is the best fit of the reported spectrum, among the several different scenarios studied in G-P, Ap.J. 1995.

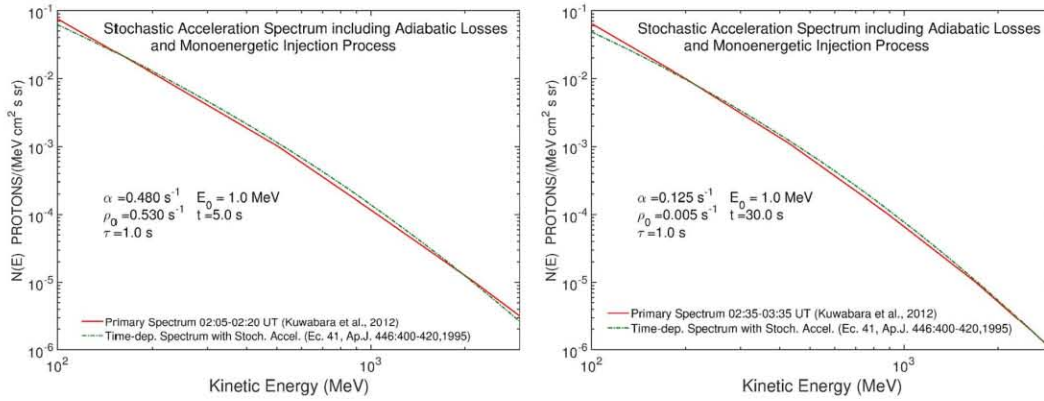


Figure 2. Confrontation of the observational spectra (Kuwabara et al., 2012) at 02:05–02:20 UT (left panel) and 02:35–03:35 UT (right panel) versus theoretical time-dependent spectra with stochastic acceleration.

Another outstanding analysis was carried out by Plainaki et al. (2014), based on their model NMBANGLE PPOLA that allows them the use of a number of stations that apparently did not register the GLE. Their work leads to two different *episodes* in the event: an initial one (prior to the arrival of the bulk of particles to NM stations), where the spectrum is rather of soft nature, and on the other hand, there is a second episode composed by particles with harder spectrum. They interpret these two phases as a possibility of the existence of two acceleration processes. Figure 3 shows our fit to the soft component just at the beginning of the event when particles belong rather to the SPE component, but high-energy protons scarcely have arrived at ground level (01:45 UT). The best fit is obtained assuming stochastic acceleration with monoenergetic injection and adiabatic energy losses in a relatively fast process at the source. Figure 3 also shows the fit of our source spectrum to their observational harder spectrum as measured by those authors at 03:05 UT. Our fitting of the spectrum at 03:05 points toward acceleration in a second episode of the event. We obtain that the best description is by stochastic acceleration with monoenergetic injection of 1-MeV protons, while particles are losing energy at the source by adiabatic deceleration. Both fittings in Figure 3 were obtained with equation (1) in the supporting information (corresponding to Equation (41) in G-P, Ap.J. 1995).

Besides, Mishev et al. (2014) develop an original method to determine the energy spectrum of the GLE71 that turns out to be quasi-independent of the latitude of NM stations. To derive a suitable spectrum the authors drew on low-latitude stations that seemingly have not recorded the GLE71. The method is based on a modern conception of the standard-kind method with a new yield function and inversion method. In fact, they

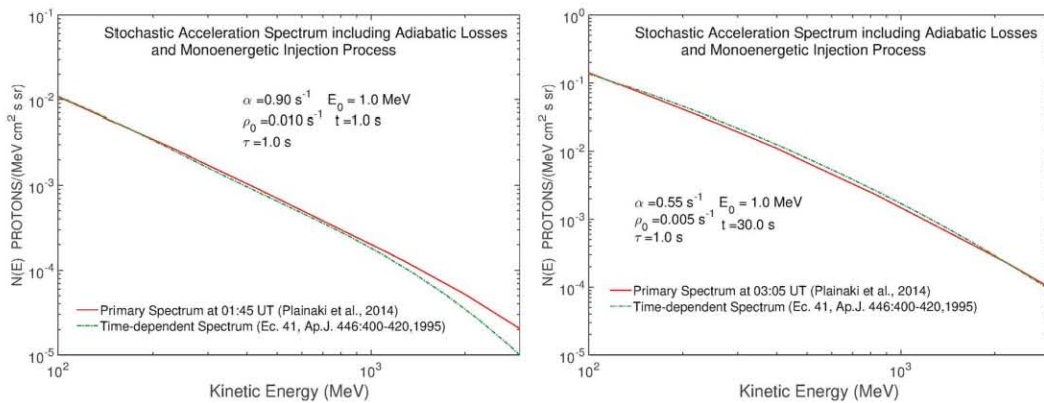


Figure 3. Confrontation of the observational spectra (Plainaki et al., 2014) at 01:45 UT (left panel) and 03:05 UT (right panel) versus theoretical time-dependent spectra with stochastic acceleration.

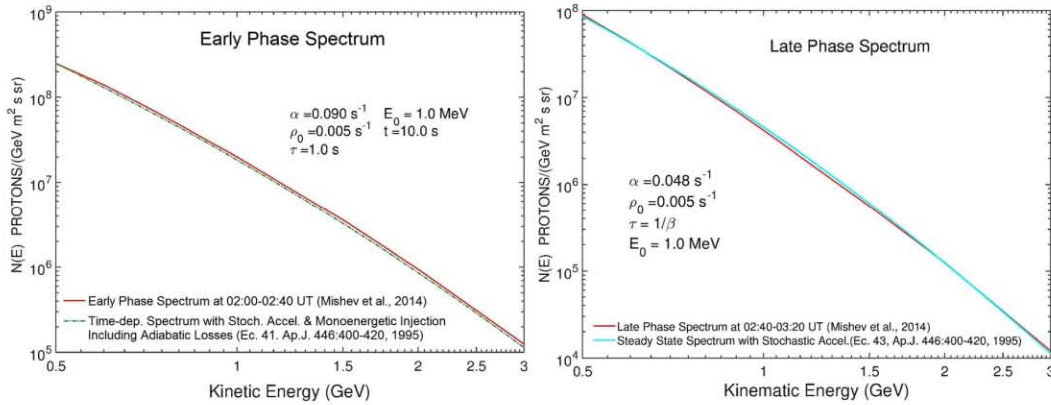


Figure 4. Confrontation of the observational early phase (02:00–02:40 UT) and late phase (02:40–03:20 UT; Figure 5 in Mishev et al., 2014) versus theoretical time-dependent and steady state spectra, respectively.

distinctly showed the presence of an “early” phase and a “late” phase in the ground NM data during the GLE71, which in some measure could be considered as equivalent to the PC and DC that were put in evidence long ago by the group of *Apatity* (e.g., Miroshnichenko et al., 1990; Vashenyuk et al., 1991, 1994, 1997, 2002, 2006, 2008, Vashenyuk, Balabin, et al., 2007, Vashenyuk, Miroshnichenko, et al., 2007). Their early phase is illustrated in Figure 4, corresponding to the angle-averaged integrated fluency from 02:00 to 02:40 UT. This can be suitably reproduced by means of the time-dependent spectrum from stochastic acceleration after 10 s, with monoenergetic injection of 1-MeV protons while undergoing adiabatic energy losses (equation (1) in the supporting information, corresponding to equation (41) in G-P, ApJ. 1995). In Figure 4 is also shown the angle-averaged integrated fluency in the time interval 02:40–03:20 UT (Mishev et al., 2014). For this time interval the best description of the spectrum is obtained with the *steady state spectrum* from stochastic acceleration and monoenergetic injection, given in equation (3) of the supporting information (corresponding to equation (43) in G-P, ApJ. 1995), where it is assumed that particle escape is inversely proportional to the velocity of the particles. In Figure 5 we show the observational spectra at specific times during the so-called late phase 02:40 and 03:10 UT. These can be reproduced with our source time-dependent spectrum from stochastic acceleration and monoenergetic injection while losing energy by adiabatic losses (equation (1) in the supporting information). It can be seen that the source spectrum, in our time-dependent approach (at two different acceleration times, 10 and 30 s), fits quite correctly the observational spectra for the two times, 02:40 and 03:10 UT. The closeness in Figure 5 between the theoretical spectrum with the observational one might indicate that even if the steady state was not yet reached, it was very near to be reached after

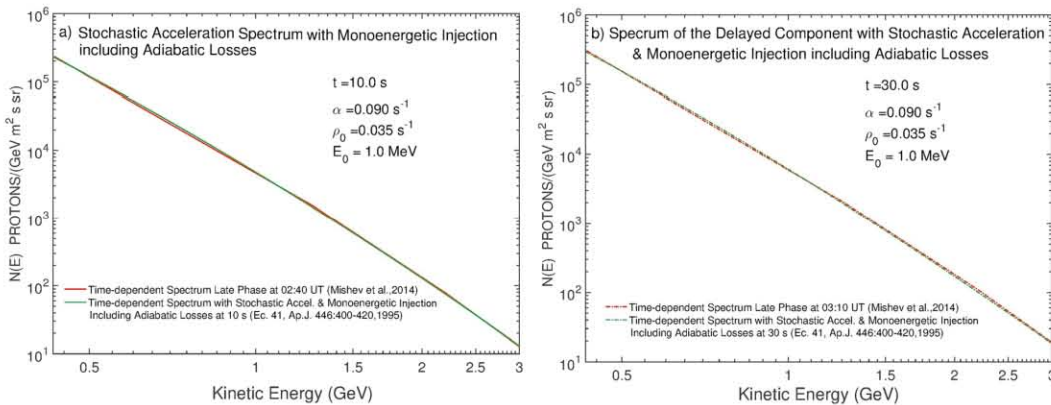


Figure 5. Confrontation of the observational late phase (02:40 and 03:10 UT; Figure 4 in Mishev et al., 2014) versus theoretical time-dependent spectra.

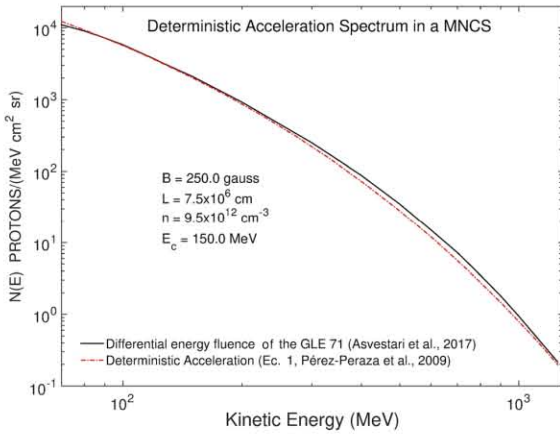


Figure 6. Confrontation of the observational spectra (Asvestari et al., 2017) versus theoretical spectra with deterministic acceleration in a magnetic neutral current sheet (MNCS).

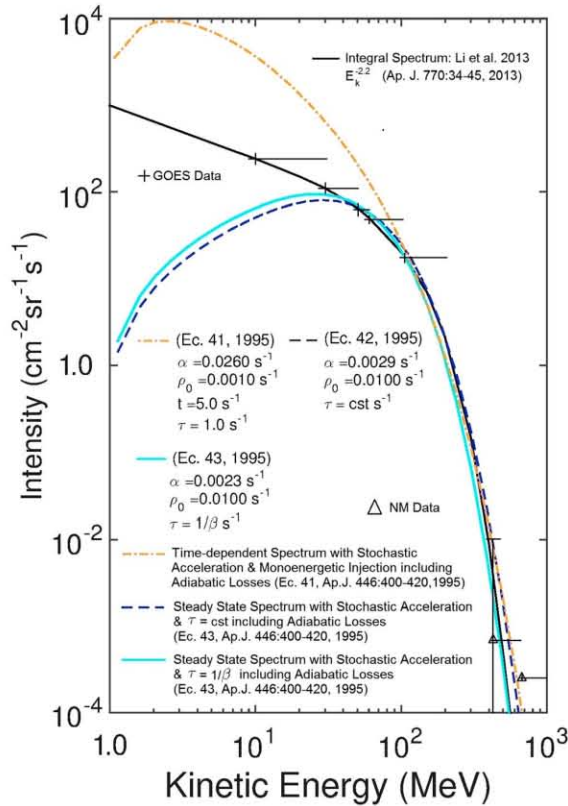


Figure 7. Confrontation of the observational spectrum (Li et al., 2013) versus theoretical time-dependent and steady state spectra.

10 s in the source (translated to the Earth level in a time interval, 02:40–03:20 UT); according to Figures 4 and 5b such steady state situation took place at an acceleration time just above 30 s, which at the Earth level occurred between 03:10 and 03:20 UT.

Recently, Asvestari et al. (2017) give a spectrum of the GL71 on the basis of the PAMELA data that differs from the GOES + NM data only at $E > 1$ GeV. The authors do not mention the specific time of their differential spectrum neither comment on different acceleration stages; it should be noted that the fluence is not per time unit and differs by several orders of magnitude with respect to the other authors. In Figure 6, it is shown that in this case the best fit to their spectrum is given with deterministic acceleration in a reconnection process of a MNCS (equation (4) in the supporting information, corresponding to equation (1) in Pérez-Peraza et al., 2009).

Regarding Figure 7, it has been argued by Li et al. (2013) that in practice, due to the limited latitude effect and to the extreme low intensity at high energies $\sim 3 \times 10^{-4}$ pfu ($\text{cm}^{-2} \cdot \text{s}^{-1} \cdot \text{sr}^{-1}$) of GLE71, no confident energy spectrum can be determined in the high-energy portion by the standard model, just in agreement with Büttikofer & Flückiger (2013). In order to avoid high controversies around the NM counting rates that appear due to statistical fluctuations, instead of the standard model used by most authors, Li et al. (2013) drew on the TOM method using data of five NM stations. They derived a spectrum that fits correctly the low-energy portion from GOES-13. The black curve in Figure 7 shows the derived TOM spectrum including data at low energies. It should be noted that in contrast to other authors, they give an integral spectrum instead of a differential one, so instead of converting their spectrum to the differential form, we have chosen to integrate our equations (1)–(3) of the supporting information. In this case, our study indicates that above 400 MeV very good fittings may be obtained with the steady state spectrum from stochastic acceleration with monoenergetic injection and adiabatic losses (equations (2) and (3) of the supporting information, corresponding to equations (42) and (43) in G-P, Ap.J. 1995) and even with the time-dependent spectrum (equation (1) in the supporting information). However, at lower energies we cannot reproduce the observational spectrum, which can be attributed, at least, to two main causes: (1) Forman et al. (1986) precluded the TOM method for low-energy particles, because it is less reliable not only due to transport effects but also because particles are more subject to convection and adiabatic deceleration, so the spectrum becomes flatter than the spectrum at the Sun; (2) the low-energy portion of the spectrum is produced by another stage of acceleration, most probable due to shock wave acceleration as argued by Li et al. (2013). This second option could be also consistent with the series of works of Bombardieri et al. (2006, 2007, 2008) who have shown that shock wave acceleration is rather effective for the nonrelativistic range, but at high energies the spectrum is broken undergoing an exponential cutoff. The result is then a significant softening of the particle spectrum and decrease of their maximum energy. Those works are in agreement with our claim in the present work, regarding the predominance of stochastic acceleration. Under these circumstances the logical scenario could be a prompt acceleration phase by reconnection in a MNCS and shock wave acceleration and a delayed stage by stochastic acceleration.

3. Discussion

The GLE of 17 May 2012 was very peculiar from the point of view that was relatively small, showing a spectrum at $E < 433$ MeV of relatively soft nature, changing to a hard one as the time elapses. There is a consensus that the lack of a latitude effect of nonpolar MN stations inhibits the standard model to derive the observational spectrum at $E > 433$ MeV. However, there is no doubt that a number of stations have registered a counting rate increase at the time of the event, originated in a class 5.1 flare that took place at about 01:25 UT. Such increase was registered also for some nonpolar stations, though on the basis of statistical fluctuations they have been disregarded by Li et al. (2013), what led those authors to derive a spectrum on the basis of the TOM model (Forman et al., 1986). Nevertheless, ignoring those statistical constraints, a number of authors derived the spectrum on the basis of different variants of the conventional standard model. The observational spectrum tends to show two different behaviors: a rather flat spectrum from 01:45 to 02:30 UT that we have identified as a PC and a steeper spectrum that we designate here as a DC. These connotations may be identified with the early and late phases of Mishev et al. (2014) and the acceleration episodes of Plainaki et al. (2014).

As we mention in section 1, the phenomena that take place at the sources of solar energetic particles can be inferred from the timing synchronization between the several electromagnetic flare emissions and CME. Another option is by means of energetic particles on the basis of the confrontation of observational spectra with theoretical source spectra. In the present work we attempt to infer about the source phenomena by this last option, that is, by fitting observational spectra with our theoretical spectra developed in Pérez-Peraza et al. (1977), Gallegos-Cruz and Pérez-Peraza (1995), and Pérez-Peraza et al. (2009). Such confrontation leads us to infer about plausible scenarios of particle generation in this peculiar GLE. The restriction of this method is that observational spectra, even at high energies, are not strictly representative of the source spectra. In fact, the closest translation is when the source is in the Sun-Earth connection ($\sim 55^\circ\text{--}88^\circ$); particles traveling out of that cone never reach Earth, so then the registered fluence is lower than that at the source level. Furthermore, there are effects of coronal azimuthal and interplanetary transport, as well as adiabatic and collisional energy losses in and out of the source (probably behind the expanding shock wave). If the source magnetic structure is momentarily closed, even the most energetic particles may be modulated by collisional energy losses before they escape to the interplanetary medium. Given the involved flare location, for the particular event, the GLE71, we have considered here the observational spectrum as a proxy of the source spectrum. The confrontation of theoretical source spectra with the observational one gives us an approximate conception of the scenarios of production, which is the involved acceleration and energy loss processes and the plausible source parameters.

We found that two main acceleration mechanisms are potentially involved: (1) a deterministic process by direct electric field acceleration from reconnection in a MNCS (the presence of reconnection processes during flare activity has been often discussed in the literature since at list from 1953; see, e.g., the excellent review by Cargill, 2013) and (2) a stochastic process by local magnetohydrodynamic turbulence in the flare body and/or turbulence generated behind the shock generated in the CME associated to the flare, when the preceding CME can provide enough enhanced turbulence to feed a particle population ahead the main CME-driven shock.

Regarding the source parameters, it should be emphasized that taking into account, there is not a unique observational spectrum, but there exist a great dispersion of results for the GLE71, even at similar record times, so one can only determine a range of the most probable source parameters. The results obtained here from stochastic acceleration point toward an acceleration efficiency in the range $\alpha = 0.9\text{--}0.0023\text{ s}^{-1}$ and the deceleration efficiency by adiabatic losses $\rho = 0.01\text{--}0.001\text{ s}^{-1}$, and the best description of the spectrum is obtained for acceleration times in the range $t \approx 1\text{--}30\text{ s}$ and for monoenergetic injection the best value is $E_0 = 1\text{ MeV}$. For the deterministic acceleration process by reconnection in a MNCS the values of the magnetic field strength are in the interval $B = 250\text{--}50\text{ Gauss}$, the density $n = 9.5 \times 10^{12}$ to $6.5 \times 10^{12}\text{ cm}^{-3}$ and the length of the neutral sheet $L = 7.5 \times 10^6$ to $1.15 \times 10^8\text{ cm}$. Such a dispersion of the physical parameters can be understood from the fact that the observational spectra given by different authors have been done using different approaches of the standard model: different sets of NM stations, different yield functions, different considerations about time evolution of pitch angle distributions and functions of asymptotic cones, and different flux intensity with different spectral indices, so that their

Table 1

Source Parameters Derived From the Best Fittings in Figures 1–7

Author	Spectrum	UT	Fit	α (s^{-1})	ρ_0 (s^{-1})	E_0 (MeV)	τ (s)	t (s)	B (gauss)	L (cm)	n (cm^{-3})	Injection
Kuwabara et al. (2012)	Time-dependent stochastic acceleration	02:05–02:20	Ec. 41, ApJ. 446,1995	0.48	0.53	1.0	1.0	5.0				Monoenergetic
Kuwabara et al. (2012)	Time-dependent stochastic acceleration	02:35–03:35	Ec. 41, ApJ. 446,1995	0.125	0.005	1.0	1.0	30.0				Monoenergetic
Li et al. (2013)	Time-dependent stochastic acceleration		Ec. 41, ApJ. 446,1995	0.026	0.001	1.0	1.0	5.0				Monoenergetic
Li et al. (2013)	Steady state stochastic acceleration		Ec. 42, ApJ. 446,1995	0.0029	0.01	1.0	1.0					Monoenergetic
Li et al. (2013)	Steady state stochastic acceleration		Ec. 43, ApJ. 446,1995	0.0023	0.01	1.0	$1/\beta$					Monoenergetic
Balabin et al. (2013)	Deterministic acceleration	2:10	Ec. 01, ApJ. 695,2009						250.0	7.50E+06	6.50E+12	
Balabin et al. (2013)	Deterministic acceleration	2:30	Ec. 01, ApJ. 695,2009						50.0	1.15E+08	3.80E+12	
Plainaki et al. (2014)	Time-dependent stochastic acceleration	1:45	Ec. 41, ApJ. 446,1995	0.9	0.1	1.0	1.0	1.0				Monoenergetic
Plainaki et al. (2014)	Time-dependent stochastic acceleration	3:05	Ec. 41, ApJ. 446,1995	0.55	0.005	1.0	1.0	30.0				Monoenergetic
Mishev et al. (2014), early phase	Time-dependent stochastic acceleration	02:00–02:40	Ec. 41, ApJ. 446,1995	0.09	0.005	1.0	1.0	10.0				Monoenergetic
Mishev et al. (2014), early phase	Steady state stochastic acceleration	02:40–03:20	Ec. 43, ApJ. 446,1995	0.048	0.005		$1/\beta$					Monoenergetic
Mishev et al. (2014), early phase	Time-dependent stochastic acceleration	2:40	Ec. 41, ApJ. 446,1995	0.09	0.035	1.0	1.0	10.0				Monoenergetic
Mishev et al. (2014), early phase	Time-dependent stochastic acceleration	3:10	Ec. 41, ApJ. 446,1995	0.09	0.035	1.0	1.0	30.0				Monoenergetic
Asvestari et al. (2017)	Deterministic acceleration		Ec. 01, ApJ. 695,2009						250.0	7.50E+06	9.50E+12	

Note. UT = universal time.

fluences and spectral indices change from author to author. It is obvious that under such circumstances, it is not feasible to have a protocol to derive observational spectra of energetic solar particles; all what we can hope is that they only differ no more of an order of magnitude. Nevertheless, it should be noted that the source parameters obtained here are within the conventional range of chromospheric and coronal solar flares values. Note that in the particular case of the spectrum of Balabin et al. (2013) at 02:10 UT and that of Asvestari et al. (2017), even if the fluence scales are different, it can be seen in Table 1 that the obtained source parameters are the same.

4. Conclusions

We have explored the sources of particles during GLE of 17 May 2017 on the basis of the spectra given by different authors, under different approaches of the standard model, and on the TOM model. In spite that authors present their results in different scale units, most of them agree, within a factor around 10 in their observed fluences, with the exception of Asvestari et al. (2017). This agreement is very important considering that one of the main goals of authors in calculating energy spectra is that the specialized community may draw inference about the source phenomena.

The main results of this work to highlight are the set of source parameters of particle generation and the involved acceleration processes driving to plausible scenario(s) during the GLE71. It is precisely the confrontation of theoretical source spectra with the observational spectra that gives us an approximate conception of the scenarios of production. The analysis of the spectra leads us to consider the presence of two different particle components during the GLE71, conspicuously the works of Kuwabara et al. (2012) and Mishev et al. (2014), with their early and late phases, and Plainaki et al. (2014), with the so-called episodes. Here we have designated those two components as the PC and DC. These two components may indicate the occurrence of two different acceleration processes or a unique acceleration mechanism in two different acceleration stages. Due to the dispersion of results of different authors, strictly one could conceive different scenarios according to different observational spectra. However, here we opt for proposing a general picture of particle generation phenomena which leads us to conclude that among all the scenarios that were able to occur during particle generation in the GLE71, those invoking two acceleration stages with different acceleration mechanism are the more likely to occur. The exceptions are the results presented by Balabin et al. (2013) and Asvestari et al. (2017), which apparently only found one single acceleration stage that we have adjusted by means of the deterministic acceleration.

The fact that in our results the magnetic field B and local density n decrease as time elapses whereas the length of the sheet L increases with time leads us to propose a tentative scenario where particles of the PC are accelerated by an impulsive and fast deterministic process, whereas the DC is produced in the source and its environment by stochastic acceleration due to the local turbulence and/or the turbulence generated by the plasma expansion behind the shock wave, while losing energy by adiabatic losses, up to the moment when the "expanding magnetic bottle" opens, allowing particles to escape to the interplanetary medium. Meanwhile, the prompt particle component is produced in a concomitant MNCS. It should be noted that, according to the theoretical spectra from stochastic acceleration, at 03:40 the steady state seems to have been reached, and consequently, under this situation the acceleration efficiency tends to be much lower than at early times (Figure 4). The fact that some spectra cannot be nicely reproduced with our theoretical spectra, that is (Kuwabara et al., 2012), in the lapse 02:05–02:20 UT (Plainaki et al., 2014), before 03:05 (Figure 4), as well as the angle average spectrum of the early phase of Mishev et al. (2014) during the lapse 02:00–02:40 UT, and (Li et al., 2013) at low energies may be indicative of the possible contribution of shock wave acceleration. It should be mentioned that modern literature favors shock wave acceleration due to the frequent presence of a CME; for the GLE71 Li et al. (2013) invoke shock wave acceleration, though we think that their work is rather of qualitative nature, in contrast with our present work. Within the frame of our scenario, pure shock acceleration does not play the mayor role for accelerating particles up to GLE energies. Our present study supports rather the results of Bombardieri et al. (2006, 2007, 2008), though it is likely that shock wave acceleration has contributed to the generation of particles registered by GEOS-13 at $E < 433$ MeV. Whatever the reason of our fail to reproduce adequately the above mentioned spectra, it must be considered that the derived spectra by several authors disagree among them not only within a factor around 10 in the magnitude of the fluency but also in the slope of their spectra.

Acknowledgments

V. Velasco-Herrera wish to thank the Consejo Nacional de Ciencia y Tecnología for the financial support through grant 180148. Data regarding Figures 1–7 can be found in <https://www.dropbox.com/sh/kbjf9hrnev5mvj6/AAA-A6olcl-hmArLbjcROY6a?dl=0>.

References

Ackermann, M., Allafort, A., Baldini, L., Barbiellini, G., Bastieri, D., Bellazzini, R., et al. (2017). Fermi-LAT observations of high-energy behind-the-limb solar flares. *The Astrophysical Journal*, *835*(2), 219–232.

Álvarez-Madrigal, M., Miroshnichenko, L. I., Pérez-Peraza, J., & Rivero-G, F. (1986). Spectrum of solar cosmic rays in the source taking into account their coronal propagation. *Soviet Astronomy*, *66*, 1169–1181.

Asvestari, E. T., Willamo, A., Gil, I. G., Usoskin, G. A., Kovaltsov, V. V., & Mikhailov, A. M. (2017). Analysis of ground level enhancements (GLE): Extreme solar energetic particle events have hard spectra. *Advances in Space Research*, *60*, 781–787.

Augusto, C. R. A., Kopenkin, V., Navia, C. E., Felicio, A. C. S., Freire, F., Pinto, A. C. S., et al. (2013). Was the GLE on May 17, 2012 linked with the M5.1-class flare the first in the 24th solar cycle? *arXiv:1301.7055, Astroph. SR*.

Balabin, Yu. V., Germanenko, A. V., Vashenyuk, E. V., & Gvozdevsky, B. B. (2013). The first GLE of the new 24th solar cycle. Proc. 33rd Int. Cosmic Ray Conf., Rio de Janeiro, Brazil, paper ICRC 2013-0021.

Band, D., Matteson, J., Ford, L., Schaefer, B., Palmer, D., Teegarden, B., et al. (1993). BATSE observations of gamma-ray burst spectra. I.—Spectral diversity. *The Astrophysical Journal*, *413*, 281–292.

Battarbee, M., Guo, J., Dalla, S., Wimmer-Schweingruber, R., Swalwell, B., & Lawrence, D. J. (2017). Multi-spacecraft observations and transport simulations of solar energetic particles for the May 17th 2012 GLE event. *arXiv preprint arXiv:1706.08458*.

Berrilli, F., Casolino, M., Del Moro, D., Di Fino, L., Larosa, M., Narici, L., et al. (2014). The relativistic solar particle event of May 17th, 2012 observed on board the International Space Station. *Weather and Space Climate*, *4*, A16. <https://doi.org/10.1051/swsc/2014014>

Bombardieri, D. J., Duldig, M. L., Michael, K. J., & Humble, J. E. (2006). Relativistic proton production during the 14 July 2000 solar event: The case for multiple source mechanisms. *Astrophysical Journal*, *644*, 565.

Bombardieri, D. J., Duldig, M. L., Michael, K. J., & Humble, J. E. (2007). Relativistic proton production during the 2001 April 15 solar event. *Astrophysical Journal*, *665*, 813.

Bombardieri, D. J., Duldig, M. L., Michael, K. J., & Humble, J. E. (2008). An improved model for relativistic solar proton acceleration applied to the 2005 January 20 and earlier events. *Astrophysical Journal*, *682*, 1315.

Bütikofer, R., & Flückiger, E. O. (2013). Differences in published characteristics of GLE60 and their consequences on computed radiation dose rates along selected flight paths, 23rd European Cosmic Ray Symposium (and 32nd Russian Cosmic Ray Conference) IOP Publishing. *Journal of Physics: Conference Series*, *409*, 012166. <https://doi.org/10.1088/1742-6596/409/1/012166>

Cargill, P. (2013). From flares to nanoflares: magnetic reconnection on the Sun. *Astronomy & Geophysics*, *54*(3), 3–16.

Ellison, D. C., & Ramaty, R. (1985). Shock acceleration of electrons and ions in solar flares. *The Astrophysical Journal*, *298*, 400–408.

Firoz, K. A., Gan, W. Q., Li, Y. P., & Rodriguez-Pacheco, J. (2014). An interpretation of a possible mechanism for the first ground-level enhancement of solar cycle 24. *Solar Physics*, *290*, 613–626. <https://doi.org/10.1007/s11207-014-0619-2>

Forman, M. A., Ramaty, R., & Zweibel, E. G. (1986). The acceleration and propagation of solar flare energetic particles. In P. A. Sturrock, et al. (Eds.), *Physics of the Sun, Geophysics and Astrophysics Monograph* (Vol. II, Chap. 13, pp. 249–290). D. Reidel Publishing Company.

Freier, P. S., & Weber, W. R. (1963). Radiation hazard in space from solar particles. *Journal of Geophysical Research*, *68*, 1605.

Gallegos-Cruz, A., & Pérez-Peraza, J. (1995). Derivation of analytical particle spectra from the solution of the transport equation by the WKBJ method. *Astrophysical Journal*, *446*, 400–420.

Heber, B., Dresing, N., Dröge, W., Gomez-Herrero, R., Herbst, K., Kartavykh, Y., et al. (2013). The first ground level event of solar cycle 24 and its longitudinal distribution in the inner heliosphere, American Geophysical Union, Fall Meeting 2013, Abstract SH33B-2079.

Kuwabara, T., Bieber, J., Clem, J., Evenson, P., Gaisser, T., Pyle, R., & Tilav, S. (2012). Ground level enhancement of May 17, 2012 observed at South Pole. Proc. 45th AGU Fall Meeting, SH21A-2183 (Poster), San Francisco.

Li, C., Kazi, A., Firoz, L., Sun, P., & Miroshnichenko, L. I. (2013). Electron and proton acceleration during the first ground level enhancement event of solar cycle 24. *Astrophysical Journal*, *770*(1), 34.

Lockwood, J. A., Webber, W. R., & Hsieh, L. (1974). Solar flare proton rigidity spectra deduced from cosmic ray neutron monitor observations. *Journal of Geophysical Research*, *79*, 4149–4155.

Malandraki, O. E., Agueda, N., Papaioannou, A., Klein, K. L., Valtonen, E., Heber, B., et al. (2012). Scientific analysis within SEPServer—New perspectives in solar energetic particle research: The case study of the 13 July 2005 event, *Solar Physics* *281*:333–352. <https://doi.org/10.1007/s11207-012-0164-9>

Malandraki, O. E., Klein, K. L., Vainio, R., Agueda, N., Nuñez, M., Heber, B., et al. (2015). “High energy solar particle events forecasting and analysis: The HESPERIA project”, Proceedings of Science, Proceedings of the 34th International Cosmic Ray Conference (Vol. 34). The Hague, Netherlands.

Martinell, J., & Pérez-Peraza, J. (1981). Coronal transport of solar flare particles. *Revista Mexicana de Astronomía y Astrofísica*, *6*, 351–355.

Miroshnichenko, L. I. (1994). On the ultimate capabilities of particle accelerators on the sun. *Geomagnetism and Aeronomy*, *34*, 29.

Miroshnichenko, L. I. (1996). Empirical model for the upper limit spectrum for solar cosmic rays at the Earth’s orbit. *Radiation Measurements*, *26*, 421–425.

Miroshnichenko, L. I. (2001). *Solar Cosmic Rays* (p. 480). Dordrecht, Netherlands: Kluwer Academic Publishers.

Miroshnichenko, L. I. (2014). *Solar cosmic rays: Fundamentals and applications* (2nd ed., p. 521). Switzerland: Springer.

Miroshnichenko, L. I., Perez-Peraza, J., Alvarez-Madrigal, M., Sorokin, M. O., Vashenyuk, E. V., & Gallegos-Cruz, A. (1990). Two relativistic solar components in some SPE, Proc. 21st Int. Cosmic Ray Conf., Australia, Adelaide, 5, 5–8.

Miroshnichenko, L. I., & Sorokin, M. O. (1985). Numerical solution of inverse problem for the reconstruction of source spectrum of solar cosmic rays. *Geomagnetism and Aeronomy*, *25*(4), 534–540.

Miroshnichenko, L. I., & Sorokin, M. O. (1986). Reconstruction of some characteristics of solar cosmic rays in the source based on observations near the Earth. *Geomagnetism and Aeronomy*, *26*(4), 535–540.

Miroshnichenko, L. I., & Sorokin, M. O. (1987a). Energy spectrum of the solar proton event of February 16, 1984. *Geomagnetism and Aeronomy*, *27*(6), 893–899.

Miroshnichenko, L. I., & Sorokin, M. O. (1987b). Solution of the inverse problem for determining solar cosmic ray parameters near the source. Proc. 20th /111. Cosmic Ray Conf., Moscow, USSR, v.3, 117–120.

Miroshnichenko, L. I., & Sorokin, M. O. (1989). Temporal and spectral characteristics of particles near the Sun for the proton events of December 7–8 1982 and November 19, 1949. *Geomagnetism and Aeronomy*, *29*(2), 309–311.

Miroshnichenko, L. I., & Pérez-Peraza, J. (2008). Astrophysical aspects in the studies of solar cosmic rays. *International Journal of Modern Physics A*, *23*, 1.

Miroshnichenko, L. I., Vashenyuk, E. V., & Pérez-Peraza, J. (2009). Two components concept of solar cosmic rays: Solar and interplanetary aspects. *Bulletin of the Russian Academy of Sciences*, *73*(3), 297–300.

- Mishev, A. L., Kocharov, L. G., & Usokin, I. G. (2014). Analysis of the ground level enhancement on 17 May 2012 using data from the global neutron monitor network. *Journal of Geophysical Research: Space Physics*, 119, 670–679. <https://doi.org/10.1002/2013JA019253>
- Papaioannou, A., Souvatzoglou, G., Paschalis, P., Gerontidou, M., & Mavromichalaki, H. (2014). The first ground-level enhancement of solar cycle 24 on 17 May 2012 and its real-time detection. *Solar Physics*, 289, 423–436. <https://doi.org/10.1007/s11207-013-0336-2>
- Pérez-Peraza, J., Velasco Herrera, V., Zapotitla Román, J., Miroshnichenko, L. I., & Vashenyuk, E. V. (2011). Classification of GLE's as a function of their spectral content for prognostic goals, 32ava ICRC, Beijing, China, SH1.5, Vol.10, 149–152.
- Pérez-Peraza, J. (1986). Coronal transport of solar flare particles. *Space Science Reviews*, 44, 91–138.
- Pérez-Peraza, J., Álvarez-Madriral, M., Rivero, F., & Miroshnichenko, L. I. (1985). Source energy spectra from demodulation of solar particle data by interplanetary and coronal transport, Proc. of the Int. Cosmic Ray Conf., XIX-4, 110–113.
- Pérez-Peraza, J., Gallegos Cruz, A., Vashenyuk, E. V., Balabin, Y. V., & Miroshnichenko, L. I. (2006). Relativistic proton production at the Sun in the October 28th, 2003 solar event. *Advances in Space Research*, 38, 418.
- Pérez-Peraza, J., Gálvez, M., & Lara-Alvarez, R. (1977). Energy spectrum of flare particles from an impulsive acceleration process, Proc. of the Int. Cosmic Ray Conf., XV-5, 23–28.
- Pérez-Peraza, J., & Juárez-Zuñiga, A. (2015). Prognosis of GLEs of relativistic solar protons. *The Astrophysical Journal*, 803(1), 9. <https://doi.org/10.1088/0004-637X/803/1/27>
- Pérez-Peraza, J., & Martinell, J. (1981). Azimuthal propagation of flare particles in the Heliosphere, Proc. of the 17th Int. Cosmic Ray Conf., 3, 55–58.
- Pérez-Peraza, J., Vashenyuk, E. V., Balabin, Y. V., Miroshnichenko, L. I., & Gallegos Cruz, A. (2009). Impulsive, stochastic and shock wave acceleration of relativistic protons in large solar events of 1989 September, 29, 2000 July 14, 2003 October 28, and 2005 January 20. *Astrophysical Journal*, 695, 865.
- Pérez-Peraza, J., Vashenyuk, E. V., Gallegos Cruz, A., Balabin, Y. V., & Miroshnichenko, L. I. (2008). Relativistic proton production at the Sun in the January 20th, 2005 solar event. *Advances in Space Research*, 41, 947–954.
- Plainaki, C., Mavromichalaki, H., Laurenza, M., Gerontidou, M., Kanellakopoulos, A., & Storini, M. (2014). The ground-level enhancement of 2012 May 17: Derivation of solar proton event properties through the application of the NMBANGLE PPOLA model. *The Astrophysical Journal*, 785, 160. (12 pp.) <https://doi.org/10.1088/0004-637X/785/2/160>
- Reinhard, R., & Wibberenz, G. (1973). Coronal transport of solar flare protons: Drift and diffusion in the corona, Proc 13th ICRC, 2, 1373–1383.
- Reinhard, R., & Wibberenz, G. (1974). The variation of solar proton energy spectra and size distribution with heliolongitude. *Solar Physics*, 36, 473.
- Schatten, K. H., & Mullan, D. J. (1977). Fast azimuthal transport of solar cosmic rays via a coronal magnetic bottle. *Journal of Geophysical Research*, 82, 5609.
- Shea, M. A., & Smart, D. F. (2012). Space weather and the ground-level solar proton events of the 23rd solar cycle. *Space Science Reviews*, 171, 161–188.
- Tylka, A., & Dietrich, W. (2009). A new and comprehensive analysis of proton spectra in ground-level enhanced (GLE) solar particle events, In: Proc. 31th International Cosmic Ray Conference. *Universal Academy Press, Lodz', Poland, p. ID 0273*, URL. Retrieved from <http://galprop.stanford.edu/elibrary/icrc/2009/preliminary/pdf/icrc0273.pdf>
- Usoskin, I. G., Kovaltsov, G. A., Mironova, I. A., Tylka, A. J., & Dietrich, W. F. (2011). Ionization effect of solar particle GLE events in low and middle atmosphere. *Atmospheric Chemistry and Physics*, 11, 1979–1988.
- Vashenyuk, E. V., Balabin, Y. V., & Miroshnichenko, L. I. (2008). Relativistic solar protons in the GLE of 23 February 1956: New study. *Advances in Space Research*, 41(6), 926–935.
- Vashenyuk, E. V., Balabin, Yu. V., Miroshnichenko, L. I., Pérez-Peraza, J., & Gallegos-Cruz, A. (2007). Two-component features of the two largest GLEs: 23 February 1956 and 20 January 2005, Proc. of the Int. Cosmic Ray Conf. XXX, 1, 249–252.
- Vashenyuk, E. V., Balabin, Y. V., Pérez-Peraza, J., Gallegos-Cruz, A., & Miroshnichenko, L. I. (2006). Some features of the sources of relativistic particles at the Sun in the solar cycles 21–23. *Advances in Space Research*, 38(3), 411–417.
- Vashenyuk, E. V., Miroshnichenko, L. I., Balabin, Yu-V, Pérez-Peraza, J., & Gallegos-Cruz, A. (2007). Relativistic solar cosmic ray events (1956–2006) from GLE modeling studies, Proc. of the Int. Cosmic Ray Conf. XXX, 1, 253–256.
- Vashenyuk, E. V., Miroshnichenko, L. I., Pérez-Peraza, J., Kananen, H., & Tanskanen, P. (1997). Generation and propagation characteristics of relativistic solar protons during the GLE of September 29, 1989, Proc. of the Int. Cosmic Ray Conf. XXV, 1, 161–164.
- Vashenyuk, E. V., Miroshnichenko, L. I., Sorokin, M. O., Pérez-Peraza, J., & Gallegos-Cruz, A. (1994). Large ground level events in solar cycle 22 and some peculiarities of relativistic proton acceleration. *Advances in Space Research*, 14(10), 711–716.
- Vashenyuk, E. V., Miroshnichenko, L. I., Sorokin, M. O., Pérez-Peraza, J., Álvarez-M, Y., & Gallegos-C, A. (1991). Dynamics of acceleration and escape of relativistic solar cosmic rays from the solar corona, *Kosmicheskiye Issledovaniya (Space Research, Leningrad Physical and Technical Institute)*, 147–160.
- Vashenyuk, E. V., Pchelkin, V., Gvozdevsky, B. B., & Pérez-Peraza, J. (2002). Primary solar cosmic ray parameters obtained by modeling technique from ground based observations, Proc. The 6th World Multiconference on Systemics, Cybernetics and Informatics XVII, 458–461.
- Wibberenz, G., & Reinhard, R. (1975). The exponential decay of solar flare particles: Eastern and western hemisphere effects, Proc. 14 Int. Cosmic Rays Conf. 5, 1681–1691.

PRESENTACION DEL ARTÍCULO: “Spectra of the Two Official GLEs of Solar Cycle 24”

Basándonos en datos a nivel del suelo y en datos satelitales, determinamos, en este trabajo, el espectro observacional de ambos eventos: GLE71 (17 de mayo de 2012) y GLE 72 (10 de septiembre de 2017). Describimos un método simplificado para obtener el espectro experimental a nivel terrestre. Los datos de los GLE71 y GLE72 indican la presencia de dos poblaciones diferentes, cada una con un espectro de energía distinto. Por otro lado, exploramos el tipo de fenómenos que tienen lugar en la fuente. En contraste con otros métodos basados en la sincronización temporal entre las emisiones electromagnéticas de las fulguraciones y las eyecciones de masa coronal (CME), aquí desarrollamos una opción alternativa basada en el estudio de las partículas aceleradas, ajustando los espectros observacionales a nuestros espectros teóricos. Los principales resultados de este trabajo son la derivación de los parámetros de la fuente y la aceleración involucrada en el proceso de generación. Estos resultados nos llevan a construir posibles escenarios de generación para cada uno de los dos GLE estudiados. Consideramos este tipo de estudio como un asunto crucial en el marco de la Astrofísica Solar.

Estatus: Aceptado para publicación.



The screenshot shows an email interface in a Google Chrome browser. The email is from Elsevier's editorial office, dated October 10, 2019, to JORGE a. PEREZ y pERAZA. The subject is 'Your Submission - ASR-D-19-00270R3'. The email body contains the following text:

Date: Oct 10, 2019
To: "JORGE a. PEREZ y pERAZA" perperaz@gmail.com
cc: ssrc@msn.com; jmarquezad@gmail.com; rogelloc@geofisica.unam.com; rob_rene199027@hotmail.com
From: "Advances in Space Research" eesserver@eesmail.elsevier.com
Reply To: "Advances in Space Research" asr-editorialoffice@elsevier.com
Subject: Your Submission - ASR-D-19-00270R3

Manuscript Number: ASR-D-19-00270R3
Section: SH - Solar and Heliospheric Physics
Article Title: SPECTRA OF THE TWO OFFICIAL GLEs OF SOLAR CYCLE 24
Advances in Space Research

Dear Professor PEREZ y pERAZA,

I am pleased to tell you that your manuscript has now been accepted for publication in Advances in Space Research and will shortly be sent to the publisher for processing.

Please note that ASR articles are published online almost directly after Acceptance, in the format as accepted by the editor. Should you wish to exclude your article from this early publication, please send a message immediately to asr-editorialoffice@elsevier.com

You should receive a galley proof for your correction and/or approval within about four weeks. Please make any necessary changes, answer all questions on the query document, and return this information as instructed in the cover letter - even if no changes are necessary.

Your final paper will not be available electronically until your galley proof is approved and returned.

Thank you for submitting your work to this journal.

Kind regards,

Peggy Ann Shea
Past Editor in Chief
Advances in Space Research

For further assistance, please visit our customer support site at <http://help.elsevier.com/app/answers/list/p/7923>. Here you can search for solutions on a range of topics, find answers to frequently asked questions and learn more about EES via interactive tutorials. You will also find our 24/7 support contact details should you need any further assistance from one of our customer support representatives.

Close

Copyright © 2019 Elsevier B.V. All rights reserved. Cookies are set by this site. To decline them or learn more, visit our [Cookies](#) page. RELX™

Manuscript Number: ASR-D-19-00270R3

Title: SPECTRA OF THE TWO OFFICIAL GLEs OF SOLAR CYCLE 24

Article Type: SH - Solar and Heliospheric Physics

Keywords: SOLAR CYCLE 24 - SOLAR FLARE PARTICLES - GROUND LEVEL ENHANCEMENTS - SOURCE ACCELERATION SPECTRUM.

Corresponding Author: Professor JORGE a. PEREZ y pERAZA, Ph.D.

Corresponding Author's Institution: UNIVERSIDAD NACIONAL AUTONOMA DE MEXICO

First Author: JORGE a. PEREZ y pERAZA, Ph.D.

Order of Authors: JORGE a. PEREZ y pERAZA, Ph.D.; Juan C Marquez-Adame, Dr; Rogelio A Caballero-Lopez, Dr; Roberto R Manzano-Islas, Master

Abstract: Based on ground-level data and on satellite data we determine in this work the observational spectrum of both, the Ground Level Enhancement of May 17, (2012) the so-called GLE71 and the Ground Level Enhancement of September 10, 2017 (GLE 72). We describe a simplified method to obtain the experimental spectrum at ground level. Data of the GLE71 and GLE72 indicate the presence of two different populations, each one with a different energy spectrum. On the other hand, we explore the kind of phenomena that take place at the source in these two particular events. In contrast with other methods based on the temporal synchronization between electromagnetic emissions of flares and coronal mass ejections (CME), here we develop an alternative option based on the study of the accelerated particles, by adjusting our theoretical spectra to the observational spectra. The main results of this work are the derivation of the source and acceleration parameters involved in the generation process. These results lead us to construct possible scenarios of particle generation in the source for each one of the two studied GLEs.

SPECTRA OF THE TWO OFFICIAL GLEs OF SOLAR CYCLE 24

Jorge A. Perez-Peraza*, Juan C. Márquez-Adame, Rogelio A. Caballero-Lopez, Roberto R. Manzano Islas,
Instituto de Geofísica, Universidad Nacional Autónoma de México, Ciudad Universitaria,
04510, CDMX, MEXICO.

ABSTRACT

Based on ground-level data and on satellite data we determine in this work the observational spectrum of both, the Ground Level Enhancement of May 17, (2012) the so-called GLE71 and the Ground Level Enhancement of September 10, 2017 (GLE 72). We describe a simplified method to obtain the experimental spectrum at ground level. Data of the GLE71 and GLE72 indicate the presence of two different populations, each one with a different energy spectrum. On the other hand, we explore the kind of phenomena that take place at the source in these two particular events. In contrast with other methods based on the temporal synchronization between electromagnetic emissions of flares and coronal mass ejections (CME), here we develop an alternative option based on the study of the accelerated particles, by adjusting our theoretical spectra to the observational spectra. The main results of this work are the derivation of the source and acceleration parameters involved in the generation process. These results lead us to construct possible scenarios of particle generation in the source for each one of the two studied GLEs.

KEY WORDS: SOLAR CYCLE 24 - SOLAR FLARE PARTICLES – GROUND LEVEL ENHANCEMENTS – SOURCE ACCELERATION SPECTRUM.

* perperaz@geofisica.unam.mx

1. INTRODUCTION

The implications of the study of Ground Level enhancements of solar particles have been addressed long ago (e.g. Sakurai, 1974, Shea et. al., 1988; Dorman and Venkatesan, 1993; Miroshnichenko and Perez-Peraza, 2008; McCracken et al., 2012; Miroshnichenko, 2014) due to its incidence at the astrophysical scale and the effects on the terrestrial level. In particular, the temporal profile of the particles provides information about the processes of interplanetary transport and the structure of the interplanetary magnetic field, while the energy spectrum provides information regarding the phenomena at the source, particularly in the acceleration process(es). As it was shown by Pérez-Peraza et al., 1985, at least for protons of $E < 480$ MeV the modulation of the fluxes may be relatively important for some events. On the other hand, in Miroshnichenko 2001, (beginning of section 1 at the end of section 8.1, there are some arguments (e.g. Reames, 1993) where the author suggested that Electric fields of the solar wind, in the first approximation, can be neglected and collisions of Solar Cosmic Rays with particles of the solar wind are insignificant. In Section 8.3.2 of the same book, there is an interesting discussion about the shift in the transport

paradigm. At any event, transport theory is a complicated matter, out of the scope of this work

Generally, synchronization of time between the electromagnetic emissions of solar flares with those of solar energy particles and coronal mass ejections (CME) is the method used to explore the physical conditions and processes that take place at the sources of solar particle generation (e.g., Gopalswamy et al., 2013). Alternatively, the comparison of the observational and the theoretical energy spectra leads us to make inferences regarding the phenomena at the source, particularly the physical parameters of the source and the type of acceleration mechanisms involved in the phenomenon (e. g., Gallegos-Cruz and Perez- Peraza, 1995; Perez-Peraza et al., 2009, 2018). At present, it is generally envisaged that the particles are accelerated due to two types of processes of a different nature: a deterministic and a stochastic acceleration processes. Among the more plausible proposals is the magnetic reconnection of the field lines in the flare body, or in its surroundings, and on the other hand in the turbulence of the flare plasma, or behind the shock waves associated with the coronal mass ejection (ME). Besides, it was observed that some GLE present two acceleration phases: a Prompt Component (PC) and a Delayed Component (DC), as was evidenced long ago by the group of the Polar Geophysical Institute of Apatity, Russia, (e.g. Vashenyuk et al., 1993, 1994, 2011) and recently designated as early and late phases of Mishev et al., 2014, or even as episodes (Plainaki et al., 2014). For the particular case of the Ground Level Enhancement of May 17, other authors (e.g. Kuwabara, et al., 2012, 2013; Berrilli et al., 2014) have also indicated two possible populations, during the GLE71, supporting the presence of a PC and a DC.

By comparing theoretical and observational spectra we attempt in this work to develop scenarios that can provide us with some insights of the phenomenon of particle acceleration during solar flares. It should be emphasized that our main goal is the study of the particle spectrum at the source level; therefore, we do not deal here with processes of particle propagation. Studies of effects of his kind on energy spectra have been done since many decades ago by a quite number of groups (Schlickeiser, R., 1989, Smart, D. F. and Shea, M. A., 1993, Miroshnichenko, L. I., 2014). In fact, since we are dealing with highly relativistic energy protons able to penetrate the magnetosphere, it is expected that interplanetary transport does not significantly alter the source spectrum of most of Ground Level Enhancements (GLEs). We will discuss later the case of satellite data of energies lower than 100 MeV.

Let us remember here that (GLEs) are events observed by detectors on the earth's surface when there is an abrupt increase in the cosmic particle count. The scientific international community recognizes at least 72 GLEs events from February 28, 1942, to September 10, 2017; currently, there is a worldwide network of neutron monitors at the earth level (NMDB, <http://www.nmdb.eu>). It has been well known for approximately the last seven decades that GLEs are characterized by a rapid increase of their maximum intensity, taking place within a few minutes, with decay being much slower than the increase; flows are highly anisotropic at the beginning and sometimes throughout the GLE (e.g. Moraal and Caballero-Lopez, 2014). The energy spectrum is softer than that of galactic cosmic radiation, and as the event progresses, it softens.

The first four figures show the time profiles of both events being considered (NMDB and satellites data).

2. DATA

There is a debate about which stations have registered the GLE of May 17, 2012, and given the smallness of the event at Ground level, however, according several works as for instance those of Poluianov et al., 2017 and Shea et al. 1985, there exist a standardized format for determining cosmic ray ground-level event data. On this basis, we claim that only nine NM stations have discernibly recorded this GLE as is shown in Figure 1, (from the NMDB). However, based on to the arguments that we will mention later, we reduce our study to two stations, SOPO and SOPB, assuming that the spectrum derived using these two high altitude polar neutron monitors give a reasonable description of the energetic flux that reach the earth ground level.

2.1. GLE OF MAY 17, 2012

This event took place due to a medium intensity solar flare (1F/M5.1, N12W83) and a high-speed CME ($1,582 \text{ km s}^{-1}$). Many researchers were involved in the study of the different characteristics of this event and its mother solar flare (e.g., Gopalswamy et al., 2013; Li et al., 2013; Balabin et al., 2013; Augusto et al., 2013; Papaioannou et al., 2014, Kuwabara et al., 2013) and so on.

High energy solar protons during this event were recorded not only by high latitude Neutron Monitor stations but also by several spacecraft close to Earth: WIND, GOES, ALTEA and ACE, Berrilli (2014), and some ground-based neutron monitors. The event was quite small, highly anisotropic and was only observed at high latitudes and at a few stations at lower latitudes with a geomagnetic cutoff $< 3 \text{ GV}$. The maximum increase was 24% according to *one minute* (NMDB) was recorded in the South Pole stations, Figure 1.

One of the interesting features about the acceleration of solar protons is to compare the behavior of the energy spectrum of low energy protons with that of relativistic protons that reach ground level. Such behavior may give some insights regarding whether the low and the high energy populations proceed from the same, or, different sources.

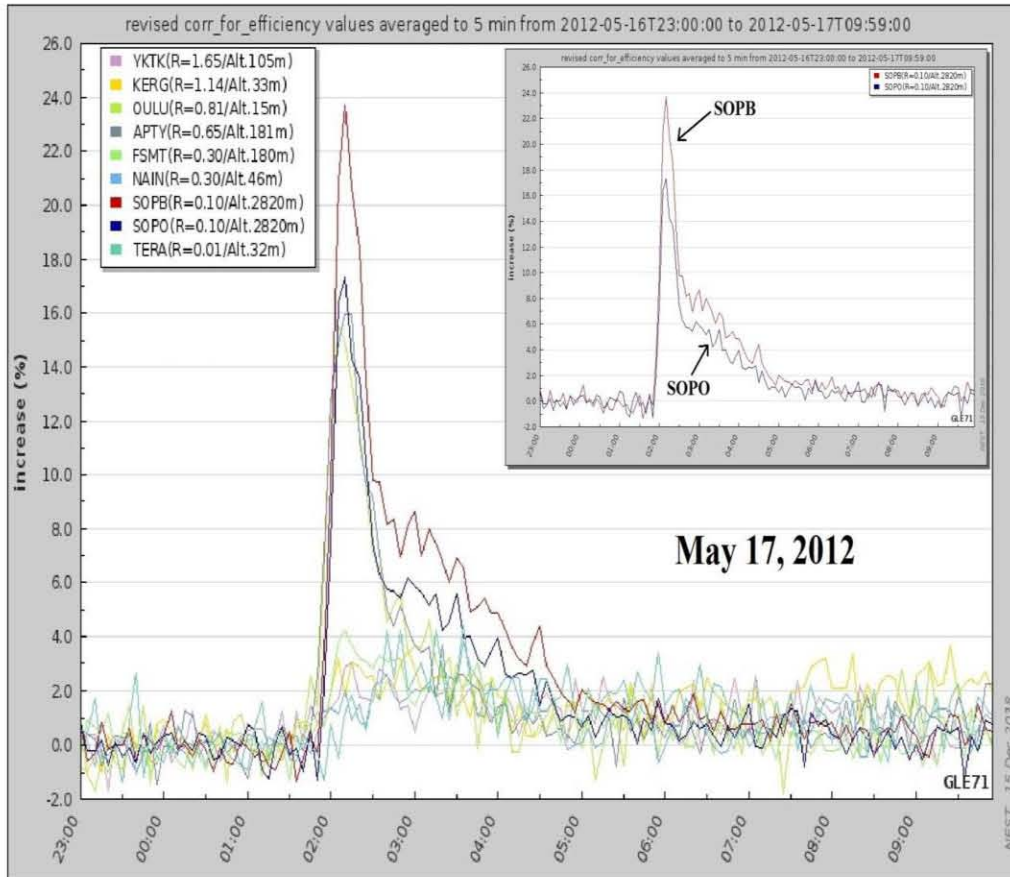


Figure 1 Increase of the proton flux of 9 stations (NMDB) including SOPO and SOPB during the GLE of May 17, 2012.

In the case of the GLE71, the time profile of low energy protons was given in terms of differential flux by Li et al., 2013 based on GOES-13 data (their Figure 3). To obtain the spectrum value at the four different energies, we use the Time of Maximum (TOM) flux (Forman et al., 1986; Li et al., 2013); Figure 2: illustrates that for 30.6 MeV, the differential flow becomes $\approx 7.9 \text{ protons} / (\text{cm}^2 \text{ s sr MeV})$, for 63.1 MeV the differential flow becomes $\approx 2.0 \text{ protons} / (\text{cm}^2 \text{ s sr MeV})$, for 165 MeV the differential flow becomes $\approx 0.18 \text{ protons} / (\text{cm}^2 \text{ s sr MeV})$ and for 433 MeV the differential flow becomes $\approx 0.058 \text{ protons} / (\text{cm}^2 \text{ s sr MeV})$. The corresponding spectra values obtained in this way are shown in the section of *Results*.

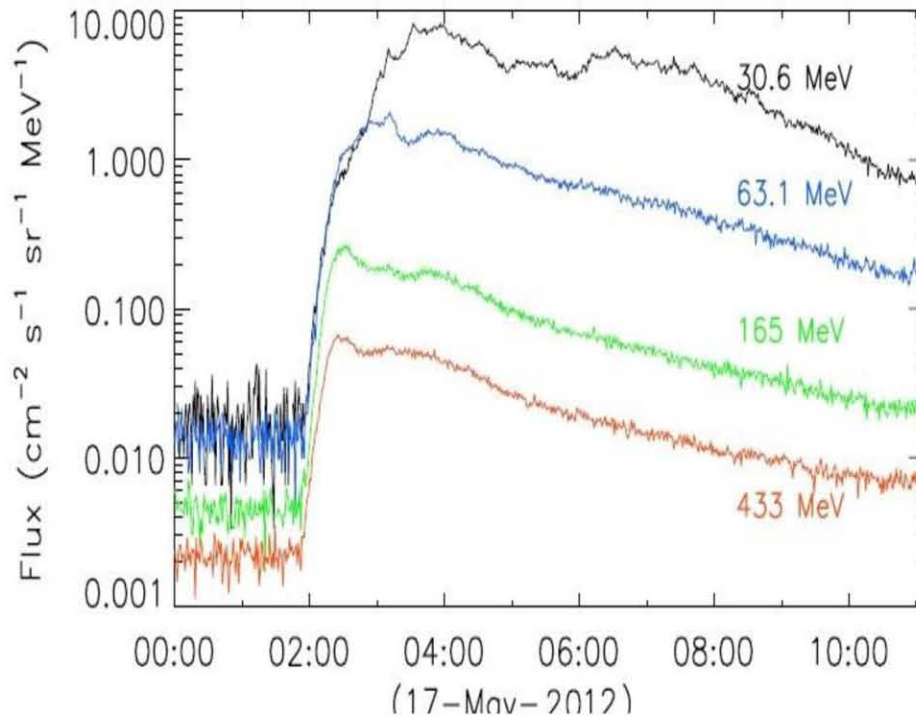


Figure 2 Differential flux of low energy solar protons as seen by the **GOES-13** satellite on May 17, 2012 during the GLE 71 (Figure 3 in Li et al. 2013).

2.2. GLE OF SEPTEMBER 10, 2017

It has been globally disseminated that at the beginning of September 2017 there was a period of extreme solar activity, precisely at the minimum of the solar cycle 24, in the Active Region AR2673 which produced four powerful class X flares, including the strongest flare of the Solar Cycle 24 (X9.3, S08W83) on September 6, 2017. This was the one that produced intensive solar-terrestrial disturbances including a severe geomagnetic storm on September 07 and 08. The corresponding solar activity center also included the second strongest flare (X8.2) of Cycle 24, on September 10, 2017, when the GLE was generated (Augusto et al., 2018; Zhao et al., 2018; Gopalswamy et al., 2018, Cohen and Mewaldt, 2018). The event was observed mainly in high-latitudes (NM) neutron monitors and stations in lower latitudes with a geomagnetic cut < 4 GV. It was also a low intensity and highly anisotropic event: the increase at SOPB was $\sim 8\%$ according to *one minute* NMDB data was recorded at the South Pole station, Figure 3.

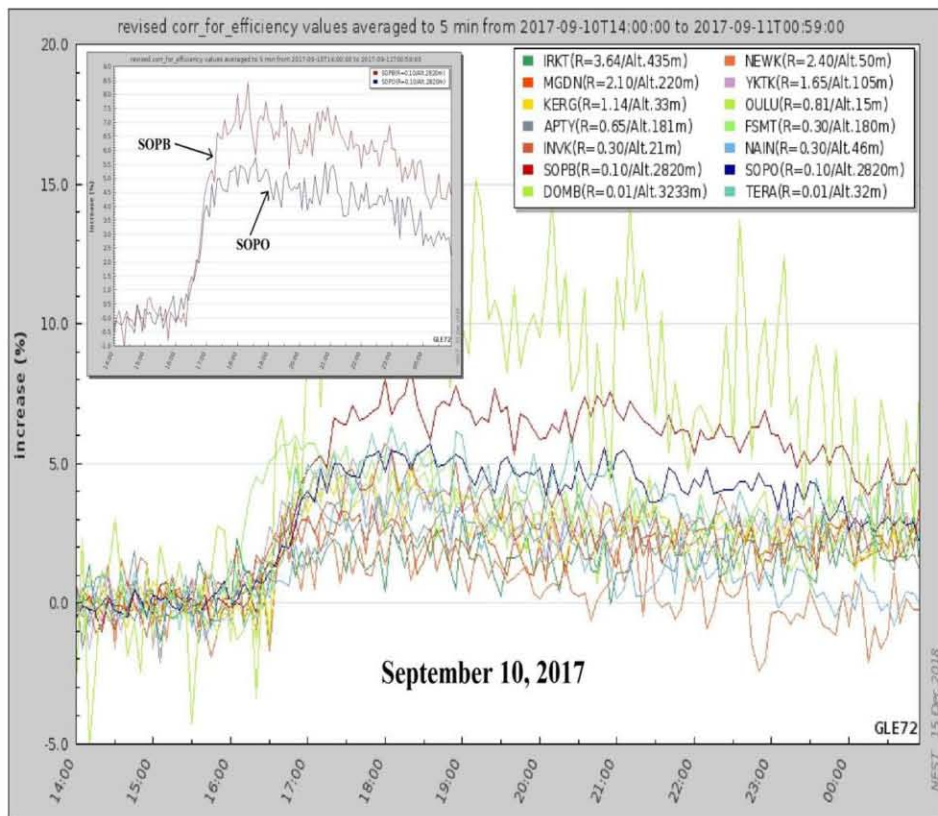


Figure 3 Increase of the proton flux of 14 stations (NMDB) including SOPO and SOPB during the GLE of September 10, 2017.

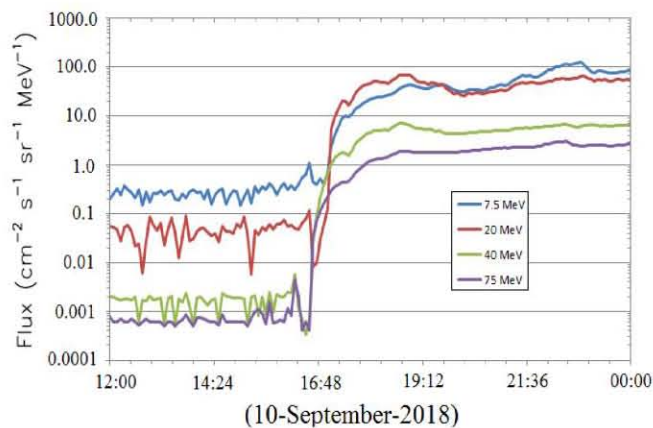


Figure 4. Differential flux of low energy solar protons as seen by the GOES-13 satellite on September 10, 2017 during the GLE 72. These profiles, in units of differential flux, were obtained from: <https://www.swpc.noaa.gov/products/goes-proton-flux>.

In the next section, we derive the energy spectrum at the ground level of this event; we are able to obtain a comparative frame by using the spectrum at low energies from the time profiles in units of differential flux, taken from: <https://www.swpc.noaa.gov/products/goes-proton-flux> (Figure 4). As in the case of the GLE 71 we take the flux for four different energies at the Time of Maximum flux (TOM) (Forman et al., 1986): for 7.5 MeV, the differential flow becomes $\approx 44.6 \text{ protons} / (\text{cm}^2 \text{ s sr MeV})$, for 20 MeV, the differential flow becomes $\approx 70 \text{ protons} / (\text{cm}^2 \text{ s sr MeV})$, for 40 MeV, the differential flow becomes $\approx 7 \text{ protons} / (\text{cm}^2 \text{ s sr MeV})$, and for 75 MeV the differential flow becomes $\approx 2.0 \text{ protons} / (\text{cm}^2 \text{ s sr MeV})$. The corresponding spectra values obtained in this way are shown in the section of *Results*.

3. ANALYSIS OF THE COSMIC RAY SPECTRUM

The counting rate N of a neutron monitor at cutoff rigidity P_c and atmospheric depth x is calculated from the following equation:

$$N(P_c, x) = \int_{P_c}^{\infty} S(P, x) J(P) dp \quad (1)$$

Here, $S(P, x)$ is the atmospheric yield function given in Caballero-Lopez and Moraal (2012) and $J(P)$ is the primary cosmic-ray spectrum at the top of the atmosphere. For the solar cosmic rays, the counting rate, N_s , is usually assumed as a power-law spectrum of the form $J=J_0 P^{-\gamma}$ at the top of the earth's atmosphere. The fractional increase, $\delta N/N$, is given by the ratio N_s/N_g , where N_s and N_g are the counting rates due to solar and galactic cosmic rays, respectively. P_c is the well-known geomagnetic threshold (cutoff rigidity), which determine the minimum energy for cosmic rays reaching the top of the atmosphere at the neutron monitor location (Smart and Shea, 2005).

In this work, we analyze both GLEs based on data from two neutron monitors at South Pole station. They are SOPO NM which is a standard 3NM64 neutron monitor and SOPB NM, a lead-free neutron monitor (LFNM), both located at an altitude of 2820 m a.s.l. with a cutoff rigidity of about 0.1 GV (see, for instance, Oh et al., 2012).

One of the most distinctive features of a GLE is its anisotropy. Therefore, if one compares the increases observed by different neutron monitors, the anisotropy must first be subtracted before spectral information is inferred. With this in mind, several techniques have been used (e.g. DeKoning 1994; Bieber et al., 2002; Ruffolo et al., 2006; and references therein). Moraal and Caballero-Lopez (2014) and Caballero-Lopez and Moraal (2016) have used the method proposed by Stoker (1985) and used in many works by the University of Delaware group (see for instance, Bieber and Evenson 1991; Oh et al., 2012; Bieber et al., 2013) to minimize the effect of the anisotropy from the spectral sensitivity. This method analyzes the ratio of increases in two neutron monitors with different rigidity response functions, but in the same location. This scenario eliminates the uncertainties due to different atmospheric pressures, temperature and other environmental conditions. Therefore, the method is much more sensitive to small anisotropies. In this work, we will use this technique based on reducing the effects of anisotropy by analyzing the ratio of increase in two

neutron monitors, with different response functions, but in the same location. Specifically, we will use the information from the pair of neutron monitors of the South Pole station: SOPO (NM64) and SOPB (LFNM). It should be mentioned that another two pairs of neutron monitors at the same location are in SANA and DOMC stations.

According to Eq. (6) of Caballero-Lopez and Moraal (2016), the ratio of the fractional increases, observed by these two neutron monitors at the South Pole station, can be written as follows:

$$\frac{(\delta N/N)_{LFNM}}{(\delta N/N)_{NM64}} = \left(\frac{N_g^{NM64}}{N_g^{LFNM}} \right) \frac{\int_{P_c}^{\infty} S_{LFNM}(P,x) P^{-\gamma} dP}{\int_{P_c}^{\infty} S_{NM64}(P,x) P^{-\gamma} dP} = f(\gamma, P_c) \quad (2)$$

Yield functions in this expression, S_{NM64} and S_{LFNM} , are from Caballero-Lopez and Moraal (2012) and Moraal and Caballero-Lopez (2014), respectively. Equation (2) means that the spectral index can be calculated from a ratio that is independent of the direction of arrival of particles. We want to emphasize that this technique has been widely used by several authors to estimate the spectrum of solar cosmic rays during a GLE. Caballero-Lopez and Moraal (2012) yield function properly reproduces the neutron monitor counting rate and is in good agreement with other yields obtained from Monte Carlo simulations (see their comparison in Caballero-Lopez, 2016).

Table 1 shows the results of applying equation (2) to the observed ratio at South Pole station, during GLE 71 and GLE 72. In our analysis, we have used 15 minutes moving averages of the data shown in Figure 1 for SOPO and SOPB. Figure 5 shows the spectral index as a function of time for both GLEs.

4. THE OBSERVATIONAL SOLAR PARTICLE SPECTRA

Regarding the obtained values of (γ) , it can be appreciated that in both GLEs there is no definite tendency of the value as time elapses, which leads us to consider that there are two different acceleration phases in both GLEs, a first one designated as the Prompt Component (PC) and a second one namely the Delayed Component (DC).

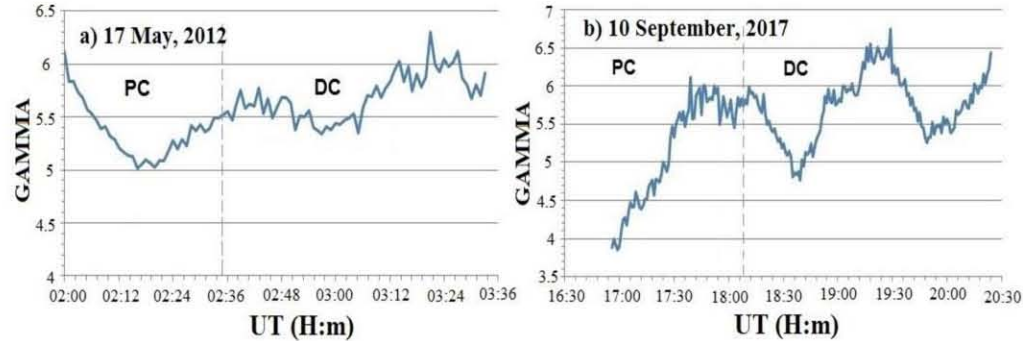


Figure 5. Time series of the 15 min. simple moving average of the parameter gamma.

neutron monitors, with different response functions, but in the same location. Specifically, we will use the information from the pair of neutron monitors of the South Pole station: SOPO (NM64) and SOPB (LFNM). It should be mentioned that another two pairs of neutron monitors at the same location are in SANA and DOMC stations.

According to Eq. (6) of Caballero-Lopez and Moraal (2016), the ratio of the fractional increases, observed by these two neutron monitors at the South Pole station, can be written as follows:

$$\frac{(\delta N/N)_{LFNM}}{(\delta N/N)_{NM64}} = \left(\frac{N_g^{NM64}}{N_g^{LFNM}} \right) \frac{\int_{P_c}^{\infty} S_{LFNM}(P,x) P^{-\gamma} dP}{\int_{P_c}^{\infty} S_{NM64}(P,x) P^{-\gamma} dP} = f(\gamma, P_c) \quad (2)$$

Yield functions in this expression, S_{NM64} and S_{LFNM} , are from Caballero-Lopez and Moraal (2012) and Moraal and Caballero-Lopez (2014), respectively. Equation (2) means that the spectral index can be calculated from a ratio that is independent of the direction of arrival of particles. We want to emphasize that this technique has been widely used by several authors to estimate the spectrum of solar cosmic rays during a GLE. Caballero-Lopez and Moraal (2012) yield function properly reproduces the neutron monitor counting rate and is in good agreement with other yields obtained from Monte Carlo simulations (see their comparison in Caballero-Lopez, 2016).

Table 1 shows the results of applying equation (2) to the observed ratio at South Pole station, during GLE 71 and GLE 72. In our analysis, we have used 15 minutes moving averages of the data shown in Figure 1 for SOPO and SOPB. Figure 5 shows the spectral index as a function of time for both GLEs.

4. THE OBSERVATIONAL SOLAR PARTICLE SPECTRA

Regarding the obtained values of (γ) , it can be appreciated that in both GLEs there is no definite tendency of the value as time elapses, which leads us to consider that there are two different acceleration phases in both GLEs, a first one designated as the Prompt Component (PC) and a second one namely the Delayed Component (DC).

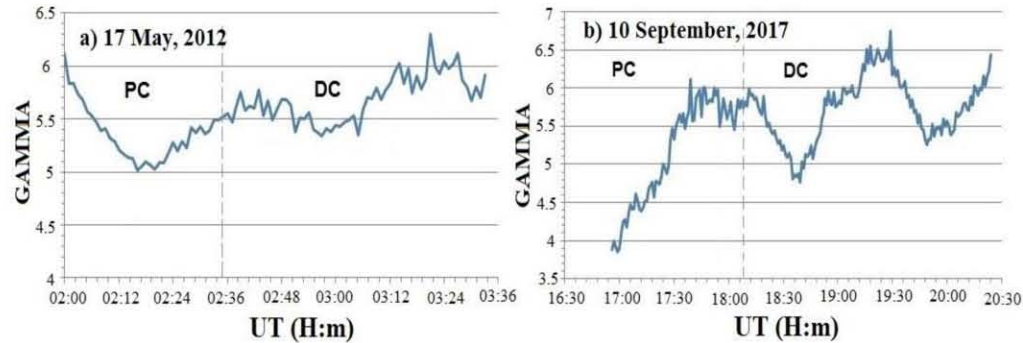


Figure 5. Time series of the 15 min. simple moving average of the parameter gamma.

Spectrum parameters at Ground Level

Date GLE	UT	Stage	J_0 [Protons/(GV m ² sr s)]	Gamma (γ)
17-may-12	02:00-02:30	PC	3.80E+04	5.3
17-may-12	02:31-03:30	DC	2.39E+04	5.6
10-sep-17	16:56-18:14	PC	1.43E+04	5.2
10-sep-17	18:15-20:24	DC	1.85E+04	5.7

TABLE 1

We must notice that if we want the flux (J_E) respect to proton kinetic energy (E) in units of $GeV^{-1} m^{-2} s^{-1} sr^{-1}$, then we must multiply the flux respect to rigidity in units of $GV^{-1} m^{-2} s^{-1} sr^{-1}$ by β^{-1} (where β is the ratio of particle speed to speed of light). Therefore, we should use the following expression:

$$J_E(E) = 10^{-7} J_0 \frac{E+E_0}{\sqrt{E(E+2E_0)}} \left(\frac{\sqrt{E(E+2E_0)}}{1000} \right)^{-\gamma} \quad (3)$$

where, J_0 is the flux respect to rigidity for 1 GV protons (and shown in column 4 of Table 1), E is in MeV, $E_0 = 938$ MeV and J_E is in units of $MeV^{-1} cm^{-2} s^{-1} sr^{-1}$. To deduce expression 3, we used the relationship between rigidity, P , proton kinetic energy, E , and as indicated in the next expression:

$$P = \sqrt{E(E + 2E_0)} = \beta(E + E_0) \quad (4)$$

From the data obtained in the Table 1 we have constructed the following energy spectra at ground level. For both events we have derived the spectrum $J_{sp}(P, t) = J_0 P^{-\gamma}$ by the method mentioned above of Caballero-Lopez and Moraal (2016). The results are illustrated in Figure 6.

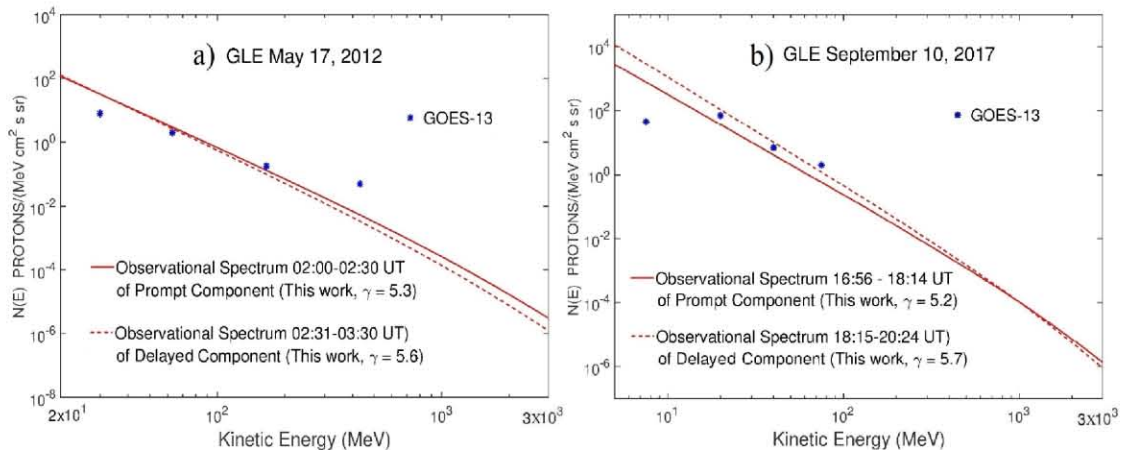
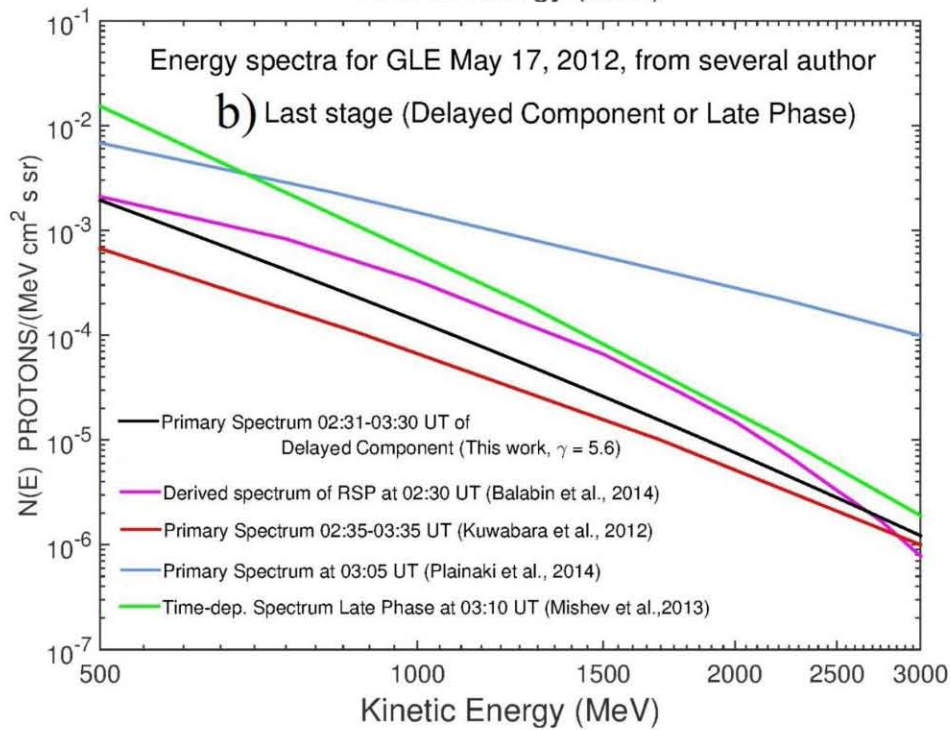
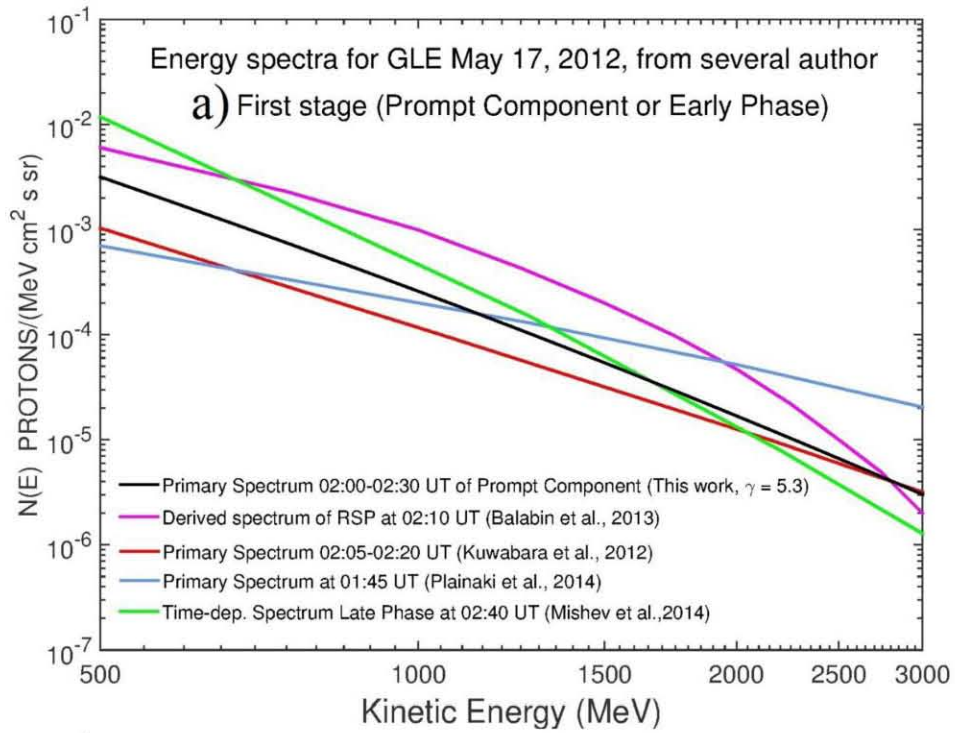


Figure 6. Observational spectra (Prompt Component and Delayed Component) obtained in this work for the GLE of May 17, 2012, Figure (a), and for the GLE of September 10, 2017, Figure (b).



10

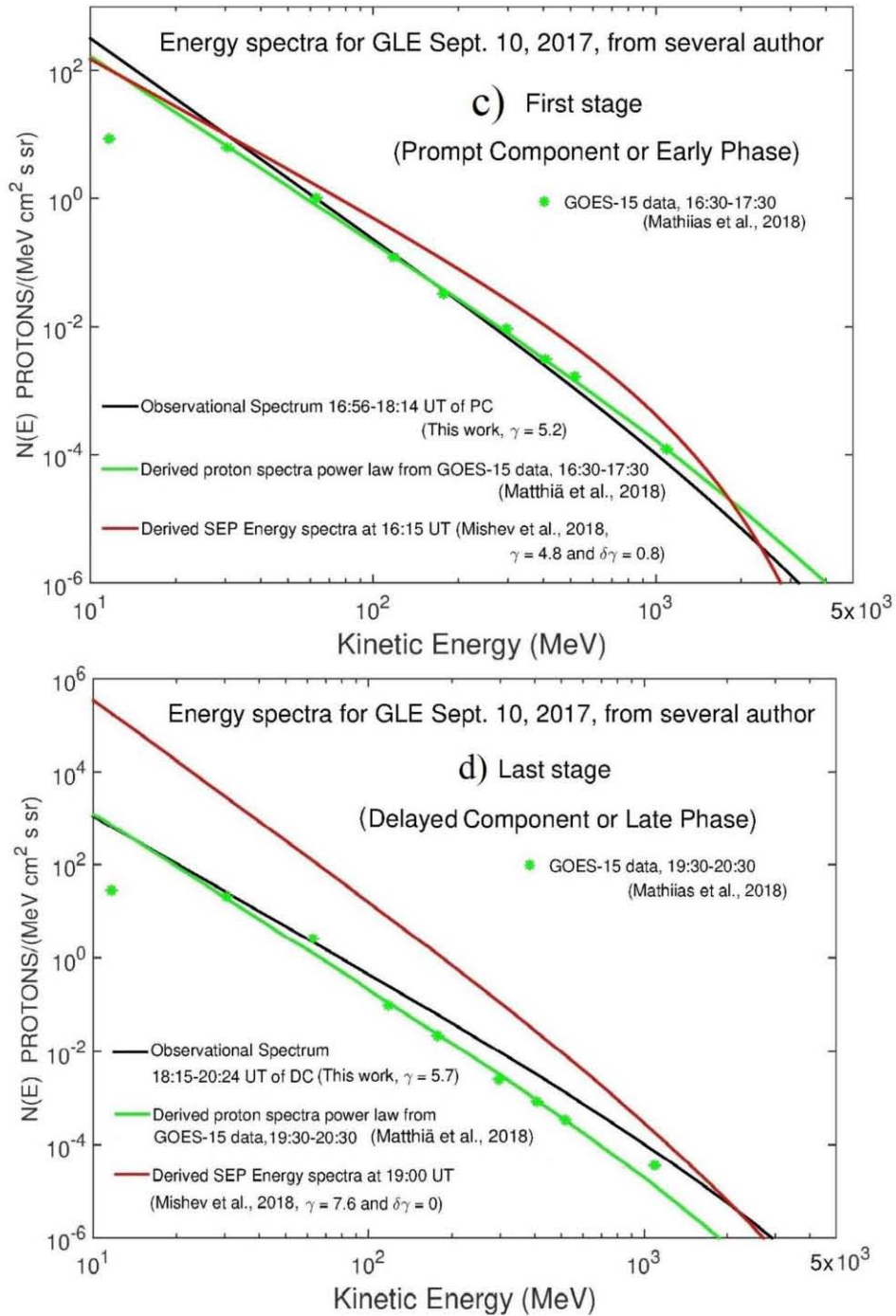


Figure 7. Energy spectrum derived in this work (in black), as compared with the spectra of other authors.

In Perez-Peraza et al. (2018), the observational spectra given by different authors (Balabin et al., 2014, Kuwabara et al., 2012, Plainaki et al., 2014 and Mishev et al., 2014) were exhaustively studied for the GLE71. The authors shown in Figure 7 published their spectra in terms of flux. The satellite data used by Matthiä et al., 2018, is shown by us in Figures 7c-d. Relative to the GLE71 (Figures 7a and 7b) it should be noted that our spectrum is included in the order of magnitude of that of other authors, who used a large number of stations; this may be understood from the use of many response functions, and that each author resorted to a different yield function. Although in the case of Kuwabara et al., 2012, the stations are the same as ours, they do not use response and yield functions as those derived Caballero-Lopez and Moraal, 2012. For the GLE72 our spectrum is very close to that of Matthiä et al., 2018, specifically at satellite energies, which correspond to the data used by these authors. Regarding Mishev et al. (2018) it can be seen in Figure 7c that the PC of the three spectra are of the same order, while the DC differs, particularly at low energies (Figure 7d).

5. - THE SOURCE SPECTRUM.

The study of the energetic distribution of non-thermal particles is a fundamental problem in Cosmic Ray Astrophysics. The particle energy spectrum contains the information about particle generation processes, the source location, and physical conditions therein. To determine particle spectra at the level of their sources several methods have been worked out ; by demodulation of the observational data back to the source , taking into account the processes that may take place during the interplanetary transport (Perez-Peraza et al., 1985, Alvarez et al., 1986), or alternatively, by inferring the particle source spectrum from the deconvolution of the non-thermal electromagnetic emissions produced by the interaction of the accelerated particles, with the local matter and electromagnetic fields. Both mentioned methods lead to a source spectrum that may be fitted by an exponential or inverse power law in energy, which by itself does not contain great information about the source phenomenology and physical conditions, but this must be inferred from additional theoretical work.

For this later goal, usually two different approaches have been worked out in the literature.; the first one consists in developing an acceleration mechanism for the particles to gain energy in the proposed electromagnetic field configuration and deriving the corresponding energy distribution predicted by the mechanism (Perez-Peraza et al., 1978; Gallegos and Perez-Peraza, 1987; Gallegos et al., 1993; Perez-Peraza et al., 1993) and on the other hand a more general method consists in solving a Fokker-Planck. type equation of continuity in the energy space, Perez-Peraza and Gallegos (1987), Perez-Peraza and Gallegos-Cruz (1994) and Gallegos-Cruz and Perez-Peraza (1995), for several types of plasma turbulence and including adiabatic energy losses (Perez-Peraza et al., 2009). Those works have been summarized in the Appendix of the present work

To infer about the physical parameters of the source and the different acceleration mechanisms involved in the GLE phenomenon, for both events, we compared the

obtained observational energy spectra in this work (Figures 6 and 7) with the theoretical energy spectra. In Perez-Peraza et al. (2017) an exhaustive study of the source spectra of the GLE71 has been done by means of the comparison of the theoretical source spectra with the experimental spectra, that several authors had published up to the end of 2017. Basically, we have dealt with stochastic acceleration, either in its time-dependent or steady state approaches. As an injection process, we are considering two options: pre-acceleration by monoenergetic flux of protons and reconnection in a Magnetic Neutral Current Sheet (MNCS) typical of flare plasma regions (Perez-Peraza et al., 1977).

6. - RESULTS

The comparison of the theoretical and experimental spectra is shown below: Figures 8 and 9 was done on basis of the theoretical energy spectra, obtained by Gallegos-Cruz and Perez-Peraza, (1995), Perez-Peraza et al., (2009), and summarized in the *Appendix*. To determine the physical parameters prevailing at the source, as well as the acceleration and deceleration from adiabatic cooling during particle generation in the two GLEs under study we employed several sets of parameters that susceptibly prevail in the sources of solar particles (e. g., Miroshnichenco and Perez-Peraza, 2008). The meaning of the symbols is described in the *Appendix*.

It should be observed in Figure 6 that our spectra are quite close to the satellite data of GOES-13. It should also be noted in Figures 7c and 7d that most of spectra are close to the data of GOES-15.

Figures 8a and 8b show the fitting of the equations, appearing in the works indicated just above, to our observational Prompt and Delayed spectra illustrated in Figures 6a. The obtained source and acceleration parameters for both components are indicated in the body of Figures.

Similarly, Figures 9a to 9f show the fitting of our observational Prompt and Delayed spectra illustrated in Figure 6b. The source parameters for both components of the spectrum are indicated in the body of the Figures.

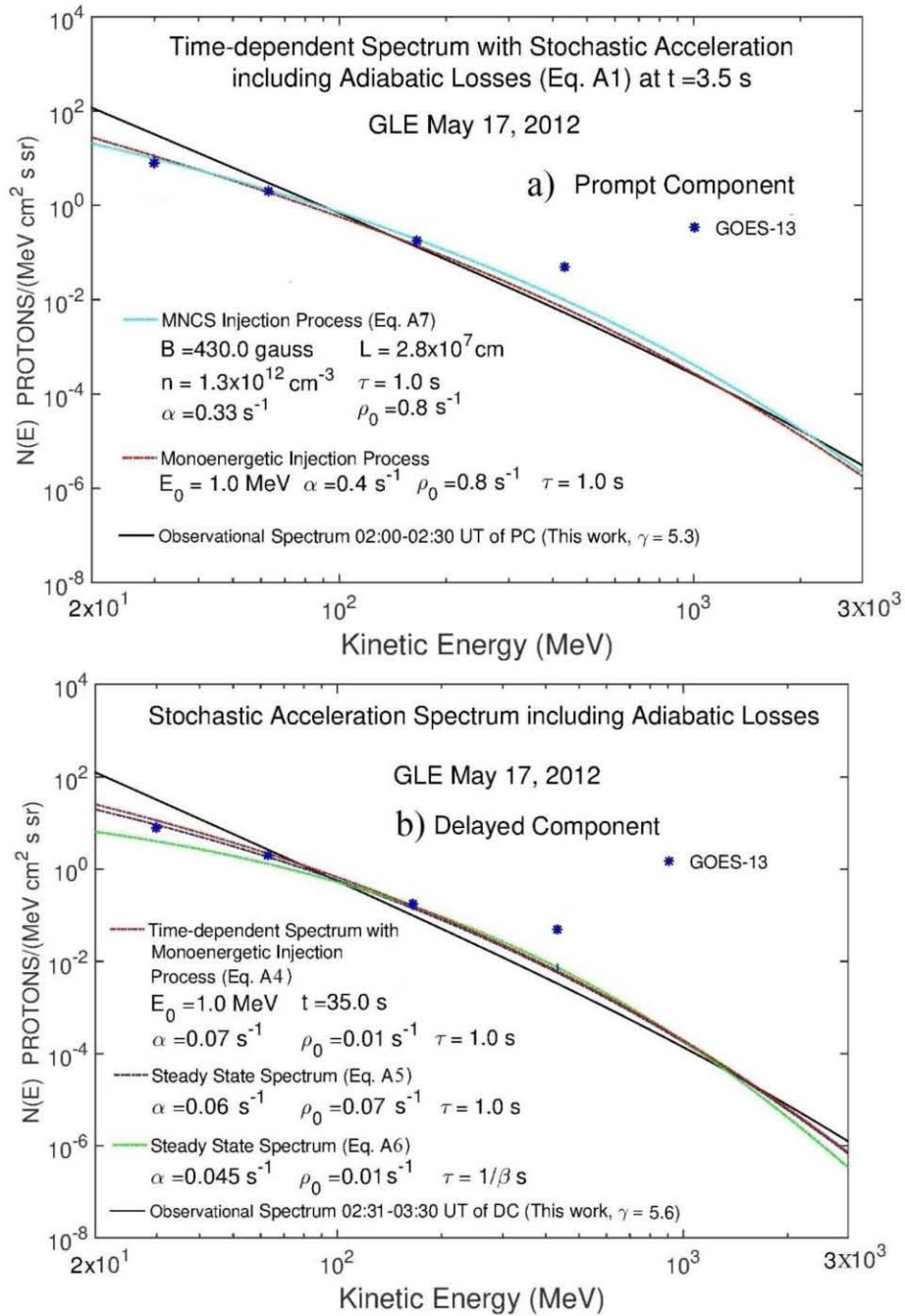
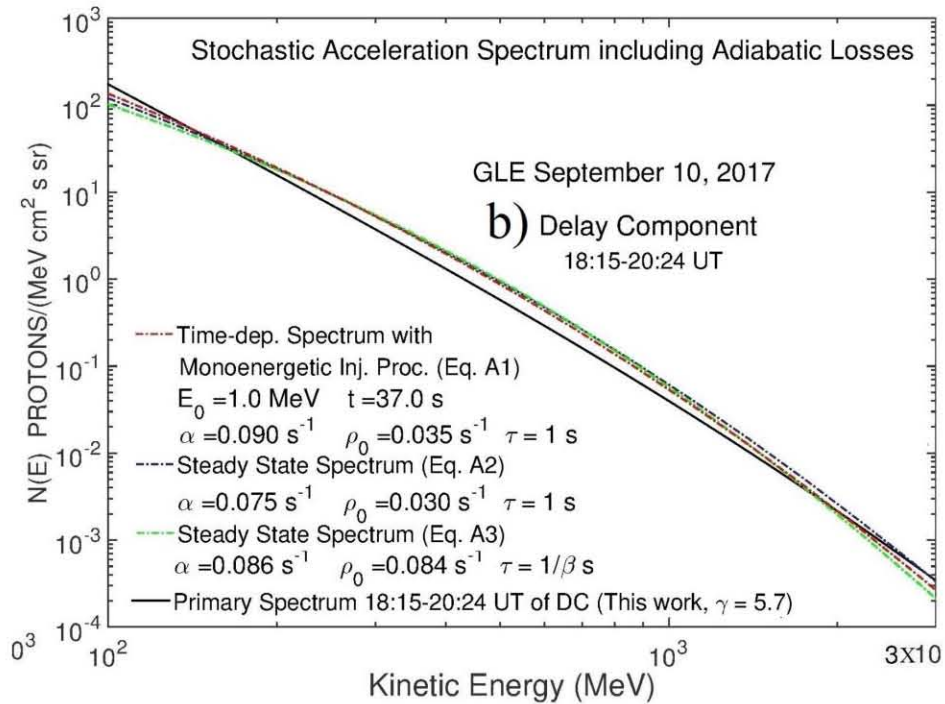
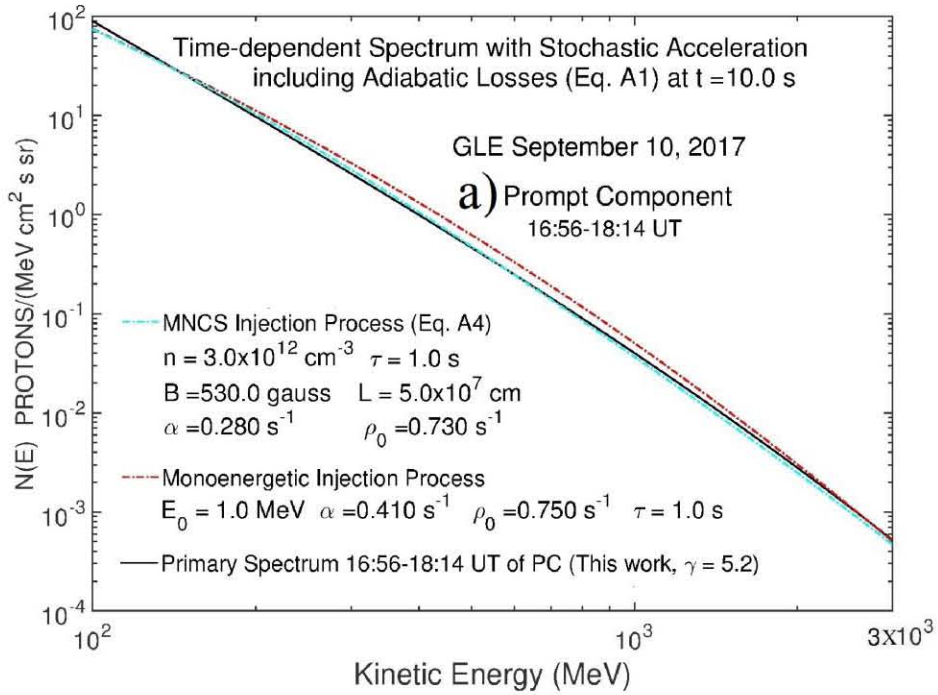
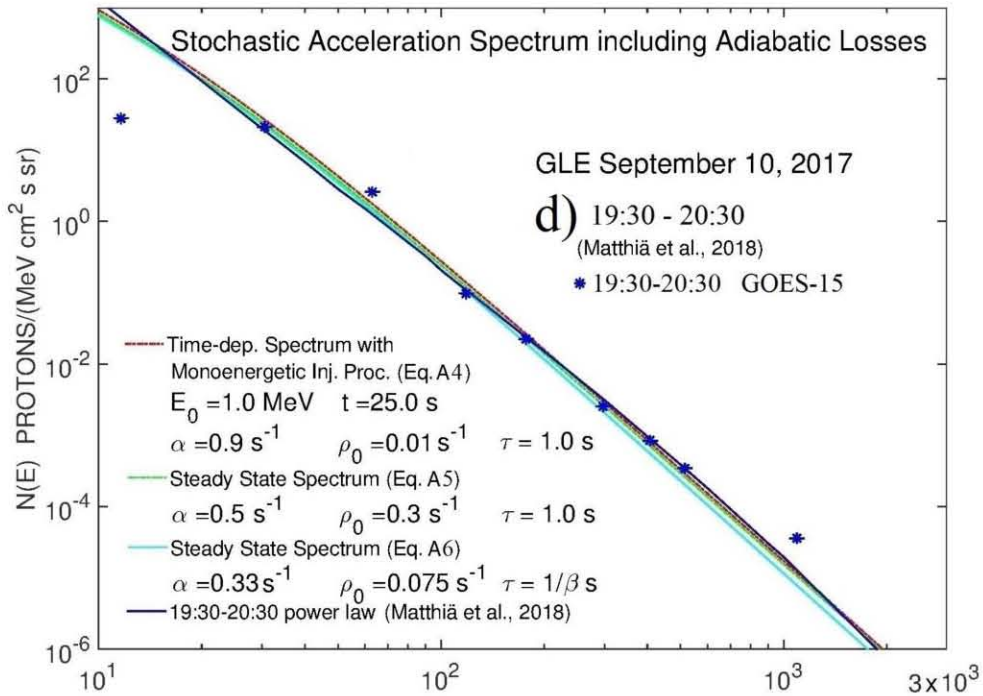
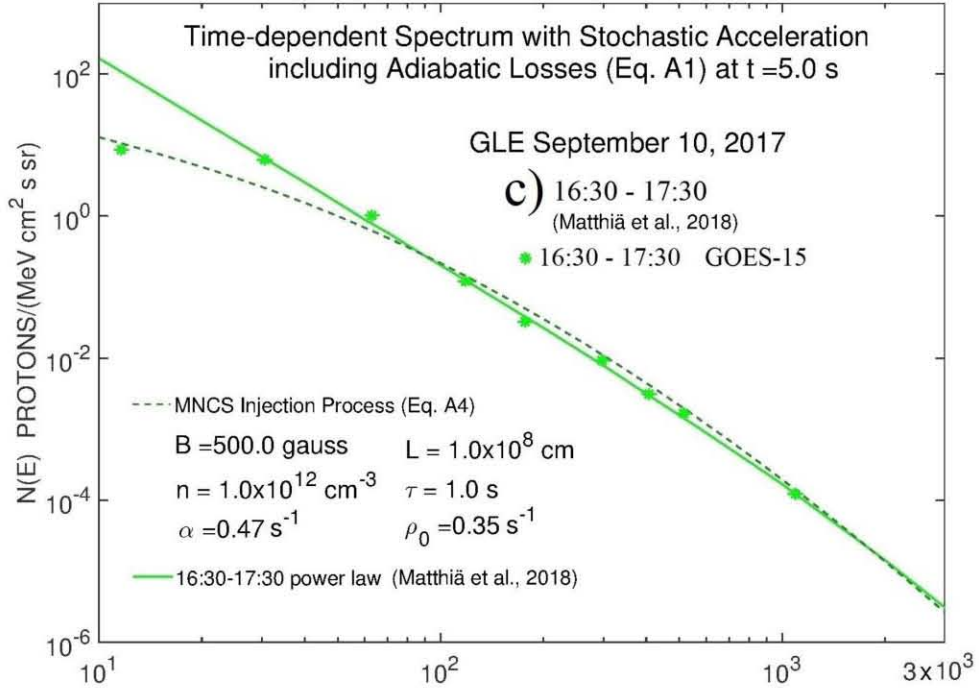


Figure 8. The comparison of the theoretical spectra to the observational spectra of this work is shown for the GLE of May 17, 2012. Figure (a) corresponds to the PC of the GLE event and Figure (b) corresponds to the DC of the same event, when it is reaching the stationary state.





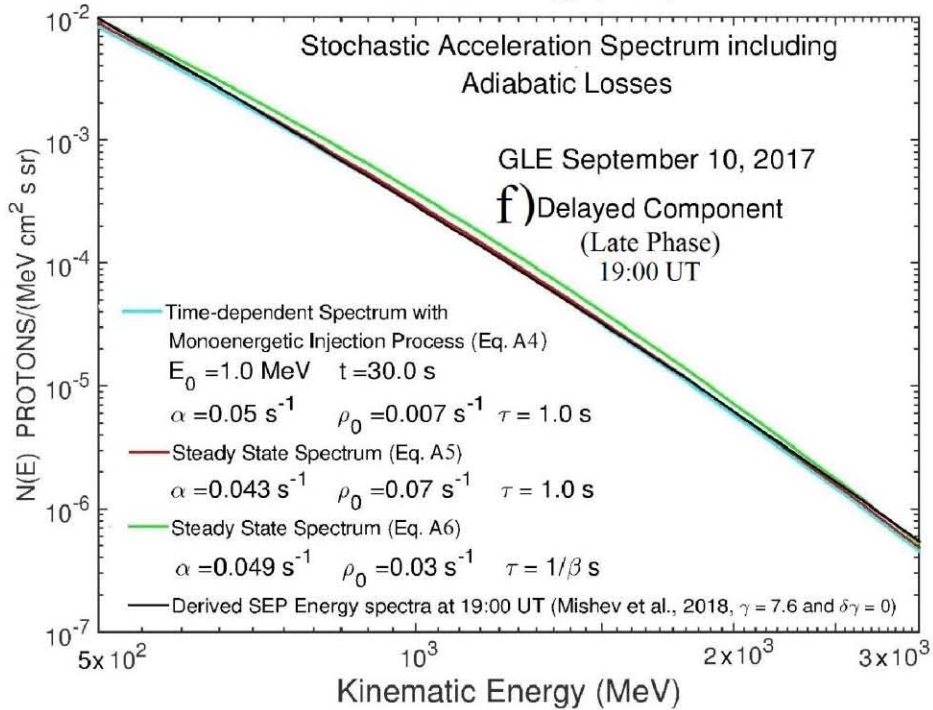
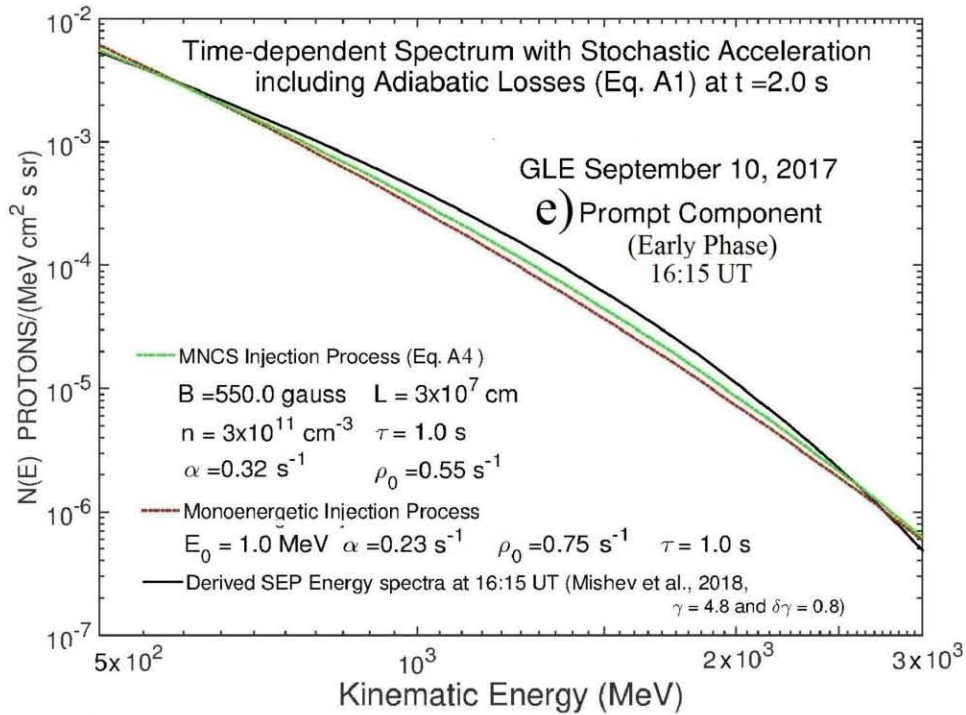


Figure 9. The comparison of the theoretical spectra to the observational spectra of this work is shown for the GLE of September 10, 2017. Figures a, c and e correspond to the PC of the GLE event, including flux values at low energies from the GOES-13 and GOES-15. Figures b, d and f correspond to the DC of the GLE event.

Source Parameters derived from the best fittings in figures 8 and 9 *

Date GLE	UT	Stage	Spectrum		FIT									Fig.	
			Observational	Theoretical	Eqs.	$\alpha(s^{-1})$	$\rho_0(s^{-1})$	$E_0(MeV)$	$\tau(s)$	$t(s)$	$B(gauss)$	$L(cm)$	$n(cm^{-3})$		Injection
17-may-12	02:00-02:30	PC	This work	Time-Dep. Stoch Accel	A4	0.400	0.800	1.0	1.0	3.5				Monoenergetic	8a
17-may-12	02:00-02:30	PC	This work	Time-Dep. Stoch Accel	A4 & A7	0.330	0.800		1.0	3.5	430.0	2.8E+07	1.3E+12	MNCS (Eq. A7)	8a
17-may-12	02:44-03:30	DC	This work	Time-Dep. Stoch Accel	A4	0.070	0.010	1.0	1.0	35.0				Monoenergetic	8b
17-may-12	02:44-03:30	DC	This work	Steady State Stoch Accel	A5	0.060	0.070		1.0					Monoenergetic	8b
17-may-12	02:44-03:30	DC	This work	Steady State Stoch Accel	A6	0.045	0.010		$1/\beta$					Monoenergetic	8b
10-sep-17	16:56-18:14	PC	This work	Time-Dep. Stoch Accel	A4	0.390	0.800	1.0	1.0	10.0				Monoenergetic	9a
10-sep-17	16:56-18:14	PC	This work	Time-Dep. Stoch Accel	A4 & A7	0.260	0.750		1.0	10.0	500.0	1.0E+08	1.0E+12	MNCS (Eq. A7)	9a
10-sep-17	18:15-20:24	DC	This work	Time-Dep. Stoch Accel	A4	0.070	0.040	1.0	1.0	37.0				Monoenergetic	9b
10-sep-17	18:15-20:24	DC	This work	Steady State Stoch Accel	A5	0.050	0.030		1.0					Monoenergetic	9b
10-sep-17	18:15-20:24	DC	This work	Steady State Stoch Accel	A6	0.067	0.093		$1/\beta$					Monoenergetic	9b
10-sep-17	16:30-17:30	PC	Matthiä et al. 2018	Time-Dep. Stoch Accel	A3 & A7	0.470	0.350		1.0	5.0	500.0	1.0E+08	1.0E+12	MNCS (Eq. A7)	9c
10-sep-17	19:30-20:30	DC	Matthiä et al. 2018	Time-Dep. Stoch Accel	A4	0.900	0.010	1.0	1.0	25.0				Monoenergetic	9d
10-sep-17	19:30-20:30	DC	Matthiä et al. 2018	Steady State Stoch Accel	A5	0.500	0.300		1.0					Monoenergetic	9d
10-sep-17	19:30-20:30	DC	Matthiä et al. 2018	Steady State Stoch Accel	A6	0.330	0.075		$1/\beta$					Monoenergetic	9d
10-sep-17	16:15	PC	Mishev et al. 2018	Time-Dep. Stoch Accel	A4	0.230	0.750	1.0	1.0	2.0				Monoenergetic	9e
10-sep-17	16:15	PC	Mishev et al. 2018	Time-Dep. Stoch Accel	A4 & A7	0.320	0.550		1.0	2.0	550.0	3.0E+07	3.0E+11	MNCS (Eq. A7)	9e
10-sep-17	19:00	DC	Mishev et al. 2018	Time-Dep. Stoch Accel	A4	0.050	0.007	1.0	1.0	30.0				Monoenergetic	9f
10-sep-17	19:00	DC	Mishev et al. 2018	Steady State Stoch Accel	A5	0.043	0.070		1.0					Monoenergetic	9f
10-sep-17	19:00	DC	Mishev et al. 2018	Steady State Stoch Accel	A6	0.049	0.030		$1/\beta$					Monoenergetic	9f

Table 2

*The meaning of the symbols is described in the Appendix.

The corresponding parameters are summarized in Table 2. Column 7 indicates the parameter of the acceleration efficiency of the stochastic process. Column 8 indicates the efficiency of the deceleration process of adiabatic cooling. Column 9 indicates the monoenergetic injection energy to the acceleration process. Column 10 indicates the mean confinement time of particles in the source. Column 11 is the acceleration time of particle, which may be assimilated to the time where the process reaches the steady-state. Column 12 is the average of the magnetic field in the magnetic neutral current sheet (MNCS). Column 13 is the average length of the MNCS. Column 14 is the density number in the source. Column 15 indicates the kind of injection into the acceleration process.

The flare conditions in these two small events are quite similar, in fact, it can be noted that there is not a considerable dispersion of the acceleration efficiency values; turbulence must have been quite similar in regions where the magnetic field strength is in the range of 400 to 550 *Gauss* and density in the range 10^{11} - 10^{12} cm^{-3} . Also, upon observing column 8 one can infer that the adiabatic deceleration efficiency (ρ_0) in these two small events is in the range of 0.01-0.8 s^{-1} . It should be noted that the accelerated particles escape from the source either with a quasi-constant mean escape time or, with an inverse dependence of their velocities ($1/\beta$).

7. - DISCUSSION

The GLE of May 17, 2012, and September 10, 2017, were very peculiar in the sense that they were relatively small, showing a hard spectrum, moving to a softer spectrum as time went by. The May 17, 2012 GLE originated in a flare of class M5.1, occurring at approximately 01:39 UT, with heliolongitude in the range of W20-W90, Li et al., (2013). According to Omodei et al., (2018) the second GLE event was associated with a X8.2 type flare in the solar zone (S08-W83), after 16:30 UT. This increase was also registered for some non-polar stations, but of high latitude.

This paper demonstrates the effectiveness of the method developed to calculate the observational energy spectrum, for the particular case where the involved instruments are at the same location. This allows to determine the spectra parameters J_0 and γ during weak events, Caballero-Lopez and Moraal (2016), and we did this here for both phases (PC and DC) of each event, and in this way, we generated the observational spectrum (Figures 6 and Table 1). We observe in Table 1 that the spectral indexes for the studied GLEs are in the order of $\gamma \approx 5 - 6$. Also, it should be noted that the spectrum of the second phase (or Delayed Component) is softer than that of the first phase (or Prompt Component). The analysis was performed in the energy range ≤ 3 *GeV*.

As was mentioned in *Section 1*, the phenomena that take place in the sources of solar energetic particles can be inferred from different standpoints, most of them appealing to the temporal synchronization between the various electromagnetic emissions of

flares and coronal mass ejections (CME). Another option is through the study of energetic particles, based on the comparison between the observational and the theoretical spectra. In the work at hand, we try to infer about source phenomena through this last option. This is done by adjusting the observational spectra to our theoretical spectra developed in (Gallegos-Cruz and Perez-Peraza, 1995; Perez-Peraza et al., 2009, Perez-Peraza et al., 2018; Perez-Peraza and Marquez-Adame, 2018) and applied, under the assumptions made of a time-dependent situation and a stationary one. The corresponding spectra developed in Gallegos-Cruz and Perez-Peraza, (1995), are synthesized in the *Appendix*. Such a comparison leads us to infer as to plausible scenarios of particle generation in these two peculiar GLEs (Table 2). In the process of comparison of the theoretical spectra with the observational one, we have employed Eq. A4, Eq. A5 and Eq. A6, as well as Eq. A7, assuming that the stochastic acceleration is preceded by an injection process, either by a local monoenergetic flux of protons of mean energy about 1 MeV, or by an injection from a deterministic process due to the intense electric fields generated in a Magnetic Neutral Current Sheet (MNCS) reconnection process (Perez-Peraza et al., 1978, 2009).

In Figures 8-9 it can be seen that the best fitting Prompt Component phase (PC) of the experimental spectra, occurred when the acceleration is still at a time $t \approx 2 - 10$ s, whereas for the Delayed Component phase (DC) the best fitting is obtained at $t \geq 25$ s. It should be noted that the September 10, 2017, Prompt Component (PC) is better described with an injection from a reconnection process; though a monoenergetic injection process cannot be disregarded, since both options reproduce the observational spectrum quite correctly. The Delayed Component (DC) seems to be systematically better described by stochastic acceleration with the injection from a monoenergetic flux. The steady-state situation seems to be reached after a time around 40 s in the source.

Figures 8 and 9 including data from the GOES-13 and GOES-15 satellite show that, data satellite may be correctly fitted by our theoretical and our experimental spectra. In addition to the authors mentioned in the text, it should be said that no other space detectors have provided public information on proton fluxes during the occurrence of GLE71 and GLE72.

Regarding the physical scenarios, in general, we have found that stochastic acceleration while losing energy by adiabatic losses during the source expansion compares much better to the observational spectra in contrast to the case when adiabatic cooling is ignored. As can be seen in Figures 8b, 9b, 9d and 9f, the possible scenario at the source of the Delayed Component for both GLEs is better described with a time-dependent spectrum of stochastic acceleration, with a monoenergetic injection and a mean confinement time of ~ 1 s (Eq. (41) in Ap. J. 446, 1995) by adding losses due to adiabatic cooling; whereas in the Prompt Component, injection from a MNCS is quite probably present as can be observed in Figures 8a, 9a, 9c and 9e. The corresponding parameters of the source processes are shown in Table 2.

We claim thus that our work leads to construct possible scenarios in the source during the generation of each GLE: throughout the enhanced solar activity of the first days of

September 2017, due to magnetic field reconfiguration, strong electric fields were generated together with high levels of turbulence; consequently, solar protons were accelerated either by a primary acceleration mechanism (most probably from reconnection in a MNCS). Alternatively, protons of $E \geq 1 \text{ MeV}$ from the high energy tail of the local plasma Maxwell distribution were accelerated by a stochastic process, either in the flare body or in its surroundings, or behind the shock wave.

8. - CONCLUSIONS

We explored the sources of particles during the GLE of May 12, 2012, and September 10, 2017 based on the observational spectrum developed here. For the GLE of September 10, 2017, we have considered also the spectra given by other authors.

In addition of deriving the observational spectra of both GLEs, the main results of this work to be emphasized are the set of source parameters for the generation of particles and the acceleration processes involved, which lead to plausible scenarios during the events under study. It is precisely the comparison of the theoretical source spectra with the observational spectra that gives us an approximate conception of the production scenarios. The analysis of the spectra leads us to consider the presence of two different particle components during the events. Some authors designate those two phases as Prompt and Delayed Components, other authors use the terms Early and Late Phases, or even stages. These two components may indicate the occurrence of two acceleration processes of a different nature, as is frequently evoked by many authors. In both phases, the main acceleration mechanism is most probably of stochastic nature, where the particle injection process to the stochastic mechanism can come from a monoenergetic proton flux that may have originated from the high energy tail of the pre-accelerated protons in the MNCS. However, in this work another option is opened: *a single acceleration mechanism in two different acceleration stages* could be generated in a deterministic process with a spectrum like that shown in Eq. A7, so that a unique stage of acceleration in a MNCS cannot be disregarded. Finally, we emphasize that the comparison between the theoretical and observational spectra gives us an approximate conception of the production scenarios, that is, of the involved processes of acceleration and loss of energy, as well as of the plausible physical parameters that prevail at the source.

Acknowledgments. R.A.C.L.'s contribution was made during the sabbatical leave supported by a PASPA-DGAPA-UNAM grant. We acknowledge the NMDB database (www.nmdb.eu), founded under the European Union's FP7 program (contract no. 213007) for providing data. The neutron monitor data from South Pole are provided by University of Wisconsin, River Falls. We acknowledge the U.S. Dept. of Commerce, NOAA, Space Weather Prediction Center for GOES data. Juan C. Marquez-Adame thanks the for economical support from the CONACyT scholarship program. Data regarding Figures 1–9 can be found in <https://drive.google.com/open?id=1LgR4ZP4wIVJUXPcVaXv0vyr7litvBoSe>

APPENDIX

By means of the quasi-linear theory, and introducing the effects of spatial transport in a time escape (Schlickeiser 1989), a diffusion equation in moment space is obtained from the Vlasov equation (collisionless Boltzmann equation). That can be also derived from the Chapman-Kolmogorov equation (eg, Schatzman 1966).

$$\frac{\partial f(p,t)}{\partial t} = \frac{1}{p^2} \frac{\partial}{\partial p} \left[p^2 D(p) \frac{\partial f(p,t)}{\partial p} \right] \quad \text{A1}$$

In Eq. A1 $f(p, t)$ is the pitch angle averaged-density of particles of momentum p interacting with turbulence at time t , and $D(p)$ is the diffusion coefficient characterizing the interaction dynamics between particles and the specific type of turbulence, which is assumed to be homogeneous and time independent (Tsytovich 1977). Furthermore, an alternative solution for this diffusion equation may be found by its transformation into a Fokker-Planck-type equation in the energy space of particles (Ginzburg & Syrovatskii 1964), Eq. A2:

$$\frac{\partial N(E,t)}{\partial t} = \frac{1}{2} \frac{\partial^2}{\partial E^2} [D(E)N(E, t)] - \frac{\partial}{\partial E} [B(E)N(E, t)] \quad \text{A2}$$

where E is the particle kinetic energy, and $N(E, t)$ is the number of particles per energy interval at time t , $D(E)$ is the diffusive energy change rate produced by the dispersion in energy gain around the value of the systematic energy gain rate, given by $B(E)$. The effect of systematic energy losses or any other systematic acceleration effect may be introduced in the second term of the right-hand of the previous equation by setting $A(E) = B(E) \pm \text{additional systematic energy change processes}$ (Ginzburg, 1958). Also, a source term $Q(E, t)$ is added, (indicating external particle injection into the acceleration region) and a sink term, assumed to describe any kind of particle disappearance process from the acceleration volume by means of characteristic disappearance (or scape) time $\tau(E, t)$, employing these arguments, the previous equation is usually rewritten as:

$$\frac{\partial N(E,t)}{\partial t} = \frac{1}{2} \frac{\partial^2}{\partial E^2} [D(E)N(E, t)] - \frac{\partial}{\partial E} [A(E)N(E, t)] - \frac{N(E,t)}{\tau(E,t)} + Q(E, t) \quad \text{A3}$$

$A(E)$ being the systematic effect of stochastic acceleration and deceleration processes as any eventual secular energy change effect. And $D(E)$ being the diffusive effects due to dispersion around the systematic energy change rate $A(E)$; $D(E)$ was discussed in Perez-Peraza and Gallegos-Cruz, 1994. There is not at present an analytical time-dependent solution for the entire particle energy range. Analytical expressions have been only derived in the asymptotic ranges, $E \ll mc^2$ and $E \gg mc^2$ (e.g., Melrose 1976, 1980; Barbosa 1979; and Ramaty 1979). However, the spectrum of protons in the transrelativistic region is very important for the production of neutrons, pions and gamma-nuclear lines in solar flares.

Among the usual simplifications to solve Eq. A3 are to assume time independence for the escape and injection functions as well as time-independent and energy-independent acceleration efficiency (constant). To avoid some of these simplifications, we herein propose the use of the WKBJ technique to solve the last equation over the complete energy range of the accelerated particles. In mathematical physics, the WKBJ approximation Wentzel, (1926) Kramer (1926), Brillouin (1926) and Jeffreys H. (1924) is a method for finding approximate solutions to linear differential equations with spatially varying coefficients. It is typically used for a semiclassical calculation in quantum mechanics in which the wavefunction is recast as an exponential function, semiclassically expanded, and then either the amplitude or the phase is taken to be changing slowly. Some people designate it as WBK, BWK or JWKB. An authoritative discussion and critical survey has been given by Balson Dingle, (1973) and Kichigin et al. 2019.

Since we have no confident inferences about the time dependence of the injection process, we retain, for simplicity, the general assumption that the flux $N(E, t)$ is being injected at a rate $Q(E) = q(E)\theta(t) \approx q(E)$ [where $\theta(t)$ is the step function] and is escaping at a rate τ^{-1} , Gallegos-Cruz and Perez-Peraza, 1995.

The theoretical spectra used in this work are:

1. The Time-dependent Spectrum for MHD turbulence, with monoenergetic injection, $\tau=cst$, and $D(p)=p^2/\beta$ has been given in the Eq. (41) in Gallegos-Cruz and Perez-Peraza (1995), Eq. (3) in Perez-Peraza et al., (2009): this formulation with the incorporation of adiabatic energy losses was employed in Perez-Peraza et al., 2018 and the inclusion of collisional energy losses will appear soon.:

$$N(E, t) \cong \frac{(\beta_0/\beta)^{1/4}(\varepsilon/\varepsilon_0)^{1/2}(\beta_0^{3/2}\varepsilon_0)^{-1}}{(4\pi\alpha/3)^{1/2}} \left[\frac{N_0}{(t^{1/2})} \exp\left(-a_f t - \frac{3J_f^2}{4\alpha t}\right) + \left(\frac{q_0}{2}\right) \left(\frac{\pi}{a_f}\right)^{1/2} R_5(\varepsilon_0, \varepsilon) \right] F(\rho_0)$$

protons / (MeV s cm² str) (A4)

where $\left(\frac{dE}{dt}\right)_{acc} = \alpha\beta E$ (MeV/s) = the stochastic acceleration rate;

and $\left(\frac{dE}{dt}\right)_{ad} = -\rho_0\beta^2 E$ (MeV/s) = deceleration rate,

With α (s^{-1}) the acceleration efficiency and $\rho_0 = (2/3)(V_r/R)$ (s^{-1}) is the deceleration efficiency due to adiabatic cooling. Furthermore V_r and R are the expanding velocity and linear extension of the expanding magnetic structure respectively; $N_0 = \text{protons}/4\pi R_{SE}^2$; $q_0 = \text{protons}/4\pi R_{SE}^2$ and $R_{SE} = 1.5 \times 10^{13}$ cm = sun-earth distance.

$$R_5(\varepsilon_0, \varepsilon) = [\text{erf}(Z_1) - 1] \exp[(3a_f/2\alpha)J_f^2] + [\text{erf}(Z_2) + 1] \exp[-(3a_f/2\alpha)J_f^2];$$

$$Z_{1,2} = (a_f t)^{1/2} \pm (3a_f/4\alpha t)^{1/2} J_f; \quad a_f = \left(\frac{\alpha}{3}\right) \left(F + \frac{3}{\alpha\tau} - 3\rho(4 - \beta^2 - \beta_0^2)/2\alpha\right);$$

$$\begin{aligned}\bar{F} &= 0.5[\beta^{-1} + 3\beta - 2\beta^3 + \beta_0^{-1} + 3\beta_0 - 2\beta_0^3]; \\ \beta &= (\varepsilon^2 - m^2 c^4)^{1/2} / \varepsilon; \quad \beta_0 = (\varepsilon_0^2 - m^2 c^4)^{1/2} / \varepsilon_0 \\ J_f &= \tan^{-1} \beta^{1/2} - \tan^{-1} \beta_0^{1/2} + 0.5 \ln \left[\frac{(1 + \beta^{1/2})(1 - \beta_0^{1/2})}{(1 - \beta^{1/2})(1 + \beta_0^{1/2})} \right]; \\ F(\rho_0) &= \left[\frac{\varepsilon_0(1 + \beta_0)}{\varepsilon(1 + \beta)} \right]^{3\rho_0/2\alpha} \quad \text{with } \varepsilon_0 \text{ the injection energy (MeV)}\end{aligned}$$

2. The Steady-State Spectrum for MHD turbulence, monoenergetic injection, $\tau = cst.$, and $D(p) = p^2/\beta$, has been given in the Eq. (42) in Gallegos-Cruz and Perez-Peraza (1995): this formulation was also developed with the inclusion of adiabatic energy losses:

$$N(E) \approx (q_0/2)(a_f \alpha/3)^{-1/2} (\beta_0^{3/2} \varepsilon_0)^{-1} (\beta_0/\beta)^{1/4} (\varepsilon/\varepsilon_0)^{1/2} \exp \left[-(3a_f/\alpha)^{1/2} J_f \right] [F(\rho_0)/4\pi R_{SE}^2] \quad \text{protons}/(MeV \text{ cm}^2 \text{ str}) \quad (\text{A5})$$

Where: $\alpha, \rho_0, a_f, \bar{F}, J_f, \beta, \beta_0, \varepsilon_0, F(\rho_0)$ and R_{SE} are the same as in Eq. A4

3. The Steady State Spectrum for MHD turbulence, monoenergetic injection, $\tau \approx 1/\beta$, and $D(p) \approx p^2/\beta$, has been given in the Eq. (43) in Gallegos-Cruz and Perez-Peraza (1995): this formulation with the incorporation of adiabatic energy losses was employed in Perez-Peraza et al., (2018):

$$N(E) = \frac{(q_0/2)(\beta_0/\beta)^{1/4} (\varepsilon/\varepsilon_0)^{1/2}}{(4\pi R_{SE}^2)(\alpha/3)^{1/2} a^4 (E) a^4 (E_0) \beta_0^2 \varepsilon_0} \left[\frac{\varepsilon + \beta \varepsilon}{\varepsilon_0 + \beta_0 \varepsilon_0} \right]^{-\left(b + \frac{1}{2b}\right)} \exp \left[\left(\frac{-1}{2b} \right) (\beta^{-1} - \beta_0^{-1}) \right] F(\rho_0) \quad \text{protons}/(MeV \text{ cm}^2 \text{ str}) \quad (\text{A6})$$

Where: $\alpha, \rho_0, a_f, \bar{F}, J_f, \beta, \beta_0, \varepsilon_0, F(\rho_0)$ and R_{SE} are the same as in Eq. A4

4. The Steady-State Spectrum of acceleration by a Direct Electric Field in a Magnetic Neutral Current Sheet (MNCS), has been given in Perez-Peraza et al., (1978) and Eq. (1) in Perez-Peraza et al., (2009):

$$N(E) = N_0 (E/E_c)^{-1/4} \exp \left[-1.12 (E/E_c)^{3/4} \right] \quad \text{protons}/(MeV \text{ cm}^2 \text{ str}) \quad (\text{A7})$$

With $N_0 = 8.25 \times 10^5 \left(\frac{nL^2}{B} \right) \left(\frac{1}{E_c} \right) / 4\pi R_{SE}^2 \text{ protons}/(MeV \text{ cm}^2 \text{ str})$, assuming anomalous conductivity; $E_c = 1.792 \times 10^3 \left(\frac{B^2 L}{n} \right) \text{ MeV}$, B = magnetic field strength (gauss), L = length of the MNCS (cm); and n = plasma number density (cm^{-3}).

REFERENCES

Álvarez, M., Miroshnichenko, L.I., Perez-Peraza, J. and Rivero-G, F., 1986, Spectrum of solar cosmic rays in the source taking into account their coronal propagation, *Soviet Astr.*, 66, p. 1169-1181.

Augusto, C. R. A., Kopenkin, V., Navia, C. E., Felicio, A. C. S., Freire, F., Pinto, A. C. S., 2013. Was the GLE on May 17, 2012 linked with the M5.1-class flare the first in the 24th solar cycle? arXiv:1301.7055, *Astroph. SR*. p. 1-9

Augusto C.R.A., Navia C.E., de Oliveira M.N., Nepomuceno A.A., Fauth A.C., Kopenkin V., Sinzi T., 2018. Relativistic proton levels from region AR2673 (GLE #72) and the heliospheric current sheet as a Sun-Earth magnetic connection. Preprint of the Alamos Laboratory, arXiv:1805.02678v1 [astro-ph.SR].

Barbosa, D.D., 1979. Stochastic Acceleration of Solar Flare Protons. *ApJ*, 233, p. 383-394; DOI: [10.1086/157399](https://doi.org/10.1086/157399)

Balabin, Yu. V., Germanenko, A. V., Vashenyuk, E. V., & Gvozdevsky, B. B., 2013. The first GLE of the new 24th solar cycle. *Proceedings 33rd International Cosmic Ray Conference, Rio de Janeiro, Brazil*, 1, p. 1467-1470.

Balson Dingle, R., *Asymptotic Expansions: Their Derivation and Interpretation* (Academic Press, 1973, London)

Berrilli F., Casolino M., Del Moro D., Di Fino L., Larosa M., Narici L., Piazzesi R., Picozza P., Scardigli S., Sparvoli R., Stangalini M., and Zaconté V., 2014. The relativistic solar particle event of May 17th, 2012 observed on board the International Space Station. *Weather and Space Clim.* 4, A16, p. 1-8, DOI: [10.1051/swsc/2014014](https://doi.org/10.1051/swsc/2014014).

Bieber, J. W., and Evenson, P., 1991. Determination of Energy Spectra for the Large Solar Particle Events of 1989. *Proceedings 22nd International Cosmic Ray Conference, Dublin*, 3, p. 129-133.

Bieber J. W., Dröge W., Evenson P. A., Pyle R., Ruffolo D., Pinsook U., Tooprakai P., Ujjarodom M., Khumlumert T. and Krucker S., 2002. Energetic Particle Observations During the 2000 July 14 Solar Event. *ApJ*. 567, p. 622-634.

Brillouin Léon, 1926. (La mécanique ondulatoire de Schrödinger: une méthode générale de résolution par approximations successives). *The wave mechanics of Schrödinger: a general method of successive approximation solving Comptes Rendus de l'Académie des Sciences*. 183, p. 24–26.

Bieber J. W., Clem J., Evenson P., Pyle R., Sáiz A., and Ruffolo D., 2013. Giant Ground Level Enhancement of Relativistic Solar Protons on 2005 January 20.I. *Spaceship Earth Observations. ApJ.*, p. 771-792.

- Caballero-Lopez, R.A. & Moraal, H., 2012. Cosmic-ray yield and response functions in the atmosphere. *J. Geophys. Res.*, Vol. 117, A12103, p. 1-11, DOI: 10.1029/2012JA017794.
- Caballero-Lopez, R.A., Moraal, H., 2016. Spectral index of solar cosmic-ray flux from the analysis of ground-level Enhancements. *Advances in Space Research* 57, p. 1314–1318.
- Cohen, C. M. S., and Mewaldt, R. A., 2018, The Ground-Level Enhancement Event of September 2017 and Other Large Solar Energetic Particle Events of Cycle 24, *Space Weather (AGU100, Advancing Earth and Space Science)*, p. 1616-1623, DOI: 10.1029/2018SW002006.
- De Koning, C.A., 1994. Significant proton events of solar cycle 22 and a comparison with events of previous solar cycles (Thesis). University of Calgary.
- Dorman, L.I., and Venkatesan, D., 1993. *Solar Cosmic Rays*, *Space Science Reviews* Vol. 64, p. 183-362, Doi: 1993SSRv.64.183D.
- Forman, M.A., Ramaty, R., Zweibel, E.G., 1986. *Physics of the Sun*, Ed. By Sturrock, P.A. et al., D. Reidel Publishing Company, Dordrecht, Holland, Chapter13, p. 249-324.
- Gallegos-C., A. and Perez-Peraza, J., 1987, Determination of energy spectra of solar electrons under different scenarios in solar flare sources, *Rev. Mexicana Astron. & Astrof.*, 14, p. 700-704.
- Gallegos-C., A., Perez-Peraza, J., Miroshnichenko, L.I. and Vashenyuk, E.V., 1993, Solar Particle Acceleration by Slow Magnetosonic Waves, *Adv. Space. Res.* 13(9), p. 187-190.
- Gallegos-Cruz, A., & Perez-Peraza, J., 1995. Derivation of analytical particle spectra from the solution of the transport equation by the WKB method. *Astrophysical Journal*, 446, p. 400–420.
- Ginzburg V. L., 1958. *Progress in Elementary Particle and Cosmic Ray Physics*, Vol. 4 (Elsevier, Amsterdam).
- Ginzburg V. L. and Syrovatskii S. I., 1964. *Origin of Cosmic Rays* (Pergamon Press. Oxford)
- Gopalswamy N., Xie H., Akiyama S., Yashiro S., Usoskin I.G., and Davila J.M., 2013. The First Ground Level Enhancement Event of Solar Cycle 24: Direct Observation of Shock Formation and Particle Release Heights. *Ap. J. Letters.*, 765: L30, p. 1-38 5, DOI: 10.1088/2041-8205/765/2/L30.
- Gopalswamy, N., Yashiro, S., Makell, P., Xie, H., Akiyama, S., and Monstein, C., 2018, Extreme Kinematics of the 2017 September 10 Solar Eruption and the Spectral Characteristics of the Associated Energetic Particles, *ApJ*, 863, L39, p. 1-6. DOI: <https://iopscience.iop.org/article/10.3847/2041-8213/aad86c>

Jeffreys Harold, 1924. On certain approximate solutions of linear differential equations of the second order. Proceedings of the London Mathematical Society. 23: p. 428–436. Doi:10.1112/plms/s2-23.1.428

Kichigin, G.N., Kravtsova, M.V., Sdobnov, V.E., 2019. Global Solar Magnetic Field and Cosmic Ray Ground Level Enhancement. Solar Phys. 294(116) p. 1-10. <https://doi.org/10.1007/s11207-019-1516-5>

Kramers, Hendrik A., 1926. Wave mechanics and half-integer quantization. (Wellenmechanik und halbzahlige Quantisierung). Zeitschrift für Physik. 39(10–11), p. 828-840. Bibcode:1926 ZPhy. 39.828. Doi:10.1007/BF01451751

Kuwabara, T., Bieber, J., Clem, J., Evenson, P., Gaisser, T., Pyle, R., and Tilav, S., 2012. Ground Level Enhancement of May 17, 2012, Observed at South Pole. 45th AGU Fall Meeting, SH21A-2183 (Poster), San Francisco.

Kuwabara, T., John Bieber, John Clem, Paul Evenson, Tom Gaisser, Rogert Pyle Serap Tilav, The Ice Cube Collaboration, 2013: Ground Level Enhancement of May 17, 2012 Observed at South Pole; Proc. 33rd ICRC, RIO DE JANEIRO 2013; The Astroparticle Physics Conference (See Special Section of these Proceedings), p. 1347-1350.

Li, C., Kazi, A., Firoz, L., Sun, P., & Miroshnichenko, L. I., 2013. Electron and proton acceleration during the first ground level enhancement event of solar cycle 24. ApJ. 770(1), 34, p. 1-11. DOI: <https://iopscience.iop.org/article/10.1088/0004-637X/770/1/34>

Matthiä D., Matthias M. M., and Berger T., 2018. The Solar Particle Event on 10–13 September 2017: Spectral Reconstruction and Calculation of the Radiation Exposure in Aviation and Space; Space Weather (AGU100, Advancing Earth and Space Science), V. 16, p. 977-986. DOI: 10.1029/2018SW001921.

McCracken, K.G., Moraal, H., Shea, M.A., 2012. The high-energy impulsive ground-level enhancement. ApJ. 761 (101), p. 1-12, DOI: 10.1088/0004-637X/761/2/101.

Melrose, D. B., 1976. Precipitation in trap models for solar hard X-ray bursts. MNRAS, 176 (1), p. 15-30, DOI: [10.1093/mnras/176.1.15](https://doi.org/10.1093/mnras/176.1.15)

Miroshnichenko, L.I., 2001. *Solar Cosmic Rays*. Ed. Kluwer Academic Publisher, The Netherlands, Astrophysics and Space Science Library, V. 260, (480 p.)

Miroshnichenko, L.I. and Perez-Peraza, J., 2008. Astrophysical Aspects in the studies of solar cosmic rays (Invited Article), International Journal of Modern Physics A, 23(1), p. 1-14

Miroshnichenko, L.I., 2014. *Solar Cosmic Rays: Fundamentals and Applications*. Second Edition, Springer, Berlin, 521 pages.

Mishev, A.L., Kocharov, L.G., Usokin I.G., 2014. Analysis of the ground level enhancement on 17 May 2012 using data from the global neutron monitor network. *J. Geophys. Res., Space Physics*, 119, p. 670-679. DOI: 10.1002/2013JA019253.

Mishev A., Usoskin I., Raukunen O., Paassilta M., Valtonen E., Kocharov L., Vainio R., 2018. First Analysis of Ground-Level Enhancement (GLE) 72 on 10 September 2017: Spectral and Anisotropy Characteristics; *Solar Phys.* 293 (136), p. 1-15
<https://doi.org/10.1007/s11207-018-1354-x>.

Moraal H. & R. A. Caballero-Lopez, 2014. The cosmic-ray ground level enhancement of 1989 september 29. *ApJ.* 790 (154), p. 1-16; DOI:10.1088/0004-637X/790/2/154.

Oh, S. Y., Bieber, J.W., Clem, J., Evenson, P., Pyle, R., Yi, Y., and Kim, Y. K., 2012. South Pole neutron monitor forecasting of solar proton radiation intensity. *Space Weather*, S05004, p. 1-13, DOI: 10.1029/2012SW000795.

Omodei N., Pesce-Rollins M., Longo F., Allafort A., Krucker S., 2018. Fermi-LAT observations of the 2017 September 10th solar flare Preprint of the Alamos Laboratory. arXiv: 1803.07654v1 [astro-ph.HE], p. 1-6; DOI: 10.3847/2041-8213/aae077.

Papaioannou, A., Souvatzoglou G., Paschalis P., Gerontidou M., Mavromichalaki H., 2014. The first ground-level enhancement of solar cycle 24 on 17 May 2012 and its real-time detection. *Solar Phys.*, 289, p. 423-436, DOI: 10.1007/s11207-013-0336-2.

Perez-Peraza, J., Gálvez, M., Lara-Alvarez, R., 1977, Energy spectrum of flare particles from an impulsive acceleration process, *Proceedings of the International Cosmic Ray Conference, XV-Vol. 5*, p. 23-28.

Perez-Peraza, J., Gálvez, M., & Lara-Alvarez, R., 1978. The Primary Spectrum of Suprathermal Solar Particles. *Adv. Space Research* 18, p. 365-368.

Perez-Peraza, J., Miroshnichenko, L.I., Rivero, F., Álvarez, M., 1985, Source energy spectra from demodulation of solar particle data by interplanetary and coronal transport, *Proceedings of the International Cosmic Ray Conference, XIX-Vol. 4*, p. 110-113.

Perez-Peraza, J. y Gallegos-C., A., 1987, Solutions of the Fokker-Planck equation for the energy distribution of suprathermal electrons, *Rev. Mexicana Astron. & Astrof.*, 14, p. 705-714.

Perez-Peraza, J., Miroshnichenko, L.I., Sorokin, O.M., Vashenyuk, E.V. and Gallegos-C., A., 1993, Spectrum of the fast solar proton component, *Geomagnetism and Aeronomy*, 32(2), 1-12; 1992 (Russian version, p. 159-171).

Perez-Peraza, J. and Gallegos-Cruz., A., 1994. Weightiness of the Dispersive Rate in Stochastic Acceleration Processes. *The Astrophysical Journal Supplement Series*, 90, p.669-682. <https://doi.org/10.1017/S0252921100077940>.

Perez-Peraza J., Vashenyuk E.V., Balabin Yu.V., Miroshnichenko L.I., Gallegos.Cruz A., 2009. Impulsive, Stochastic, and Shock Wave Acceleration of Relativistic Protons in Large Solar Events of 1989 September 29, 2000 July 14, 2003 October 28, and 2005 January 20. *ApJ*, 695, p. 865-873; DOI: 10.1088/0004-637X/695/2/865.

Perez-Peraza, Jorge, Márquez-Adame, Juan C.; Miroshnichenko, L., and Velasco-Herrera, V., 2018. Source Energy Spectrum of the 17 May 2012 GLE. *J. Geophys. Res.: Space Physics*, 123, p. 3262–3272, DOI: 10.1002/2017JA025030.

Perez-Peraza, Jorge; Márquez-Adame Juan C., 2018 in Book 1 Cosmic Rays, chapter 7, p. 121-161, Ed. by InTech, London, ISBN: 978-1-78923-593-7, ISBN: 978-953-51-6247-6.

Plainaki, C., Mavromichalaki H., Laurenza M., Gerontidou M., Kanellakopoulos A., and Storini M., 2014. The Ground-Level Enhancement of 2012 May 17: Derivation of Solar Proton Event Properties Through the Application of the NMBANGLE PPOLA Mode. *Astrophys. J.*, 785(160), p. 1-12, DOI: 10.1088/0004-637X/785/2/160.

Poluianov S.V., Usoskin I.G., Mishev A.L., Shea M.A., Smart, D.F., (2017), GLE and Sub-GLE Redefinition in the Light of High-Altitude Polar Neutron Monitors, *Solar Phys* (2017) 292(176) p. 1-7, DOI 10.1007/s11207-017-1202-4.

Ramaty, R., 1979, *Particle Acceleration Mechanisms in Astrophysics*, AIP Conf. Proceedings 56, Ed. J.Arons, C.Max, & C. McKee (New York: AIP), p. 135.

Ruffolo, D., Tooprakai, P., Rujiwarodom, M., Khumlumlert, T., Wechakama, M., Bieber, J.W., Evenson, P., Pyle, R., 2006. Relativistic Solar Protons on 1989 October 22: Injection and Transport along both Legs of a Closed Interplanetary Magnetic Loop. *ApJ*, 639, p. 1186–1205. <http://dx.doi.org/10.1086/499419>.

Sakurai, K., *Physics of Solar Cosmic Rays*, Ed. by University of Tokyo Press., 1974, UTP 22 3402, 68026-5149, Tokyo, ISBN 0-86008-105-2.

Schatzman, E., 1966. *Summer School of Theoretical Phys. Les Hooches* (New York: Gordon & Breach).

Shea, M. A., Smart, D. F. Wada, M., and Inoue, A., 1985, A suggested standardized format for cosmic ray ground-level event data, in Proceedings of 19th International Cosmic Ray Conference, La Jolla, 5, p. 510-520.

Shea, M. A., Smart, D. F., Adams, J. H., Chennette, D., Feyman J., Hamilton, D. C., Heckman, G., Konradi, A., Lee, M. A., Nachtwey, D. S., and Roelof, E. C., 1988. Toward a descriptive model of solar particle in the heliosphere; Interplanetary particle environment, JPL Publication, p. 1-13, N89-28455.

Schlickeiser, R., 1989. Cosmic-Ray Transport and Acceleration. I. Derivation of the Kinetic Equation and Application to Cosmic Rays in Static Cold Media. *ApJ*, 336(243), p. 243-293; DOI: [10.1086/167009](https://doi.org/10.1086/167009)

Smart, D. F. and Shea, M. A., 1993, *Predicting and modeling solar flare generate proton fluxes in the inner heliosphere*, in: Biological Effects and Physics of Solar and Galactic Cosmic Radiation, Part B, Eds: Swenberg et al., Plenum Press. New York, p. 101-117.

Smart, D. F. and Shea, M. A., 2005. A review of geomagnetic cutoff rigidities for earth-orbiting spacecraft. *Advances in Space Research* 36, p. 2012–2020; DOI: [10.1016/j.asr.2004.09.015](https://doi.org/10.1016/j.asr.2004.09.015)

Stoker, P. H., 1985, Spectra of solar proton ground level 1 events using neutron monitor and neutron moderated detector recordings, *Proceedings 19th International Cosmic Ray Conference*, La Jolla, Vol. 4, p. 114-117.

Tsytovich, V. N., 1977. *Theory of Turbulent Plasma* (New York: Consultants Bureau).

Vashenyuk, E. V., Miroshnichenko, L. I., Sorokin, M.O., Perez-Peraza, J. y Gallegos-Cruz, A., 1993. Search for Peculiarities of Proton Events in Solar Cycle 22 by Ground Observation Data. *Geomagnetism & Aeronomy* 33(5), p. 1-10.

Vashenyuk, E.V., Miroshnichenko, L.I. Sorokin, M.o., Perez-Peraza, J. and Gallegos A., 1994. Large Ground Level Events in Solar Cycle 22 and some peculiarities of Relativistic Proton Acceleration. *Adv. Space Res.* 14(10), p. 711-716.

Vashenyuk, E. V.; Balabin, Yu. V.; Gvozdevsky, B. B., 2011. Features of relativistic solar proton spectra derived from ground level enhancement events (GLE) modeling. *Astrophysics and Space Sciences Transactions*, Volume 7, Issue 4, 2011, p. 459-463, DOI: [10.5194/astra-7-459-2011](https://doi.org/10.5194/astra-7-459-2011)

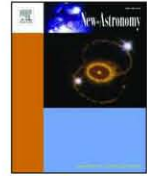
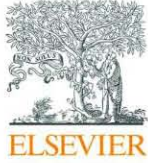
WentzeL Gregor, 1926, A generalization of the quantum conditions for the purposes of wave mechanics (Eine Verallgemeinerung der Quantenbedingungen für die Zwecke der Wellenmechanik). *Zeitschrift für Physik*, 38(6–7), p. 518–529. Bibcode:1926 ZPhy 38.518W. Doi:10.1007/BF01397171

Zhao, M.-X., Le, G.-M., & Chi, Y.-T., 2018, Investigation of the possible source for solar energetic particle event of 2017 September 10, *RAA (Research in Astronomy and Astrophysics)*-2018-0009, p. 1-13, arXiv:1805.01082v1 [astro-ph.SR] 3 May 2018

PRESENTACION DEL ARTÍCULO: “*The Quasi-Biennial Oscillation of 1.7 years in Ground Level Enhancement Events*”

Los llamados eventos de incremento a nivel del suelo son incrementos esporádicos de partículas solares relativistas medidos a nivel terrestre por una red de detectores de rayos cósmicos en todo el mundo. Generalmente se asume que estos eventos esporádicos ocurren aparentemente por azar. Sin embargo, encontramos que al estudiar los últimos 56 eventos registrados desde 1966 hasta 2014, estos eventos ocurren preferentemente en la fase positiva de la oscilación cuasi-bienal de la periodicidad de 1,7 años. Estos eventos discretos muestran que hay otro tipo de emisión solar (es decir, paquetes en forma de onda) que ocurre solo en una fase específica de una oscilación muy particular. Interpretamos este resultado empírico para admitir que los eventos de incremento a nivel del suelo no son el resultado de procesos estocásticos puros. Utilizamos la wavelet de Morlet para analizar la fase de cada una de las periodicidades encontradas y las variaciones locales de la densidad espectral de potencia en estos eventos esporádicos. Encontramos periodicidades cuasi regulares de 10.4, 6.55, 4.12, 2.9, 1.73, 0.86, 0.61, 0.4 y 0.24 años. Aunque algunas de estas periodicidades de oscilación cuasi-bienales (es decir, oscilaciones que operan entre 0.6 y 4 años) pueden interpretarse simplemente como armónicos del ciclo solar fundamental del fenómeno subyacente del magnetismo de las manchas solares. Las fuentes de estas periodicidades aún no están claras. Tampoco existe un mecanismo claro para la variabilidad de las periodicidades de oscilación cuasi-bienales. Las periodicidades de las oscilaciones cuasi-bienales se consideran en general una variación de la actividad solar, asociada con el proceso de dinamo solar. Además, la intensidad de estas periodicidades es más importante alrededor de los años de máxima actividad solar porque las periodicidades de oscilación cuasi-bienales están moduladas por el ciclo solar, donde el Sol aumenta su energía durante los máximos de actividad. Para identificar las relaciones entre los incrementos a nivel del suelo y los índices de los rayos solares y cósmicos en el marco tiempo-frecuencia, nosotros aplicamos el análisis de coherencia Wavelet. Las huellas dactilares de la actividad solar y los rayos cósmicos galácticos en estos fenómenos también se pueden discernir en términos de la prominente oscilación cuasi bienal de aproximadamente 1.7 años.

Estatus: Publicado.



The quasi-biennial oscillation of 1.7 years in ground level enhancement events



V.M. Velasco Herrera^{a,*}, J. Pérez-Peraza^a, W. Soon^b, J.C. Márquez-Adame^c

^a Instituto de Geofísica, Universidad Nacional Autónoma de México, Ciudad Universitaria, Coyoacán, México D.F., 04510, Mexico

^b Harvard-Smithsonian Center for Astrophysics, Cambridge, MA, USA

^c Posgrado en Ciencias de la Tierra, Universidad Nacional Autónoma de México, Ciudad Universitaria, Coyoacán, México D.F., 04510, Mexico

ARTICLE INFO

Keywords:

Solar flares
Ground level enhancements
Cosmic rays
Wavelet analysis

PACS:

Physics
Astronomy

ABSTRACT

The so-called Ground Level Enhancement events are sporadic relativistic solar particles measured at ground level by a network of cosmic ray detectors worldwide. These sporadic events are typically assumed to occur by random chance. However, we find that by studying the last 56 ground level enhancement events reported from 1966 through 2014, these events occur preferentially in the positive phase of the quasi-biennial oscillation of 1.7 year periodicity. These discrete ground level enhancement events show that there is another type of solar emission (i.e., wavelike packets) that occurs only in a specific phase of a very particular oscillation. We interpret this empirical result to support that ground level enhancement events are not a result of purely stochastic processes. We used the Morlet wavelet to analyze the phase of each of the periodicities found by the wavelet analyses and local variations of power spectral density in these sporadic events. We found quasi-regular periodicities of 10.4, 6.55, 4.12, 2.9, 1.73, 0.86, 0.61, 0.4 and 0.24 years in ground level enhancements. Although some of these quasi-biennial oscillation periodicities (i.e., oscillations operating between 0.6 and 4 years) may be interpreted as simply harmonics and overtones of the fundamental solar cycle from the underlying sun-spot magnetism phenomenon. The sources of these periodicities are still unclear. Also there is no clear mechanism for the variability of the quasi-biennial oscillation periodicities itself. The quasi-biennial oscillation periodicities are broadly considered to be a variation of solar activity, associated with the solar dynamo process. Also, the intensity of these periodicities is more important around the years of maximum solar activity because the quasi-biennial oscillation periodicities are modulated by the solar cycle where the Sun is more energetically enhanced during activity maxima. To identify the relationships among ground level enhancement, solar, and cosmic rays indices in time-frequency framework, we apply the wavelet coherence analysis. The fingerprints of solar activity and galactic cosmic rays on these phenomena can also be discerned in terms of the prominent quasi-biennial oscillation of about 1.7 years.

1. Introduction

The occurrence of solar proton events is a rather frequent phenomenon, which up to now is considered as a random event associated mostly with solar flares. At the same time, their close relations to magnetically active centers on the surface of the Sun and even to shock wave phenomena in the heliosphere is also presently recognized. In broad extent, their occurrence rate follows the 11-year Schwabe cycle of solar activity intimately related to the sunspot phenomenon.

Sporadically, with an average rate of 1.1 year^{-1} , a relativistic solar proton event occurs when protons acquire energies above 433 MeV (up to $\geq 10 \text{ GeV}$). This particular kind of events are also known as ground level enhancements of relativistic solar particles. These sporadic events

are associated with solar flares and eventually with shock waves, and are assumed to be quasi-random in nature. Their study turns out to be very important for both astrophysical and terrestrial aspects: the study of their energy spectrum and intensity-time profile gives us important information about their physical sources and propagation processes, respectively. To a certain extent, these occasional phenomena follow the time behaviour of the 11-year cycle of solar activity; however, they do not strictly follow the intensity of the solar activity cycle.

In a preliminary work (Pérez-Peraza et al., 2009) we established, for the first time, the intrinsic periodicities modulating ground level enhancement events: mid-term periodicities, in the range of months to years, short-term periodicities in the order of months and ultra-short term in the order of days. Most of them are seemingly harmonics of the

* Corresponding author:

E-mail address: vmv@geofisica.unam.mx (V.M. Velasco Herrera).

<http://dx.doi.org/10.1016/j.newast.2017.09.007>

Received 19 May 2017; Received in revised form 25 August 2017; Accepted 17 September 2017

Available online 20 September 2017

1384-1076/© 2017 Elsevier B.V. All rights reserved.

11 year solar activity cycles. Many of these periodicities are quite similar to those existing in sub-photospheric and coronal layers (i.e., sunspot and coronal activity indices) as well as in solar activity phenomena.

Later, an exhaustive study of the periodicities of ground level enhancement and galactic cosmic rays was given in Miroshnichenko et al. (2012). Recently, in Pérez-Peraza et al. (2015) it was established that some of the dominant periodicities that are present in galactic cosmic rays 11, 4.7, 2.8, 1.7, 0.4, 0.25 and 0.075 years, which in turn coincide with those of solar activity 11, 7, 4.7, 3.5, 1.3, 0.9 and 0.4 years based on the sunspot number. With the exclusion of the 11 years periodicity of the solar cycle, it was determined that the most prominent periodicity in galactic cosmic rays and the sunspot number is that of 4.7 years. We claim that such similarity is a necessary condition, but it is however not sufficient to draw physical inferences on the phenomena that are taking place in the solar atmosphere.

The periodicities between 0.6 and 4 years are broadly categorized as the quasi-biennial oscillation of solar activity (see Bazilevskaya et al. (2014, 2016)), speculated to be associated with the underlying solar dynamo processes. In addition, the inter-relationship between quasi-biennial variations of solar activity and galactic cosmic rays was also analyzed by Bazilevskaya et al. (2014), Bazilevskaya et al. (2016).

In the analysis of quasi-biennial oscillation of solar activity, different filters are usually adopted (for more details, see e.g., Rivin (1989); Bazilevskaya et al. (2016)). But there is a practical problem, it is not clear what are the criteria to choose the correct and appropriate filters. Here we propose to use the wavelet coherence to resolve this problem Velasco Hererra (2008a). A first wavelet coherence analysis was performed by Velasco Hererra (2008b) and those authors found that many of the relativistic solar particles periodicities are in common with different facets of the solar atmosphere. Following this work, in Pérez-Peraza et al. (2011) we proposed a classification of ground level enhancement of relativistic solar particles on the basis of their spectral content: we delimited three main groups according to the level of enhancement over the galactic cosmic rays background.

Based on the ground works established previously, we have advanced the idea that the agreement in the modulation timescales found with wavelet coherence analysis between ground level enhancement periodicities and those of different layers of the solar atmosphere, indicates that ground level enhancement phenomena are not locally isolated phenomena but that there is apparently a well organized synchronization involving the whole Sun and even including the associated modulation of the incoming galactic cosmic rays fluxes. This empirical evidence argues against the pure stochasticity of ground level enhancement production.

It should be emphasized that even if the sunspot number is a representative proxy of solar activity phenomena, sunspots are not the ultimate source of ground level enhancement, which in turn is generally placed in the context of solar flare activity phenomenon (see e.g., attempts to connect solar flares to the underlying magnetic sunspot features in Eren et al. (2017)). A more direct proxy is now available from the Boğaziçi University Kandilli Observatory, Istanbul, Turkey which we will use in this paper.

Following our synchronization hypothesis, we attempt in this work by considering the effect of the source itself of ground level enhancement, that is the generating mechanisms of solar flare. We study, using the wavelet coherence analysis, directly the solar flare index for the period 1966 to 2014, which is a close-enough proxy of the particle acceleration source itself. We ignore here the ground level enhancement statistics available from 1942–1965 interval mainly because the solar flare index dates only from 1966 onward. In addition, we also carry out here a wavelet coherence analysis pairwise among galactic cosmic rays, ground level enhancement and solar flare index indices.

2. Data

The network of neutron monitors stations worldwide furnishes data of the ground level enhancement and galactic cosmic rays. Data since 1964 with high reliability are available from many neutron monitors stations; for the period from 1966 up to 2014 we have used monthly averaged galactic cosmic rays data from the Oulu neutron monitor station: <http://cosmicrays oulu.fi/>.

The fact that the solar flare index is available only since 1966, we consider here 57 events (see Table 3 below) from the ground level enhancement-event no. 15 (July 07, 1966) up to ground level enhancement-event no. 71 (May 17, 2012) and digitally transformed into a binary signal (Velasco Herrera and Cordero, 2016), as follows:

$$F = \begin{cases} 1 & \text{there are GLE in given month} \\ 0 & \text{no GLE or no reported} \end{cases} \quad (1)$$

We note that the use of the binary function (F) does not produce spurious or fictitious periodicities but only influence the decrease in amplitude of spectral power per scale.

In our previous works, we have studied the coherence between the sunspot number and ground level enhancement activity variations. Since the relativistic solar protons are basically produced in solar flares and only indirectly through the sunspot index, in this work we take a new step forward by using the source of the phenomenon itself, that is, solar flare, solar flare index, statistics.

The solar flare index is a value related to the measure of this short-lived explosive activity on the Sun (Ataç, 1987; Özgüç and Ataç, 1989; 1996; 2003; Ataç and Özgüç, 1996; 1998; 2001). Here we used the monthly averaged data on total solar flare index from the Boğaziçi University Kandilli Observatory, Istanbul, Turkey <http://www.koeri.boun.edu.tr/astronomy/>, from 1966 up to 2014.

3. Wavelet analysis

Concerning the methodology employed, let us remind here that in order to analyze local variations of power within a single non-stationary time series at multiple periodicities, (such as the galactic cosmic rays, ground level enhancement and solar flare index), we apply the wavelet tool using the Morlet wavelet (Torrence and Compo, 1998) because it provides a relatively higher resolution of the periodicity (frequency) scales. And because the basis analyzing function for the wavelet transform is a complex function, we are also able to calculate the phase information accurately (e.g. Velasco Herrera et al., 2015).

Meaningful wavelet periodicities (confidence level greater than 95%) must be contained inside the cone of influence (lightly shaded zones in Figs. 1 and 2) of solar flare index and the interval of 95% confidence (Torrence and Compo, 1998) is marked by red dotted lines (left panels in all figures). The global spectra (left panels in all figures) have been included in the wavelet plot in order to show the power contribution of each periodicity inside the cone of influence. To determine the statistical significance levels of the global wavelet power spectrum, it is necessary to choose an appropriate background spectrum. For many phenomena, an appropriate background spectrum is either white noise (with a flat Fourier spectrum) or red noise (increasing power with decreasing frequency). We established our significance levels in the global wavelet spectra with a simple red noise model (Gilman et al., 1963).

The uncertainties of each meaningful periodicities (peak in global wavelet spectrum) are obtained from the full-width at half maximum values (Mendoza et al., 2006).

The squared coherency is used to identify frequency bands within which two time series are covarying and is a measure of the intensity of the covariance of the two series in time-frequency space. The wavelet transform coherence (WTC) is especially useful in highlighting the time and periodicity intervals, when the two phenomena (X and Y) have a

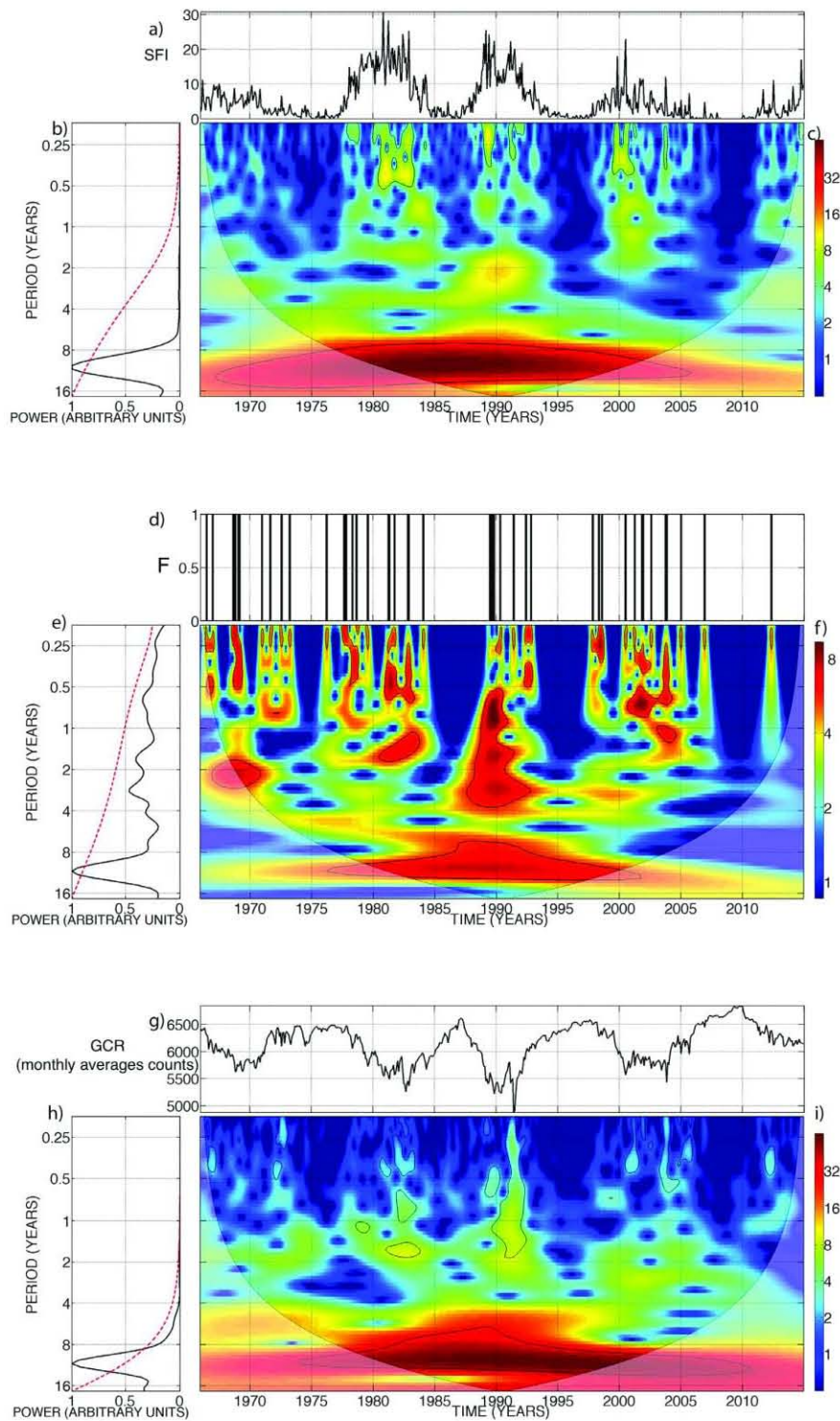


Fig. 1. Wavelet transform analysis of solar flare index (SFI), ground level enhancements (F) and galactic cosmic rays (GCR) time series (black line in a, d, and g) between 1966 and 2014. The wavelet powers are shown in the central panel (c, f, and i), where the curved outlines mark zones of the cone of influence. The color bar shows the wavelet spectral power in arbitrary normalized units. The thick contour is the 95% confidence level for the corresponding red-noise spectrum. The global wavelet is shown in the left panel (b, e, and h). The red dotted lines marked the 95% red-noise levels of the global spectra. (For interpretation of the references to colour in this figure legend, the reader is referred to the web version of this article.)

strong coupling, and is defined (Torrence and Compo, 1998) as:

$$WTC_n^{XY}(s) = \frac{\langle |W_n^{XY}(s)|^2 \rangle}{\langle s^{-1} |W_n^X(s)|^2 \rangle \langle s^{-1} |W_n^Y(s)|^2 \rangle} \quad (2)$$

where $W_n^{XY}(s)$ is the cross wavelet spectrum of two time series X and Y , with wavelet transforms $W_n^X(s)$ and $W_n^Y(s)$ respectively, $\langle \cdot \rangle$ indicates smoothing both in time and scale (e.g. Grinsted et al., 2004; Velasco Herrera et al., 2017), n is the time index and s is the wavelet scale. The factor s^{-1} is used to convert to energy density.

The global wavelet coherence spectrum (GWTC) is defined (Velasco and Mendoza, 2008) as:

$$GWTC = \sum_n WTC_n^{XY}(s)$$

The statistical significance level of the wavelet coherence is estimated using Monte Carlo methods with red noise to determine the 5% significance level (Torrence and Webster, 1999). The Monte Carlo estimation of the significance level uses on the order of 1000 surrogate data set pairs (Grinsted et al., 2004).

If the wavelet spectrum is calculated individually for two or more time series and these spectra show that they have some periodicities in common, this does not necessarily mean there is a physical relationship between them. However, if the global wavelet coherence spectrum shows that there are common periodicities; this implies that there is a physical mechanism and/or certain medium connecting these two phenomena. It is precisely such frequency synchronization that may indicate that there is coupling, modulation and/or resonance between these two distinct phenomena studied.

Broadly speaking, the WTC metric measures the degree of similarity between the input (X) and the system output (Y), as well as the consistency of the output signal (X) due to the input (Y) for each frequency component. If the coherence between two series is high, the arrows in the coherence spectra show the phase between the phenomena: arrows at 0° (horizontal right) indicate that both phenomena are in phase and arrows at 180° (horizontal left) indicate that they are in anti-phase. It is very important to point out that these two cases imply a linear relationship between the considered phenomena; arrows at 90° and 270° (vertical up and down, respectively) indicating an out of phase situation which means that the two phenomena have a non-linear relationship (i.e., see Soon et al., 2014; Velasco Herrera and Cordero, 2016; Velasco Herrera, 2016; Velasco Herrera et al., 2017).

4. Results and discussion

Fig. 1 shows the wavelet spectra of the solar flare index, the ground level enhancement and the galactic cosmic rays records, respectively. The time series are shown in the top panels (black line in Fig. 1a, d, and g), and the wavelet powers are shown in the central panels in time-frequency representation (Fig. 1c, f, and i). The global-averaged wavelet spectra (GWS) indicating the main periodicities appears in the left panel of each figure (Fig. 1b, e, and h).

In Fig. 1a, we show the wavelet analysis of the solar flare index from 1966 to 2014. The GWS (Fig. 1b) presents periodicities of 10.4, 5.2, 3.27, 2.45, and 1.73 years and of 262, 146, and 76 days. It is noted that in the central panel where a periodicity of 10.4 years is shown, the spectral power is distributed evenly throughout the whole time interval (1966–2014), whereas the spectral powers of periodicities under 10.4 years are most visible only around the time of solar activity maxima (Fig. 1c).

The wavelet analysis of the ground level enhancement from 1966 to 2014 is shown in Fig. 2d. The GWS (Fig. 1e) presents periodicities of 10.4, 6.55, 4.12, 2.9, and 1.73 years and of 313, 222, 146, and 87 days. The frequency spectral power for 10.4 years is present throughout the time interval. Once again, the modulations of ground level enhancement events on periodicities shorter than 10.4 years mainly occur

around the phase of solar activity maxima (Fig. 1f).

The wavelet analysis of the galactic cosmic rays between 1966 and 2014 is shown in Fig. 1g. The GWS (Fig. 1g) presents periodicities of 10.4, 5.2, 3.09, 1.83, and 1.22 years and of 281 and 156 days. For the periodicity of 10.4 years, the spectral power is distributed evenly throughout the whole record from 1966 to 2014, whereas the spectral powers of the periodicities under 10.4 years are most prominent only around solar maxima (Fig. 1i).

The periodicity of 10.4 years corresponds to the Schwabe cycle and is present in all of the time series, with the main power concentrated in this periodicity. This periodicity has been detected at a confidence level greater than 95%. The periodicity of 5.2 years corresponds to the quasi-quinquennial cycle Velasco Hererra (2008a), while the periodicities between 0.6 and 4 years are noted as the quasi-biennial oscillation of solar activity (Bazilevskaya et al., 2014; 2016), presumably associated with the solar dynamo process. Regarding the 4.7–5.5 years periodicity, Djurović and aquet (1996) reported these periodicities in sunspot areas, as well as in the coronal activity index, Wolf numbers and solar flux at 10.7 cm.

We wish to note that the periodicity of 1.8 years in Total Solar Irradiance index has been contemplated and reported by Li et al. (2010). The plausible connection of such short-term periodicity to the underlying intrinsic solar magnetism or solar dynamo operation can be further motivated by the recent exciting discovery of such a mid-term periodicity by Egeland et al. (2015) in a young (about 1 Gyr old) Sun analog, HD 30495. Apparently, the solar and stellar dynamo generation and/or modulation of such mid-term 1.7–1.8 years oscillation is nearly universal.

The periodicity of 146 days is the Rieger-type cycle, and 76 days is a short periodicity. The intensity of these periodicities is more important around the years of maximum solar activity because the mid-term, short and ultra-short periodicities are modulated by the solar cycle where the Sun is more energetically enhanced during activity maxima Valdés-Galicia and Velasco (2008). The intermediate-term periodicities (87–106, 159–175, 194–219, 292–318 and ~ 389 days) in sunspot areas has been reported by Chowdhury et al. (2009). In Table 1, we summarize the main periodicities with their uncertainties for the solar flare index, ground level enhancement and galactic cosmic rays records deduced in our analyses.

The pairwise wavelet coherence analyses between solar flare index, ground level enhancement, and galactic cosmic rays time series from 1966 to 2014 are shown in Fig. 2. Fig. 2a and c illustrates the wavelet coherence (WTC) spectrum between solar flare index and ground level enhancement statistics (black line and black bars, respectively). It can be seen from the corresponding global wavelet coherence spectra (Fig. 2b) that the common periodicities between these two phenomena are 10.4, 4.74, 3.04, 1.67, 0.9 and 0.59 years. All these periodicities have confidence levels greater than 95%, with the exception of the periodicity of 4.74. Other than the 11 years periodicity of the solar cycle, the most prominent one is that of 1.67 years, called hereafter as the 1.7 years periodicity (taking into account the uncertainty margin for the wavelet basis in resolving this timescale/period). It should be noted that this periodicity divides the ground level enhancement into five intervals, each of which are well defined within solar Schwabe Cycles 20–24: 1966–1972, 1975–1985, 1986–1994, 1996–2006 and 2011–2014. It can be seen that they are linearly correlated most of time with the exception of Cycle 22 where the correlation is of a rather complex nature.

Fig. 2d and f shows the wavelet coherence spectrum between galactic cosmic rays and ground level enhancement (black line and blue bars, respectively): the common periodicities in this case are 10.4, 4.52, 2.89, 1.59, 0.7 and 0.44 years. Here the periodicities between galactic cosmic rays and ground level enhancement are in anticorrelation and all these periodicities have confidence levels greater than 95%, with the exception of the periodicity of 4.79. The 1.59 years periodicity (confidence level greater than 95%) designated from here on as the 1.7-year

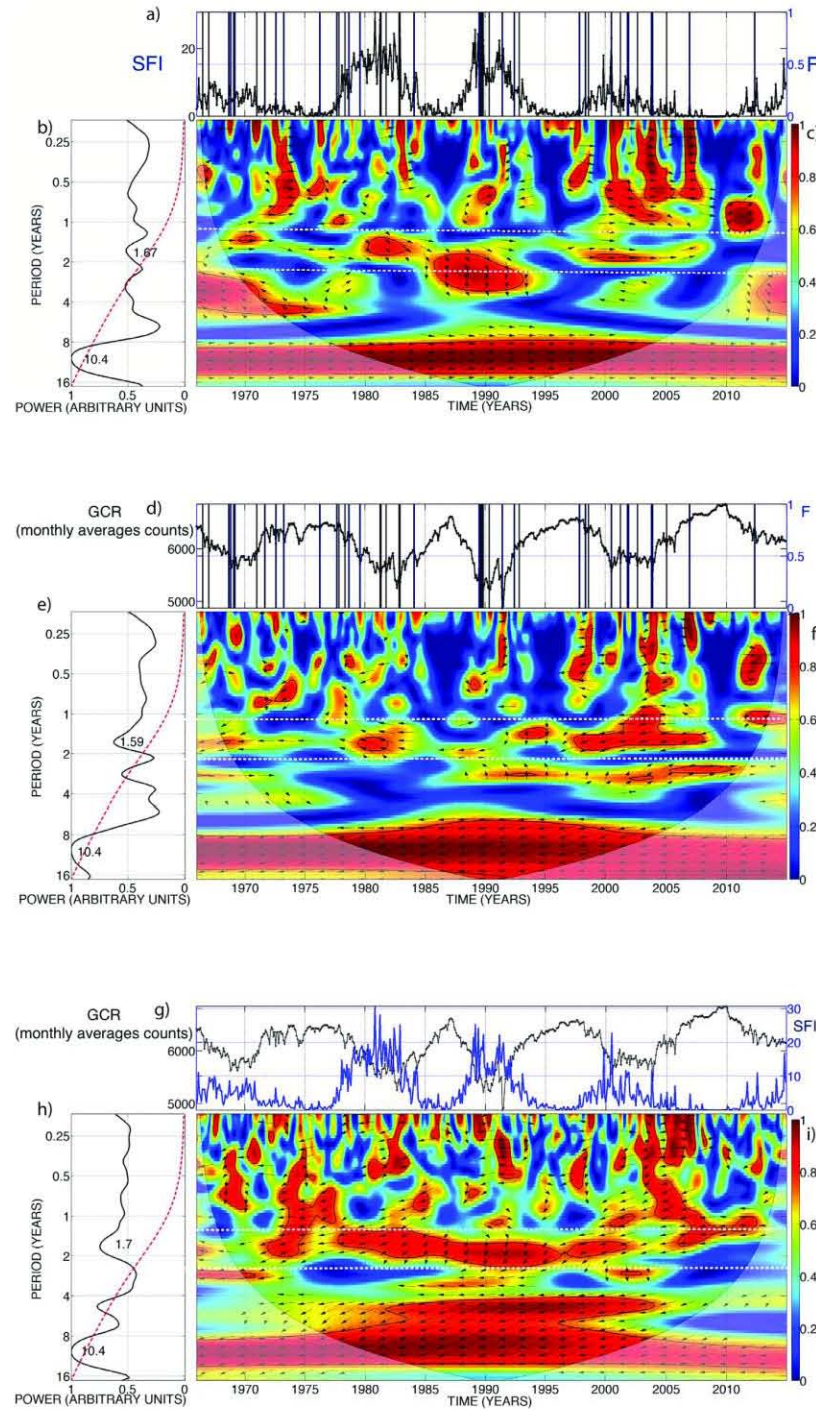


Fig. 2. Results of the wavelet coherence (WTC) analysis for the solar flare index and ground level enhancement (black line and black bars respectively in a), galactic cosmic rays and ground level enhancement (black line and black bars respectively in d), and solar flare index and galactic cosmic rays (blue line and black line respectively in Fig. 2g) time series from 1966 to 2014. The left panels (Fig. 2b, 2e, and 2h) shows the global spectrum of the wavelet coherence power. The red dotted line represents the significance level of the global spectrum and refers to the power of red noise level at the 95% confidence interval, as described in Fig. 1. The center panels show the wavelet coherence power (c, f, and i). The color bar scale shows the wavelet coherence power. The orientation of the arrows shows relative phasing of the two time series at each timescale; arrows at 0° (pointing to the right) indicate that both time series are perfectly positively correlated (in phase) and arrows at 180° (pointing to the left) indicate that they are perfectly negatively correlated (180° out of phase), both of these two perfect cases implying a linear relationship between the considered phenomena; non-horizontal arrows indicate an out of phase situation and a more complex non-linear relationship. (For interpretation of the references to colour in this figure legend, the reader is referred to the web version of this article.)

periodicity that divides the ground level enhancement in 5 intervals: 1966–1974, 1976–1985, 1988–1995, 1997–2006 and 2010–2014.

Fig. 2g and i presents the wavelet coherence spectrum between the solar flare index and galactic cosmic rays (blue line and black line, respectively). Here, the common periodicities are 10.4, 4.79, 3.19, 1.76, 1.13, 0.76, 0.3 and 0.23 years. Again, these two phenomena are

anticorrelated. All these periodicities have confidence levels greater than 95%, with the exception of the periodicity of 2.89 years. In Table 2, we present the main periodicities detected with their uncertainties from the pairwise wavelet coherence calculations among the three time series records: solar flare index, ground level enhancement and galactic cosmic rays statistics.

Table 1

Main periodicities (in years) that contribute to solar flare index, ground level enhancement and galactic cosmic rays.

Periodicities	Solar flare index	ground level enhancement	Galactic cosmic rays
Short (≤ 1 years)	0.72 ± 0.3	0.86 ± 0.2	0.77 ± 0.2
	0.40 ± 0.2	0.61 ± 0.3	
	0.21 ± 0.01	0.40 ± 0.1	
Mid-term periodicities (1–2 years)	2.45 ± 0.5	2.9 ± 0.5	1.73 ± 0.6
	1.73 ± 0.5	1.73 ± 0.6	1.22 ± 0.5
		0.24 ± 0.1	2.75 ± 0.5
3 years cycle (Quasi-triennial)	3.3 ± 0.7	4.12 ± 0.7	3.09 ± 0.8
5 years cycle (Quasi-quinquennial)	5.2 ± 1.1	6.55 ± 0.9	5.20 ± 1.4
Decadal	10.4 ± 2.3	10.4 ± 2.1	10.4 ± 1.9

Table 2

Main common periodicities (in years) in the pairwise wavelet coherence between solar flare index, ground level enhancement and galactic cosmic rays.

Periodicities	Galactic cosmic rays	Ground level enhancement
Solar flare index	10.40 ± 2.1	10.4 ± 2.3
	4.79 ± 1.3	4.74 ± 1.1
	3.19 ± 0.5	3.04 ± 0.7
	1.76 ± 0.3	1.67 ± 0.3
	1.13 ± 0.2	0.90 ± 0.1
	0.76 ± 0.1	0.59 ± 0.1
	0.30 ± 0.03	
	0.23 ± 0.01	
ground level enhancement	10.40 ± 2.3	
	4.52 ± 1.2	
	2.89 ± 0.5	
	1.59 ± 0.2	
	0.70 ± 0.1	
	0.44 ± 0.03	

The quasi-biennial oscillation of 1.7 years divides all ground level enhancement events into five intervals, and is one of the most prominent periodicities in the wavelet coherence. This empirical observation permits the assumption that there is a connection between this oscillation and the occurrence of the ground level enhancement events. To identify the relationships between ground level enhancement and quasi-biennial oscillation of 1.7 year as a function of time, we apply the inverse wavelet transform in wavelet spectrum of the ground level enhancement events (Torrence and Compo, 1998; Velasco Herrera et al., 2017).

Fig. 3 shows the time variation of the 1.7 years oscillation (obtained with inverse wavelet transform) and the discrete ground level enhancement events (dotted red line and black bars, respectively) analyzed from 1966 to 2014 (see Table 3 for all recorded ground level enhancement events). In addition, the sunspots (gray shaded area) are shown to describe the solar cycles. It can be observed that of the 57 ground level enhancement events analyzed, none of the events occurred during solar minima of Cycles 20 to 23. In the solar Cycle 20, the ground level enhancement-no. 15 to ground level enhancement-no. 26 events were registered, in the solar Cycle 21 the ground level enhancement-no. 27 to ground level enhancement-no. 39 events occurred, during the Cycle 22 of the ground level enhancement-no. 40 to ground level enhancement-no. 54 events occurred, in the solar Cycle 23 of ground level enhancement-no. 55 to ground level enhancement-no. 70 events were recorded. During the solar Cycle 24 only the ground level enhancement-no. 71 event is reported around May 17, 2012.

It is often assumed that ground level enhancement events are random phenomena. However, it can be deduced from the 57 ground level enhancement events analyzed that they occur preferentially in the

Table 3

57 Ground level enhancement events from 1966 through 2014.

Event	Event date	Event	Event date			
15	7 July	1966	44	22	October	1989
16	28 January	1967	45	24	October	1989
17	28 January	1967	46	15	November	1989
18	29 September	1968	47	21	May	1990
19	18 November	1968	48	24	May	1990
20	25 February	1969	49	26	May	1990
21	30 March	1969	50	28	May	1990
22	24 January	1971	51	11	June	1991
23	1 September	1971	52	15	June	1991
24	4 August	1972	53	25	June	1992
25	7 August	1972	54	2	November	1992
26	29 April	1973	55	6	November	1997
27	30 April	1976	56	2	May	1998
28	19 September	1977	57	6	May	1998
29	24 September	1977	58	24	August	1998
30	22 November	1977	59	14	July	2000
31	7 May	1978	60	15	April	2001
32	23 September	1978	61	18	April	2001
33	21 August	1979	62	4	November	2001
34	10 April	1981	63	26	December	2001
35	10 May	1981	64	24	August	2002
36	12 October	1981	65	28	October	2003
37	26 November	1982	66	29	October	2003
38	7 December	1982	67	2	November	2003
39	16 February	1984	68	17	January	2005
40	25 July	1989	69	20	January	2005
41	16 August	1989	70	13	December	2006
42	29 September	1989	71	17	May	2012
43	19 October	1989				

positive phase of the oscillation of 1.7 years. This could possibly mean that the ground level enhancement events, apparently not quite a random process, but that they appear in packages in the positive phase of this periodicity, most likely when there are certain favorable conditions in the solar chromosphere. This result is surprising, since solar phenomena have almost always been considered to be quasi-continuous events. These ground level enhancement events show that there is apparently another type of solar manifestation, i.e., the “solar packets” that, occur only in a selected phase of a very particular persistent oscillation.

The fact that the ground level enhancement events, can occur at any time of the positive phase of the quasi-biennial oscillation of 1.7 years, has indeed been suggested that these events are a consequence of random processes. However, from the point of view of solar packets, the ground level enhancement events may ultimately not a random process at all. The occurrence of these events are very well determined in the positive phase of the quasi-biennial oscillation of 1.7 years. We admit, that within this phase, there is an indeterminacy of when ground level enhancement events can or will occur. But, we have managed to limit in time, the occurrence of these relativistic sporadic wave-packet-like events. The periodicity of 1.7 years has been reported in different quasi-continuous solar indices (see for example Bazilevskaya et al., 2014; 2016; Mendoza et al., 2006; Valdés-Galicia and Velasco, 2008 and the cited references). What is surprising about the ground level enhancement events is that it is a discrete time series but that it also has this periodicity.

5. Conclusions

We have applied wavelet transform to study the time-frequency characteristics of ground level enhancement events and we found quasi-regular periodicities of 10.4, 6.55, 4.12, 2.9, 1.73, 0.86, 0.61, 0.4 and 0.24 years.

It can be noted that the quasi-biennial oscillation of 1.7 years divides the ground level enhancement events into five intervals, each of which are well defined within solar Cycles 20–24.

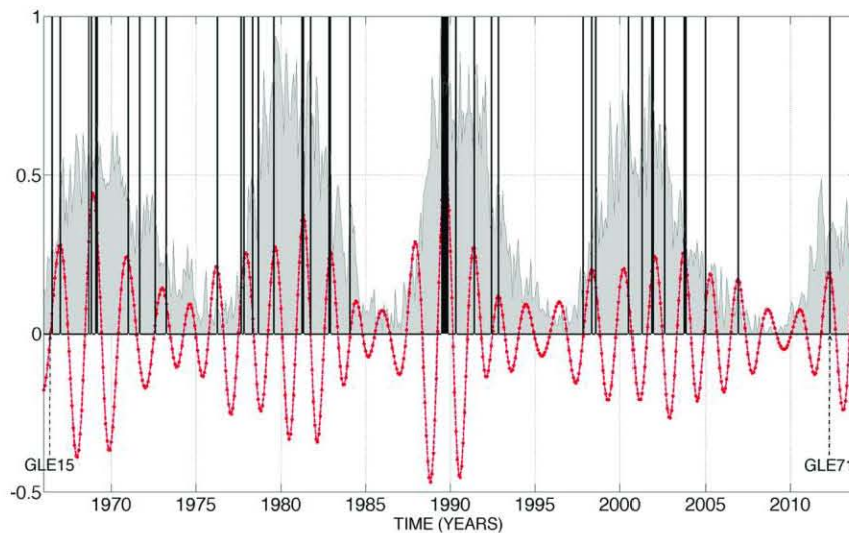


Fig. 3. The distribution of discrete ground level enhancement events (black bars marking events 15 to 71) in solar Schwabe Cycles 20–24 (gray shaded area). These events occur preferentially in the positive phase of the quasi-biennial oscillation of 1.7 years (dotted red line). (For interpretation of the references to colour in this figure legend, the reader is referred to the web version of this article.)

The ground level enhancement sporadic events are typically assumed to be of a random nature. However, we find that the last 57 ground level enhancement events reported from 1966 to 2012 occur preferentially in the positive phase of the quasi-biennial oscillation of 1.7 years. This empirical result suggests that the ground level enhancement events may not simply be of chance occurrences after all.

In order to understand the physical relationship among solar activity, galactic cosmic rays and ground level enhancement, we have performed a wavelet coherence analysis of three inter-related phenomena involved: galactic cosmic rays, ground level enhancement and the source itself of ground level enhancement, that is, solar flare index. As it can be expected galactic cosmic rays are in anti-correlation with phenomena of solar activity, specifically in our case, with solar flare index and ground level enhancement. In contrast, the relationship between ground level enhancement and the solar flare index is positively related and roughly linear in its correlation.

The changes in galactic cosmic rays provide information about the occurrence when ground level enhancement can be related to the synchronization of some periodicities of galactic cosmic rays with those developed in solar flare index and ground level enhancement during the gestation of an ground level enhancement event. Thus, the empirical relation deduced here may ultimately be used as a predictor of ground level enhancement occurrences.

In Table 1, we summarize the most prominent periodicities for each of the studied phenomena. It can be appreciated that in spite of slight differences, these periods can be grouped in five categories.

In Table 2 we show the common periodicities between the studied phenomena. It can be observed that they are quite close, within the limits of the detection uncertainty: among the most prominent periodicities involved in the coupling of these three phenomena are the 1.7 year periodicity (1.67, 1.76 and 1.59 years) as well as the 4.7 years (4.74, 4.79 and 4.52) which likely played a prominent role for the synchronization between solar flare index, ground level enhancement and galactic cosmic rays. Our independent analyses confirm the mid-term flare periodicities previously reported by Kilcik et al. (2010). Finally, the physical reality (rather than a mere statistical chance or even artefact) of the mid-term 1.7 years periodicity can find independent confirmation from a recent result on the study of a young Sun analog, HD 30495 (Egeland et al., 2015).

Acknowledgments

Pérez-Peraza thanks the support of UNAM, DGAPA-PAPIIT by

means of grant IN106214. Velasco Herrera V.M. acknowledges the support from CONACyT-180148 and PAPIIT IN107618 grants. Willie Soon's work was partially supported by the SAO grant with proposal ID: 00000000003010-V101. We express our sincere gratitude to T. Ataç and A. Özgüç from Bogazici University Kandilli Observatory, Istanbul, Turkey for providing us with the flare index data used in this study.

References

- Ataç, T., 1987. *Astron. Astrophys. Suppl.* 135, 201.
- Ataç, T., Özgüç, A., 1996. *Solar Phys.* 166, 201.
- Ataç, T., Özgüç, A., 1998. *Solar Phys.* 198, 399.
- Ataç, T., Özgüç, A., 2001. *Solar Phys.* 198, 399.
- Bazilevskaya, G., Broomhall, A.M., Elsworth, Y., Nakariakov, V.M., 2014. *Space Sci. Rev.* 186, 359.
- Bazilevskaya, G., Kalinin, M.S., Krainev, M.B., Makhmutov, V.S., Svirzhevskaya, A.K., Svirzhevsky, N.S., Stozhkov, Y.I., 2016. *Cosmic Res.* 54 (3), 171.
- Chowdhury, P., Khan, M., Ray, P.C., 2009. *Mon. Not. R. Astron. Soc.* 392, 1159.
- Djurović, D., Pâquet, P.P., 1996. *Solar Phys.* 167, 427.
- Egeland, R., Metcalfe, T., Hall, J.C., Henry, G.W., 2015. *Astrophys. J.* 812 (12).
- Eren, S., Kilcik, A., Atay, T., Miteva, R., Yurchyshyn, V., Rozelot, J.P., Özgüç, A., 2017. *Mon. Not. R. Astron. Soc.* 465, 68.
- Gilman, D.L., Fuglister, F.H., Mitchell, J.M.J., 1963. *Atmos. Sci.* 20, 182.
- Grinsted, A., Moore, J.C., Jevrejeva, S., 2004. *Nonlinear Process Geophys.* 11, 561.
- Kilcik, A., Özgüç, A., Rozelot, J.P., Ataç, T., 2010. *J. Atmos. Solar-Terr. Phys.* 264, 255.
- Li, K.J., Xu, J.C., Liu, X.H., Gao, P.X., Zhan, L.S., 2010. *Solar Phys.* 267, 295.
- Mendoza, B., Velasco, V.M., Valdés-Galicia, J.F., 2006. *Sol Phys.* 233, 319.
- Miroshnichenko, L.I., Pérez-Peraza, J., Velasco Herrera, V.M., Zapotitla, J., Vashenyuk, E.V., 2012. *Geomagn. Aeronomy* 52, 547.
- Özgüç, A., Ataç, T., 1989. *Solar Phys.* 123, 357.
- Özgüç, A., Ataç, T., 1996. *Solar Phys.* 163, 183.
- Özgüç, A., Ataç, T., 2003. *Solar Phys.* 214, 375.
- Pérez-Peraza, J., Velasco Herrera, V.M., Zapotitla, J., Miroshnichenko, L.I., Vashenyuk, E., Ya, I., 2009. 10, 1.
- Pérez-Peraza, J., Velasco Herrera, V.M., Zapotitla, J., Miroshnichenko, L.I., Vashenyuk, E., Libin, Ya., 2011. *Proc. of the 32nd ICRC*, SH 10, pp. 151.
- Pérez-Peraza, J., Juárez, A., Juárez, J., *Astron. J.* 2015, 803, 27.
- Rivin, Y.R., 1989. *The cycles of The Earth and the Sun*. Moscow, Nauka.
- Soon, W., Velasco Herrera, V.M., Selvaraj, K., Traversi, R., Usoskin, I., Chen, C.T.A., Lou, J.Y., Kao, S.J., Carter, R.M., Pipin, V., Severi, M., Becagli, S.A., 2014. *Earth-Sci. Res.* 134, 1.
- Torrence, C., Compo, G., 1998. *Bull. Am. Meteorol. Soc.* 79, 61.
- Torrence, C., Webster, P.J., 1999. *J. Clim.* 12, 2679.
- Valdés-Galicia, J.F., Velasco, V., 2008. *Adv. Space Res.* 41, 297.
- Velasco, V., Mendoza, B., 2008. *Adv. Space Res.* 42, 866.
- Velasco Herrera, V.M., Soon, W., Velasco-Herrera, G., Traversi, R., Horiuchi, K., 2017. *New Astron.* 56, 86.
- Velasco Herrera, V., 2008a. 37th COSPAR scientific assembly. E21-0049-08.
- Velasco Herrera, V., 2008b. 37th COSPAR scientific assembly. E21-0050-08.
- Velasco Herrera, G., 2016. *Adv. Space Res.* 58 (10), 2104.
- Velasco Herrera, V.M., Cordero, G., 2016. *Earth Planets Space* 42, 866.
- Velasco Herrera, V.M., Mendoza, B., Velasco Herrera, G., 2015. *New Astron.* 34, 221.

PRESENTACION DEL ARTÍCULO:




“Determination of GLE of Solar Energetic Particles by Means of Spectral Analysis”

Utilizando tres series de tiempo solares no estacionarias: Solar Flare index (FS), Sunspots Index (SS) y Solar Flux index (F10.7), aplicamos el análisis de Coherencia de Wavelet de Morlet para determinar los armónicos dominantes de la actividad solar, 1.73, 3.27, 4.9, 10.4 y 11 años. Las periodicidades obtenidas se procesan mediante el método de Lógica Difusa que nos permite reproducir las fechas de ocurrencia de los Incrementos a nivel del suelo (GLE) de partículas solares relativistas registradas en la red global de Monitores de Neutrones, desde 1942 a 2006. En las técnicas espectrales mencionadas utilizamos dichas fechas como línea base de entrenamiento para determinar la ocurrencia de los incrementos de partículas solares en los Ciclos Solares. El resultado en Lógica Difusa se extiende a tiempos posteriores al período de entrenamiento para cubrir el final del ciclo 24 y el inicio del ciclo 25. Además del aspecto previsorio de este trabajo, los resultados obtenidos son de gran interés en vista de la reciente controversia despertada en relación con la aparición de GLEs débiles (es decir, Sub-GLEs), durante el presente Ciclo Solar 24.

Estatus: Publicado.



Determination of GLE of Solar Energetic Particles by Means of Spectral Analysis

Juan C. Márquez-Adame , Jorge Pérez-Peraza , and Victor Velasco-Herrera 
Instituto de Geofísica, Universidad Nacional Autónoma de México, C.U., Coyoacán, 04510, México, D.F., Mexico¹
Received 2019 February 23; revised 2019 April 20; accepted 2019 May 15; published 2019 June 25

Abstract

Using three nonstationary solar series, the solar flare index (FS), the sunspots index (SS), and the solar flux (F10.7) index, we apply the Morlet wavelet analysis to determine the most dominant harmonics of solar activity, 1.73, 3.27, 4.9, 10.4, and 11 yr. The periodicities obtained are processed by the fuzzy logic method, which allows us to reproduce the occurrence dates of ground level enhancements (GLE), since 1942–2006, which we use as a training baseline of these spectral techniques to determine the occurrence of solar particle enhancements in solar cycles. Then, the result of fuzzy logic is extended to periods later than the training period so as to cover the end of cycle 24 and the beginning of cycle 25. In addition to the forecastable aspect of this work, the obtained results are of high interest in view of the recent controversy that has arisen in relation to the occurrence of small GLE (namely sub-GLE), during cycle 24.

Key words: Sun; flares – Sun; particle emission

1. Introduction

The solar energy particles that arrive to the ground have been given several names: relativistic solar proton events and/or ground level enhancements (GLE). The latter name has remained the general one, and a subdivision has even been presupposed. The GLE are measured at the terrestrial level by the worldwide network of neutron monitor (MN) detectors. These sporadic events are associated with solar flares and are assumed to be of a solar quasi-stochastic nature: their occurrence is not always connotative of solar activity intensity. Taking into account that even when solar cycle 22 was much more intense than cycle 23, the latter had more GLE than cycle 22; for example, there were 13 GLEs in the period from 1989 July to 1991 June, and not a single event since the end of 2006 December up to 2012 May. A previous study that establishes the synchronization between some periodicities of the various layers of the solar atmosphere argues against a complete stochasticity of the relativistic particle production phenomenon. This leads to the determination of precursors that are not seen in the galactic cosmic radiation outside the periods of GLE occurrences (Pérez-Peraza et al. 2009). Such synchronization seems to indicate that the production of GLE is not an isolated local phenomenon, but rather it involves global regions of the Sun's atmosphere. In this last study, it was shown that despite the quasi-stochastic nature of GLEs, it is possible to predict them with relative precision, months or even years before they occur: even for the next solar cycle. Additionally, in this work, we can clearly distinguish the occurrence of 10 GLE during solar cycle 24 that had not been comprehensively categorized.

2. Data and Methodology

2.1. Morlet Wavelet Analysis

To determine the main oscillation periodicities as well as their time evolution in nonstationary series, such as those of solar energetic particles, we apply the Morlet wavelet technique (Torrence & Compo 1998). This is a very well-known tool for analyzing localized variations of power within a given time series for many different periodicities when one is dealing with a nonstationary series and the coherence between two

nonstationary series. The so-called global wavelet spectrum (GWS) is an average of the power spectra at each resolution level. That is to say, it is assumed that the time series has an average power spectrum relative to the red noise of the Fourier series: harmonics above this average spectrum (the slashed line in the right panels of Figure 1) represent real signals with levels of reliability higher than 95%. The importance of the GWS is in the distribution of signals with the same characteristics in order to determine which harmonics contain greater power (Torrence & Webster 1999).

We apply the wavelet analysis to the series of monthly data obtained from the following index that pertains to solar activity: number of sunspots (SS) from 1749 to 2017 (<http://www.sidc.be/silso/datafiles>), solar flux index (F10.7) from 1947 to 2017 (<https://www.esrl.noaa.gov/psd/data/correlation/solar.data>; Xiao et al. 2017; Chatterjee 2001; Henney et al. 2012), and the Flare Index (FI) from 1966 to 2014 (http://www.koeri.boun.edu.tr/astronomy/fi_nedir.htm; Ataç & Özgüç 1998, 2001). Figure 1 demonstrates the wavelet spectrum and the global energy spectrum (intermediate panels) of each of the series. In order to discern high frequencies, we apply the Daubechies filter (Daubechies 1992) so as to eliminate the 11 yr harmonic or its approximate in the case of Index F10.7, that contains a much higher level of energy and thus conceals the shorter periods.

The dominant periodicities that are present in different series that we use in our analysis refer to sunspots: 11 and 4.9 yr; for the index F10.7: 11 and 3.27 yr; and for FI: 10.4, 3.27 and 1.73 yr. It should be mentioned that in the case of the FI, we found the quasi-biennial periodicity (1.73 yr) proposed by Velasco Herrera et al. (2018).

2.2. Fuzzy Logic

The procedure of Fuzzy Logic consists of calculating the time intervals of occurrence of the GLEs, by means of creating membership functions (MFs) for the selected periodicities of greater energy, in the wave power spectrum of the studied series, as described by Mendel (1995). We observe that the amplitude of the dominant periodicities, and their behavior during the occurrence of a GLE event, have similar

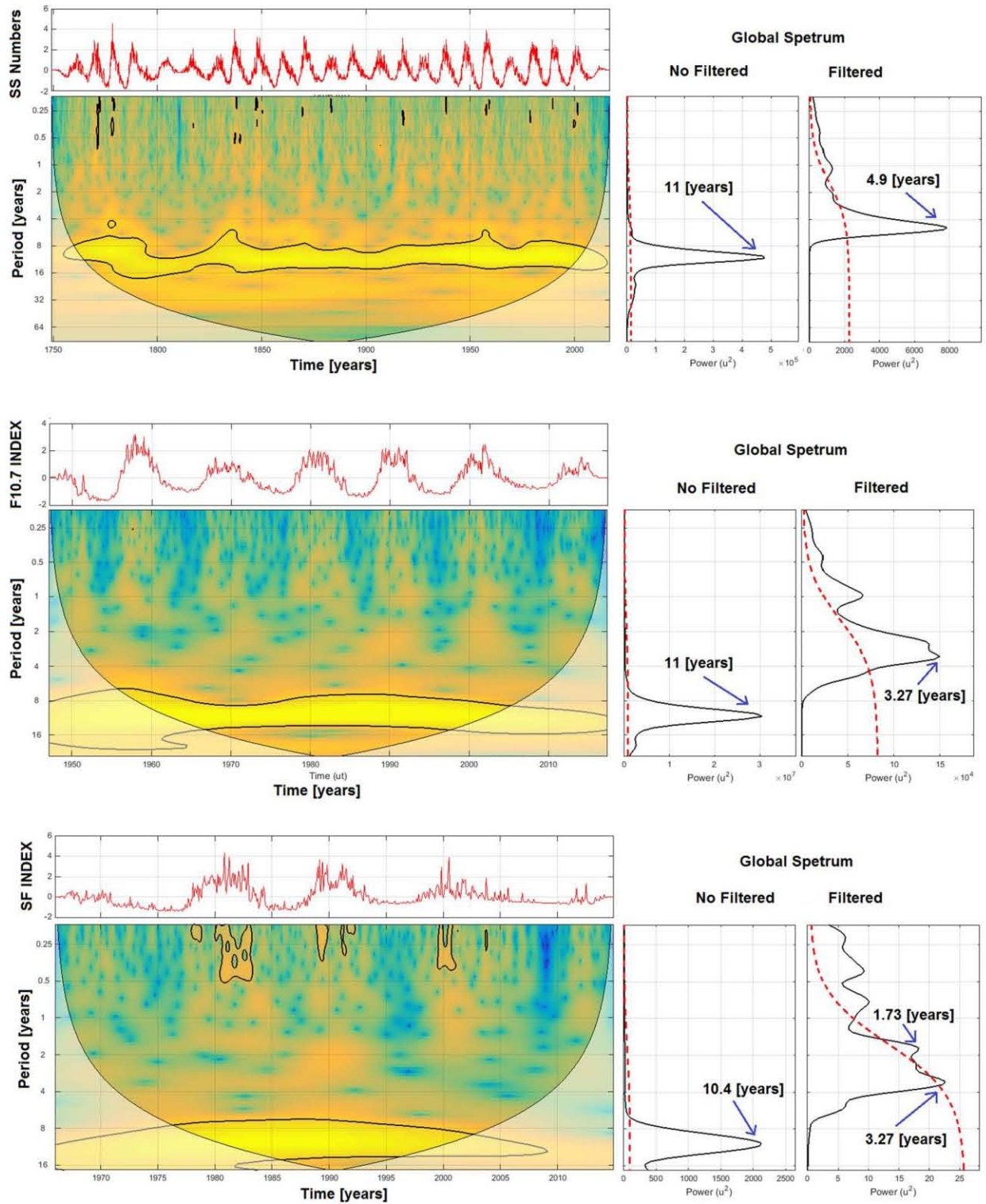


Figure 1. Spectral analysis: the upper panel of the first box shows the time series of the number of sunspots, the central panel of the box refers to the wavelet spectrum, and the right panel is its global energy spectrum before and after filtering. Similarly, in the central box we have the F10.7 series and below, the corresponding Wavelet and its global spectrum. Similarly, in the lower panel the corresponding information of the FI can be found.

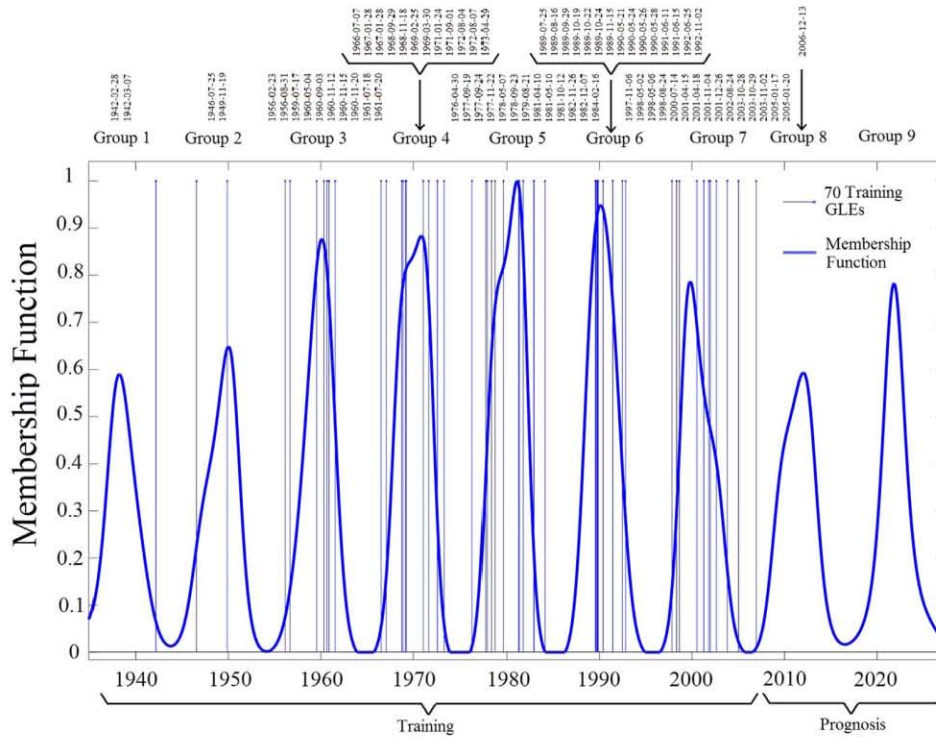


Figure 2. Fuzzy Logic results of the 70 training GLE.

characteristics that allow us to estimate the time intervals in which subsequent events may occur in the future.

The MFs are usually built according to criteria of experts in the area of study or, alternatively, these can be calculated by using mathematical data analysis algorithms, which are applied mainly in the Theory of Control Systems (e.g., Chuen 1990). In our case, the MF is the curve that describes the degree to which an element of the set of amplitudes of a certain periodicity in the 70 GLEs belongs. The concept of fuzzy logic emerges from the fact that an MF can describe the occurrence of a given GLE. In our analysis, the MF was constructed with the product of the equations of two standard Gaussian curves expressed in Equation (1): the mean and the standard deviation are obtained with the data and the amplitudes of the frequency and its derivate during the occurrence of the studied events.

$$\mu_A = \frac{1}{\alpha_A \sqrt{2\pi}} e^{-\frac{(t-\beta_A)^2}{2\alpha_A^2}} \times \frac{1}{\alpha_{dA} \sqrt{2\pi}} e^{-\frac{(t-\beta_{dA})^2}{2\alpha_{dA}^2}}. \quad (1)$$

Equation (1) represents the function of the membership of the frequencies, according to the studied periodicities, α_A and β_A , that represent the average and the standard deviation of the frequency amplitudes, respectively; α_{dA} and β_{dA} , which are calculated from the amplitude of the derivative of periodicity; in both cases, the average and the standard deviation are calculated with the data of the amplitudes of the frequency at the moment in which the events of interest (or training) occurred in the past, that is, the known GLE.

Finally, t is the variable that represents the distribution of the amplitudes of the frequencies. Therefore, although the proposal of an MF is somewhat arbitrary, in the sense of selecting the

Table 1
First GLE and Last GLE of the First Eight Groups

Group	First GLE	Last GLE
1	***	(1942 Mar 7)
2	(1946 Jul 25)	(1949 Nov 19)
3	(1956 Feb 23)	(1961 Jul 20)
4	(1966 Jul 7)	(1973 Apr 29)
5	(1976 Apr 30)	(1984 Feb 16)
6	(1989 Jul 25)	(1992 Nov 02)
7	(1997 Nov 6)	(2005 Jan 20)
8	(2006 Dec 13)	***

Table 2
Intervals Calculated for the Two Subgroups of GLE: The First and the Last of Each Group

Group	Begin	End
8	2006 Aug 26	2015 Aug 3
9	2017 Jun 13	2005 Mar 5

we assume that our data can approximate a Gaussian bell, and the MF is statistically related to our data.

Figure 2 shows the MF constructed with the 70 training GLE mentioned. By definition, MFs have maximum unit amplitude, and 0 indicates that there is no membership (Mendel 1995).

To predict the amplitude of the MF, we base our calculations on the prospective behavior (periodic behavior in the future) of the amplitude of a certain frequency. The information of the MFs calculated for all analyzed periodicities leads us to define time intervals for the probable occurrence of an event. Once the MFs for each frequency are constructed, the next step is to

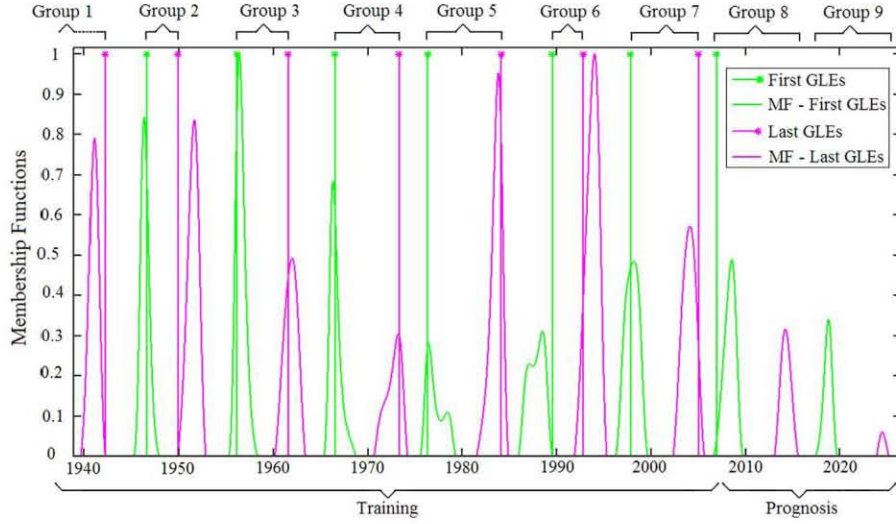


Figure 3. Membership Functions of the first GLE and last GLE subgroups.

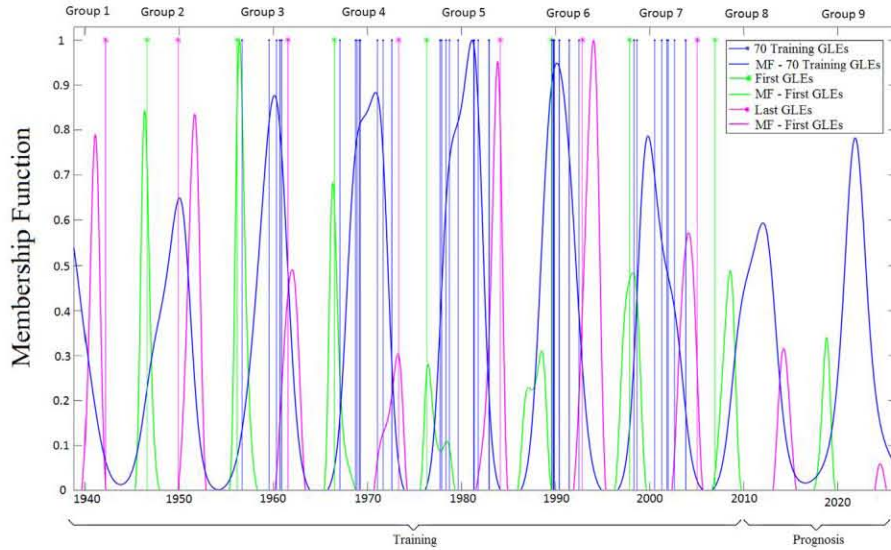


Figure 4. Membership function graph of the initial 70 GLE training, and the membership functions of the first GLE and the last GLE subgroups.

the product.

$$\Pi = \mu_A \cap B \cap C \cap \dots = \mu_A \times \mu_B \times \mu_C \times \dots, \quad (2)$$

where $\mu_A \cap B \cap C \cap \dots$ denotes the intersection function and $\mu_A, \mu_B, \mu_C, \dots$ the MFs of each of the selected periodicities.

Figure 2 shows the results of fuzzy logic: the 70 GLE training events are illustrated in light blue. The resulting MF is in dark blue.

In this work we continue with the previous assumptions by using the behavior of periodicities to describe the occurrence of the GLE. The behavioral characteristics of periodicities determine the time intervals in which a GLE may occur. The procedure for calculating time intervals is to create MFs for the periodicities with higher energy in the wavelet power spectra, of the three indexes. Unlike to previous work, Pérez-Peraza & Juárez-Zuñiga (2015), for “training” purposes the GLE were

grouped into three categories: first, last, and intermediate, which were previously classified on the basis of the 11 yr solar cycle. Later, the MF of each of those three groups was obtained. On this basis the GLE occurrence intervals were determined.

Instead, in this work, we use the first 70 GLEs (from 1942 to 2006) as initial training data, and together with the seven periodicities (Figure 1 and Equation (2)) we obtained a more accurate MF. From this MF the first and last subgroups were obtained, see Table 1.

Nine groups are formed from the 70 GLE training. Thus we call the training zone the first seven groups and the beginning of the eighth group. We call the rest of the eighth group and the entire ninth group the prognosis zone.

In Figure 2, we show the harmonic behavior of the dates of occurrence of the GLE, according to the selected periodicities of the indexes worked on (Equation (2)). This result is in

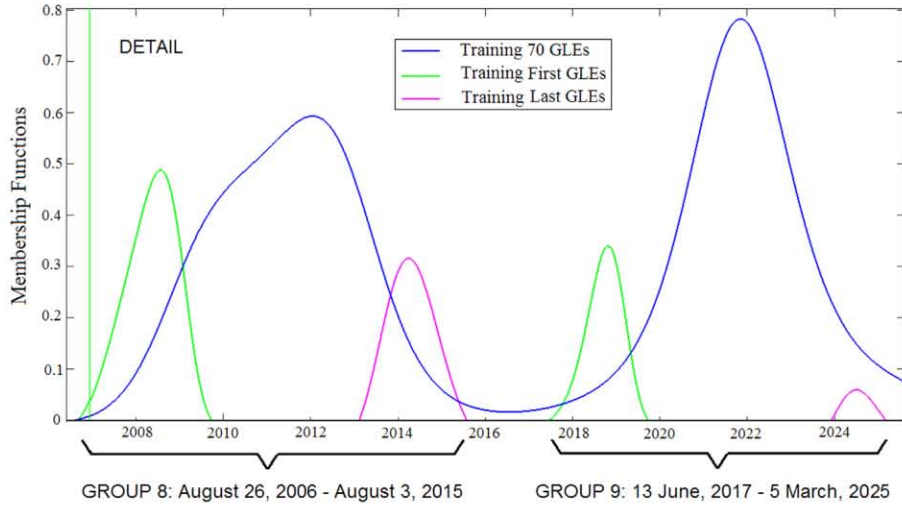


Figure 5. Detail of Groups 8 and 9 from Figure 4.

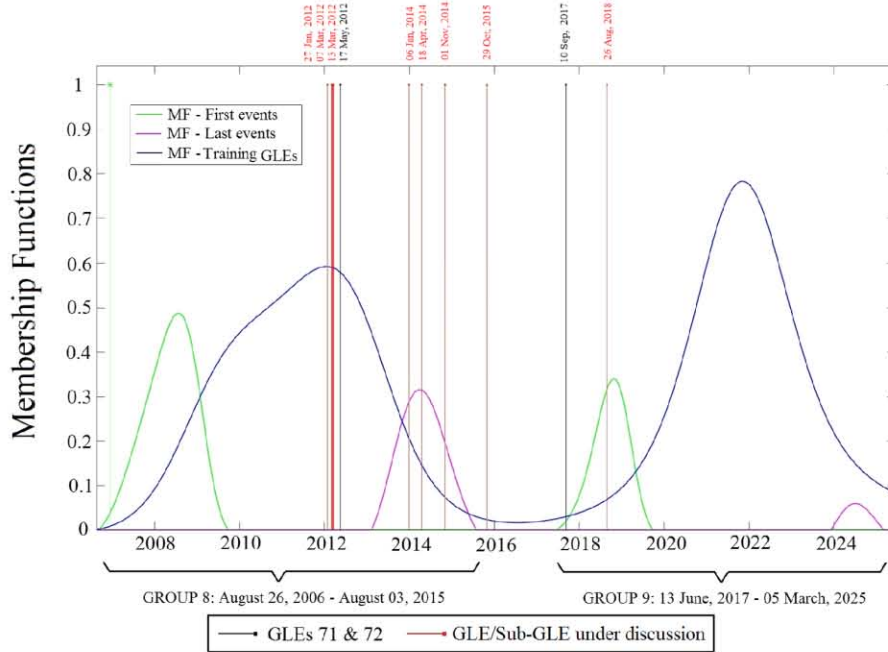


Figure 6. GLE in the prognosis zone.

agreement with previous works where the periodic nature of the GLE events had already been included as evidence, Pérez-Peraza et al. (2011).

Based on this MF, we can extend the analysis to later times after the 70 GLE of training. This is where the importance of our study lies, as it gives us a powerful tool to calculate the values of the MF associated with the possible occurrence of the events under study (Groups 8 and 9 of Figure 1). However, as we can see in Figure 2 even when groups can be defined very clearly for the 70 GLE of training, we observe that the date ranges for groups 8 and 9 are not well defined. In order to refine such a limitation, two subgroups are defined of each group established in Figure 2, see Table 2: a first GLE and a last GLE.

Using these subgroups as training groups, we obtain Figure 3.

In Figure 3 the ranges of groups 8 and 9 are extracted from the MFs of the first GLE and last GLE subgroups.

In order to better visualize the above, we combine Figures 2 and 3 in a new figure (Figure 4).

The above graph now allows us to obtain the prediction ranges that clearly define the end date of group 8 and the beginning and end of group 9, which is shown in detail of Figure 5. In Figure 6, we indicated the specific dates of the prognosis of events disclosed in Figure 5.

As we observed, cycle 24 was a particular period due to the appearance of peculiarly weak GLE as reported in different

works in the literature; this led to the discussion in the international scientific community about the occurrence or not of certain GLE events, such questions were derived in the reconceptualization due to the fact that there is at present a high discrepancy in the classification of events of cycle 24.

3. Discussion

In this discussion, the contribution we intend to render through our work is to provide more tools within the framework of the Wavelet technique and Fuzzy Logic in order to extend the study to cycles 24 and 25, as well as to corroborate the previous studies of the harmonic behavior of the GLE evidenced in Pérez-Peraza et al. (2011) and Pérez-Peraza & Juárez-Zuñiga (2015).

In Pérez-Peraza & Juárez-Zuñiga (2015), two indices were used, one of solar activity (SS) and another modulated by solar activity (RCG): eight periodicities or harmonics were obtained for each index, so in the process of working with Fuzzy Logic, 16 periodicities were applied. As mentioned above, it is important to note that in the present work only indices of solar activity were used (SS Index, F10.7 Index, and Flare Index) and the periodicities that best grouped the occurrence of the 70 GLE of logic training were selected through the obtained MF, Figure 1. This is of great importance since previously only the 11 yr periodicity of the sunspot index was used to try to group the occurrence of GLE. In our present study, we note that the grouping is more precise, Figure 2, since the grouping comes from the MF resulting from the selected harmonics, Figure 1 and Equation (2). This is to be taken into account as an important sample of the periodic behavior of the phenomenon of solar flares, which is broader and more precise than just considering the 11 yr period of sunspots.

Subsequently, we focused our analysis on the time zone after the 70 GLE of training, which we designate as the area of prognosis, where two groups were clearly formed. The treatment in fuzzy logic to obtain the start and end dates of groups eight and nine of prognosis, Table 2, was limited to the first GLE and last GLE of each group obtained in the training zone, Figure 3 and Table 1.

Once the time ranges of groups eight and nine have been obtained in the prognosis area, in order to corroborate the validity we used the method developed in Pérez-Peraza & Juárez-Zuñiga (2015). The relative profiles in the global MN network were reviewed to identify the events that actually indicate an increase at ground level.

From the above, we can observe that seven events, including GLE71, fall within the predicted time range for group eight; one more, the event of 2015 October 29, falls very close to the end of the same group eight predicted for 2015 August 3. Finally, we see that the two remaining events, including the GLE72, occur within the range of the first events predicted for group nine.

4. Conclusions

Among the important conclusions, we point out the following:

- a. Indexes specific to solar activity are used.

- b. The conjunction of Wavelet and Fuzzy Logic methods allows us to find the seven harmonics that accurately describe the periodic behavior of the phenomenon of solar flares. In so far as the 70 GLE of training, we define in a precise way seven groups of GLE and the beginning of an eighth group.
- c. The MFs obtained, extrapolated to later times, in the prognosis area, defined the completion of group eight and the entire interval of group nine.
- d. To verify the veracity of the prognosis, we contrast it with the events that occurred in cycle 24, which have been mentioned in the literature.
- e. It was found that nine events fall within the two groups of the prognosis area and one more falls very close to the end of group eight.

In summary, the above corroborates the potential of the method for the study of the periodic nature of the occurrence of GLE events.

To the Instituto de Geofísica de UNAM for his economical support and to the CONACyT for the economical support by means of a scholar grant. To the institutions where we obtained the databases of solar indices:

- a. Number of Sunspots (SS) from 1749 to 2017 (<http://www.sidc.be/silso/datafiles>).
- b. Solar Flux Index (F10.7) from 1947 to 2017 (<https://www.esrl.noaa.gov/psd/data/correlation/solar.data>).
- c. Flare Index (FI) from 1966 to 2014 (http://www.koeri.boun.edu.tr/astronomy/fi_nedir.htm).

ORCID iDs

Juan C. Márquez-Adame  <https://orcid.org/0000-0002-3126-0775>

Jorge Pérez-Peraza  <https://orcid.org/0000-0001-8998-3653>

Victor Velasco-Herrera  <https://orcid.org/0000-0002-0100-8878>

References

- Ataç, T., & Özgüç, A. 1998, *SoPh*, **180**, 397
 Ataç, T., & Özgüç, A. 2001, *SoPh*, **198**, 399
 Chatterjee, T. N. 2001, *MNRAS*, **323**, 101
 Chuen, L. 1990, *ITSMC*, **20**, 2
 Daubechies, I. 1992, in CBMS-NSF Regional Conf. Ser. Applied Mathematics 61 (Philadelphia, PA: SIAM) 1162107
 Henney, C. J., Toussaint, W. A., White, S. M., & Arge, C. N. 2012, *SpWea*, **10**, S02011
 Mendel, J. 1995, *IEEEP*, **83**, 3
 Pérez-Peraza, J., & Juárez-Zuñiga, A. 2015, *ApJ*, **803**, 27
 Pérez-Peraza, J., Velasco Herrera, V. M., Zapotitla, J., et al. 2011, *Proc. ICRC (Beijing)*, **10**, 151
 Pérez-Peraza, J., Velasco Herrera, V. M., Zapotitla, J., Vashenyuk, E. V., & Miroshnichenko, L. I. 2009, *Proc. ICRC (Lodz)*, 31
 Torrence, C., & Compo, G. 1998, *BAMS*, **79**, 61
 Torrence, C., & Webster, P. J. 1999, *JCLI*, **12**, 2679
 Velasco Herrera, V. M., Pérez-Peraza, J., Soon, W., & Márquez-Adame, J. C. 2018, *NewA*, **60**, 7
 Xiao, C., Cheng, G., Zhang, H., et al. 2017, *ChJSS*, **37**, 1

PRESENTACION DEL ARTICULO:

“An Alternative Classification of Solar Particle Events that Reach the Earth Ground Level”

Actualmente existe una controversia en la literatura acerca de la denominación de Protones Solares Energéticos, que generalmente se designan como incrementos a nivel del suelo (GLE por sus siglas en ingles), Sub-GLE o simplemente Partículas energéticas solares (SEP). Tales clasificaciones dependen de la naturaleza del comportamiento de un evento dado. Hay algunos criterios de discrepancia entre los diferentes autores que hemos señalado en la primera parte de este trabajo. Para unificar criterios, aquí realizamos un análisis de varias bases de datos y diferentes catálogos de eventos de partículas. Observamos que existe cierta discrepancia en la conceptualización de los eventos en la literatura especializada, y por lo tanto proponemos una re-conceptualización en el sentido de que todos los GLE cumplen con los criterios dados en la literatura para ser considerados como GLE, incluso aquellos que se han clasificado recientemente como Sub-GLE/GLE para el caso particular del presente ciclo 24. Para discernir el tipo de incremento de partículas solares que ocurren durante el presente Ciclo Solar, basamos nuestro trabajo en diferentes bases de datos de Monitores de Neutrones, datos del catálogo de satélites SOHO y catálogos SEP. Esto nos lleva a recomendar una re-conceptualización del tipo de eventos involucrados.

Estatus: Aceptado para publicación.

An alternative classification of solar particle events that reach the earth ground level

Abstract

There is currently a controversy in the literature about the denomination of Energetic Solar Protons, which are usually designated as Ground Level Enhancements (GLE), Sub-GLE or simply Solar Energetic Particles (SEP). Such classifications depend on the nature of a given event behavior. There is some criteria discrepancy among different authors that we have pointed out in the first part of this work. In order to unify criteria, here we carry out an analysis of several data bases and different catalogs of particle events. We observe that there is some discrepancy in the conceptualization of events in the specialized literature, and we hereby propose a reconceptualization in the sense that all GLE fulfill the criteria given in the literature to be considered as GLE, even those that have been classified recently as Sub-GLE/GLE for the particular case of the present cycle 24. To discern the kind of solar particle enhancements occurring during the present Solar Cycle, we base our work on different database of NM, data from the SOHO satellite catalogue and SEP catalogs. This leads us to recommend a reconceptualization of the kind of involved events. Our proposal is to name the event according to its date of occurrence, which leads us to avoid renumbering in case of detecting an intermediate event between two others already officially numbered, in the specific case of GLE. We propose, for instance, the following nomenclature: GLE dd/mm/yyyy. Another option is to consider all events that reach the terrestrial level simply as GLE with the first nomenclature just given above, which obviously includes GLE and Sub-GLE.

Keywords: ground level enhancements, sub-gles-seps, diurnal variation

Volume 3 Issue 5 - 2019

J Pérez-Peraza, JC Márquez Adame

Instituto de Geofísica, Universidad Nacional Autónoma de México, Coyoacán, 04510, México, Mexico

Correspondence: J Pérez-Peraza, Instituto de Geofísica, Universidad Nacional Autónoma de México, Coyoacán, 04510, CDMX, Mexico, Email perpera@gmail.com

Received: August 28, 2019 | **Published:** September 05, 2019

Abbreviations: GLE, ground level enhancements; SEP, solar energetic particles; SA, solar activity; GCR, galactic cosmic rays

Introduction

GLE of relativistic solar protons are sporadic phenomena associated with solar flares and are assumed to be of a quasi-random nature. These energetic particles span over most of the earth's latitudes. To a certain extent they follow the time behavior of the 11-year cycle of solar activity (SA); however, they do not follow the intensity of the SA: for instance, solar cycle 22 was much more intense than cycle 23, but the latter had more GLE than cycle 22: there were 13 GLE in the period from July 1989 to June 1991, and not a single event from the end of December of 2006 up until 2012. In principle, only 72 GLE have been officially recorded: the first measurement was on February 28, 1942 (GLE01) and the last one on September 10, 2017 (GLE72). Though the average occurrence rate is ~ 1.05 year⁻¹, their occurrence may stretch at times for almost six years, as was the case between GLE70 and GLE71. GLE are measured at ground level by the worldwide network of Neutron Monitor (MN) detectors spanning over most latitudes and altitudes (from sea level up to high mountains).

The original definition of a GLE is basically the detection of a statistically significant increases of particles of solar origin in counting rates, in common times, and at least in two neutron monitor stations located in different places, at high latitudes, and one/two low or middle latitudinal stations. This definition is accepted by quite a number of scientists, however, since the decade of the 70s. In fact, all GLE since 1942 have had significant increases in some stations at sea level (<300m).

This definition was proposed by the community of cosmic rays in the 1970s, when there was only one station at high latitudes and

altitudes (South Pole). With the installation of another station at high latitudes and altitudes (DOMC/DOMB), for weak events, the conditions of the original definition could be given without requiring any station at sea level to detect the increase. According Miroshnichenko¹ if particles are recorded by spacecrafts in the Earth's orbit, with no clear evidence of penetration at the earth ground level, these are conventionally designated as SEP (Solar Energetic Particles) events.

In the current solar cycle there were a great number of notably weak events, which caused great confusion in designating them as GLE, thus giving them a suitable nomenclature. Recently, a new kind of GLE has been defined, the so called *Sub-GLE* events^{2,3} which differ from the GLE definition in that no statistically significant enhancement in the count rates of NM at the sea level (>300 m) is required, in which case the count rate must be registered by at least two different located high-altitude NM station.

In the course of solar cycle 24, only two GLE have been "formally" recognized; one is that of May, 17 2012, the so called GLE71,⁴⁻¹⁹ and the second one is the GLE of September 10, 2017, that has been "formally" designated as GLE72 by many authors Tassev et al.,²⁰⁻²² However, there are some authors who claim that the GLE72 corresponds to the 06 January, 2014 event Augusto et al.,²³⁻²⁶ as can be observed in Table 1 there is a high discrepancy in the nomenclature assigned to the same event. For instance, Augusto et al.,²⁷ have designated GLE73 the event of October 29, 2015. Table 1 shows the high dispersion in the classification of different authors for a given event. In view of such a discrepancy of nomenclatures as can be seen in Table 1, our goal in this work is to attempt to elucidate the real nature of each event and to propose a more easily manageable reclassification on the basis of specific conditions.

Methodology

As can be seen in Table 1, there is a wide conception of a given event according to the different authors. In view of these discrepancies, an exhaustive analysis was made of all the events treated in the literature for the solar cycle 24, Table 1. This implies a reclassification of the concept of a GLE. Such a reclassification considers to some extent some of the conditions previously established in the literature:^{3,16}

I. A GLE event is registered when there are near-time coincident and statistically significant enhancements of the count rates of at least two differently located neutron monitors including at least one neutron monitor near sea level and a corresponding enhancement in the proton flux measured by a space-borne instrument(s).

II. A sub-GLE event is registered when there are near-time coincident and statistically significant enhancements of the count rates of at least two differently located high-elevation neutron monitors and a corresponding enhancement in the proton flux measured by a space-borne instrument(s), but no statistically significant enhancement in the count rates of neutron monitors near sea level.

We begin for analyzing which of the studied events coincided with an appreciable overlap effect of Diurnal Variation during one or two days before the beginning of each event. This was done on basis to the database www.nmdb.eu. We found that only two events where all stations were strongly affected by the Diurnal Variation March 13, 2012, and the event of 18 April 2018. Consequently, no increment at ground level can be perceived; though some authors claim to have perceived them as a possible Sub-GLE/GLE.^{28,19}

Table 1 Events of cycle 24, and their classification according different authors

Event	Author or database	Observations
January 23, 2012	Bazilevskaya, et al., ³² Gopalswamy et al., ²⁶ Li et al., ¹³ Makumoto et al., 2013	SEP
	This work based in www.nmdb.eu	No discernible enhancement
January 27-28, 2012	Bazilevskaya, et al., ³⁵ Gopalswamy et at., ³⁴ Li et al. ^{12,13}	SEP
	Augusto et al., ²³	"almost" GLE
	Belov et al., ²⁸	possible GLE
	Velinov et al., ²⁹	Contender for GLE
	GLE database University of Oulu	Sub-GLE
	This work based in www.nmdb.eu (Figure 1a: INVK, NAIN, THUL, SOPO, SOPB, MRNY, TERA, MCMU, MXCO, NEWK, FSMT)	Discernible enhancement
March 7, 2012	Augusto et al., ²⁷ Bazilevskaya, et al., ³⁵ Gopalswamy et al., ²⁶ Li et al., ^{12,13} Ding et al., ³³	SEP
	Belov et al., ²⁸	possible GLE
	Velinov et al., ²⁹	Contender for GLE
	GLE database University of Oulu: Mishev et al., ¹⁶	Sub-GLE
	This work based in www.nmdb.eu (Figure 1b: KERG: APTY, SOPB, SOPO, TERA, MCMU, MXCO, ARNM, NANM, AATB, ROME, BKSJ, JUNG1, LMK5, IRKS, IRKT, MOSC, KIEL, KIEL2, YKTK)	Discernible enhancement
March 13, 2012	Bazilevskaya et al., ³² Gopalswamy et al., ²⁶ Li et al., ¹³	SEP
	Belov et al., ²⁸	possible GLE
	Velinov et al., ²⁹	Contender for GLE
	This work based in www.nmdb.eu (Figure 1c: THUL, SOPB, SOPO, TERA, MCMU, MXCO, NEWK, FSMT, NAIN, INVK)	Discernible enhancement
May 17, 2012	Augusto et al., 2013, Asvestari et al., ⁴ Balabin et al., ^{6,24} Berrilli et al., 2014 Firoz et al., ⁸ Gopalswamy et al., ^{9,25,26} Krastova and Sdobnov et al., ¹⁰ Li et al., 2013, 2015, 2016 Mishev et al., ^{15,16} Papaioannou et al., ¹⁷ Perez-Peraza et al., 2018, Plainaki et al., ¹⁸ Thakur et al., ²⁶ Velinov et al., ²⁹ The IceCube Collaboration et al., ¹⁹ Kühl et al., 2015 GLE database University of Oulu; This work based in www.nmdb.eu	GLE 71
	Bazilevskaya et at., ³²	SEP
	Belov et al., ²⁸ Ding et al., ²³ Thakur et al., ²⁶	GLE
July 23, 2012	Gopalswamy et at., ⁹	Small GLE
	This work based in www.nmdb.eu	No discernible enhancement
May 22, 2013	Gopalswamy et al., ²⁶ ; Li et al., ¹⁶	SEP
	This work based in www.nmdb.eu	No discernible enhancement

Table Continues...

Event	Author or database	Observations
January 6, 2014	Augusto et al., ²³ Balabin et al., 2015 Gopalswamy et al., ^{25,26} Krastsova and Sdobnov, 2017; Kühl et al., 2015; Velinov et al., 2016 The IceCube Collaboration et al., ¹⁹	GLE 72
	Li et al., ¹⁶ Thakur et al., ^{25,26}	GLE 72 (Small OLE)
	Belov et al., 2015	GLE
	GLE database University of Oulu; Mishev et al., ³	Sub-GLE
	This work based in www.nmdb.eu (Figure 1 d): APTY, SOPB, SOPO, MCMU, OULU, MWSN	Discernible enhancement
January 7, 2014	Li et al., ¹⁶	SEP
	This work based in www.nmdb.eu	No discernible enhancement
April 18, 2014	Augusto et al., ²³	Favorable conditions for the formation of a GLE
	This work based in www.nmdb.eu (Figure 1e: MXCO, NEWK, PWNK, MWSN, SOPO, SOPB, NAIN)	Discernible enhancement
November 1, 2014	Augusto et al., ²¹	Signals at ground level of relativistic solar particles
	This work based in www.nmdb.eu (Figure 1f: SOPO, SOPB, MCMU, NAM, PWNK)	Discernible enhancement
June 07, 2015	Gil et al., ³⁰	ACRE (Anisotropic Cosmic-Ray Enhancement)
	GLE database University of Oulu	Sub-GLE
	This work based in www.nmdb.eu (Figure 1g: SOPB, SOPO, TERA, MCMU, NEWK, PWNK)	Discernible enhancement
October 29, 2015	Augusto et al., ²³ The IceCube Collaboration et al., ¹⁹	GLE 73
	Velinov et al., ²⁹	—
	GLE database University of Oulu; Mishev et al., ³	Sub-GLE
	This work based in www.nmdb.eu (Figure 1b: JUNG, KERG, TXBY, MWSN, SOPB, SOPO, KIEL)	Discernible enhancement
September 10, 2017	Augusto et al., ²¹ Kurt et al., 2018 Tassev et al., ²⁰ ; GLE database University of Oulu; This work based in www.nmdb.eu	GLE 72
August 26, 2018	GLE database University of Oulu	Sub-GLE
	Gil et al., 2018	Possible ACRE
	This work based in www.nmdb.eu (Figure 2: TSMB, HRMS, MOSC, ICEFtG, OULU, APTY, NAIN, THUL, SOPB, SOPO, MRNY, MEN, AATB, ROME, BKSJ, JUNGt, LMKs, IRKT)	Discernible enhancement

Results

In the case of events of 27 January, 2012, 07 March, 2012, 6 January 2014, 1, November, 2014 and 29 October, 2015, a number of stations were not totally masked by the Diurnal Variation, as we will mention later. These events that were partially affected by Diurnal Variation. For all these events we analyzed the relative increase of particles with respect to the Background of Galactic Cosmic Rays (GCR), two hours before the events were detected, as indicated in Table 2 and Figure 1. Also, as we mention before we consider the information two days before the event in order to determine the intensity of the Diurnal Variation. An interesting analysis of the event of 07 June 2015 indicates that this is an anisotropic cosmic ray enhancements of the type ACRE.³⁰ They also argue that the event of 26 August, 2018 is most probably also an ACRE. Obviously, in these cases there are not associated flares nor increases of particles in the satellites detectors (Figure 1g).

For each event, the relative increase with respect to the GCR background was obtained, considering a range of two hours prior to the event. It can have been observed in Figure 1 that the start of the

associated SEP event to the ground level enhancement is substantially similar with the start of particle enhancement at the level of satellite data, (Table 3) and (Figure 1). In view that the determination of the start of the GLE is not easy, mainly when there is an overlapping Diurnal wave we have considered the associated SEP start time. Note that Figure 1 refers to the satellite-level count which excludes Diurnal Variation, while Figure 2 refers to the count rate at the terrestrial level where sometimes the Diurnal Variation is intense enough to mask small increments of particles solar, of the type that took place in Solar Cycle 24, as the events that occurred on March 13, 2012 and April 18, 2014 (Table 2).

Taking into a count the ample discrepancy in the classification and the corresponding dates as exposed in Table 1, we proceeded to a new reclassification on the basis of the existing database. For the events of January 27, 2012, March, 2012, 6 January 2014, 1, November, 2014 and 29 October, 2015 (Figure 2) we have the following analysis: for each event, the relative increase with respect to the GCR background was analyzed, considering a range of two hours prior to the event (Figure 1). The five selected events, (Table 2), were chosen because they meet the above mentioned criteria 2.I.

Table 2 Summary of stations that distinguished particle increment in spite of the Diurnal Variation

Event	Station that distinguished the event
27/01/2012	THUL, SOPB, SOPO, FSMT
07/03/2012	KERG, SOPB, SOPO, MCMU, MXCO, BKSJ
13/03/2012	All stations were affected by the diurnal wave
06/01/2014	SOPB, SOPO, OULU, MWSN
18/04/2014	All stations were affected by the diurnal wave
01/11/2014	SOPB, SOPO
07/06/2015	ACRE ³⁰
29/10/2015	TXBY, SOPB, SOPO
26/08/2018	Possible ACRE ³⁰

(<https://www.ngdc.noaa.gov/stp/satellite/goes/doc/SPE.txt>; <https://umbra.nascom.nasa.gov/SEP/>)

Table 3 SEP corresponding to selected events from Table 2

Year	Particle event			Associated CME, FLARE, and active region				
	Start (Day/UT)	Maximum (Day/UT)	Proton Flux (pfu @ >10 MeV)	CME	Maximum (Day/UT)	Importance (X ray/Opt)	Location	NOAA SEC Region No.
2012	Jan 27/1905	Jan 28/0205	796	Halo NW/27 1827	Jan 27/1837	X1/1F long duration	N27W71	I1402
2012	Mar 07/0510	Mar 08/1115	6530	Halo NF/07 0036	Mar 07/0024	X5/3B	N17E15	I1429
2012	Mar 13/1810	Mar 13/2045	469	Halo NW/13 1736	Mar 13/1741	M7	N18W62	I1429
2014	Jan 06/0915	Jan 09/0340	1033	Asymm. Partial Halo SW/07 1824	Jan 07/1832	X1/2N	S15W11	I1944
2014	Apr 18/1525	Apr 19/0105	58	CME (C3)/181325	18/1303	M7	S16W41	I2036
2014	Nov 01/1400	N/A	N/A	N/A	N/A	C2.7-class flare	southeastern region	N/A
2015	Oct 29/0550	Oct 29/1000	23	Far-sided on W limb, S11/29 0236	(Farside)	N/A	N/A	I2434

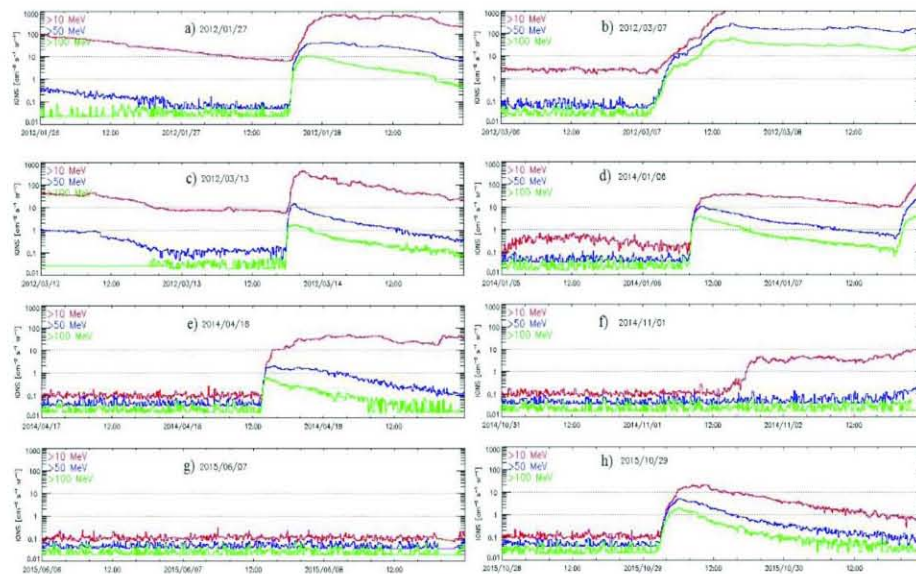


Figure 1 Integral Flux for each event (SOHO LASCO CME CATALOG: https://cdaw.gsfc.nasa.gov/CME_list/).

Citation: Pérez-Peraza J, Adame JCM. An alternative classification of solar particle events that reach the earth ground level. *Phys Astron Int J.* 2019;3(5):163–170. DOI: 10.15406/paij.2019.03.00177

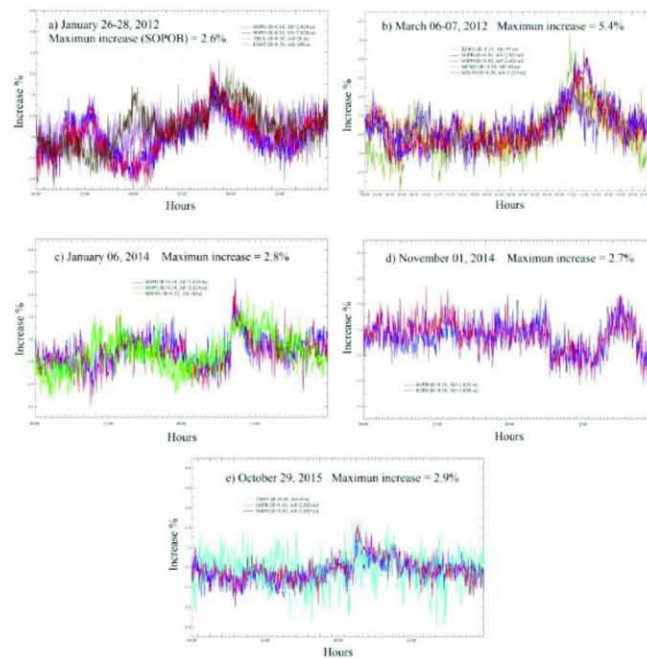


Figure 2 Increments obtained for potential GLEs or Sub-GLEs selected from table I, based on the data of the worldwide network of Neutron Monitors (www.nmdb.eu).

January 27, 2012

Figure 2a shows the relative rate of increase from the count to every 5 minutes of the SOPB, SOPO, THUL and FSMT stations for the days 26-28 January 2012, normalized to the count interval from 5:00 to 7:00 UT of the GCR background of January 27, 2012 (Table 2) and (Figure 1a), which indicate the start of the event. As we observed in Figure 2a, in these stations a certain effect of Diurnal variability is observed, however, it is possible to clearly distinguish the relative increment of the event. Applying the criteria indicated in:^{3,16}

- I. The event was detected by spatial instruments at 19:05 UT from the flare of class X1/1F (N27W71) (Table 2).
- II. The event was detected at the South Pole station (SOPB and SOPO) of high latitude and altitude.
- III. The event has been seen at the THUL and FSMT stations, both of high latitude, but of altitude at mean sea level (<300 m mid-level sea).
- IV. Due to these criteria this event is classified as a **GLE** (According to 2.I).

March 7, 2012

Figure 2b shows the relative rate of increase from the count to every 5 minutes of the SOPB, SOPO, KERG, MCMU and MXCO stations for the days 06-07 March 2012, normalized to the counting interval of 03:00–05:00 UT of the GCR background of March 7, 2012 (Table 2) and (Figure 1b), which indicate the start of the event. As we observe in Figure 2b in these stations, no effect of Diurnal variability is observed and it is clearly distinguished the relative increase of the event without any doubt. Applying the criteria indicated in: Poluianov et al.,^{3,16}

- I. The event was detected by spatial instruments at 05:10 UT from the flare class X5 / 3B (N17E15) (see Table 2).
- II. The event was detected at the South Pole station (SOPB and SOPO) of high latitude and altitude.
- III. The event has been seen at the KERG and MCMU stations, both at altitude at mean sea level (<300 m mid-level sea).
- IV. The event was detected at the low latitude and high altitude MXCO station.
- V. Due to these criteria this event is classified as **GLE** (According to 2.I).

January 6, 2014

Figure 2c shows the relative rate of increase from the count to every 5 minutes of the SOPB, SOPO and MWSN stations for the days 05-06 January 2014, normalized to the counting interval of 07: 00-09: 00 UT of the GCR background of January 06, 2014 (Table 2) and (Figure 1d), which indicate the start of the event. As we observe in the Figure in these stations a slight effect of daytime variability is observed from the day before the event, however, it is possible to clearly distinguish the relative increase of the event without any doubt. Applying the criteria indicated in: Poluianov et al.,^{3,16}

- I. The event was detected by spatial instruments at 09:15 UT from the flare class X1/2N (S15W11) (Figure 1d) and (Table 2).
- II. The event was detected at the South Pole station (SOPB and SOPO) of high latitude and altitude.
- III. The event has been seen at the MWSN station, of high latitude, but of altitude at mean sea level (<300 m mid-level sea).

IV. Due to these criteria this event would be classified as **GLE** (According to 2.I).

November 1, 2014

Figure 2d shows the relative increase rate from the count to every 5 minutes of the SOPB, SOPO stations for the days 10-11 November 2014, normalized to the counting interval of 11:00-13:00 UT of the background of GCR of November 01, 2014 according to Table 2 and Figure 1f, which indicate the start of the event. As we observe in the figure in these stations no effect of Diurnal variability is observed, however, there is a systematic drop in the count approximately at 07 UT on November 1, later it is possible to distinguish the relative increase of the event. Applying the criteria indicated in: Poluianov et al.,^{3,16}

- I. The event was detected by spatial instruments at 14:00 UT from the flare class C2.7 (Southeastern region) (Figure 1f) and (Table 2)
- II. The event was detected at the South Pole station (SOPB and SOPO) of high latitude and altitude.
- III. The event was not detected by any other station.
- IV. Since both monitors (SOPB and SOPO) are in the same station, the criteria for classifying the event as a possible GLE (as assumed by Augusto et al.,³¹) are not met, whereas according to this work only can be classified as a **SEP**.

October 29, 2015

Figure 2E shows the relative increase rate from the count to every 5 minutes of the SOPB, SOPO and TXBY stations for the days 28-29 October 2015, normalized to the counting interval from 04: 00-05: 00 UT of the GCR background of October 1, 2015 according to Table 2 and Figure 1H, which indicate the beginning of the event. The noise behavior of the TXBY station could indicate probable affectation due to the daytime variability, while the monitors of the South Pole station do not show this affectation. Applying the criteria indicated in: Poluianov et al.,^{3,16}

- I. The event was detected by spatial instruments at 05:50 UT whose source was apparently a CME (Figure 1H) and (Table 2).
- II. The event was detected at the South Pole station (SOPB and SOPO) of high latitude and altitude.

III. The event has been seen at the TXBY station, of altitude at the mean sea level (<300 m mid-level sea).

IV. In our opinion these events can be classified as **GLE** (According to 2.I).³²⁻³⁶

Conclusion

On the basis to criteria popular in the scientific community we have made an analysis of all Solar Particle events (of any kind) that have taken place during cycle 24 as is shown in Table 1. Basically, what we have done in the present work consists of an exhaustive revision of all the events that have been reported in the literature related to the solar cycle 24. We have found 15 events which appear in Table 1: the first column contains the date of the studied event, the second column displays the data source, and/or the corresponding authors, and finally the third column indicates the kind of event, as has been assigned by each of the authors. It is precisely in these two columns where the conflict in the classification of the events as reported by the different authors, can be appreciated. In virtue of this, we have proceeded to carefully examine the information regarding the particle counting rate in the available data basis existing for this purpose: (www.nmdb.eu, GLE Database University of OULU and Databases of neutron monitors of McMurdo, Mirny and Kiel; data from the SOHO satellite catalogue and SEP catalogs).

Basically, our study consists in making sure that a ground level enhancement really existed. Of the above, procedure we have selected nine events that presumable have shown a possible increment (Table 2). Among these nine events, two of them are not solar particle enhancements (the so called ACRE) and other two are indiscernible due to the effect of Diurnal Variation. After confirming the enhancements of the other five events, we proceed to identify the generator SEP of each event (Figure 1) and (Table 3) in order to reclassify each one of the five selected events (Table 4) on basis to the criteria established in section 2 Poluianov et al.,^{3,16} According to our results (Table 4), it can be observed that we are demonstrating that there are two GLE events which occurred between the officially accepted GLE70 and GLE71 (January 27, 2012 and March 13, 2012), as well as two between the GLE71 and the GLE72 (January 6, 2014 and October 29, 2015); which comply with the established criteria to be considered as GLE, which leads us to claim that the nomenclature of GLE events carried out to date, based on consecutive numbering is not adequate. This was made clear by the significant number of relatively weak events that occurred in the mentioned solar cycle between GLE70 and GLE72.

Table 4 Reclassification of the category of events

Event	Author or database	Previous class	Station [R(GV),ALT(m)]	Reclassification
January 27-28, 2012	Bazilevskaya et al., ³² Gopalswamy et al., ²⁶ Li et al., ^{12,13}	SEP	SOPB(R=0.10,Alt=2820m), SOPO(R=0.10,Alt=2820m), THUL(R=0.30,Alt 26m), FSMT(R=0.30,Alt=180m)	GLE
	Augusto et al., ²³	"almost" GLE		
	Belov et al., ²⁸	possible GLE		
	Velinov et al., 2016	Contender for GLE		
	GLE database University of Oulu	Sub-GLE		
	This work based in www.nmdb.eu (Figure 1a)	Discernible enhancement		

Table Continues...

Event	Author or database	Previous class	Station [R(GV),ALT(m)]	Reclassification
March 7, 2012	Augusto et al., ²³ Bazilevskaya, et al., 2013 Gopalswamy et al., ²⁶ Li et al., ^{12,13} Ding et al., ³³	SEP	KERG(R=1.14,Alt=33m), SOPB(R=0.10,Alt=2820m), SOPO(R=0.41.10,Alt=2820m), MCMU(R=0.30,Alt=48m) MXCO(R=8.28,Alt=2274m)	GLE
	Belov et al., ²⁸	possible GLE		
	Velinov et al., 2016	Contender for GLE		
	GLE database University of Oulu; Mishev et al., ³	(R41•30 Alt=48m), Sub-GLE		
	This work based in www.nmdb.eu (Figure 1b)	Discernible enhancement		
January 6, 2014	Augusto et al., ²³ Balabin et al., 2015 Gopalswamy et al., ^{25,26} Kratsova and Sdobnov, 2017; Kühn et al., 2015; Velinov et al., 2016 The IceCube Collaboration et al., ¹⁹	GLE 72	SOPB(R=0.10,Alt=2820m), SOPO(R=0.10,Alt=2820m), MWSN(R=0.22,Alt=30m)	GLE
	Li et al., ¹² Thakur et al., ^{25,26}	GLE 72 (Small GLE)		
	Belov et al., ²⁸	GLE		
	GLE database University of Oulu; Mishev et al., ³	Sub-GLE		
	This work based in www.nmdb.eu (Figure 1c)	Discernible enhancement		
November 1, 2014	Augusto et al., ³¹	Signals at ground level of relativistic solar particles	SOPB(R=0.10,Alt=2820m), SOPO(R=0.10,Alt=2820m)	SEP
	This work based in www.nmdb.eu (Figure 1d)	Discernible enhancement		
October 29, 2015	Augusto et al., ²³ The IceCube Collaboration et al., ¹⁹	GLE 73	TXBY(R=0.48,Alt=0m), SOPB(R=0.10,Alt=2820m), SOPO(R=0.10,Alt=2820m)	GLE
	Velinov et al., 2016	Contender for GLE		
	GLE database University of Oulu; Mishev et al., ³	Sub-GLE		
	This work based in www.nmdb.eu (Figure 1e)	Discernible enhancement		

In our detailed analysis of all solar particle events of solar cycle 24, we observe the confusion existing between different authors; which generates a great discrepancy regarding the consideration of such events as GLE or not, as well as their nomenclature. In this paper we classify, based on precise criteria (Section 2), 4 events as GLE, which leads us to indicate that the consecutive numbering method for GLE events is not adequate. Our proposal is to name the event according to its date of occurrence, which leads us to avoid renumbering in case of detecting an intermediate event between two others already officially numbered, in the specific case of GLE. We propose, for instance, the following nomenclature: GLE dd/mm/yyyy. Another option is to consider all events that reach the terrestrial level simply as GLE with the first nomenclature just given above, which obviously includes GLE and Sub-GLE; entailing that the Sub-GLE can not necessarily be seen by stations near sea level; while a 100% of the GLE up to now have been registered at least by one station near sea level (including the four GLE of Table 4 that have been seen in at least one station at the sea level). On the other hand, in view that both of these two types have a SEP counterpart, in reality there is not a sharp distinction between them. In summary, according to our study, small and intensive events that come to earth could be considered all them as GLE.

Acknowledgments

We acknowledge the NMDB database (www.nmdb.eu), founded under the European Union's FP7 programme (contract no. 213007) for providing data. The neutron monitors data from Oulu, Mirny, McMurdo and Kiel for providing data. We acknowledge the U.S. Dept. of Commerce, NOAA, Space Weather Prediction Center for GOES and SEP data. Data regarding Figure 1 can be found in <https://drive.google.com/open?id=1iVGJ6RffHpuccM57kdjCPp-KcQeBRNrP>. We acknowledge to INSTITUTO DE GEOFISICA of the UNIVERSIDAD NACIONAL AUTONOMA DE MEXICO for economic support.

Conflicts of interest

The author declares there is no conflict of interest.

References

- Miroshnichenko LI. *Solar cosmic rays: Fundamentals and applications*. 2nd edn. Switzerland: Springer. 2014. p. 521.
- Atwell W, Tylka AJ, Dietrich W, et al. *Sub-GLE Solar Particle Events and the Implications for Lightly-Shielded Systems Flown During an Era of Low Solar Activity*. 45th International Conference on Environmental Systems, 12-16 July 2015, Bellevue, WA, ICES-2015-340. 2015. p. 1-15.

3. Poluianov SV, Usoskin IG, Mishev AL, et al. GLE and Sub-GLE Redefinition in the Light of High-Altitude Polar Neutron Monitors. *Solar Phys.* 2017;292:176.
4. Asvestari ET, Willamo A, Gil IG, et al. Analysis of ground level enhancements (GLE): Extreme solar energetic particle events have hard spectra. *Advances in Space Research.* 2017;60(4):781–787.
5. Augusto CRA, Kopenkin V, Navia CE, et al. Was the GLE on May 17, 2012 Linked with the M5.1-Class Flare the First in the 24th Solar Cycle?, *arXiv:1301.7055v1.* 2013.
6. Balabin YV, Germanenko AV, Vashenyuk EV, et al. *The first GLE of the new 24th solar cycle.* Proc. 33rd Int. Cosmic Ray Conf., Rio de Janeiro, Brazil, paper ICRC 2013-0021. 2013. p. 1–3.
7. Berrilli F, Casolino M, Del Moro D, et al. The relativistic solar particle event of May 17th, 2012 observed on board the International Space Station. *Weather and Space Climate.* 2014;4:A16.
8. Firoz KA, Gan WQ, Li YP, et al. An interpretation of a possible mechanism for the first ground-level enhancement of solar cycle 24. *Solar Physics.* 2014;290:613–626.
9. Gopalswamy N, Xie H, Akiyama S, et al. The First Ground Level Enhancement Event of Solar Cycle 24: Direct Observation of Shock Formation and Particle Release Heights. *The Astrophysical Journal Letters.* 2013;765:L30:5.
10. Kravtsova MV, Sdobnov VE. Ground Level Enhancements of Cosmic Rays in Solar Cycle 24. *Astronomy Letters.* 2017;43(7):501–506.
11. Kühn P, Banjac S, Dresing N, et al. Proton intensity spectra during the solar energetic particle events of May 17, 2012 and January 6, 2014. *A&A.* 2015;576:A120.
12. Li C, Kazi A, Firoz L, et al. Electron and proton acceleration during the first ground level enhancement event of solar cycle 24. *Astrophysical Journal.* 2013;770(1):34.
13. Li C, Miroshnichenko LI, Fang C. Proton activity of the Sun in current solar cycle 24. *Research in Astronomy and Astrophysics.* 2015;15(7):1036–1044.
14. Li C, Miroshnichenko LI, Sdobnov VE. Small Ground-Level Enhancement of 6 January 2014: Acceleration by CME-Driven Shock?. *Solar Phys.* 2016;291(3):975–987.
15. Mishev AL, Kocharov LG, Usoskin IG. Analysis of the ground level enhancement on 17 May 2012 using data from the global neutron monitor network. *Journal of Geophysical Research: Space Physics.* 2014;119(2):670–679.
16. Mishev A, Poluianov S, Usoskin I. Assessment of spectral and angular characteristics of sub-GLE events using the global neutron monitor network. *J Space Weather Space Clim.* 2017;17:A28.
17. Papaioannou A, Souvatzoglou G, Paschalis P, et al. The First Ground-Level Enhancement of Solar Cycle 24 on 17 May 2012 and Its Real-Time Detection. *Solar Phys.* 2013;289(1):423–436.
18. Plainaki C, Mavromichalaki H, Laurenza M, et al. The ground-level enhancement of 2012 May 17: Derivation of solar proton event properties through the application of the NMBANGLE PPOLA model. *The Astrophysical Journal.* 2014;785(12):160.
19. The IceCube Collaboration, Manganard PS, Muangha P, et al. *GeV Solar Energetic Particle Observation and Search by IceTop from 2011 to 2016.* 35th International Cosmic Ray Conference - ICRC2017, 10–20 July, 2017, Bexco, Busan, Korea. 2017.
20. Tassev Y, Velinov PIY, Tomova D. Analysis of Extreme Solar Activity in Early September 2017: G4–Severe Geomagnetic Storm (07–08.09) and GLE72 (10.09) in Solar Minimum. *Comptes rendus de l'Acad'emie bulgare des Sciences.* 2017;70(10).
21. Augusto CRA, Navia CEMN de Oliveira, Nepomuceno AA, et al. Relativistic Proton Levels from Region AR 12673 (GLE #72) and the Heliospheric Current Sheet as a Sun-Earth Magnetic Connection. *Astronomical Society of the Pacific.* 2018.
22. Kurt V, Belov A, Kudela K, et al. Some characteristics of the GLE on 10 September 2017, *Contrib. Astron. Obs Skalná'e Pleso.* 2018;48:329–338.
23. Augusto CRA, Navia CE, de Oliveira MN, et al. Ground level observations of relativistic solar particles on Oct 29th, 2015: Is it a new GLE on the current solar cycle ?, *Astrophysics Solar and Stellar Astrophysics.* 2016.
24. Balabin YV, Germanenko AV, Gvozdevsky BBI. Analysis of the Event GLE72 of 6 January 2014; *Journal of Russian Academy of Sciences. Series Physical.* 2015;79(5):612–614.
25. Gopalswamy N, Yashiro S, Thakur N, et al. The 2012 July 23 Backside Eruption: an Extreme Energetic Particle Event?, *The Astrophysical Journal.* 2016;833:216:20.
26. Thakur N, Gopalswamy N, Xie H, et al. Ground Level Enhancement in the 2014 January 6 Solar Energetic Particle Event. *The Astrophysical Journal Letters.* 2014;790:L13L5.
27. Augusto C, Navia C, de Oliveira MN, et al. Signals at ground level of relativistic solar particles associated with a radiation storm on 2014 April 18. *Publ Astron Soc Japan.* 2016;68(1):8(1–12).
28. Belov AV, Eroshenko EA, Kryakunova ON, et al. Possible Ground Level Enhancements of Solar Cosmic Rays in 2012, ISSN 1062. 8738. *Bulletin of the Russian Academy of Sciences Physics.* 2015;79(5):561–565.
29. Velinov P. *Extended Categorisation of Ground Level Enhancements (GLEs) of Cosmic Rays Due to Relativistic Solar Energetic Particles.* Bulgarian Academy of Sciences. Space Research and Technology Institute. Aerospace Research in Bulgaria. 28, 2016, Sofia. 2016.
30. Gil A, Kovaltsov GA, Mikhailov VV, et al. An Anisotropic Cosmic-Ray Enhancement Event on 07-June-2015: A Possible Origin. *Solar Phys.* 2018;293:154.
31. Augusto CRA, Navia CE, de Oliveira MN, et al. Signals at ground level of relativistic solar particles associated to the All Saints' filament eruption on 2014. *arXiv:1507.03954v1.* 2015;1–13.
32. Bazilevskaya GA, Mayorov AG, Malakhov VV, et al. Solar energetic particle events in 2006-2012 in the PAMELA experiment data. *Journal of Physics: Conference Series.* 2013;409:012188.
33. Ding LG, Cao XX, Wang ZW, et al. Large solar energetic particle event that occurred on 2012 March 7 and its VDA analysis. *Research in Astron Astrophys.* 2016;0(200x):No.0, 000–000.
34. Gopalswamy N, Xie H, Akiyama S, et al. Major solar eruptions and high-energy particle events during solar cycle 24. *Earth Planets and Space.* 2014;66:104.
35. Makhmutov VS, Bazilevskaya GA, Stozhkovy YI, et al. *Solar proton event on January 23, 2012.* 33RD International Cosmic Ray Conference, Rio de Janeiro 2013, The Atroparticle Physics Conference. 2013. p. 1–4.
36. Pérez-Peraza J, Márquez-Adame JC, Miroshnichenko L, et al. Source Energy Spectrum of the 17 May 2012 GLE. *Journal of Geophysical Research: Space Physics.* 2018;123(5):3262–3272.

DISCUSIÓN Y CONCLUSIONES GENERALES

Con respecto a las secciones del Marco Teórico y de Resultados podemos considerar lo siguiente:

En el Capítulo en libro (Pérez-Peraza & JC Márquez-Adame, 2018) los espectros de energía en estado estacionario se trabajaron de forma independiente para los diferentes casos (aceleración, compresión y expansión adiabática, desaceleración por colisiones coulombianas y p-p), posteriormete se sumarizaron varias combinaciones y de ahí se obtuvieron los parámetros de la fuente de producción de las partículas solares relativistas, así como el tipo de evento (caliente, cálido o frío). En el Marco Teórico en el punto 6 desarrollamos la solución a la ecuación de transporte (3) por medio de la aproximación WKBJ a partir de la cual obtenemos el espectro de energía dependiente del tiempo para turbulencia MHD, con inyección monoenergética, deceleración adiabática, deceleración por pérdidas colisionales y deceleración por degradación energética por colisiones protón-protón, Ec. 12, en este caso en una sola solución incluimos todos los casos anteriormente citados. Enseguida mencionamos las más importantes consideraciones y resultados obtenidos:

- Los tiempos para los ajustes teóricos por medio de la aproximación WKBJ se consideraron a $t > 10$ s, para ser acordes a las soluciones estacionarias dadas en el estudio inicial correspondiente al capítulo en libro (Pérez-Peraza & JC Marquez-Adame, 2018).
- La curva resultante de la solución teórica por medio de la aproximación WKBJ se ajusta mejor al espectro observacional en los 12 eventos trabajados.
- El parámetro de aceleración (α) en el estudio original toma un valor diferente para cada tipo de ajuste por evento, en cambio en la Ec 12, al igual que los demás parámetros (n , ρ , T , t , τ , etc.) son valores únicos por ajuste y por evento, en donde encontramos que los valores de aceleración (α) obtenidos con la aproximación WKBJ son del orden de los obtenidos en el Capítulo en libro (Pérez-Peraza & JC Márquez-Adame, 2018) para cada evento.
- Para el parámetro de la temperatura (T) también obtenemos congruencia entre ambos estudios.
- La solución de la ecuación de transporte (3) por medio de la aproximación WKBJ nos da por resultado un **modelo unificado** para el estudio de los espectros de energía observacionales de los GLEs, a partir de su modelación teórica y de esta forma obtener los parámetros en la fuente de producción de las partículas solares relativistas.
- El presente método nos provee de suficientes parámetros libres, lo cual potencia el proceso de ajuste para darnos los escenarios mas plausibles de la producción de partículas solares relativistas en la fuente.

También se ajustaron teóricamente con la Ec. 12 los espectros observacionales de los GLEs 71 y 72 obtenidos por nuestro grupo de trabajo.

Con respecto a los artículos ya publicados y/o aceptados para publicación podemos considerar lo siguiente:

El trabajo aquí presentado se extendió hacia el estudio de tres puntos muy importantes relativos a los incrementos de partículas solares relativistas detectadas a nivel del suelo por la red global de Monitores de Neutrones, los cuales son el estudio de sus espectros de **energía observacionales y teóricos**. A partir de la confrontación de dichos espectros se obtienen los parámetros de la fuente, de esta forma podemos prever posibles escenarios de generación. El siguiente punto importante fue el estudio y confirmación, **del carácter periódico de dichos eventos** y en base a esto se desarrolló un método basado en el análisis de coherencia Wavelet y de Lógica Difusa para su descripción y prognosis. Finalmente se realizó un estudio exhaustivo concerniente a la clasificación y denominación de los eventos GLEs, aplicando los últimos criterios aceptados por la comunidad internacional y proponiendo una nueva nomenclatura basada en su fecha de ocurrencia y no en una numeración consecutiva, para evitar futuras confusiones al respecto.

Debido a que cada trabajo contiene su respectiva sección de conclusiones, aquí resumimos las siguientes conclusiones generales:

- De los 6 trabajos que se están presentando como Tesis Doctoral, los tres primeros tienen que ver con los espectros de energía de los GLE. Los principales resultados a destacar de *“Exploration of Solar Cosmic Ray Sources by Means of Particle Energy Spectra”* (Cosmic Rays, Ed. IntechOpen, 2018, Cap. 7, Pág. 121-161), *“Source Energy Spectrum of the 17 May 2012 GLE”* (JGR: Space Physics, 2017, 10.1002/2017/JA0225030) y *“Spectra of the Two Official GLEs of Solar Cycle 24”* (aceptado para publicación: *Advanced in Space Research*, 2019), son la obtención del conjunto de parámetros de la fuente para la generación de partículas solares relativistas y la descripción de los procesos de aceleración involucrados, que conducen a escenarios plausibles durante los eventos bajo estudio, basados en un marco teórico que abarca la dependencia del tiempo y el estado estacionario en todo el rango de energías. Es precisamente la confrontación de los espectros de energía teóricos contra los espectros de energía observacionales lo que nos da una concepción aproximada de los escenarios de producción. El análisis de los espectros nos lleva a considerar la presencia de dos componentes de partículas diferentes durante los eventos. Algunos autores designan esas dos fases como componentes Prompt (Prompt) y Retardada (Delayed). Estas dos componentes indican la ocurrencia de dos procesos de aceleración de naturaleza diferente, como lo evocan muchos autores. En ambas fases, el principal mecanismo de aceleración es probablemente de naturaleza estocástica, donde el proceso de inyección de partículas al mecanismo estocástico también puede provenir de un flujo de protones monoenergéticos que puede haberse originado en la parte de altas energías de los protones preacelerados en la Lamina Magnética de Corriente Neutra (MNCS por sus siglas en inglés). Sin embargo, en el segundo trabajo se abre otra opción, en donde se podría generar un solo mecanismo de aceleración en dos etapas diferentes en un proceso determinista con un espectro como el que se muestra en la Ecuación 7, de modo que la etapa de aceleración única debido a la MNCS no se puede ignorar. Finalmente, enfatizamos que la confrontación entre los espectros teóricos y observacionales nos da una concepción aproximada de los

escenarios de producción, es decir, de los procesos involucrados de aceleración y pérdida de energía, así como de los parámetros físicos plausibles que prevalecen en la fuente.

- En los trabajos *“The Quasi-Biennial Oscillation of 1.7 years in Ground Level Enhancement Events”* (**New Astronomy, 2018, 60: 7-13**) y *“Determination of GLE of Solar Energetic Particles by Means of Spectral Analysis”* (**The Astrophysical Journal, 878:154 6pp, 2019**) concluimos que queda claramente demostrado el comportamiento periódico en la ocurrencia de los incrementos de partículas solares relativistas a nivel terrestre, GLEs. En este sentido, fuimos capaces de caracterizar con gran precisión el comportamiento armónico de dichos eventos, haciendo uso de los principales índices de la actividad solar: Solar Flare index (FSI), Sunspots Index (SS) y Solar Flux index (F10.7), gracias a la combinación de las técnicas de coherencia Wavelet y de Lógica Difusa, siendo herramientas muy poderosas también para realizar trabajos de prognosis con dichos eventos.

- La peculiaridad de este Ciclo Solar 24 en cuanto a la producción de GLE's débiles conllevó a la redefinición de los criterios para clasificarlos y proponer un nuevo tipo de evento (Sub-GLE), haciendo una revisión exhaustiva de los 15 eventos en controversia encontrados en la literatura, en el trabajo *“An Alternative Classification of Solar Particle Events that Reach the Earth Ground Level”* (**aceptado para publicación: Phys Astron Int J. 2019; 3-5:161–170**), concluimos que solo 4 eventos cumplen con los nuevos requisitos establecidos. En vista de tal controversia proponemos denominar a los eventos GLE por su fecha de ocurrencia y no de manera consecutiva.

Por último, como conclusión general podemos resaltar que la presente Tesis terminó siendo un estudio muy completo acerca de las características de la generación en la fuente de las partículas solares relativistas que arriban a la Tierra y provocan los incrementos a nivel terrestre (GLE) detectados por la red global de Monitores de Neutrones, así como de la ocurrencia, periodicidad, prognosis y nomenclatura de dichos eventos.

REFERENCIAS

- Ackermann, M., Allafort, A., Baldini, L., Barbiellini, G., Bastieri, D., Bellazzini, R., et al. (2017). Fermi-LAT observations of high-energy behind-the-limb solar flares. *The Astrophysical Journal*, 835(2), 219–232.
- Aleksanyan, T. M., Blokh, Y. L., Dorman, L. I. & Starkov, F. (1979). Coupling and barometer coefficients for measurements of cosmic-ray variations at altitudes of 260-400 mb. *Proc. 16th ICRC* 4, 321.
- Alhualia 1971, 12th ICRC, Tasmania, Hobart, p. 468.
- Álvarez-Madrigal, M., Miroshnichenko, L. I., Pérez-Peraza, J., & Rivero-G, F. (1986). Spectrum of solar cosmic rays in the source taking into account their coronal propagation. *Soviet Astronomy*, 66, 1169–1181.
- Asvestari, E. T., Willamo, A., Gil, I. G., Usoskin, G. A., Kovaltsov, V. V., & Mikhailov, A. M. (2017). Analysis of ground level enhancements (GLE): Extreme solar energetic particle events have hard spectra. *Advances in Space Research*, 60, 781–787.
- Ataç T. and Özgüç A., 1998, Flare Index of Solar Cycle 22, *Solar Physics* 180: 397–407.

- Ataç T. and Özgüç A., 2001, Flare Index during the Rising Phase of Solar Cycle 23, *Solar Physics* 198: 399–407.
- Ataç, T., 1987. *Astron. Astrophys. Suppl.* 135, 201.
- Ataç, T., Özgüç, A., 1996. *Solar Phys.* 166, 201.
- Ataç, T., Özgüç, A., 1998. *Solar Phys.* 198, 399.
- Ataç, T., Özgüç, A., 2001. *Solar Phys.* 198, 399.
- Atwell W., Tylka A. J., Dietrich W., Rojdev K., Matzkind C., (2015), Sub-GLE Solar Particle Events and the Implications for Lightly-Shielded Systems Flown During an Era of Low Solar Activity, 45th International Conference on Environmental Systems, 12-16 July 2015, Bellevue, WA, ICES-2015-340, <https://ntrs.nasa.gov/search.jsp?R=20150009484> 2019-01-29T01:42:05+00:00Z
- Augusto, C. R. A., Kopenkin, V., Navia, C. E., Felicio, A. C. S., Freire, F., Pinto, A. C. S., et al. (2013). Was the GLE on May 17, 2012 linked with the M5.1-class flare the first in the 24th solar cycle? ArXiv:1301.7055, *Astroph. SR*.
- Augusto C. R. A., Navia C. E., de Oliveira M. N. and Shigueoka H., Nepomuceno A., Fauth A. C., (2015), Signals at ground level of relativistic solar particles associated to the All Saints" filament eruption on 2014, arXiv:1507.03954v1 [astro-ph.SR]
- Augusto C. R. A., Navia C. E., de Oliveira M. N., Nepomuceno A. A., Fauth A. C., (2016), Ground level observations of relativistic solar particles on Oct 29th, 2015: Is it a new GLE on the current solar cycle ?, arXiv:1603.08863v1 [astro-ph.SR].
- Augusto C., Navia C., de Oliveira M. N., Fauth A., and Nepomuceno A., (2016), Signals at ground level of relativistic solar particles associated with a radiation storm on 2014 April 18, *Publ. Astron. Soc. Japan* (2016) 68 (1), 8 (1–12) doi: 10.1093/pasj/psv111.
- Augusto C. R. A., Navia C. E. M. N. de Oliveira, Nepomuceno A. A., Fauth A. C., Kopenkin V., Sinzi T., (2018), Relativistic Proton Levels from Region AR 12673 (GLE #72) and the Heliospheric Current Sheet as a Sun-Earth Magnetic Connection, Article in Publications of the Astronomical Society of the Pacific, arXiv:1805.02678v2 [astro-ph.SR], DOI: 10.1088/1538-3873/aaeb7f.
- Balabin, Y. V., Germanenko, A. V., Vashenyuk, E. V., & Gvozdevsky, B. B. (2013). The first GLE of the new 24th solar cycle, *Proc. 33rd Int. Cosmic Ray Conf.*, Rio de Janeiro, Brazil, paper ICRC 2013-0021.
- Balabin Y. V., Germanenko A. V., Gvozdevsky B. B., Vashenyuk E. V.; (2015); Analysis of the Event GLE72 of 6 January 2014; *Journal of Russian Academy of Sciences. Series Physical*, 2015, Vol. 79, No. 5, p. 612–614; DOI: 10.7868/S0367676515050099.
- Barbosa, D.D. (1979). Stochastic Acceleration of Solar Flare Protons. *ApJ*, 233, 383; DOI: [10.1086/157399](https://doi.org/10.1086/157399).
- Band, D., Matteson, J., Ford, L., Schaefer, B., Palmer, D., Teegarden, B., et al. (1993). BATSE observations of gamma-ray burst spectra. I— Spectral diversity. *The Astrophysical Journal*, 413, 281–292.
- Barcus, J.G. 1969, *Solar Pys.* 8, 186.
- Battarbee, M., Guo, J., Dalla, S., Wimmer-Schweingruber, R., Swalwell, B., & Lawrence, D. J. (2017). Multi-spacecraft observations and transport simulations of solar energetic particles for the May 17th 2012 GLE event, arXiv preprint arXiv: 1706.08458.
- Bazilevskaya, G.A, Charakhchyan, A.N., Charakhchyan, T.N., Lozutin, I.L, 1971,, 12th I.C.R.C., Tasmania 5, 1825
- Bazilevskaya, G., Broomhall, A.M., Elsworth, Y., Nakariakov, V.M., 2014. *Space Sci. Rev.* 186, 359.
- Bazilevskaya, G., Kalinin, M.S., Krainev, M.B., Makhmutov, V.S., Svirzhevskaya, A.K., Svirzhevsky, N.S., Stozhkov, Y.I., 2016. *Cosmic Res.* 54 (3), 171.

- Bazilevskaya G. A., Mayorov A. G., Malakhov V. V., et al., (2013), Solar energetic particle events in 2006-2012 in the PAMELA experiment data, 23rd European Cosmic Ray Symposium (and 32nd Russian Cosmic Ray Conference), IOP Publishing, Journal of Physics: Conference Series 409 (2013) 012188 doi:10.1088/1742-6596/409/1/012188.
- Belov A. V., Eroshenko E. A., Kryakunova O. N., Nikolayevskiy N. F., Malimbayevb A. M., Tsepakinab I. L., and Yanke V. G., (2015), Possible Ground Level Enhancements of Solar Cosmic Rays in 2012, ISSN 1062_8738, Bulletin of the Russian Academy of Sciences. Physics, 2015, Vol. 79, No. 5, pp. 561–565. © Allerton Press, Inc., DOI: 10.3103/S1062873815050147.
- Berrilli F., Casolino M., Del Moro D., Di Fino L., Larosa M., Narici L., Piazzesi R., Picozza P., Scardigli S., Sparvoli R., Stangalini M., and Zacont V. (2014). The relativistic solar particle event of May 17th, 2012 observed on board the International Space Station. *Weather and Space Clim.* 4, A16, DOI: 10.1051/swsc/2014014.
- Bieber, J. W., and Evenson, P. (1991). Determination of Energy Spectra for the Large Solar Particle Events of 1989. *Proc. 22d Int. Cosmic-Ray Conf. (Dublin)*, 3, 129.
- Bieber J. W., Dröge W., Evenson P. A., Pyle R., Ruffolo D., Pinsook U., Tooprakai P., Ujiwarodom M., Khumlumlert T. and Krucker S. (2002). Energetic Particle Observations During the 2000 July 14 Solar Event. *ApJ.* 567:622–634.
- Bieber J. W., Clem J., Evenson P., Pyle R., Sáiz A., and Ruffolo D. (2013). Giant Ground Level Enhancement of Relativistic Solar Protons on 2005 January 20. I. Spacecraft Earth Observations. *ApJ.* 771:92 (13pp).
- Biswas, S and Radhakishnan, B.: 1973, *Solar Phys*, 28, 211.
- Bland, 1966 *Nuovo Cim* 13 427.
- Bombardieri, D. J., Duldig, M. L., Michael, K. J., & Humble, J. E. (2006). Relativistic proton production during the 14 July 2000 solar event: The case for multiple source mechanisms. *Astrophysical Journal*, 644, 565.
- Bombardieri, D. J., Duldig, M. L., Michael, K. J., & Humble, J. E. (2007). Relativistic proton production during the 2001 April 15 solar event. *Astrophysical Journal*, 665, 813.
- Bombardieri, D. J., Duldig, M. L., Michael, K. J., & Humble, J. E. (2008). An improved model for relativistic solar proton acceleration applied to the 2005 January 20 and earlier events. *Astrophysical Journal*, 682, 1315.
- Brazil, paper ICRC 2013-0021.
- Bruzek, A.: 1972, *Solar Phys*, 26, 94
- Bryant, D.A., Cline, T.L., Desai, V.D. and McDonald, F.B., 1965, *ApJ.* 141, 478.
- Bukata, R.P., Gronstal, P.I., Palmeira, R.A.R, McCracken, K.G., Rao, U.R., 1969, *Solar Phys.* 10, 198
- Burlaga, 1970, *Solar Physics*; 13, 348
- Buttler, S.T. and Buckingham, M.J. 1962 *Phys. Rev.*, 126, 1.
- Bütikofer, R., & Flückiger, E. O. (2013). Differences in published characteristics of GLE60 and their consequences on computed radiation dose rates along selected flight paths, 23rd European Cosmic Ray Symposium (and 32nd Russian Cosmic Ray Conference) IOP Publishing. Journal of Physics: Conference Series, 409, 012166. <https://doi.org/10.1088/1742-6596/409/1/012166>
- Caballero-Lopez, R.A. & Moraal, H. (2012). Cosmic-ray yield and response functions in the atmosphere. *JGR*, Vol. 117, A12103, DOI: 10.1029/2012JA017794.
- Caballero-Lopez, R.A., Moraal, H. (2016). Spectral index of solar cosmic-ray flux from the analysis of ground-level Enhancements. *Advances in Space Research* 57, 1314–1318.

- Cargill, P. (2013). From flares to nanoflares: magnetic reconnection on the Sun. *Astronomy & Geophysics*, 54(3), 3–16.
- Ellison, D. C., & Ramaty, R. (1985). Shock acceleration of electrons and ions in solar flares. *The Astrophysical Journal*, 298, 400–408.
- Cameron, A.G.W. 1967 *ApJ. Letters* 1, 35.
- Cheng, C. C. 1972, *Solar Physics*, 22, pp 178–188.
- Chupp, E. L. 1971: *Space Sci. Rev.* 12, 486.
- Chupp, E.L., Forrest, D.J., Higbie, P.R., Suri, A.N., Tsai, C. and Dunphy, P.P., 1974, *Nature*, 241, 333.
- Cline, T, 1970, NASA-X-661-7133, GSFC, Greenbelt, Maryland.
- Chatterjee, T. N., 2001, On the Application of Information Theory to the Optimun State-space Reconstruction of the Short-term Solar Radio Flux (10.7 cm), and its Prediction Via a Neural Network, *Mon. Not. R. Astron. Soc.* 323, 101-108.
- Chuen L., 1990, Fuzzy logic in control systems. *IEEE transactions on systems, man, and cybernetics*. Vol. 20, num. 2.
- Chowdhury, P., Khan, M., Ray, P.C., 2009. *Mon. Not. R. Astron. Soc.* 392, 1159.
- Datlowe, D. 1971 *Solar Physics* 17, 436
- Daubechies, I., 1992, in *CBMS-NSF Regional Conf. Ser. Applied Mathematics*, Vol. 61 (Philadelphia, PA: SIAM), 1162107.
- Davis, L., 1966, in *The Solar Wind*, Ed. by R.J. Mackin and M. Neugebauer, Pergamon Press, N.Y.
- De Jager, C.: 1967 *Solar Phys.*, 2, 327
- De Jager C., 1969, in C. De Jager and Z. Svestka (eds), *Solar Flares and Space Res.* 1
- De Koning, C.A. (1994). Significant proton events of solar cycle 22 and a comparison with events of previous solar cycles (Thesis). University of Calgary.
- Dessai, U.D. 1971 *Canadian Journal of Physics*, 49, . 265.
- Ding L.-G., Cao X.-X., Wang Z.-W. and Le G.-M., (2016), Large solar energetic particle event that occurred on 2012 March 7 and its VDA analysis, *Research in Astron. Astrophys.* Vol.0 (200x) No.0, 000–000, arXiv: 1604.05303v1 [astro-ph.SR]
- Djurović, D., Pâquet, P.P., 1996. *Solar Phys.* 167, 427.
- Dorman, L.I., and Venkatesan, D. (1993). *Solar Cosmic Rays*, *Space Science Reviews* Vol. 64, 183-362, Code: 1993SSRv.64.183D.
- Duggal, S.P., Guidi, I., Pomerantz, M.A, 1971, *Solar Phys.* 18, 234.
- Duggal, S.P., 1979 *Reviews of Geophysics. Space Physics* 17, 1021.
- Dulk, G. A., Altschuler, M. D., and Smerd, S. F.: 1971, *Astrophys. Letter* 8, 235
- Elliot H. 1952, *Progress in Cosmic Ray Physics* Ed. by Wilson, J.G., Vol 1
- Elliot, H.: 1964, *Planet Space Sci.* 12, 657
- Elliot, H 1969 in *Solar Flares and Space Research* (Ed. by De Jager, C. and Svestka, Z.) North Holand Pub. Amsterdam, p.356.
- Elliot, H.: 1972,) *Solar-Terrestrial Physics*, Part I, p.134, Ed. by C. De Jager
- Englade, R.C. 1971, 12th Int. Cosmic Ray Conf., Tasmania, 2, 502.
- Englade, R.C. 1972, *J. Geophys. Res.* 77, 6266
- Ellison, M.A., McKena, S.M.P. and Reid 1961, *Dunsink Obs. Publ.* 53.
- Ellison, M.A. and Reid, J.A., 1964 *Research in Geophys.* , M.I.T. Press 1, 43.
- Egeland, R., Metcalfe, T., Hall, J.C., Henry, G.W., 2015. *Astrophys. J.* 812 (12).
- Eren, S., Kilcik, A., Atay, T., Miteva, R., Yurchyshyn, V., Rozelot, J.P., Özgüc, A., 2017. *Mon. Not. R. Astron. Soc.* 465, 68.

- Fichtel, C.E. and McDonald, F.B. 1967 *Ann. Rev. of Astron. And Astrophysics* 5, 359.
- Fisk, L.A. and Axford, W.I. (1968). *Journal of Geophysical Research* 73: doi: 10.1029/JA073i013p04396. ISSN 0148-0227.
- Fisk, L.A., 1975, 14th ICRC; Munich.
- Friedman, H.: 1969, in C. De Jager and Z. Sveztko (eds), *Solar Flares and Space Research*, p. 87
- Fritzova-Svestkova and Svetska, 1967, *Solar Phys.*, 2, 87.
- Firoz, K. A., Gan, W. Q., Li, Y. P., & Rodriguez-Pacheco, J. (2014). An interpretation of a possible mechanism for the first ground-level enhancement of solar cycle 24. *Solar Physics*, 290, 613–626. <https://doi.org/10.1007/s11207-014-0619-2>
- Firoz, K. A., Gan, W. Q., Li, Y. P., & Rodriguez-Pacheco, J. (2014). An interpretation of a possible mechanism for the first ground-level enhancement of solar cycle 24. *Solar Physics*, 290, 613–626. <https://doi.org/10.1007/s11207-014-0619-2>
- Forman, M. A., Ramaty, R., & Zweibel, E. G. (1986). The acceleration and propagation of solar flare energetic particles. In P. A. Sturrock, et al. (Eds.), *Physics of the Sun, Geophysics and Astrophysics Monograph* (Vol. II, Chap. 13, pp. 249–290). D. Reidel Publishing Company.
- Forman, M.A., Ramaty, R., Zweibel, E.G. (1986). *Physics of the Sun*, Ed. By Sturrock, P.A. et al., D. Reidel Publishing Company, Chapter 13, p.249-324.
- Freier, P. S., & Weber, W. R. (1963). Radiation hazard in space from solar particles. *Journal of Geophysical Research*, 68, 1605.
- Gallegos-Cruz, A. and Pérez-Peraza, J. 1995, *ApJ*, 446, 669.
- Gallegos-Cruz, A., & Pérez-Peraza, J. (1995). Derivation of analytical particle spectra from the solution of the transport equation by the WKB method. *Astrophysical Journal*, 446, 400–420.
- Gallegos-Cruz, A., & Pérez-Peraza, J. (1995). Derivation of analytical particle spectra from the solution of the transport equation by the WKB method. *Astrophysical Journal*, 446, 400–420.
- Gil A., Kovaltsov G. A., Mikhailov V. V., Mishev A., Poluianov S., Usoskin I. G., (2018), An Anisotropic Cosmic-Ray Enhancement Event on 07-June-2015: A Possible Origin, *Solar Phys*, 293:154, <https://doi.org/10.1007/s11207-018-1375-5>
- Gilman, D.L., Fuglister, F.H., Mitchell, J.M.J., 1963. *Atmos. Sci.* 20, 182.
- Ginzburg V. L. (1958). *Progress in Elementary Particle and Cosmic Ray Physics*, Vol. 4 (Elsevier, Amsterdam) p. 339.
- Ginzburg, V. L. 1969, *Elementary Processes for Cosmic Ray Astrophys*, Gordon & Breach.
- Ginzburg V. L. and Syrovatskii S. I. (1964). *Origin of Cosmic Rays* (Pergamon Press. Oxford)
- Gopalswamy N., Xie H., Akiyama S., Yashiro S., Usoskin I.G., and Davila J.M. (2013). The First Ground Level Enhancement Event of Solar Cycle 24: Direct Observation of Shock Formation and Particle Release Heights. *The Astrophysical Journal Letters*, 765: L30 (5pp), DOI: 10.1088/2041-8205/765/2/L30.
- Gopalswamy N., Xie H., Akiyama S., Yashiro S., Usoskin I. G., and Davila J. M., (2013), The First Ground Level Enhancement Event of Solar Cycle 24: Direct Observation of Shock Formation and Particle Release Heights, *The Astrophysical Journal Letters*, 765:L30 (5pp), doi:10.1088/2041-8205/765/2/L30
- Gopalswamy N., Xie H., Akiyama S., Mäkelä P. A. and Yashiro S., (2014), Major solar eruptions and high-energy particle events during solar cycle 24, *Earth, Planets and Space* 2014, 66:104, <http://www.earth-planets-space.com/content/66/1/104>
- Gopalswamy N., Yashiro S., Thakur N., Mäkelä P., Xie H. , and Akiyama S., (2016), The 2012 July 23 Backside Eruption: an Extreme Energetic Particle Event?, *The Astrophysical Journal*, 833:216 (20pp),, doi:10.3847/1538-4357/833/2/216

- Grinsted, A., Moore, J.C., Jevrejeva, S., 2004. *Nonlinear Process Geophys.* 11, 561.
- Heber, B., Dresing, N., Dröge, W., Gomez-Herrero, R., Herbst, K., Kartavykh, Y., et al. (2013). The first ground level event of solar cycle 24 and its longitudinal distribution in the inner heliosphere, American Geophysical Union, Fall Meeting 2013, Abstract SH33B-2079.
- Henney C. J., Toussaint W. A., White S. M., and Arge C. N., 2012, Forecasting F10.7 with solar magnetic flux transport modeling, *Space Weather*, Vol. 10, S02011, DOI: 10.1029/2011SW000748
- Heristchi Dj., Kangas, JKremser, G., Legrand, J.P.Masse, P. PalousM.Pfotzer, G. Riedler, W, Whilhem, K., 1967 *Ann of the IQSY*, 3, 267 196.7
- Heristchi,Dj. and Trottet, G., 1971, *Phys. Rev. Letters*, 26, 197.
- Heristchi Perez-Peraza, J. Trottet, G. 1972 *Bull. Of the Worl Data Center A, Upper Atmosphere Geophysics*, ed. by Virginia Lincoln, Boulder Colorado, 24, 182.
- Heristchi ,Dj., Perez-Peraza ,J., and Trottet, G., 1975, paper SP-5.3-9 14th International Cosmic Rays Conference, 5, 1841
- Heristchi, Dj, Trottet, G. and, Perez-Peraza, J. 1976, *Solar Physics* 49, 141
- Hess, W. N., 1958, *Rev. Mod. Phys.* 30, 368.
- Ifideli, S. O.: 1974, *Solar Phys.*, 2, 327
- Jokipii, J. R., 1971, Propagation of Cosmic Rays in the Solar Wind, *Reviews of Geophysics and Space Physics*, 9, No. 1.
- Kilcik, A., Özgüç, A., Rozelot, J.P., Ataç, T., 2010. *J. Atmos. Solar-Terr. Phys.* 264, 255.
- King, J.H. 1974, *J. Spacecraft Rockets*, 11, 40l.
- Korchak,A.A. and Sirovatskii, S.I. 1958, *Soviet Doklady*, 3, 983.
- Korchak,A.A. and Sirovatskii, S.I. 1960, *Proc of the 6th ICRC 3,,216*, (Moscow:Izd AN SSSR(in Russian)
- Korchak, A.A. 1967a, *Astron. Zhurn* 11, 258
- Korchak, A.A. 1967b *Doklady AN SSSR* 12, 192.
- Korchak,, A.A, and Platov, Yu. V., 1968 *Astron Zh* 45(6), 1185.
- Kravtsova M. V. and Sdobnov V. E., (2017), Ground Level Enhancements of Cosmic Rays in Solar Cycle 24, ISSN 1063-7737, *Astronomy Letters*, 2017, Vol. 43, No. 7, pp. 501–506., Pleiades Publishing, Inc., DOI: 10.1134/S1063773717070040
- Krimigis, S. M.:1965, *J. Geophys. Res.* 70, 2943.
- Krivsky, 1970, *Acta Phys. Acad. Sci. Hungar.* 29, 427.
- Krivsky, L 1965, *Nuovo Cimento Ser.10-27*, 1017.
- Kurochka, L. N.: 1970, *Astron. Zh.* 47,111.
- Kurt V., Belov A., Kudela K. and Yushkov B., (2018), Some characteristics of the GLE on 10 September 2017, *Contrib. Astron. Obs. Skalnat´e Pleso* 48, 329 – 338, arXiv:1806.00226v1 [physics.space-ph]
- Kuwabara, T. et al., 2013 (The Ice Cube Collaboration), Ground Level Enhancement of May 17, 2012 Observed at South Pole; 33 ICRC, RIO DE JANEIRO 2013; The Astroparticle Physics Conference (See Special Section of these Proceedings).
- Kuwabara, T., Bieber, J., Clem, J., Evenson, P., Gaisser, T., Pyle, R., & Tilav, S. (2012). Ground level enhancement of May 17, 2012 observed at South Pole, *Proc. 45th AGU Fall Meeting*, SH21A-2183 (Poster), San Francisco.
- Kühl P., Banjac S., Dresing N., Gómez-Herrero R., Heber B., Klassen A., and Terasa C., (2015), Proton intensity spectra during the solar energetic particle events of May 17, 2012 and January 6, 2014, *A&A* 576, A120, DOI: 10.1051/0004-6361/201424874

- Li, C., Kazi, A., Firoz, L., Sun, P., & Miroshnichenko, L. I. (2013). Electron and proton acceleration during the first ground level enhancement event of solar cycle 24. *Astrophysical Journal*, 770(1), 34.
- Li C., Miroshnichenko L. I. and Fang C., (2015), Proton activity of the Sun in current solar cycle 24, *Research in Astronomy and Astrophysics* 2015 Vol. 15 No. 7, 1036–1044 doi: 10.1088/1674-4527/15/7/011
- Li C., Miroshnichenko L.I., Sdobnov V.E., (2016), Small Ground-Level Enhancement of 6 January 2014: Acceleration by CME-Driven Shock?, *Solar Phys*, DOI 10.1007/s11207-016-0871-8
- Li, C., Kazi, A., Firoz, L., Sun, P., & Miroshnichenko, L. I. (2013). Electron and proton acceleration during the first ground level enhancement event of solar cycle 24. *Astrophysical Journal*, 770(1), 34.
- Li, K.J., Xu, J.C., Liu, X.H., Gao, P.X., Zhan, L.S., 2010. *Solar Phys.* 267, 295.
- Li, C., Kazi, A., Firoz, L., Sun, P., & Miroshnichenko, L. I. (2013). Electron and proton acceleration during the first ground level enhancement event of solar cycle 24. *ApJ*. 770(1), 34.
- Lin, R.P., 1968, *J. Geophys. Res.* 73, 3066.
- Lin, R.P. Kahler, S.W. and Roelof, E.C., 1960 *Solar Phys.* 4, 338.
- Lingelfelter, R.E., and Ramaty, R.1967 *High Energy Nuclear Reactions in Astrophysics*, Ed, by Shen. B.S.P, Benjamin W, A, Inc.p.99.
- Lockwood, J. A., Friling, L. A., 1968, *Cosmic-ray flare effect of Januar28, 1967 as record by neutron J. Geophy. Res.* 73, 427.
- Lockwood, J. A., Webber, W. R., & Hsieh, L. (1974). Solar flare proton rigidity spectra deduced from cosmic ray neutron monitor observations. *Journal of Geophysical Research*, 79, 4149–4155.
- Lockwood,J.A., Webber,W.R. and Hsieh, L., 1974,*J. Geophys Res.*79, 4149.
- Lust, R. and Simson, J.A., 1957. *The Phys. Rev.* 108, 1563.
- Makhmutov V. S., Bazilevskaya G. A., Stozhkovy Y. I., Raulin J. P., Soncco C., Correia E., Marun A., (2013), Solar proton event on January 23, 2012, 33RD International Cosmic Ray Conference, Rio de Janeiro 2013, The Aatroparticle Physics Conference
- Malandraki, O. E., Agueda, N., Papaioannou, A., Klein, K. L., Valtonen, E., Heber, B., et al. (2012). Scientific analysis within SEPServer—New perspectives in solar energetic particle research: The case study of the 13 July 2005 event, *Solar Physics* 281:333–352. [https://doi.org/ 10.1007/s11207-012-0164-9](https://doi.org/10.1007/s11207-012-0164-9)
- Malandraki, O. E., Klein, K. L., Vainio, R., Agueda, N., Nuñez, M., Heber, B., et al. (2015). “High energy solar particle events forecasting and analysis: The HESPERIA project”, *Proceedings of Science, Proceedings of the 34th International Cosmic Ray Conference (Vol. 34)*. The Hague, Netherlands.
- Malville, J.M. and Smith, S.F., 1963, *J. geophys. Res.* 68, 3181.
- Martinell, J., & Pérez-Peraza, J. (1981). Coronal transport of solar flare particles. *Revista Mexicana de Astronomia y Astrofisica*, 6, 351–355.
- Matthiä D., Matthias M. M., and Berger T. (2018). The Solar Particle Event on 10–13 September 2017: Spectral Reconstruction and Calculation of the Radiation Exposure in Aviation and Space; German Aerospace Center (DLR). Institute of Aerospace Medicine, Cologne, Germany; Space Weather Events of 4-10, DOI: 10.1029/2018SW001921.
- McCracken, K.G., Moraal, H., Shea, M.A. (2012). The high-energy impulsive ground-level enhancement. *ApJ*. 761, 101. DOI: 10.1088/0004-637X/761/2/101.
- McCracken K.G., 1969 in *Solar Flares and Space Research* , Ed. by De Jager, C. and Svetska, Z. North Holland Pub, Amsterdam, p. 202.

- McDonald F.B. and Dessai, 1971, *J. Geophys. Res.*76, 808.
- Melrose, D. B. (1976). Precipitation in trap models for solar hard X-ray bursts. *MNRAS*, 176, 15; DOI: [10.1093/mnras/176.1.15](https://doi.org/10.1093/mnras/176.1.15)
- Mendel, J., 1995, Fuzzy logic systems for engineering: A tutorial. *Proceedings of the IEEE*, vol. 83, num. 3.
- Mendoza, B., Velasco, V.M., Valdés-Galicia, J.F., 2006. *Sol Phys.* 233, 319.
- Miroshnichenko, L. I., & Sorokin, M. O. (1985). Numerical solution of inverse problem for the reconstruction of source spectrum of solar cosmic rays. *Geomagnetism and Aeronomy*, 25(4), 534–540.
- Miroshnichenko, L. I., & Sorokin, M. O. (1986). Reconstruction of some characteristics of solar cosmic rays in the source based on observations near the Earth. *Geomagnetism and Aeronomy*, 26(4), 535–540.
- Miroshnichenko, L. I., & Sorokin, M. O. (1987a). Energy spectrum of the solar proton event of February 16, 1984. *Geomagnetism and Aeronomy*, 27(6), 893–899.
- Miroshnichenko, L. I., & Sorokin, M. O. (1987b). Solution of the inverse problem for determining solar cosmic ray parameters near the source, *Proc. 20th /111. Cosmic Ray Conf , Moscow, USSR, v.3*, 117–120.
- Miroshnichenko, L. I., & Sorokin, M. O. (1989). Temporal and spectral characteristics of particles near the Sun for the proton events of December 7-8 1982 and November 19, 1949. *Geomagnetism and Aeronomy*, 29(2), 309–311.
- Miroshnichenko, L. I., Perez-Peraza, J., Alvarez-Madrigal, M., Sorokin, M. O., Vashenyuk, E. V., & Gallegos-Cruz, A. (1990). Two relativistic solar components in some SPE, *Proc. 21st Int. Cosmic Ray Conf., Australia, Adelaide*, 5, 5–8.
- Miroshnichenko, L. I., & Pérez-Peraza, J. (2008). Astrophysical aspects in the studies of solar cosmic rays. *International Journal of Modern Physics A*, 23, 1.
- Miroshnichenko, L. I. (1994). On the ultimate capabilities of particle accelerators on the sun. *Geomagnetism and Aeronomy*, 34, 29.
- Miroshnichenko, L. I. (1996). Empirical model for the upper limit spectrum for solar cosmic rays at the Earth's orbit. *Radiation Measurements*, 26, 421–425.
- Miroshnichenko, L. I. (2001). *Solar Cosmic Rays* (p. 480). Dordrecht, Netherlands: Kluwer Academic Publishers.
- Miroshnichenko, L. I., Vashenyuk, E. V., & Pérez-Peraza, J. (2009). Two components concept of solar cosmic rays: Solar and interplanetary aspects. *Bulletin of the Russian Academy of Sciences*, 73(3), 297–300.
- Miroshnichenko, L.I., Pérez-Peraza, J., Velasco Herrera, V.M., Zapotitla, J., Vashenyuk, E.V., 2012. *Geomagn. Aeronomy* 52, 547.
- Miroshnichenko, L. I. (2014). *Solar cosmic rays: Fundamentals and applications* (2nd ed., p. 521). Switzerland: Springer.
- Miroshnichenko, L. I. (2014). *Solar cosmic rays: Fundamentals and applications* (2nd ed., p. 521). Switzerland: Springer.
- Miroshnichenko, L., 2015, *Solar Cosmic Rays: Fundamental and Applications*, *Astrophysics and Space Science Library* 405.
- Mishev , A.L., Kocharov, L.G. and Usoskin, G., 2014, *J.G.R.: Space Physics* 119, 670.

- Mishev, A. L., Kocharov, L. G., & Usokin, I. G. (2014). Analysis of the ground level enhancement on 17 May 2012 using data from the global neutron monitor network. *Journal of Geophysical Research: Space Physics*, 119, 670–679. <https://doi.org/10.1002/2013JA019253>
- Mishev A., Poluianov S. and Usoskin I., (2017), Assessment of spectral and angular characteristics of sub-GLE events using the global neutron monitor network, *J. Space Weather Space Clim.* 2017, 7, A28, DOI: 10.1051/swsc/2017026
- Mishev A., Usoskin I., Raukunen O., Paassilta M., Valtonen E., Kocharov L., Vainio R. (2018). First Analysis of Ground-Level Enhancement (GLE) 72 on 10 September 2017: Spectral and Anisotropy Characteristics; *Solar Phys.* 293:136. <https://doi.org/10.1007/s11207-018-1354-x>.
- Mishev, A. L., Kocharov, L. G., & Usokin, I. G. (2014). Analysis of the ground level enhancement on 17 May 2012 using data from the global neutron monitor network. *Journal of Geophysical Research: Space Physics*, 119, 670–679. <https://doi.org/10.1002/2013JA019253>
- Moraal H. & R. A. Caballero-Lopez (2014). The cosmic-ray ground level enhancement of 1989 september 29. *ApJ.* 790:154 (16pp); DOI:10.1088/0004-637X/790/2/154.
- Ogilvie, K.W., Bryant, D.A. and Davis, L.R., 1962, *J.Geophys. Res.* 67(3), 929.
- Oh, S. Y., Bieber, J.W., Clem, J., Evenson, P., Pyle, R., Yi, Y., and Kim, Y. K. (2012). South Pole neutron monitor forecasting of solar proton radiation intensity. *Space Weather*, S05004, DOI: 10.1029/2012SW000795.
- Omodei N., Pesce-Rollins M., Longo F., Allafort A., Krucker S. (2018). Fermi-LAT observations of the 2017 September 10th solar flare Preprint of the Alamos Laboratory. arXiv: 1803.07654v1 [astro-ph.HE] (6 pages); DOI: [10.3847/2041-8213/aae077](https://doi.org/10.3847/2041-8213/aae077).
- Özgüç, A., Ataç, T., 1989. *Solar Phys.* 123, 357.
- Özgüç, A., Ataç, T., 1996. *Solar Phys.* 163, 183.
- Özgüç, A., Ataç, T., 2003. *Solar Phys.* 214, 375.
- Palmer, I.A.(1982, *Rev. Geophys. Space Phys.*20, 335.
- Papaioannou A., Souvatzoglou G., Paschalis P., Gerontidou M., Mavromichalaki H., (2013), The First Ground-Level Enhancement of Solar Cycle 24 on 17 May 2012 and Its Real-Time Detection, *Solar Phys*, DOI 10.1007/s11207-013-0336-2
- Parker E.N., 1963a, *Interplanetary Dynamical Processes*, John Wiley & Sons, Interscience, New York.
- Parker E.N., 1963b, *ApJ Suppl* 77, 177.
- Parker 1965, *Planet.and Space Sc.*13 (1), 9.
- Parker, E.N. 1969, *Space Sci. Rev.* 9, 325.
- Perez-Peraza, J. 1975, *J. Geophys. Res.*, 80, 3535.
- Perez-Peraza, J. and Galindo Trejo, J. 1975_ " *Rev. Mexicana Astron. & Astroph.* 1, 273
- Pérez-Peraza, J., Gálvez, M., & Lara-Alvarez, R. (1977). Energy spectrum of flare particles from an impulsive acceleration process, *Proc. of the Int. Cosmic Ray Conf.*, XV-5, 23–28.
- Pérez-Peraza, J., Gálvez, M., & Lara-Alvarez, R. (1978). The Primary Spectrum of Suprathermal Solar Particles. *Adv. Space Research* 18, 365-368.
- Pérez-Peraza, J., Lara-Alvarez, , 1979 , “The required range for the acceleration efficiency when particles undergo energy losses” *R. Proc. of the Int. Cosmic Ray Conf.* XVI-12, 259-264, 1979 (XVI-5, 10, 1979).
- Perez-Peraza J., 1981, *Selective Acceleration in Cosmic Ray Source, Nucleosintesis*, *Proc. Of the Summer Workshop held in TIFR, Bombay, and May 19-23, 1980.* Editors S. Biswas, S. Ramadurai, M. N. Vahia, Tata Institute of Fundamental Research, Bombai.

- Pérez-Peraza, J., & Martinell, J. (1981). Azimuthal propagation of flare particles in the Heliosphere, Proc. of the 17th Int. Cosmic Ray Conf., 3, 55–58.
- Pérez-Peraza, J., Álvarez-Madrigal, M., Rivero, F., & Miroshnichenko, L. I. (1985). Source energy spectra from demodulation of solar particle data by interplanetary and coronal transport, Proc. of the Int. Cosmic Ray Conf., XIX-4, 110-113.
- Pérez-Peraza, J. (1986). Coronal transport of solar flare particles. *Space Science Reviews*, 44, 91–138.
- Pérez-Peraza, J. and Gallegos-Cruz, A., 1994a, *Ap. J. Suppl.*, 90-2, 669.
- Pérez-Peraza, J. and Gallegos-Cruz, A., 1994b, *Geofísica Internacional* 33-2, 311.
- Pérez-Peraza, J. and Gallegos-Cruz, A. (1994). Weightiness of the Dispersive Rate in Stochastic Acceleration Processes. *The Astrophysical Journal Supplement Series*, 90:669-682. <https://doi.org/10.1017/S0252921100077940>.
- Pérez-Peraza, J., Gallegos Cruz, A., Vashenyuk, E. V., Balabin, Y. V., & Miroshnichenko, L. I. (2006). Relativistic proton production at the Sun in the October 28th, 2003 solar event. *Advances in Space Research*, 38, 418.
- Pérez-Peraza, J., Vashenyuk, E. V., Gallegos Cruz, A., Balabin, Y. V., & Miroshnichenko, L. I. (2008). Relativistic proton production at the Sun in the January 20th, 2005 solar event. *Advances in Space Research*, 41, 947–954.
- Pérez-Peraza J., Vashenyuk E.V., Balabin Yu.V., Miroshnichenko L.I., Gallegos.Cruz A. (2009). Impulsive, Stochastic, and Shock Wave Acceleration of Relativistic Protons in Large Solar Events of 1989 September 29, 2000 July 14, 2003 October 28, and 2005 January 20. *ApJ*. 695, 865; DOI: 10.1088/0004-637X/695/2/865.
- Pérez-Peraza, V.M. Velasco Herrera, J. Zapotitla, E.V. Vashenyuk, L.I. Miroshnichenko., 2009, Pulse with Modulation Analysis of Ground Level Enhancements of Solar Cosmic Rays, Proc. de la 31ava Conf. Int. de Rayos C6smicos, SH.1.5-8.
- Pérez Peraza, J., Velasco Herrera, V., Zapotitla Román, J., Miroshnichenko, L. I., & Vashenyuk, E. V., Libin I. YA., (2011). Classification of GLE's as a function of their spectral content for prognostic goals, 32ava ICRC, Beijing, China, SH1.5, Vol.10, 149–152.
- Pérez-Peraza, J., Juarez, A., Juarez, J., *Astron. J.* 2015. 803, 27.
- Pérez-Peraza Jorge and Juárez-Zuñiga Alan, Prognosis of GLEs of Relativistic Solar Protons, 2015, *The Astrophysical Journal*, 803:27 (9pp). <https://doi.org/10.1088/0004-637X/803/1/27>
- Pérez-Peraza, Jorge; Márquez-Adame Juan C. (2018) in Book *Cosmic Rays*, Ed. by InTech. ISBN: 978-1-78923-593-7, chapter: 7, ISBN: 978-953-51-6247-6.
- Pérez-Peraza J., Márquez-Adame J. C., Miroshnichenko L. and Velasco-Herrera V., (2018), Source Energy Spectrum of the 17 May 2012 GLE, *Journal of Geophysical Research: Space Physics*, DOI: 10.1002/2017JA025030
- Pérez-Peraza J, Adame JCM. An alternative classification of solar particle events that reach the earth ground level. *Phys Astron Int J.* 2019;3(5):163–170. DOI: 10.15406/paij.2019.03.00177
- Pinter, S. 1969, *Solar Phys.* 8, 149.
- Pinter, S. 1972 Proc. IV Leningrad Cosmic Phys. Seminar, Phys. Techn. Inst., Leningrad, p.63.
- Plainaki, C., Mavromichalaki H., Laurenza M., Gerontidou M., Kanellakopoulos A., and Storini M. (2014). The Ground-Level Enhancement of 2012 May 17: Derivation of Solar Proton Event Properties Through the Application of the NMBANGLE PPOLA Mode. *Astrophys. J.*, 785, 160 (12 pp.), DOI: 10.1088/0004-637X/785/2/160.

- Plainaki, C., Mavromichalaki, H., Laurenza, M., Gerontidou, M., Kanellakopoulos, A., & Storini, M. (2014). The ground-level enhancement of 2012 May 17: Derivation of solar proton event properties through the application of the NMBANGLE PPOLA model. *The Astrophysical Journal*, 785, 160. (12 pp.) <https://doi.org/10.1088/0004-637X/785/2/160>
- Poluianov S.V., Usoskin I.G., Mishev A.L., Shea M.A., Smart, D.F., (2017), GLE and Sub-GLE Redefinition in the Light of High-Altitude Polar Neutron Monitors, *Solar Phys* (2017) 292:176, DOI 10.1007/s11207-017-1202-4
- Pomerantz and Duggal, 1974, *J. Geophys. Res.* 79, 913
- Ramaty, R and Lingelfelter, R.E, 1967 *J Geophys. Res.*72, 879.
- Ramaty, R. (1979). *Particle Acceleration Mechanisms in Astrophysics*. (AIP Conf. Proc.56). Ed. J.Arons, C.Max, & C. McKee (New York: AIP), 135.
- Ramaty R.,and Lingelfetter, R.E.,1973, in *High Energy Phenomenon on the sun* NASA SP-342, 301.
- Ramaty R.,and Lingelfetter, R.E.,1975, in *Solar Gamma, X and EUV Radiation*, IAU Symposium 68, Ed. by R.S. Kane, Reidel Pub. Co.Dordrecht, Holland, p.363.
- Ramudurai,S. and Biswas,S. 1971,12th International Cosmic Rays Conference 2, 793.
- Ramudurai,S. and Biswas, S. 1974, *Astrophys and Space Sci.*, 30, 187.
- Reames, D.F. and Fichtel, C.E. 1967, 10th ICRC, Calgary. 2, 546.
- Reid, J.H., 1961, *Dunsink Obs. Publ.* 53.
- Reinhard, R., & Wibberenz, G. (1973). Coronal transport of solar flare protons: Drift and diffusion in the corona, *Proc 13th ICRC*, 2, 1373–1383.
- Reinhard, R., & Wibberenz, G. (1974). The variation of solar proton energy spectra and size distribution with heliolongitude. *Solar Physics*, 36, 473.
- Rivin, Y.R., 1989. *The cycles of The Earth and the Sun*. Moscow, Nauka.
- Rotwell. P.L., 1976, *J. Geophys. Res.* 81, 709.
- Ruffolo, D., Tooprakai, P., Rujivarodom, M., Khumlumlert, T., Wechakama, M., Bieber, J.W., Evenson, P., Pyle, R. (2006). Relativistic Solar Protons on 1989 October 22: Injection and Transport along both Legs of a Closed Interplanetary Magnetic Loop. *ApJ*. 639, 1186–1205. <http://dx.doi.org/10.1086/499419>.
- Sakurai, K., 1963, *J. Geomag. Geoelect.*14, 144.
- Sakurai, K., 1965, *Pub. Of the Astron. Soc. of Japan*, 19, 408.
- Sakurai, K. 1966a, *Pub. Of the Astron. Soc. of Japan* 18, 77.
- Sakurai, K. 1966b, *Rept. Ionosph. Space Res. of Japan* 20, 519; 20, 233.
- Sakurai, K 1967, *Rept. Ionosph. Space Res. of Japan* 21, 113; 21, 213.
- Sakurai, K. 1971 NASA Report X- 693-71-268 GSFC, Greenbelt Md.
- Sakurai, K. 1973, *Solar Phys* 31, 483.
- Sakurai, K., *Physics of Solar Cosmic Rays*, Ed. by University of Tokyo Press. (1974). UTP 3402, 68026-5149.; ISBN 0-86008-105-2.
- Sakurai, K. 1976 *Pub. Astron. Society of Japan* 28, 177.
- Schatten, K. H., & Mullan, D. J. (1977). Fast azimuthal transport of solar cosmic rays via a coronal magnetic bottle. *Journal of Geophysical Research*, 82, 5609.
- Schatzman, E. (1966). *Summer School of Theoret. Phys. Les Hooches* (New York: Gordon & Breach). 229.
- Schatzman, E., 1967, *Solar Phys.* 1,411.

- Schlickeiser, R. (1989). Cosmic-Ray Transport and Acceleration. I. Derivation of the Kinetic Equation and Application to Cosmic Rays in Static Cold Media. *ApJ*, 336, 243; DOI: [10.1086/167009](https://doi.org/10.1086/167009)
- Severnii and Shabanskii (1961). The generation of cosmic rays in flares, *Soviet Astrophys. AJ.*, 4, 583.
- Shea, M. A., Smart, D. F., Adams, J. H., Chennette, D., Feyman J., Hamilton, D. C., Heckman, G., Konradi, A., Lee, M. A., Nachtwey, D. S., and Roelof, E. C., (1988). Toward a descriptive model of solar particle in the heliosphere; Interplanetary particle environment, JPL Publication 88-28
- Shea, M. A., & Smart, D. F. (2012). Space weather and the ground-level solar proton events of the 23rd solar cycle. *Space Science Reviews*, 171, 161–188.
- Simnet, 1971, *Solar Phys.* 20, 448.
- Smart, D. F. and Shea, M. A. (1993), Predicting and modeling solar flare generate proton fluxes in the inner heliosphere, in: *Biological Effects and Physics of Solar and Galactic Cosmic Radiation, Part B*, Eds.: Swenberg et al., Plenum Press. New York, p. 101-117.
- Smart, D. F. and Shea, M. A. (2005). A review of geomagnetic cutoff rigidities for earth-orbiting spacecraft. *Advances in Space Research* 36, 2012–2020; DOI: [10.1016/j.asr.2004.09.015](https://doi.org/10.1016/j.asr.2004.09.015)
- Smerd, S.F. and Dulk, G.A. 1971 in *Solar Magnetic Fields*, IAU 43, 616.
- Smith E.V.P.1968, in *Mass Motions in Solar Flares and Related Phenomena*, Nobel Symposium 9, Ed. by Y Oman, Almqvist Wiksell, Stockholm p. 137.
- Smith S.F. and Ramsay, H.E., 1967, *Solar Phys.* 2, 158.
- Smith D.F. 1986 *Adv. Space Res.* 6(6), 135.
- Somov, B.V. and Syrovatskii, S.I., 1974, *Solar Phys.*, 39, 415.
- Sonnerup 1973, in R. Ramaty and R. G. Stone (eds.), *High Energy Phenomena on the Sun*, NASA X-693-73-193, p. 357.
- Soon, W., Velasco Herrera, V.M., Selvaraj, K., Traversi, R., Usoskin, I., Chen, C.T.A., Lou, J.Y., Kao, S.J., Carter, R.M., Pipin, V., Severi, M., Becagli, S.A., 2014. *Earth-Sci. Rev.* 134, 1.
- Stoker, P. H. (1985), Spectra of solar proton ground level events using neutron monitor and neutron moderated detector recordings, *Proc. 19th ICRC*, La Jolla, 4, 114.
- Suemoto and Hiei 1959, *Publ. astr. Soc. Japan* 11, 185.
- Suemoto and Hiei 1962, 1962, *Publ. astr. Soc. Japan* 14, 33.
- Svestka, Z, 1963, *BAC*, 14, 234
- Svetska,Z. 1966 Proton flares before 1956. *Astr. Insts. Czech. Bulletinm*, 17, 262.
- Svetska, Z., 1968 on long-term forecasts of proton flares, *Solar Physics*, 4(1), 18.
- Svetska,Z. 1969 in *Solar Flares and Space Research* (ed. By de Jager, C. and Svestka, Z.) North-Holland Pub., Amsterdam, p. 16.
- Svetska, Z. 1976 *Solar Flares Geophysical and Astrophysics Monographs*, Ed. Reidel Publishing Company
- Syrovatskii,S.I., 1961, *Sov. Phys. JET?* 13, 1257.
- Syrovatskii,S.I. and Shmeleva, O.P., 1972:-*Sov. Astron. AJ*, 16, 273.
- Takakura, T. 1966, *Space Sci. Rev.* 5, 80.
- Takakura, T., 1969, *Solar Phys.* 6, 133.
- Tassev Y., Velinov P. I. Y., Tomova D., Mateev L., (2017), Analysis of Extreme Solar Activity in Early September 2017: G4 – Severe Geomagnetic Storm (07–08.09) and GLE72 (10.09) in Solar Mininum, *Comptes rendus de l’Acad’emie bulgare des Sciences*, Tome 70, No 10, 2017, SCIENCES COSMIQUES Météorologie de l’espace

- Thakur N., Gopalswamy N., Xie H., Mäkelä P., Yashiro S., Akiyama S., and Davila J. M., (2014), Ground Level Enhancement in the 2014 January 6 Solar Energetic Particle Event, *The Astrophysical Journal Letters*, 790: L13 (5pp), 2014 July 20 doi:10.1088/2041-8205/790/1/L13
- The IceCube Collaboration, Manganard P. S., Muangha P., Pyle R., Ruffolo D., and Sáiz A.; (2017), GeV Solar Energetic Particle Observation and Search by IceTop from 2011 to 2016; 35th International Cosmic Ray Conference - ICRC2017, 10-20 July, 2017, Bexco, Busan, Korea, PoS(ICRC2017)132, http://icecube.wisc.edu/collaboration/authors/icrc17_icecube
- Torrence, C., Compo, G., 1998. *Bull. Am. Meteorol. Soc.* 79, 61.
- Torrence, C., Webster, P.J., 1999. *J. Clim.* 12, 2679.
- Torrence, C. and Compo, G., 1998, *A Practical Guide to Wavelet Analysis*, *Bull. American Meteorol. Soc.* 79, 61-78.
- Torrence, C. and Webster, P.J., 1999, Interdecadal Changes in the ENSO-Monsoon System. *Journal of Climate*, 12, 2679-2690. [https://doi.org/10.1175/1520-0442\(1999\)012<2679:ICITEM>2.0.CO;2](https://doi.org/10.1175/1520-0442(1999)012<2679:ICITEM>2.0.CO;2)
- Tsyтович, V. N. (1977). *Theory of Turbulent Plasma* (New York: Consultants Bureau)
- Tylka, A., & Dietrich, W. (2009). A new and comprehensive analysis of proton spectra in ground-level enhanced (GLE) solar particle events, In: *Proc. 31th International Cosmic Ray Conference*. Universal Academy Press, Lodz', Poland, p. ID 0273, URL. Retrieved from <http://galpropstanford.edu/elibrary/icrc/2009/preliminary/pdf/icrc0273.pdf>
- Usoskin, I. G., Kovaltsov, G. A., Mironova, I. A., Tylka, A. J., & Dietrich, W. F. (2011). Ionization effect of solar particle GLE events in low and middle atmosphere. *Atmospheric Chemistry and Physics*, 11, 1979–1988.
- Valdés-Galicia, J.F., Velasco, V., 2008. *Adv. Space Res.* 41, 297.
- Vashenyuk, E. V., Miroshnichenko, L. I., Sorokin, M. O., Pérez-Peraza, J., Álvarez-M, Y., & Gallegos-C, A. (1991). Dynamics of acceleration and escape of relativistic solar cosmic rays from the solar corona, *Kosmicheskyye Issledovaniya (Space Research, Leningrad Physical and Technical Institute)*, 147–160.
- Vashenyuk, E. V., Miroshnichenko, L. I., Sorokin, M.O., Pérez-Peraza, J. y Gallegos-Cruz, A. (1993). Search for Peculiarities of Proton Events in Solar Cycle 22 by Ground Observation Data. *Geomagnetism & Aeronomy* 33(5), 1-10.
- Vashenyuk, E.V., Miroshnichenko, L.I., Sorokin, M.O., Pérez-Peraza, J. y Gallegos- Cruz, A., *Geomag. y Aeron.* 33-5, 563-575 (1994).
- Vashenyuk, E. V., Miroshnichenko, L. I., Sorokin, M. O., Pérez-Peraza, J., & Gallegos-Cruz, A. (1994). Large ground level events in solar cycle 22 and some peculiarities of relativistic proton acceleration. *Advances in Space Research*, 14(10), 711–716.
- Vashenyuk, E. V., Miroshnichenko, L. I., Pérez-Peraza, J., Kananen, H., & Tanskanen, P. (1997). Generation and propagation characteristics of relativistic solar protons during the GLE of September 29, 1989, *Proc. of the Int. Cosmic Ray Conf. XXV*, 1, 161–164.
- Vashenyuk, E. V., Pchelkin, V., Gvozdevsky, B. B., & Pérez-Peraza, J. (2002). Primary solar cosmic ray parameters obtained by modeling technique from ground based observations, *Proc. The 6th World Multiconference on Systemics, Cybernetics and Informatics XVII*, 458–461.
- Vashenyuk, E. V., Balabin, Y. V., Perez-Peraza, J., Gallegos-Cruz, A., & Miroshnichenko, L. I. (2006). Some features of the sources of relativistic particles at the Sun in the solar cycles 21-23. *Advances in Space Research*, 38(3), 411–417.

- Vashenyuk, E. V., Balabin, Yu. V., Miroshnichenko, L. I., Pérez-Peraza, J., & Gallegos-Cruz, A. (2007). Two-component features of the two largest GLEs: 23 February 1956 and 20 January 2005, *Proc. of the Int. Cosmic Ray Conf.* XXX, 1, 249–252.
- Vashenyuk, E. V., Miroshnichenko, L. I., Balabin, Yu-V, Pérez-Peraza, J., & Gallegos-Cruz, A. (2007). Relativistic solar cosmic ray events (1956–2006) from GLE modeling studies, *Proc. of the Int. Cosmic Ray Conf.* XXX, 1, 253–256.
- Vashenyuk, E. V., Balabin, Y. V., & Miroshnichenko, L. I. (2008). Relativistic solar protons in the GLE of 23 February 1956: New study. *Advances in Space Research*, 41(6), 926–935.
- Vashenyuk, E.V. 2011, *Bulletin of the Russian Academy of Sciences* 75(6), 767.
- Vashenyuk, E. V.; Balabin, Yu. V.; Gvozdevsky, B. B. (2011). Features of relativistic solar proton spectra derived from ground level enhancement events (GLE) modeling. *Astrophysics and Space Sciences Transactions*, Volume 7, Issue 4, 2011, pp.459-463, DOI: [10.5194/astra-7-459-2011](https://doi.org/10.5194/astra-7-459-2011)
- Velasco, V., Mendoza, B., 2008. *Adv. Space Res.* 42, 866.
- Velasco Herrera, V., 2008a. 37Th COSPAR scientific assembly. E21-0049-08.
- Velasco Herrera, V., 2008b. 37Th COSPAR scientific assembly. E21-0050-08.
- Velasco Herrera, V.M., Mendoza, B., Velasco Herrera, G., 2015. *New Astron.* 34, 221.
- Velasco Herrera, G., 2016. *Adv. Space Res.* 58 (10), 2104.
- Velasco Herrera, V.M., Cordero, G., 2016. *Earth Planets Space* 42, 866.
- Velasco Herrera V.M., Pérez-Peraza J., Soon W., and Márquez-Adame J.C, The Quasi-Biennial Oscillation of 1.7 years in Ground Level Enhancement Events, 2017, *New Astronomy*, DOI: [10.1016/j.newast.2017.09.007](https://doi.org/10.1016/j.newast.2017.09.007)
- Velasco Herrera, V.M., Soon, W., Velasco-Herrera, G., Traversi, R., Horiuchi, K., 2017. *New Astron.* 56, 86.
- Velinov P., (2016), Extended Categorisation of Ground Level Enhancements (GLEs) of Cosmic Rays Due to Relativistic Solar Energetic Particles, Bulgarian Academy of Sciences. Space Research and Technology Institute. Aerospace Research in Bulgaria. 28, 2016, Sofia.
- Webber, W.R. 1964, AAS-NASA SP-50 Symp. On the physics of solar flares, GSFC, Ed, W.W. Hess, p. 515.
- Wentzel, D.G. 1965, *J. Geophys. Res.*, 70, 2716.
- Wentzel, D.G. 1969a, *ApJ* 156, 303.
- Wentzel, D.G. 1969b, *ApJ* 157, 545
- West, H.I Jr., Buck, R.M., Walton, J.R. and D'Arcy, R.G., Jr.1972, *Upper Atmosph. Geophys World Data Center A*, NOAA, Rep. 24., p. 113.
- Widding, K.G., 1975, *IAU Symposium* 68, 153
- Wild, J.P., 1962, *J. Phys. Soc. Japan* 17 Suppl. An II, 249.
- Wibberenz, G., & Reinhard, R. (1975). The exponential decay of solar flare particles: Eastern and western hemisphere effects, *Proc. 14 Int. Cosmic Rays Conf.* 5, 1681–1691.
- Xiao C., Cheng G., Zhang H., Rong Z., Shen C., Zhang B., Hu H., 2017, Using Back Propagation Neural Network Method to Forecast Daily Indices of Solar Activity F10.7. *Chin. J. Space Sci.*, 2017, 37(1): 1-7, DOI:10.11728/cjss2017.01.001.
- Yordan Tassev, Peter I.Y. Velinov, Dimitrinka Tomova, Lachezar Mateev. (2017). *Comptes rendus de l'Academie bulgare des Sciences*, Tome 70, No 10, Sciences Cosmiques.